mgr Izabela Domańska

Sterylizacja radiacyjna implantacyjnych postaci leków przeciwnowotworowych

Rozprawa na stopień doktora nauk medycznych i nauk o zdrowiu w dyscyplinie nauki farmaceutyczne

Promotorzy: prof. dr hab. inż. Marcin Sobczak

dr hab. inż. Krystyna Cieśla, Prof. Instytutu

Katedra i Zakład Chemii Farmaceutycznej i Biomateriałów

Obrona rozprawy doktorskiej przed Radą Dyscypliny Nauk Farmaceutycznych Warszawskiego Uniwersytetu Medycznego

Warszawa 2023

Słowa kluczowe: nanocząstki, sterylizacja radiacyjna, wiązka elektronów, promieniowanie γ, paklitaksel, polimery biodegradowalne, poliestry alifatyczne, systemy dostarczania substancji leczniczej

Keywords: nanoparticles, radiation sterilization, electron beam, γ-irradiation, paclitaxel, biodegradable polymers, aliphatic polyesters, drug delivery systems

Pragnę złożyć serdeczne podziękowania
Panu prof. dr hab. inż. Marcinowi Sobczakowi,
za opiekę naukową i wsparcie na każdym etapie pracy
oraz ogromny wkład
w mój rozwój naukowy i intelektualny.

Chciałabym również bardzo podziękować
Pani dr hab. inż Krystynie Cieśli, Prof. Instytutu,
za ogrom życzliwości, nieocenioną pomoc oraz cenne rady.

Źródło finansowania

Badania zrealizowane w ramach niniejszej rozprawy doktorskiej zostały sfinansowane ze środków Ministerstwa Edukacji i Nauki w ramach działalności statutowej Warszawskiego Uniwersytetu Medycznego.

Grant Młodego Badacza WUM

Tytuł projektu: Badanie wpływu procesu sterylizacji radiacyjnej na nowe biodegradowalne systemy terapeutyczne zawierające paklitaksel.

Źródło finansowania: FW231/1/F/MBS/N/21 (2021-2023).

Rozprawa doktorska została wykonana w ramach uczestnictwa w projekcie *Interdyscyplinarnych Studiów Doktoranckich „RadFarm”* realizowanego w konsorcjum czterech jednostek:

1. Narodowego Centrum Badań Jądrowych w Otwocku
2. Warszawskiego Uniwersytetu Medycznego
3. Uniwersytetu Warszawskiego
4. Instytutu Chemii i Techniki Jądrowej w Warszawie

Tytuł projektu: *Radiofarmaceutyki dla ukierunkowanej mole kularnie diagnostyki i terapii medycznej* (POWR.03.02.00-00-I009/17-00).

Projekt *Radiofarmaceutyki dla ukierunkowanej molekularnie diagnostyki i terapii medycznej* jest współfinansowany ze środków Europejskiego Funduszu Społecznego Programu Operacyjnego Wiedza Edukacja Rozwój 2014-2020.

Spis treści

1. Aktywność naukowa

Wykształcenie

- 2015–2016 – Uniwersytet Warszawski, Centrum Metrologii Chemicznej; Warszawa
  Studia podyplomowe, kierunek: Metrologia Chemiczna
- 2013–2014 – l'Ecole Nationale Supérieure de Chimie et de Physique de Bordeaux (ENSCPB), Bordeaux, Francja
  Master of sciences: Polymers Engineering and Formulation
- 2012–2013 – Université de Reims Champagne-Ardenne (URCA), Reims, Francja
  Międzynarodowy program wymiany studenckiej Erasmus; Instytut Chemii Molekularnej
  Studia magisterskie; kierunek: Chemia
- 2008–2013 – Uniwersytet Marii Curie-Skłodowskiej (UMCS) w Lublinie; Lublin
  Studia magisterskie; kierunek: chemia; specjalizacja: Chemia Środków Bioaktywnych i Kosmetyków

Autorstwo w publikacjach naukowych

- Domańska, I.M., Zalewska, A., Cieśla, K., Plichta, A., Głuszewski, W., Łyczko, M., Kowalczyk, S., Oledzka, E., Sobczak, M., The influence of electron beam and gamma irradiation on paclitaxel-loaded nanoparticles of fully randomized copolymers in relation to potential sterilization. *Journal of Drug Delivery Science and Technology* 2023, 90, 105115.
- Domańska, I.M., Figat, R., Zalewska, A., Cieśla, K., Kowalczyk, S., Kędra, K., Sobczak, M., The influence of ionizing radiation on paclitaxel-loaded nanoparticles based on PLGA. *Applied Sciences* 2023, 13, 11052.
- Oledzka E, Paśnik K., Domańska I., Zielińska-Pisklak M., Piotrowska U., Sobczak M., Szeleszczuk Ł., Laskowska, A., Poly(amidoamine) Dendrimer/Camptothecin Complex: From Synthesis to In Vitro Cancer Cell Line Studies. *Molecules* 2023, 28, 2696.
- Domańska, I.M., Zgadzaj, A., Kowalczyk, S., Zalewska, A., Oledzka, E., Cieśla, K., Plichta, A., Sobczak, M., A Comprehensive Investigation of the Structural, Thermal, and Biological Properties of Fully Randomized Biomedical Polyesters Synthesized with a Nontoxic Bismuth(III) Catalyst. *Molecules* 2022, 27, 1139.
- Domańska, I.M., Oledzka, E., Sobczak, M., Sterilization process of polyester based anticancer-drug delivery systems. *International Journal of Pharmaceutics* 2020, 587, 119663.
- Vleugels, L.F.W., Domańska, I., Voets, I.K., Tuinier, R., On the driving forces for complexation of methyl orange with polycations. *Journal of Colloid and Interface Science* 2017, 491, 141–150.

Granty badawcze

- Kierownik projektu:
  2021-2023 – „Badanie wpływu procesu sterylizacji radiacyjnej na nowe biodegradowalne systemy terapeutyczne zawierające paklitaksel", Projekt Młodego Badacza nr FW231/1/F/MBS/N/21, Warszawski Uniwersytet Medyczny.
  Opiekun projektu: prof. dr hab. inż. Marcin Sobczak

Uczestnictwo w konferencjach naukowych

Zagadnienia wchodzące w skład niniejszej rozprawy doktorskiej były prezentowane na krajowych konferencjach naukowych:

- Domańska, I., Zalewska, A., Plichta, A., Łyczko, M., Cieśla, K., Sobczak, M. Studies on the influence of ionizing radiation on new, biodegradable drug delivery systems containing paclitaxel. ACCORD. *Interdisciplinary Conference on Drug Sciences*, Warszawa, 26-28.05.2022.
- Domańska, I., Rybak, D., Kowalczyk, S., Łyczko, M., Olędzka, E., Cieśla, K., Sobczak, M. Mikrocząstki poliestrowe jako nośniki paklitakselu – otrzymywanie, badania strukturalne, analiza kinetyki uwalniania substancji leczniczej w warunkach in vitro. *XVII Warszawskie Seminarium Doktorantów Chemików - ChemSession'21,* Warszawa, 24.09.2021.
- Domańska, I., Oledzka, E., Cieśla, K., Plichta, A., Sobczak, M. Synteza i charakterystyka strukturalna biodegradowalnych matryc polimerowych do zastosowań biomedycznych. *III Ogólnopolska Konferencja „Fizyka Medyczna Farmacja Fizyczna"*, Warszawa, 25.09.2020.
- Domańska, I., Oledzka, E., Sobczak, M. Biodegradowalne matryce polimerowe jako nośniki leków przeciwnowotworowych – synteza i charakterystyka strukturalna. *Pierwsza Wirtualna Konferencja Naukowa Kampusu Ochota,* Warszawa, 30.06-01.07.2020.

2. Wykaz skrótów

$BiOct_3$ – 2-etyloheksanian bizmutu/oktanian bizmutu

CL – ε-kaprolakton

CPA – cyklofosfamid

CPT – kamptotecyna

$Đ$ – współczynnik dyspersyjności

DDS – system dostarczania substancji leczniczej (ang. *drug delivery systems*)

DLS – technika dynamicznego rozpraszania światła (ang. *dynamic light scattering*)

DOX – doksorubicyna

DSC – różnicowa kalorymetria skaningowa (ang. *differential scanning calorimetry*)

EB – wiązka elektronów

EE – efektywność enkapsulacji

5-FU – 5-fluorouracyl

GA – glikolid

GPC – chromatografia żelowa (ang. *gel permeation chromatography*)

HPLC – wysokosprawna chromatografia cieczowa (ang. *high-performance liquid chromatography*)

l – średnia długość bloków w łańcuchu polimeru

LA – laktyd

L-LA – L-laktyd

MALDI-TOF MS – spektrometryczna metoda laserowej jonizacji/desorpcji próbki wspomagana matrycą z analizatorem czasu przelotu (ang. *matrix-assisted laser desorption/ionization with time-of-flight analyzer mass spectrometry*)

M_n – liczbowo średnia masa molowa

NMR – spektroskopia magnetycznego rezonansu jądrowego (ang. *nuclear magnetic resonance*)

NRU – test pochłaniania czerwieni obojętnej (ang. *neutral red uptake*)

PCL – poli(ε-kaprolakton)

PCLGA – kopolimer ε-kaprolaktonu i glikolidu

PEG200 – glikol polioksyetylenowy

PGA – poliglikolid

PLA – poli(L-laktyd)

PLACL – kopolimer L-laktydu i ε-kaprolaktonu

PLGA – kopolimer L-laktydu i glikolidu

PTX – paklitaksel

R – współczynnik randomizacji

ROP – polimeryzacja z otwarciem pierścienia (ang. *ring opening polymerization*)

SAL – poziom zapewnienia sterylności (ang. *sterility assurance level*)

SEM – skaningowa mikroskopia elektronowa (ang. *scanning electron microscopy*)

T_c – temperatura zimnej krystalizacji

T_g – temperatura zeszklenia

TGA – termograwimetria

T_m – temperatura topnienia (ang. *temperature of melting*)

T_I – transestryfikacja I rodzaju

T_{II} – transestryfikacja II rodzaju

WHO – Światowa Organizacja Zdrowia (ang. *World Health Organization*)

X_c – udział fazy krystalicznej

3. Streszczenie

Choroby nowotworowe są jedną z najczęstszych przyczyn zgonów na całym świecie. Zgodnie z danymi opublikowanymi przez Światową Organizację Zdrowia (ang. *World Health Organization*, WHO), najczęstszą przyczyną zachorowań na nowotwory w 2020 r. były nowotwory piersi (2,26 miliona nowych przypadków) i płuc (2,21 miliona nowych przypadków). Rak płuc był również najczęstszą przyczyną zgonów (1,8 miliona zgonów) [1].

W przypadku nowotworów piersi, wczesne wykrycie pozwala zastosować terapie mogące prowadzić do pełnego wyleczenia (685 tys. zgonów odnotowanych w 2020 r.) [1]. Tym samym, niezwykle ważne jest poszukiwanie nowych substancji leczniczych i praca nad opracowaniem nowych formulacji znanych już cytostatyków.

Paklitaksel (PTX) jest substancją leczniczą o działaniu cytostatycznym. Jest wykorzystywany m.in. w leczeniu nowotworów piersi, raka jajnika, niedrobnokomórkowego raka płuc i mięsaka Kaposi`ego. Jednakże, ze względu na słabą rozpuszczalność w wodzie, jego zastosowanie jest utrudnione. Rozwiązaniem tego problemu mogą być systemy terapeutyczne o kontrolowanym uwalnianiu substancji leczniczej. Na szczególną uwagę zasługują nanocząstki otrzymywane z biodegradowalnych i biokompatybilnych poliestrów alifatycznych, które po wprowadzeniu do organizmu są rozkładane metabolicznie do prostych związków nietoksycznych. Odpowiednio opracowane nośniki substancji leczniczej charakteryzują się wyjątkową farmakokinetyką, precyzyjnym transportem substancji leczniczej w organizmie oraz zmniejszają prawdopodobieństwo wystąpienia efektów ubocznych. Proces sterylizacji polimerowych nanocząstek może być jednak utrudniony. Poliestry są termicznie niestabilne, co w znacznym stopniu redukuje liczbę potencjalnie dostępnych technik końcowej sterylizacji. Tym samym, niezwykle ważne jest znalezienie efektywnej metody sterylizacji, która nie powodowałaby znaczącej zmiany struktury oraz właściwości fizykochemicznych sterylizowanych materiałów.

Celem niniejszej pracy doktorskiej było zbadanie wpływu promieniowania jonizującego w odniesieniu do możliwości zastosowania fotonów γ i wiązki elektronów (EB) przy użyciu dawki 25 kGy jako potencjalnej metody sterylizacji opracowanych poliestrowych systemów terapeutycznych o kontrolowanym uwalnianiu substancji leczniczej. Otrzymane zostały nowe poliestrowe nośniki substancji leczniczej, zdolne do kontrolowanego uwalniania PTX. Proces syntezy poliestrów prowadzony był metodą polimeryzacji z otwarciem pierścienia (ang. *ring opening polymerization*, ROP) L-laktydu (L-LA), ε-kaprolaktonu (CL) oraz glikolidu (GA) w obecności 2-etyloheksanianu bizmutu ($BiOct_3$) jako katalizatora. Otrzymane polimery nie wykazywały cyto- i genotoksyczności, co jest warunkiem krytycznym w zastosowaniach biomedycznych. Niniejsza praca badawcza zawiera kompleksowe badania wpływu promieniowania jonizującego na strukturę i właściwości fizykochemiczne opracowanych poliestrowych nośników PTX, a w szczególności, wpływu na kinetykę uwalniania z nich substancji leczniczej. Zmiany te zostały omówione w odniesieniu do procesów radiacyjnych zachodzących w polimerach poddanych działaniu promieniowania jonizującego (degradacja i sieciowanie).

4. Abstract

Cancer is one of the leading cause of death worldwide. According to the World Health Organization (WHO), the most common cancer types in 2020 were breast and lung cancer, responsible for 2.26 million and 2.21 million of new cases respectively. Additionally, lung cancer was the most common cause of cancer deaths, accounting for 1.8 million deaths in 2020.

However, some of the common cancer types, such as breast cancer (685 000 deaths in 2020), have high cure probabilities when detected early [1]. Therefore it is very important to study on the development of new active substances and new formulations of the drug substances already known.

Paclitaxel (PTX) is an active substance widely used in anticancer therapy, in the treatment of breast, ovarian, non-small cell lung cancers, and Kaposi's sarkoma. However, its low aqueous solubility is challenging in relation to the method of administration. In recent years, in order to develop safe and effective system of PTX administration, the encapsulation of PTX in nanoparticulate drug delivery systems (DDSs) is extensively studied. The most desirable are drug carriers obtained from biodegradable and biocompatible polyesters. The advantage of polyesters is their biodegradability and biocompatibility. These polymers, introduced to the organism, are metabolically decomposed into completely removable and non-toxic products. Nevertheless, polymer drug carriers administered parenterally, are required to withstand harsh conditions of the sterilization process. Considering biodegradable polyester drug carriers, the assurance of sterility is particularly demanding. Polyesters are thermally unstable, therefore, the number of potentially available sterilization methods is limited. This is therefore of great interest to establish an effective, alternative method of the sterilization process, that does not affect physicochemical properties and the structure of the sterilized material.

The main purpose of the study was to investigate the influence of ionizing radiation, by both, γ-rays and fast electrons (sterilization dose, 25 kGy), in relation to possible sterilization of new, self-developed anticancer DDSs. The properly developed drug carriers are able to reduce the side effects of cytostatics and enhance their tumor deposition with highly controlled pharmacokinetics, and thus, improved therapeutic efficacy. In this regard, the first goal of the study was to develop novel polyester drug carriers, capable of controlled release of PTX. The research involved the synthesis of aliphatic polyesters via ring-opening polymerization of L-lactide (L-LA), *ε*-caprolactone (CL) and glycolide (GA) in the presence of bismuth catalyst (bismuth 2-ethylheksanoate, $BiOct_3$).The use of the bismuth catalyst system allowed to obtain the polymers not cyto– nor genotoxic, that is critical in terms of medical applications.

The research is a complex study on the influence of ionizing radiation on the physicochemical properties and the structure of developed polyester carriers of PTX, as well as the kinetic of PTX release from the nanoparticles obtained. The structural and physicochemical changes in the examined polymers were evaluated in relation to potential processes (chain scission and cross-linking), participating during the irradiation of the polymers, as well as their effects on the kinetic of PTX release.

5. Wykaz publikacji wchodzących w skład cyklu stanowiącego rozprawę doktorską

Podstawą o ubieganie się o nadanie stopnia doktora nauk medycznych i nauk o zdrowiu w dyscyplinie nauki farmaceutyczne jest cykl czterech prac opublikowanych w latach 2020-2023.

Łączny wskaźnik Impact Factor: 18,175

Łączna punktacja MEiN: 410

P1 (praca przeglądowa)

Domańska, I., Oledzka, E., Sobczak, M.*

Sterilization process of polyester based anticancer-drug delivery systems.

International Journal of Pharmaceutics **2020**, 587, 119663

IF_{2020}: 5,875

MEiN: 100

P2 (praca oryginalna)

Domańska, I.M., Zgadzaj, A., Kowalczyk, S., Zalewska, A., Oledzka, E., Cieśla, K., Plichta, A., Sobczak, M.*

A Comprehensive Investigation of the Structural, Thermal, and Biological Properties of Fully Randomized Biomedical Polyesters Synthesized with a Nontoxic Bismuth(III) Catalyst.

Molecules **2022**, 27, 1139

IF_{2022}: 4,600

MEiN: 140

P3 (praca oryginalna)

Domańska, I.M., Zalewska, A., Cieśla, K., Plichta, A., Głuszewski, W., Łyczko, M., Kowalczyk, S., Oledzka, E., Sobczak, M.*

The influence of electron beam and gamma irradiation on paclitaxel-loaded nanoparticles of fully randomized copolymers in relation to potential sterilization.

Journal of Drug Delivery Science and Technology 2023, 90, 105115.

IF_{2023}: 5,000

MEiN: 70

P4 (praca oryginalna)

Domańska, I.M., Figat, R., Zalewska, A., Cieśla, K., Kowalczyk, S., Kędra, K., Sobczak, M., The influence of ionizing radiation on paclitaxel-loaded nanoparticles based on PLGA. *Applied Sciences* 2023, 13, 11052.

IF_{2023}: 2,700

MEiN: 100

6. Wprowadzenie

6.1. Paklitaksel

PTX jest wysoce efektywną substancją leczniczą o działaniu cytostatycznym, a tym samym jedną z najczęściej stosowanych substancji czynnych w chemioterapii [2]. PTX jest związkiem należącym do grupy taksanów, pozyskiwanym pierwotnie z kory cisu zachodniego, *Taxus brevifolia* [3]. Aktywność biologiczna PTX uwarunkowana jest obecnością łańcucha bocznego przy węglu 13 oraz czteroczłonowego pierścienia oksetanowego w pozycji C4-C5 (Schemat 1) [4]. PTX jest związkiem antymikrotubulinowym, ograniczającym proliferację komórek nowotworowych. Jest czynnikiem promującym powstawanie mikrotubul poprzez wiązanie się łańcuchem bocznym przy węglu 13 z białkami uczestniczącymi w ich tworzeniu i stabilizacji [4]. Zahamowanie rozpadu mikrotubul z kolei uniemożliwia ich reorganizację. W efekcie, nieprawidłowe funkcjonowanie tych struktur skutecznie zaburza przebieg mitozy komórek oraz transport wewnątrzkomórkowy, co z kolei kończy się obumarciem komórek w wyniku apoptozy oraz ograniczeniem rozwoju nowotworu [4,5].

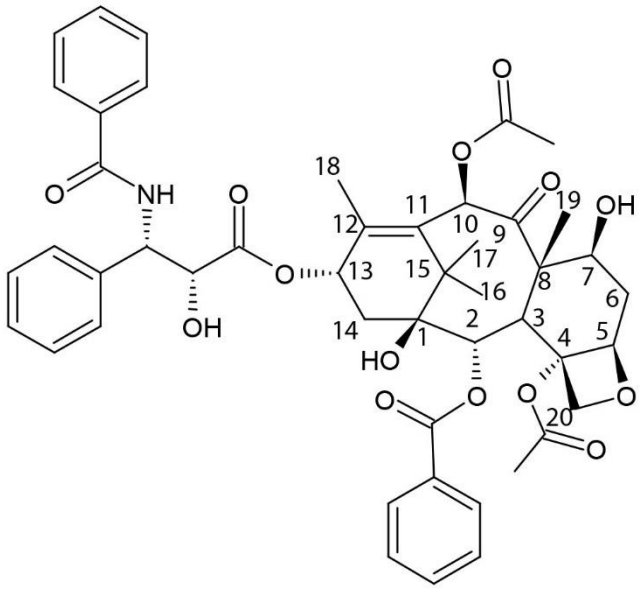

Schemat 1. Paklitaksel ($C_{47}H_{51}NO_{14}$) [6].

Szerokie spektrum działania PTX obejmuje zastosowanie m.in. w terapii raka jajnika, piersi, niedrobnokomórkowego raka płuc oraz mięsaka Kaposi'ego i białaczki [5,7,8]. PTX może być stosowany samodzielnie (np. Taxol, Abraxane) lub w leczeniu skojarzonym (np. z gemcytabiną w terapii przerzutowego gruczolakoraka trzustki oraz z karboplatyną w leczeniu niedrobnokomórkowego raka płuc) [9]. PTX nie jest jednak dobrze tolerowany a jego zastosowanie wiąże się z poważnymi niepożądanymi działaniami, takimi jak np. reakcje nadwrażliwości, toksyczność hematologiczna, neuropatia obwodowa, zaburzenia rytmu serca oraz mielosupresja [3,10]. Ze względu na mechanizm działania, niepożądane interakcje PTX dotyczą szczególnie szybko dzielących się komórek. PTX hamuje m.in. czynność krwiotwórczą szpiku kostnego oraz powoduje stany zapalne błony śluzowej przewodu pokarmowego. Ponadto PTX charakteryzuje się słabą rozpuszczalnością w wodzie i brakiem odpowiedniej

biodystrybucji [8], co ogranicza jego zastosowanie w formie tradycyjnej. Jest to przyczyną, dla której prowadzone są badania nad nowymi postaciami leków zawierającymi tę substancję czynną. Do chwili obecnej, Europejska Agencja Leków dopuściła do obrotu podawane we wlewie dożylnym produkty lecznicze pod nazwami Abraxane oraz Pazenir, a zawierające kompleksy albuminy z PTX w postaci nanocząstek. Podanie leku w tej formie ułatwia jego rozpuszczenie we krwi.

Obecnie, nowym obiecującym kierunkiem są badania nad polimerowymi systemami terapeutycznymi o kontrolowanym uwalnianiu PTX. Prowadzi się je w celu zmniejszenia skutków ubocznych terapii przeciwnowotworowej poprzez dostarczenie substancji leczniczej w sposób ciągły, dzięki czemu wydłużają okres jej działania. Umożliwiają też specyficzne dostarczenie substancji aktywnej do określonego miejsca w organizmie, a w przypadku substancji leczniczych takich jak PTX, rozwiązują dodatkowo problem ich słabej rozpuszczalności.

6.2. Poliestrowe nośniki substancji leczniczych

6.2.1. Systemy terapeutyczne o kontrolowanym uwalnianiu substancji leczniczych

Kontrolowane dostarczanie substancji leczniczych za pomocą systemów terapeutycznych (DDSs, ang. *drug delivery systems*) jest obecnie obiecującą strategią w leczeniu nowotworów. Zamknięcie cząsteczek PTX w mikro- lub nanocząstkach polimerowych ma za zadanie wydłużenie czasu ich utrzymywania w organizmie, ponieważ są one dostarczane w sposób ciągły (Rysunek 1). Ponadto, odpowiednio opracowany układ zapewnia uwalnianie substancji aktywnej nie tylko z kontrolowaną szybkością, ale dodatkowo, w określonym miejscu organizmu, co w rezultacie umożliwia zmniejszenie stosowanej dawki. Obydwa te czynniki umożliwiają ograniczenie niepożądanych działań leku, zapewniając przy tym maksymalną efektywność farmakologiczną substancji czynnej. W tym celu, najbardziej pożądane jest zastosowanie biokompatybilnych i biodegradowalnych nośników substancji leczniczych. Należą do nich matryce otrzymane z poliestrów alifatycznych, które w wyniku procesów metabolicznych ulegają degradacji do prostych, nietoksycznych związków, które są łatwo usuwane z organizmu.

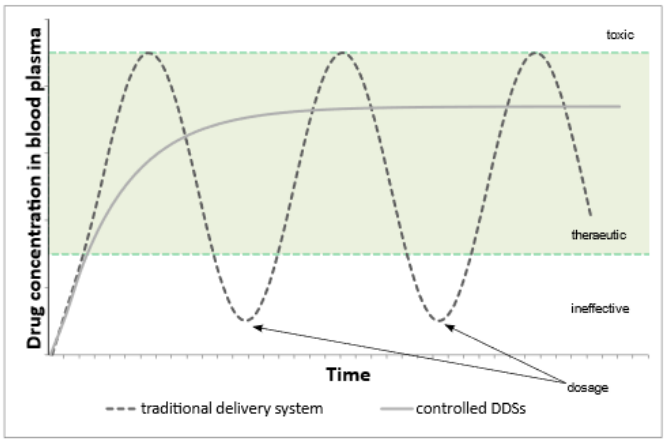

Rysunek 1. Porównanie profili uwalniania substancji czynnej z tradycyjnego nośnika (linia przerywana) oraz z DDS (linia ciągła).

6.2.2. Poliestry do zastosowań biomedycznych

Rozwój farmacji związany jest z ciągłym poszukiwaniem rozwiązań w zakresie opracowywania nowych substancji leczniczych. Działania takie wymagają długiego czasu i spotykają się z ograniczeniami związanymi z wprowadzeniem nowego leku na rynek. Drugim istotnym kierunkiem jest opracowanie najbardziej efektywnych i najmniej obciążających organizm metod dostarczania mu substancji leczniczych już znanych [11]. Warunki takie spełniają systemy terapeutyczne o kontrolowanym uwalnianiu substancji aktywnych, w których znakomicie sprawdzają się biokompatybilne i biodegradowalne poliestry alifatyczne, a w szczególności homo-, ko- i terpolimery glikolidu, laktydu i ε-kaprolaktonu [12]. Poliestry te są nietoksyczne i nie akumulują się w organizmie. W organizmie ulegają rozkładowi do produktów będących jego metabolitami, a następnie z niego usuwanych w postaci substancji nietoksycznych, takich jak CO_2 i H_2O [13]. Ze względu na swoje właściwości, polimery te znalazły szerokie zastosowanie w wielu obszarach medycyny. Są one stosowane m.in. jako bioresorbowalne nici chirurgiczne, implanty chirurgiczne, opatrunki oraz nośniki substancji czynnych.

Zaletą stosowania powyższych poliestrów jest łatwość, z jaką można sterować ich strukturą. Prowadzenie procesu syntezy w sposób kontrolowany prowadzi do otrzymania polimerów o założonej budowie chemicznej i właściwościach, co z kolei przekłada się na możliwość „zaprogramowania" czasu ich rozkładu oraz szybkości uwalniania substancji czynnej. Polimery do zastosowań biomedycznych powinny odznaczać się wysoką czystością [12]. Jest to niezwykle ważne, ponieważ nawet niewielkie pozostałości katalizatora użytego na etapie ich syntezy mogą działać toksycznie na organizm. Dodatkowo, otrzymane polimery powinny charakteryzować się niskim współczynnikiem dyspersyjności masy molowej ($Đ$), wpływającym na właściwości fizykochemiczne.

Poliestry alifatyczne mogą być otrzymywane różnymi metodami, jednak najważniejsze z nich, to: (1) polimeryzacja z otwarciem pierścienia (ROP, ang. *ring opening polymerization*) oraz (2) polikondensacja (Schemat 2) [13,14]. Mechanizm polikondensacji oparty jest na procesie estryfikacji hydroksykwasów. Główną zaletą polikondensacji jest dostępność prekursorów polimerów alifatycznych, tj. odpowiednich hydroksykwasów. Ograniczeniami metody są jednak m.in. trudności z otrzymaniem polimerów o założonej liczbowej średniej masie molowej (M_n) oraz związane z tym względnie wysokie indeksy dyspersyjności mas molowych otrzymywanych polimerów ($Đ$). Ograniczenia te nie mają miejsca w przypadku procesu ROP. Proces ROP laktonów pozwala zsyntetyzować polimery o wysokich M_n, i niskich wartościach $Đ$ [15]. Proces polimeryzacji laktonów jest jednak niezwykle skomplikowany. Na jego przebieg może wpływać wiele czynników, takich jak: rodzaj monomerów, katalizatora i inicjatora uczestniczącego w procesie syntezy oraz warunki, w jakich jest prowadzony (temperatura, czas, obecność wody i tlenu, itp.). Dodatkowo, procesowi polimeryzacji mogą towarzyszyć procesy uboczne, takie jak transestryfikacja oraz makrocyklizacja.

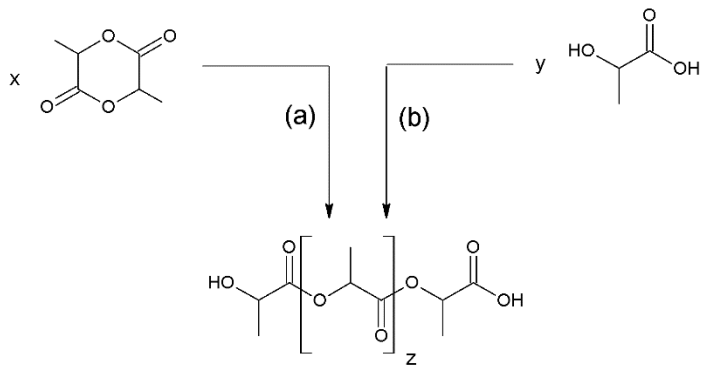

Schemat 2. Schemat otrzymywania (a) PLA w procesie ROP laktydu oraz (b) poli(kwasu mlekowego) w procesie polimeryzacji stopniowej.

Dzięki zastosowaniu metody ROP można różnymi sposobami sterować mikrostrukturą łańcuchów poliestrów, na przykład stosując odpowiednią kombinację monomerów oraz dobór systemu katalitycznego i warunków reakcji. Parametry te wpływają jednak na udział reakcji transestryfikacji. Procesy te mogą być reakcjami wewnątrzcząsteczkowymi (cyklizacja łańcucha) lub międzycząsteczkowymi. Wyróżniamy dwa rodzaje reakcji transestryfikacji. W transestryfikacji I rodzaju (T_I), jednostkami strukturalnymi łańcucha polimeru są jednostki monomeryczne, takie jak jednostki laktydylowe (–LL–), glikolidylowe (–GG–). Natomiast w przypadku transestryfikacji II rodzaju (T_{II}) następuje otwarcie jednostek laktydylowych i glikolidylowych, prowadzące do formowania się charakterystycznych jednostek laktylowych (–L–) i glikolilowych (–G–). Obecność obu tych procesów prowadzi do tworzenia nowych sekwencji jednostek, a w efekcie randomizacji łańcucha polimeru. Określenie udziału transestryfikacji I lub II rodzaju oraz mikrostruktury łańcucha polimeru (średnia długość bloków, współczynnik randomizacji) jest możliwe dzięki wykorzystaniu spektroskopii magnetycznego rezonansu jądrowego (NMR, ang. *nuclear magnetic resonance*).

Jednym z pierwszych otrzymanych biodegradowalnych polimerów był poliglikolid (PGA). Już na początku lat 70-tych XX wieku zyskał szerokie zastosowanie w medycynie, m.in. w produkcji resorbowalnych nici DEXON®. Jednak nie znalazł on większego zastosowania w inżynierii tkankowej ze względu na niepożądane stany zapalne, które prawdopodobnie były wynikiem obecności kwasu glikolowego, będącego produktem degradacji PGA, oraz na pogarszające się właściwości mechaniczne materiału. W przypadku polilaktydu (PLA), obecność dodatkowych grup metylowych w strukturze polimeru sprawia, że jest on bardziej hydrofobowy, a tym samym stabilniejszy hydrolitycznie od PGA [16]. Jednak to kopolimery LA i GA zostały najszerzej zbadane oraz znalazły liczne zastosowania w systemach terapeutycznych o kontrolowanym uwalnianiu substancji leczniczych [17]. Możliwość kontroli syntezy oraz struktury uzyskiwanych polimerów na drodze modyfikacji udziału monomerów sprawia, że otrzymane poliestry charakteryzują się wyjątkowymi parametrami dostosowanymi do wartości oczekiwanych dla potencjalnego zastosowania. Obecnie prowadzone są intensywne badania nad nowymi poliestrami alifatycznymi i optymalizacją procesu ich syntezy. Szczególny nacisk kładziony jest na „zieloną chemię” oraz na zastąpienie powszechnie

stosowanych, jednak kontrowersyjnych z punktu widzenia toksyczności, katalizatorów metaloorganicznych innymi układami katalitycznymi.

6.3. Sterylizacja produktów leczniczych

Farmakopea Europejska określa standardy jakości dotyczące leków. Precyzuje m.in. metody badań oraz wymagania jakościowe produktów leczniczych wprowadzanych na rynek europejski [18]. Jednym z takich wymagań jest zapewnienie sterylności. Dotyczy to w szczególności produktów podawanych pozajelitowo. Celem procesu sterylizacji jest otrzymanie produktu wolnego od mikroorganizmów na poziomie SAL (ang. *sterility assurance level*). SAL jest parametrem, który w sposób ilościowy określa prawdopodobieństwo obecności mikroorganizmu w produkcie poddanym procesowi sterylizacji, a jego wartość graniczną przyjęto na poziomie 10^{-6} mikroorganizmów w 1 g (lub 1 ml) produktu [18].

Wymagania sterylności produktu mogą być osiągnięte na dwa sposoby: wytwarzanie w warunkach aseptycznych lub poddanie go sterylizacji końcowej. Ze względu na wrażliwość właściwości fizykochemicznych na działania podejmowane w ramach procedur sterylizacyjnych, wytworzenie produktu w warunkach aseptycznych jest często jedyną metodą zapewnienia jego sterylności. Jest to jednak metoda niekorzystna ze względu na relatywnie wysokie ryzyko jego późniejszego zanieczyszczenia. Dodatkowo, praca w warunkach aseptycznych wymaga przestrzegania wysokich norm jakościowych, co z kolei implikuje wysokie nakłady finansowe [19,20]. Sterylizacja końcowa jest metodą łatwiejszą z punktu widzenia technologicznego, jednak dobranie odpowiedniej metody jest często utrudnione ze względu na ewentualną degradację sterylizowanego produktu, inne zmiany strukturalne lub powstanie toksycznych produktów ubocznych [21].

Enkapsulacja substancji leczniczej w polimerowej otoczce poprawia jej biodystrybucję oraz chroni przed wpływem czynników zewnętrznych. Poliestrowe nośniki substancji leczniczych są jednak termicznie niestabilne, co ogranicza liczbę potencjalnych technik sterylizacyjnych. Niewłaściwie dobrany proces sterylizacji może zatem przyczynić się do zmian strukturalnych polimerowych nośników substancji leczniczych, co z kolei wpływa na kinetykę ich degradacji oraz profil uwalniania substancji leczniczej. Konieczne jest zatem przeprowadzenie walidacji oraz oceny wpływu procesu sterylizacji niezależnie dla każdego, poszczególnego systemu terapeutycznego.

6.3.1. Techniki sterylizacji

Wśród najczęściej stosowanych technik sterylizacji wyróżnia się: sterylizację przy użyciu środków chemicznych, promieniowania jonizującego, promieniowania UV, a także sterylizację termiczną oraz filtrację w warunkach aseptycznych.

Wyróżnia się dwa rodzaje sterylizacji termicznej – sterylizację gorącym powietrzem (160 °C - 180 °C) oraz parą wodną w podwyższonej temperaturze (min. 121 °C) [18]. Jak jednak wiadomo, poliestry alifatyczne są wrażliwe na podwyższoną temperaturę i wilgoć, co czyni te metody bezużytecznymi w odniesieniu do ich potencjalnej sterylizacji. Wysokie temperatury używane w procesie sterylizacji mogą przekraczać charakterystyczne temperatury przemian termicznych polimerów, a tym samym powodować ich deformację i wpływać niekorzystnie

na właściwości fizykochemiczne, mechaniczne i strukturalne [22,23]. Podobnie, ze względu na mechanizm procesu opierający się na działaniu wolnych rodników, sterylizacja plazmą może powodować sieciowanie lub degradację polimerów. Sterylizacja przy użyciu UV (260 nm [24], UV-C) jest z kolei ograniczona głównie do sterylizacji wody oraz powierzchni materiałów. Sterylizacja przy użyciu środków chemicznych wymaga zastosowania lotnych związków organicznych, takich jak tlenek etylenu (EtO) oraz formaldehyd. Jednak pomimo możliwości prowadzenia procesu w niskich temperaturach, metoda ta jest niekorzystna ze względu na szkodliwe substancje, które mogą pozostać na powierzchni lub wewnątrz matrycy polimerowej. Dodatkowo, EtO należy do grupy związków alkilujących i może oddziaływać z grupami funkcyjnymi polimerów, powodując zmiany ich właściwości fizykochemicznych [25]. W przypadku filtracji w warunkach aseptycznych stosowane są membrany nieoddziałujące z substancją poddawaną sterylizacji, przez co metoda ta nie wpływa na ich właściwości fizykochemiczne oraz może być stosowana dla substancji termowrażliwych. Ograniczeniem tej metody jest jednak wielkość porów membrany. Zgodnie z wytycznymi Farmakopei Europejskiej, w procesie sterylizacji należy używać membran o maksymalnej średnicy porów 0,22 μm [18].

W związku z powyższym, większego znaczenia nabiera zastosowanie do sterylizacji mikro- i nanocząstek polimerowych promieniowania jonizującego (promieniowania γ lub wiązki elektronów) przy użyciu dawki sterylizacyjnej wynoszącej 25 kGy [18,26]. Jest to metoda odpowiednia w szczególności dla termowrażliwych nośników substancji czynnych, w przypadku których rozmiary porów membrany wykluczają zastosowanie metody filtracyjnej. Należy mieć jednak na uwadze, że promieniowanie jonizujące może powodować zmiany strukturalne, w tym sieciowanie lub degradację polimerów, co wpłynie na ich właściwości fizykochemiczne i kinetykę uwalniania substancji leczniczej. Wymagane są zatem szczegółowe badania pod kątem wpływu promieniowania jonizującego w odniesieniu do ewentualnych zmian strukturalnych nośnika oraz samej substancji aktywnej.

6.3.2. Promieniowanie jonizujące

Pierwsza nagroda Nobla w dziedzinie fizyki przypadła w 1901 r. Wilhelmowi Conradowi Roentgenowi, za odkrycie w 1895 r. nieobserwowanego dotychczas rodzaju promieniowania, nazwanego przez samego odkrywcę promieniami X. Efektem badań Roentgena nad przenikliwością promieni X (wydostających się ze szklanej lampy z odpompowanym powietrzem i wtopionymi elektrodami) względem różnych materiałów, było pierwsze zdjęcie rentgenowskie dłoni ludzkiej, należącej do jego żony Berty, zatytułowane „dłoń z pierścionkiem”. Promienie Roentgena są do dziś niezastąpione m.in. w medycynie do oceny urazów kości.

Odkrycie Roentgena było jedynie wierzchołkiem góry lodowej, zapoczątkowującym serię kolejnych odkryć w dziedzinie fizyki. Wśród nich znalazło się odkrycie elektronu przez Thompsona oraz odkrycie naturalnej promieniotwórczości, które przypisuje się Henry`emu Becquerelowi (uran jako źródło promieniowania) oraz Marii i Piotrowi Curie (nowe pierwiastki, tj. rad i polon). Kolejne badania doprowadziły do hipotezy, że promieniowanie nie jest jednorodne i występują trzy rodzaje promieniowania: α, β i γ, różniące się

przenikliwością zależną m.in. od ośrodka materii. Był to impuls do rozwoju badań radiacyjnych.

Biorąc pod uwagę obecny stan wiedzy, promieniowanie jonizujące dzieli się ze względu na swoją naturę na dwa główne rodzaje: promieniowanie korpuskularne i elektromagnetyczne. promieniowanie korpuskularne występuje w postaci cząstek naładowanych, obejmujących promieniowanie elektronowe, ciężkie cząstki naładowane (protony, deuterony, jony helu, jony atomów ciężkich), promieniowanie α i cząstek nienaładowanych (neutrony). Prmieniowanie elektromagnetyczne obejmuje promieniowanie γ i promieniowanie X. W wyniku oddziaływania promieniowania jonizującego z materią mogą zachodzić zmiany biologiczne, jak też rozmaite przekształcenia fizyczne i chemiczne. Część z tych zmian może być korzystna i wykorzystania w praktyce na przykład w celach sterylizacji (np. w medycynie) lub modyfikacji materiałów, w tym polimerów. Warto jednak zaznaczyć, że korzystnemu działaniu sterylizującemu mogą towarzyszyć niekorzystne zmiany struktury napromieniowanych materiałów. W efekcie oddziaływania z materią, promieniowanie powoduje jonizację ośrodka przez który przechodzi. Istotną wielkością, pozwalającą na ocenę interakcji promieniowania z materią jest dawka pochłonięta, określająca ilość energii przekazanej przez promieniowanie jednostce masy materiału (mierzona w grejach, Gy).

Obecnie na skalę przemysłową w procesie sterylizacji radiacyjnej wykorzystuje się głównie wiązki elektronów przyspieszane w akceleratorach (EB) i promieniowanie gamma (γ) oraz, w ograniczonym jeszcze zakresie, promieniowanie Roentgena. Warto zaznaczyć, że w przypadku zastosowania promieniowania gamma, zderzenie fotonu z atomem powoduje wybicie elektronu z powłoki walencyjnej po czym wzbudzona cząsteczka emituje wtórny foton (o mniejszej energii w porównaniu do fotonu pierwotnego) i powraca do stanu podstawowego. Tak więc w przypadku napromieniowania zarówno elektronami jak i fotonami gamma, bezpośrednią przyczyną procesów chemicznych w materiałach są oddziaływania z elektronami. Natomiast wybite elektrony są zdolne do wywołania dalszych procesów jonizacji i wzbudzenia (jonizacja wtórna). Dodatkowym efektem pochłaniania energii przez napromieniowany ośrodek jest wzrost jego temperatury (efekt termiczny). Promieniowanie stopniowo wytraca energię na swojej drodze w materiale, powodując tworzenie w „śladzie" reaktywnych form chemicznych, co z kolei inicjuje dalsze reakcje chemiczne. Jakkolwiek prawdopodobieństwo oddziaływania promieniowania z atomami i cząsteczkami zależy od gęstości elektronowej materiału, odporność na promieniowanie i przebieg procesów chemicznych zależą od jego struktury cząsteczkowej. Również w przypadku poliestrów wrażliwość na promieniowanie może być zróżnicowana w zależności od ich struktury. Należy pamiętać przy tym, że wykorzystywane w procesie sterylizacji promieniowanie jonizujące (γ i EB) nie powoduje wzbudzenia w napromieniowanych materiałach promieniotwórczości, ponieważ może być ona wywoływana dopiero przez promieniowanie o energii powyżej 12,5 MeV [27].

Jak wspomniano, proces sterylizacji z wykorzystaniem promieniowania jonizującego (zarówno elektromagnetycznego, jak i szybkich elektronów), można przeprowadzić w dowolnych temperaturach, zwykle w temperaturze otoczenia ale również w warunkach kriogenicznych. Zastosowanie tzw. „zimnego procesu wyjaławiania" jest niezwykle ważne w odniesieniu do poliestrów wrażliwych na wysokie temperatury. Promieniowanie γ i EB znacznie się jednak różnią pierwotnymi zjawiskami jonizacji, a w konsekwencji mocą dawki i zasięgiem. Warto

podkreślić, że w obu przypadkach praktycznie cała energia przekazywana jest przez elektrony wtórne. W porównaniu do szybkich elektronów, promieniowanie γ charakteryzuje się wysoką zdolnością przenikania. Dla przykładu, elektrony o energii E = 10 MeV (akcelerator Elektronika 10/10, ICHTJ, Polska) posiadają maksymalny zasięg w wodzie równy ok. 5,2 cm, a zatem dużo mniej niż w porównaniu do promieniowania γ (źródło ^{60}Co, dwa rodzaje kwantów o energiach 1,17, 1,33 MeV), którego zasięg połówkowy (wartość połowicznego osłabienia promieniowania w jednostkach zasięgu) wynosi w wodzie $d_{1/2}$ = 11,1 cm [28]. Niestety, w przypadku promieniowania γ, konieczne jest wykorzystanie radioizotopów, społecznie postrzeganych jako bardziej niebezpieczne. Najczęściej stosuje się źródło ^{60}Co z okresem półtrwania $T_{1/2}$ = 5,27 lat oraz, alternatywnie ^{137}Cs o $T_{1/2}$ = 30,08 lat (rzadziej stosowane ze względu na wysoką reaktywność i rozpuszczalność jego związków). Oba te źródła są beta-promieniotwórcze. Promieniowanie gamma emitują produkty ich rozpadu, tj. jądra wzbudzone ^{60}Ni* i ^{137}Ba* (Schemat 3). Szybkie elektrony charakteryzują się z kolei wysoką mocą dawki (np. 14 MGy h^{-1} dla mocy akceleratora 10 kW), co jednak wiąże się z ryzykiem ogrzania napromieniowanego materiału o kilkanaście stopni. Proces sterylizacji w wiązce elektronów z użyciem dawki 25 kGy jest jednak znacznie krótszy (około 10 s w przypadku akceleratora o mocy 10 kW) w porównaniu do wykorzystanego w obecnych badaniach źródła ^{60}Co o mocy dawki 1,8 kGy h^{-1}, wymagającego długiego czasu ekspozycji (ok. 14 h).

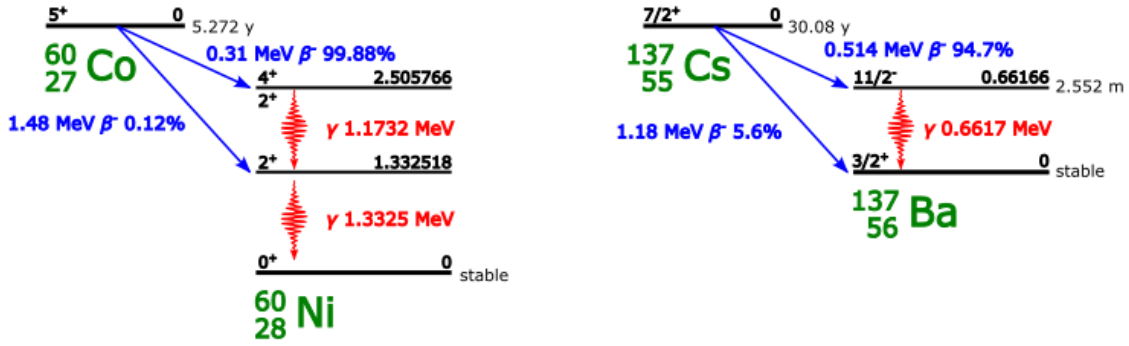

Schemat 3. Schemat rozpadu jądra kobaltu-60 (a) oraz cezu-137 (b) [29].

Celem procesu sterylizacji jest zniszczenie wszystkich form mikroorganizmów. W procesie sterylizacji, Farmakopea Europejska [18] rekomenduje zastosowanie dawki 25 kGy, niezależnie od rodzaju promieniowania (γ, EB). Promieniowanie jonizujące powoduje poważne uszkodzenia radiacyjne oddziałując bezpośrednio na elementy budowy komórki (nici DNA), lub pośrednio, powodując radiolizę wody i wytworzenie wolnych rodników (·OH, $O_2^{\cdot}$), mogących następnie prowadzić do zerwania wiązań między dwiema helisami DNA (publikacja P1, Figure 1) lub rozerwania łańcuchów białek [26,28,30]. W przypadku promieniowania o niskiej gęstości jonizacji (tj. promieniowanie γ i EB) większy udział w mechanizmie oddziaływania ma efekt pośredni [31,32].

6.3.3. Sterylizacja radiacyjna poliestrowych nośników substancji leczniczych

Techniki radiacyjne są szczególnymi metodami wykorzystywanymi w procesie sterylizacji produktów. Pozwalają w krótkim czasie wysterylizować materiał w całej jego objętości oraz, w odróżnieniu do metod chemicznych, nie pozostawiają szkodliwych zanieczyszczeń. Dodatkowo, proces sterylizacji może być prowadzony w atmosferze gazu ochronnego oraz w obniżonej temperaturze, co jest niezwykle istotne w przypadku termowrażliwych poliestrowych nośników leków. Poza warunkami, w jakich prowadzona jest sterylizacja, efekty radiacyjne zależą również od struktury polimeru. W trakcie napromieniowania, materiały te na skutek pochłonięcia energii promieniowania jonizującego, ulegają charakterystycznym procesom. Z łańcuchów polimerów odrywane są atomy wodoru, co prowadzi do powstawania aktywnych centr wolnorodnikowych [33]. Wolne rodniki mogą z kolei ulegać kolejnym reakcjom, a tym samym prowadzić do modyfikacji struktury cząsteczkowej polimeru na skutek dwóch konkurencyjnych procesów; sieciowania i degradacji. Procesom tym zazwyczaj towarzyszy uwalnianie produktów gazowych. Wskazane jest zatem wykonanie szczegółowych badań dot. wpływu promieniowania jonizującego na opracowane postaci leków, ponieważ nieprzewidziany profil degradacji polimeru może wpłynąć negatywnie na efektywność i bezpieczeństwo zastosowanej terapii.

Podatność polimerów na degradację pod wpływem promieniowania jonizującego zależy od wielu czynników, takich jak skład polimeru i długość jego łańcuchów oraz mikrostruktura, jak też zaabsorbowana dawka promieniowania [22,34,35,36]. Degradacja i sieciowanie są procesami konkurencyjnymi. Dotychczasowe dane uzyskane dla PLA wskazują jednak, że przy zastosowaniu stosunkowo niskich dawek promieniowania (<25 kGy) mechanizm degradacji ma większy udział w zachodzących procesach w porównaniu do sieciowania [35]. Natomiast po zastosowaniu dawki 45 kGy, względny udział obu procesów zmienia się na rzecz mechanizmu sieciującego [36]. W napromieniowanych materiale zwiększa się gęstość wolnych rodników, które łatwiej mogą się spotkać i rekombinować (tworząc np. rozgałęzione struktury o zwiększonej masie cząsteczkowej). Najważniejszym czynnikiem wpływającym na wrażliwość polimerów na promieniowanie jonizujące jest ich struktura. Można uważać, że wrażliwość poliestrów na rozerwanie jest spowodowana przez wysoką podatność grup estrowych oraz III-rzędowych atomów węgla [22,34]. Z kolei pierścienie aromatyczne mają zdolność pochłaniania energii, chroniąc tym samym przed szkodliwym działaniem promieniowania jonizującego (efekt ochronny) [37]. Ponadto, na podstawie wyników badań uzyskanych dla PLGA, wyciągnięto wniosek, że obecność krótszych łańcuchów polimerów sprzyja procesom rekombinacji powstających rodników i zapobiega ich dalszej propagacji [38].

6.4. Podsumowanie przeglądu literatury

Promieniowanie jonizujące wykazuje duży potencjał jako metoda sterylizacji poliestrowych nośników substancji leczniczych, wrażliwych na działanie podwyższonych temperatur. Proces sterylizacji radiacyjnej charakteryzuje się wysoką skutecznością niszczenia mikroorganizmów bez konieczności wprowadzenia dodatkowych substancji do produktu poddanego sterylizacji, a realizowany jest w opakowaniu finalnym, co pozwala uniknąć wtórnego zanieczyszczenia. Promieniowanie jonizujące może jednak inicjować tworzenie reaktywnych form w polimerach,

prowadząc do zmian strukturalnych oraz właściwości fizykochemicznych tych materiałów. Na przykład krótsze łańcuchy polimerowe powstające w wyniku rozrywania pod wpływem promieniowania jonizującego pierwotnego łańcucha polimeru (co pokazuje zmniejszenie jego M_n), mogą ulegać w organizmie pacjenta szybszej degradacji w porównaniu do nienapromieniowanego materiału. W przypadku znacznej części polimerów, użycie dawki sterylizacyjnej powoduje jednak niewielkie zmiany radiacyjne. Ponadto istnieje szereg strategii ograniczających niepożądane skutki napromieniowania polimerów, takie jak: napromieniowanie w niskiej temperaturze oraz zastosowanie atmosfery ochronnej (beztlenowej), co ogranicza propagację wolnych rodników, a także modyfikacja struktury polimeru (krystaliczność, obecność segmentów aromatycznych charakteryzujących się większą odpornością radiacyjną od segmentów alifatycznych) oraz napromieniowanie w krótkim czasie, z użyciem dużej dawki promieniowania, co blokuje dyfuzję tlenu do wnętrza materiału i powoduje efekt podobny do napromieniowania w atmosferze gazu ochronnego.

W literaturze istnieje wiele prac opisujących wpływ promieniowania jonizującego na właściwości strukturalne i fizykochemiczne poliestrów, jednak jedynie nieliczne prace dotyczą badań wpływu promieniowania γ i/lub EB na mikro-/nanocząstki zawierające PTX. W związku z powyższym, celem niniejszej pracy doktorskiej były kompleksowe badania nad otrzymywaniem nowych systemów terapeutycznych o kontrolowanym uwalnianiu substancji leczniczej do których wprowadzano PTX oraz kompleksowa analiza wpływu promieniowania jonizującego na opracowane DDSs.

7. Założenia i cel pracy

Głównym celem badawczym pracy doktorskiej było określenie wpływu promieniowania jonizującego w odniesieniu do możliwości sterylizacji nowych systemów terapeutycznych o kontrolowanym uwalnianiu PTX. Szczegółowe cele pracy były następujące:

I. Opracowanie oraz optymalizacja metody syntezy biodegradowalnych matryc poliestrowych o założonej strukturze i właściwościach fizykochemicznych w obecności nowego, biozgodnego systemu katalitycznego ($BiOct_3$–PEG200).
II. Otrzymanie systemów terapeutycznych zawierających substancję przeciwnowotworową (PTX).
III. Napromieniowanie otrzymanych DDSs oraz zbadanie wpływu promieniowania jonizującego (promieniowanie γ, EB) na otrzymane nanocząstki poliestrowe zawierające PTX, ze szczególnym uwzględnieniem wpływu promieniowania jonizującego na: mikrostrukturę i właściwości fizykochemiczne matryc polimerowych, morfologię i właściwości fizykochemiczne otrzymanych nanocząstek, kinetykę uwalniania z DDSs substancji leczniczej oraz stabilność substancji leczniczej po napromieniowaniu.

8. Etapy realizacji pracy doktorskiej

I. Studium literaturowe dotyczące aktualnego stanu wiedzy na temat wpływu promieniowania jonizującego na poliestrowe systemy terapeutyczne o kontrolowanym uwalnianiu substancji leczniczych o działaniu przeciwnowotworowym [P1].
II. Optymalizacja procesu syntezy biodegradowalnych matryc polimerowych [P2].
III. Ocena cyto- i genotoksyczności opracowanych matryc polimerowych [P2, P4].
IV. Analiza wpływu promieniowania jonizującego na opracowane matryce polimerowe [P3, P4].
V. Otrzymanie nośników leku przeciwnowotworowego – nanocząstek polimerowych zawierających PTX [P3, P4].
VI. Analiza wpływu promieniowania jonizującego na otrzymane nanocząstki polimerowe zawierające PTX, analiza kinetyki uwalniania substancji leczniczej z nośników polimerowych w warunkach in vitro [P3, P4].

9. Wyniki własne i dyskusja

Niniejszy cykl oparto na czterech publikacjach: 1 przeglądowej i 3 pracach oryginalnych. Prace te są efektem badań zrealizowanych w Katedrze i Zakładzie Chemii Farmaceutycznej i Biomateriałów Warszawskiego Uniwersytetu Medycznego, we współpracy z Instytutem Chemii i Techniki Jądrowej w Warszawie, dotyczących wpływu promieniowania jonizującego na poliestrowe systemy terapeutyczne o kontrolowanym uwalnianiu PTX. W publikacjach przedstawiono wyniki badań związanych z syntezą, charakterystyką biologiczną, fizykochemiczną i strukturalną matryc polimerowych oraz nanocząstek zawierających PTX. Materiały te zostały otrzymane z wykorzystaniem biodegradowalnych poliestrów alifatycznych. Matryce polimerowe (Tabela 1) zsyntetyzowano na drodze polimeryzacji z otwarciem pierścienia L-LA, CL i GA w obecności biozgodnego 2-etyloheksanianu bizmutu(III) jako katalizatora. Ocena wpływu promieniowania jonizującego z zastosowaniem dawki sterylizacyjnej (25 kGy) oraz dwóch rodzajów promieniowania jonizującego (promieniowanie γ i EB) została przeprowadzona w odniesieniu do matryc polimerowych oraz formulacji finalnych zawierających substancję leczniczą (PTX). W tym celu wykorzystane zostały techniki, takie jak: spektroskopia magnetycznego rezonansu jądrowego (ang. *nuclear magnetic resonance*, NMR), chromatografia żelowa (ang. *gel permeation chromatography*, GPC), spektrometryczna metoda laserowej jonizacji/desorpcji próbki wspomagana matrycą z analizatorem czasu przelotu (ang. *matrix-assisted laser desorption/ionization with time-of-flight analyzer mass apectrometry* MALDI-TOF MS), analiza termiczna z wykorzystaniem termograwimetrii (ang. *thermogravimetric analysis*, TGA) oraz różnicowej kalorymetrii skaningowej (ang. *differential scanning calorimetry*, DSC). Dodatkowo, przeprowadzono badania cyto- i genotoksyczności matryc polimerowych za pomocą testu *umu* oraz testu pochłaniania czerwieni obojętnej (ang. *neutral red uptake*, NRU). Analiza morfologiczna cząstek została przeprowadzona przy użyciu skaningowej mikroskopii elektronowej (ang. *scanning electron microscopy*, SEM), natomiast ich wielkość została określona za pomocą

techniki dynamicznego rozpraszania światła (ang. *dynamic light scattering*, DLS). Analiza efektywności enkapsulacji (*EE*) PTX w nośnikach leku oraz ilości uwolnionej substancji w czasie przeprowadzono techniką wysokosprawnej chromatografii cieczowej (ang. *high-performance liquid chromatography*, HPLC).

Tabela 1. Polimery zsyntetyzowane i poddane badaniom w ramach pracy doktorskiej.

Symbol	Nazwa, skład	Publikacja
PCL	poli(ε-kaprolakton)	P2, P3
PLA	poli(L-laktyd)	P2, P3
PLACL	kopolimer L-laktydu i ε-kaprolaktonu (L-LA : CL = 0,5 : 0,5)	P2, P3
PCLGA	kopolimer ε-kaprolaktonu i glikolidu (CL : GA = 0,85 : 0,15)	P2, P3
PLGA	kopolimer L-laktydu i glikolidu (L-LA : CL = 0,85 : 0,15)	P4

W pracy P1 przedstawiono przegląd literatury dotyczący powszechnie stosowanych technik sterylizacyjnych oraz wpływu procesu sterylizacji radiacyjnej na właściwości fizykochemiczne i strukturę polimerów mających zastosowanie w systemach dostarczania substancji czynnych, tj. homo- ko- i terpolimerów LA, CL, GA i węglanu trimetylenu, oraz wybranych substancji leczniczych o działaniu przeciwnowotworowym, takich jak doksorubicyna (DOX), kamptotecyna (CPT), paklitaksel (PTX), cyklofosfamid (CPA) i 5-fluorouracyl (5-FU). Metody radiacyjne są powszechnie stosowanymi technikami końcowej sterylizacji wyrobów medycznych. Proces sterylizacji radiacyjnej może być wykonywany z wykorzystaniem promieniowania γ lub szybkich elektronów (EB). Zgodnie z zaleceniami Farmakopei Europejskiej, w celu uzyskania poziomu zapewnienia sterylności SAL 10^{-6} mikroorganizmów ml^{-1} (lub $gram^{-1}$), standardowo stosuje się dawkę 25 kGy. Pomimo dużego potencjału tej metody, należy jednak mieć na uwadze różną wrażliwość polimerów na działanie promieniowania jonizującego. Warto też pamiętać, że przekształcenia chemiczne zachodzą w polimerach nie tylko w trakcie napromieniowania, ale również w ciągu pewnego czasu po napromieniowaniu, zazwyczaj kilku dni (procesy post-radiacyjne, efekt post-radiacyjny). W polimerach poddanych działaniu promieniowania jonizującego, procesy rozrywania łańcucha (degradacji radiacyjnej) konkurują z procesami sieciowania, co w zależności od udziału obu typów procesów, może znacząco wpłynąć na strukturę polimeru, a tym samym jego właściwości fizykochemiczne. Warto zaznaczyć, że dane literaturowe wskazują na stabilność PTX, poddanego działaniu promieniowania γ z użyciem dawki 25 kGy. Świadczy o tym fakt, że po napromieniowaniu nie wykryto obecności produktów jego degradacji. Stabilność PTX została potwierdzona również po upływie 2 miesięcy od napromieniowania.

Analiza danych literaturowych wykazała, że korzystniej jest prowadzić proces sterylizacji z wykorzystaniem EB w porównaniu do komór gamma. Efekt ten może jednak w znacznym stopniu wynikać z krótszego czasu napromieniowania z użyciem EB, niezbędnego do

uzyskania równoważnej dawki promieniowania. Wykazany został wpływ struktury polimerów na przebieg i ukierunkowanie procesów radiacyjnych i mogących im towarzyszyć zmian fizykochemicznych i strukturalnych, oraz warunków procesu (temperatura, obecność gazu obojętnego). Wyniki badań wskazują, że po napromieniowaniu polimerów przy użyciu dawki sterylizacyjnej, 25 kGy, udział mechanizmu rozrywania łańcuchów (ang. *chain scission*) przeważa nad sieciowaniem (ang. *cross-linking*). Istotne znaczenie dla ukierunkowania procesów radiacyjnych ma jednak struktura materiału poddanego sterylizacji. Wykazano, że wiązania estrowe oraz trzeciorzędowe atomy węgla są najbardziej podatne na działanie promieniowania jonizującego. Natomiast odporność polimeru na działanie promieniowania jonizującego rośnie wraz ze zmniejszeniem jego masy molowej. Ponadto obecność pierścieni aromatycznych w strukturze polimeru lub w odpowiednio bliskim kontakcie z matrycą polimerową wywiera efekt ochronny w stosunku do polimerów wystawionych na działanie promieniowania jonizującego, co jest tłumaczone możliwością przenoszenia przez te pierścienie ładunku.

Jest wiele prac dotyczących wpływu promieniowania jonizującego na matryce polimerowe oraz systemy dostarczania leków przeciwnowotworowych. Są to m.in. prace opublikowane przez Tapia-Guerrero i in. [39], Maksimenko i in. [40], Song i in. [41]. Jednak do chwili obecnej pojawiły się zaledwie nieliczne prace opisujące wpływ promieniowania jonizującego na polimerowe systemy terapeutyczne w postaci mikro-/nanocząstek o kontrolowanym uwalnianiu PTX. Ponadto opublikowane wyniki uzyskano w przypadku dostępnych komercyjnie matryc polimerowych [41,42]. W związku z powyższym, uznano za celowe podjęcie badań w tej tematyce.

W publikacji P2 przedstawiono wyniki badań dotyczące optymalizacji procesu syntezy matryc polimerowych w obecności biozgodnego, rzadko dotychczas wykorzystywanego katalizatora $BiOct_3$. Optymalizację przeprowadzono poprzez modyfikację warunków syntezy (temperatura, czas) oraz ilość użytego katalizatora, oceniając wydajność procesu polimeryzacji oraz stopień konwersji monomerów. Otrzymane matryce poddano analizie strukturalnej, fizykochemicznej, jak również aktywności biologicznej. W kolejnym etapie badań wytypowano matryce, które zostały wykorzystane do dalszych badań.

Materiały poliestrowe otrzymano na drodze polimeryzacji z otwarciem pierścienia L-LA, CL i GA przy różnych stosunkach molowych monomerów (Tabela 1). W wyniku optymalizacji procesu syntezy, otrzymano 5 matryc polimerowych: PCL, PLA, PLACL, PCLGA i PLGA. Synteza matryc polimerowych prowadzona była w obecności katalizatora $BiOct_3$ oraz glikolu polioksyetylenowego (PEG200), pełniącego funkcję koinicjatora procesu polimeryzacji (publikacja P2, P4). Wybór katalizatora $BiOct_3$ podyktowany był jego opisaną w literaturze efektywnością katalityczną [43]. Dodatkowo, Bi(III) charakteryzuje się najniższą toksycznością wśród metali ciężkich [44,45], co czyni go korzystniejszym inicjatorem procesu z punktu widzenia „zielonej chemii", w porównaniu do tradycyjnie stosowanych katalizatorów metaloorganicznych, takich jak 2-etyloheksanian cyny(II). Uzyskane materiały poliestrowe poddano analizie fizykochemicznej, strukturalnej i termicznej.

W publikacji P2 przedstawiono wyniki badań, dotyczące efektywność procesu polimeryzacji CL, L-LA i GA w obecności katalizatora $BiOct_3$. W tym celu, na podstawie widm ^{1}H NMR mieszaniny poreakcyjnej, przeanalizowano stopień konwersji monomerów, natomiast M_n i $Đ$ zostały określone przy użyciu techniki GPC, z zastosowaniem polistyrenu jako wzorca. Dla każdego materiału wytypowano najlepsze warunki syntezy. Homopolimer L-LA, zsyntetyzowany w temperaturze 110 °C oraz w czasie 24 h, charakteryzował się M_n = 12 300 g mol^{-1} oraz $Đ$ = 1,29. W przypadku pozostałych matryc polimerowych, temperatura reakcji została podwyższona do 130 °C. Uzyskane matryce PCL, PLACL i PCLGA charakteryzowały się średnimi masami molowymi odpowiednio: 10 800 g mol^{-1}, 12 600 g mol^{-1} i 11 800 g mol^{-1} oraz współczynnikiem dyspersyjności: $Đ_{PCL}$ = 1,59; $Đ_{PLACL}$ = 1,55 oraz $Đ_{PCLGA}$ = 1,75. Zastosowane warunki reakcji umożliwiły uzyskanie niemal całkowitej konwersji monomerów (≥ 98%) z wydajnością procesu w zakresie 70 % – 90 %.

Struktura łańcuchów polimerowych jest pewnego rodzaju „odciskiem palca" polimeru. Można ją jednak modyfikować poprzez zastosowanie różnych warunków reakcji lub zmianę rodzaju katalizatora. Dodatkowo, w trakcie syntezy może zachodzić proces transestryfikacji I lub II rodzaju, w wyniku którego następuje redystrybucja jednostek w łańcuchu polimeru, a w efekcie, powstają polimery o strukturze losowej. Do badania mikrostruktury obu kopolimerów użyto spektroskopii ^{1}H NMR (w przypadku PCLGA) i ^{13}C NMR (w przypadku PLACL). Charakterystyczne sygnały widoczne na widmach zostały przypisane do odpowiednich sekwencji jednostek łańcuchów obu polimerów (publikacja P2, Table 5, Table 6), zgodnie z danymi dostępnymi w literaturze [46–49]. Analiza mikrostrukturalna została przeprowadzona w odniesieniu do średnich długości bloków w łańcuchu (l), współczynnika randomizacji (R) oraz udziału transestryfikacji II rodzaju (T_{II}) w procesie polimeryzacji. Oba kopolimery charakteryzowały się strukturą losową (R_{PLACL} = 1,07 i R_{PCLGA}=1,33) oraz krótkimi sekwencjami bloków w łańcuchu: l_{LL} = 1,60 i l_{Cap} = 1,41 (PLACL) oraz l_{GG} = 0,53 i l_{Cap} = 2,82 (PCLGA), będących efektem znacznego udziału procesu transestryfikacji II rodzaju, towarzyszącego procesowi syntezy obu polimerów (publikacja P2). Określenie struktury polimerów jest niezwykle ważne, ponieważ wynikają z niej właściwości makroskopowe materiałów, jak np. właściwości termiczne. Badane polimery charakteryzowały się pojedynczą temperaturą zeszklenia, co potwierdza ich jednorodność. Dodatkowo, analiza termiczna polimerów z wykorzystaniem techniki DSC pozwoliła oszacować zawartość fazy krystalicznej w polimerach (PCL, PLA oraz PCLGA). W przypadku PLACL, krótkie bloki laktydylowe (LL) i ε-kaproilowe (Cap) o dużej losowości ułożenia w łańcuchu wpłynęły negatywnie na proces krystalizacji, tworząc polimer amorficzny (o czym świadczył brak efektu cieplnego topnienia na termogramie DSC).

W przypadku polimerów dla zastosowań biomedycznych, niezwykle ważne jest, aby nie były one toksyczne. Poliestry alifatyczne należą do grupy polimerów biodegradowalnych, które ulegają procesom rozkładu do nietoksycznych produktów, łatwo usuwanych z organizmu [50]. Jednak w procesie ich syntezy używane były rozpuszczalniki organiczne oraz katalizator metaloorganiczny, które mogą negatywnie wpływać na właściwości biologiczne otrzymywanych matryc. W związku z powyższym, zsyntetyzowane materiały zostały poddane badaniom toksyczności, które wykluczyły ich cyto- i genotoksyczność (publikacja P2).

Opisane w publikacji P2 matryce PCL, PLA, PLACL i PCLGA stanowiły przedmiot dalszych badań. W kolejnym etapie pracy (publikacja P3), matryce te zastosowano do uzyskania systemów terapeutycznych, zdolnych do kontrolowanego uwalniania PTX. Wprowadzenie PTX do nośnika polimerowego miało na celu m.in. ominięcie problemu słabej rozpuszczalności substancji leczniczej oraz zapewnienie kontrolowanego uwalniania tej substancji w organizmie. Nanocząstki zawierające PTX otrzymano metodą pojedynczej emulsji (o/w) z odparowaniem rozpuszczalnika, przy zastosowaniu poli(alkoholu winylowego) (PVA) jako stabilizatora. Otrzymano sferyczne cząstki o średniej wielkości mieszczącej się w zakresie 172,4 nm – 257,9 nm. Wielkość ta wyklucza ich sterylizację z wykorzystaniem filtracji w warunkach aseptycznych, ponieważ stosuje się w tym celu membrany o maksymalnej wielkości porów równej 0,22 μm. W związku z powyższym, zasadne wydaje się poszukiwanie alternatywnych metod końcowej sterylizacji. Obecnie zaproponowano sterylizację z wykorzystaniem promieniowania jonizującego. Zgodnie z zaleceniami Farmakopei Europejskiej [18,51], w badaniach została użyta dawka sterylizacyjna 25 kGy. Dodatkowo, w badaniach wykorzystano dwa rodzaje promieniowania, tj. promieniowanie γ i elektronowe. W takich warunkach zachodzą procesy radiacyjne prowadzące do bezpośredniego rozrywania wiązań w łańcuchu polimeru lub zapoczątkowujące szereg procesów, w których w pierwszym stadium następuje nieodwracalne odrywanie z łańcuchów atomów wodoru. Skutkuje to powstaniem reaktywnych centr wolnorodnikowych, które w dalszym etapie ulegają procesom radiacyjnym, prowadzącym do konkurencyjnych procesów: degradacji na skutek rozrywania wiązań oraz sieciowania. Może to w istotnym stopniu wpływać na strukturę polimeru, a tym samym jego właściwości fizykochemiczne oraz kinetykę degradacji, która z kolei warunkuje kinetykę uwalniania substancji leczniczej.

Wpływ promieniowania jonizującego został przeanalizowany w odniesieniu do opracowanych matryc polimerowych oraz otrzymanych nanocząstek zawierających PTX, co pozwoliło na kompleksową ocenę wpływu procesu sterylizacji radiacyjnej na przygotowane postaci leku. Otrzymane wyniki badań (przedstawione szczegółowo w publikacji P3) wskazują, że zarówno promieniowanie γ, jak i EB nie wpłynęły znacząco na strukturę otrzymanych polimerów. Niezależnie od zastosowanego rodzaju promieniowania nie zaobserwowano pojawienia się nowych sygnałów w widmach ^{1}H i ^{13}C NMR po ich napromieniowaniu. Analiza mikrostrukturalna kopolimerów (PLACL oraz PCLGA) nie wykazała również po napromieniowaniu istotnych zmian średnich długości bloków w łańcuchach polimerów ani znaczących zmian wartości współczynnika randomizacji, czy parametru T_{II}, będącego odzwierciedleniem stosunku stężenia sekwencji [CLC] oraz [CGC] do stężenia tych sekwencji w całkowicie bezładnym łańcuchu. Analiza fizykochemiczna matryc polimerowych przed i po napromieniowaniu wykazała jednak zauważalne zmiany M_n. Zmiany te były jednak różne w zależności od rodzaju zastosowanego promieniowania. Jakkolwiek najwyższe zmniejszenie M_n zaobserwowano w przypadku kopolimerów poddanych promieniowaniu γ ($\Delta M_{nPLACL}^{\gamma}$ = -12,7 %, $\Delta M_{nPCLGA}^{\gamma}$ = -28,2 %), wszystkie próbki napromieniowane przy użyciu fotonów γ wykazały obniżenie średniej masy molowej, któremu towarzyszyło podwyższenie $Đ$ polimerów. Obniżenie M_n prawdopodobnie wynika z rozrywania łańcuchów polimerów. W przypadku próbek poddanych działaniu promieniowania elektronowego, zmiany M_n były mniejsze. Homopolimery po napromieniowaniu wykazały spadek M_n (ΔM_{nPCL}^{EB} = -5,8 %,

ΔM_{nPLA}^{EB} = -6,9 %), podobnie jak w przypadku napromieniowania fotonami γ (jakkolwiek mniejszy). Jednak w przypadku kopolimerów, M_n nieznacznie wzrosła (ΔM_{nPLACL}^{EB} = +5,5 %, ΔM_{nPCLGA}^{EB} = +3,2 %), co wskazuje na zwiększenie udziału konkurencyjnych procesów sieciowania. Mniejsza redukcja M_n po napromieniowaniu za pomocą EB homopolimerów, oraz zwiększenie M_n po napromieniowaniu kopolimerów w porównaniu do napromieniowania fotonami γ wskazuje na zwiększenie udziału w tych warunkach konkukrencyjnych procesów sieciowania, przy czym w przypadku napromieniowania kopolimerów udział procesów sieciowania zaczyna przeważać nad degradacją. Należy jednak mieć na uwadze, że użyte do sterylizacji źródło ^{60}Co miało względnie niską aktywność (w porównaniu do mocy użytego akceleratora), a tym samym wymagało długiego czasu ekspozycji próbek na promieniowanie (ok. 14 h), podczas gdy uzyskanie tej samej dawki promieniowania (25 kGy) z użyciem wiązki elektronów było możliwe w czasie poniżej 1 min. Tym samym, czas ekspozycji próbek na promieniowanie mógł w znaczącym stopniu wpłynąć na procesy radiacyjne zachodzące w napromieniowanych materiałach. W przypadku sterylizacji, zastosowana wiązka elektronów o energii 10 MeV charakteryzowała się dużą mocą dawki, co dodatkowo mogło stworzyć warunki podobne do napromieniowania w próżni (tlen nie zdąży dyfundować do wnętrza materiału, a tym samym zapoczątkować procesów oksydegradacji). Jednocześnie, duża gęstość rodników ułatwiała ich rekombinację, a tym samym sprzyjała procesom sieciowania. W przypadku promieniowania γ z zastosowanego źródła ^{60}Co o względnie niskiej mocy dawki (ok. 1,8 kGy h^{-1}), stała ekspozycja polimeru na promieniowanie prowadziła do ciągłego tworzenia się wolnych rodników w czasie, a ich mała gęstość mogła utrudniać rekombinację.

Analiza termogramów DSC wykazała nieznaczne przesunięcia charakterystycznych temperatur, tj. temperatury zeszklenia (T_g), topnienia (T_m) oraz zimnej krystalizacji (T_c) polimerów po napromieniowaniu. W większości przypadków, zmiany te korelowały ze zmianami M_n próbek po napromieniowaniu i były bardziej widoczne dla próbek poddanych działaniu promieni γ. W przypadku PCLGA, spadek M_n po napromieniowaniu fotonami γ spowodował znaczne obniżenie T_g. Przesunięciu po napromieniowaniu uległy również obydwa efekty endotermiczne (co wynika prawdopodobnie z obecności różnych form krystalicznych i amorficznych w polimerze, uformowanych z łańcuchów o różnej długości i/lub różnej strukturze). Zmiany te wynikały najprawdopodobniej z degradacji PCLGA. Efekt endotermiczny przypisany topnieniu frakcji PCLGA o krótszych łańcuchach, przesunął się w kierunku wyższych temperatur, natomiast najprawdopodobniej na skutek rozrywania wiązań, obniżeniu uległa temperatura topnienia przypisana frakcji PCLGA o dłuższych łańcuchach i początkowo bardziej uporządkowanej strukturze (publikacja P3, Figure 7).

Wprowadzenie PTX do nośnika polimerowego miało na celu stworzenie systemu terapeutycznego o kontrolowanym profilu uwalniania, który eliminuje ograniczenia aplikacyjne, wynikające ze słabej rozpuszczalności tej substancji leczniczej. Analiza SEM nie wykazała widocznych zmian w morfologii badanych próbek po napromieniowaniu (publikacja P3, Figure 11). Badania uwalniania PTX z otrzymanych nanocząstek zostały przeprowadzone w warunkach in vitro z wykorzystaniem metody dializy. Analiza HPLC wykazała, że PTX uwalniał się w sposób kontrolowany, zgodnie z kinetyką I rzędu, niezależnie od rodzaju nośnika (PCL, PLA, PLACL, PCLGA). Dodatkowo, wyniki dopasowania uzyskanych profili do modelu Korsmeyer'a-Peppas'a wskazują na anomalne uwalnianie

substancji leczniczej, w którym biorą udział dwa mechanizmy, tj. dyfuzja cząsteczek substancji czynnej przez polimerową otoczkę oraz erozja matrycy polimerowej. Świadczą o tym wartości obliczonych współczynników wykładniczych, które mieściły się w przedziale $0{,}45 < n < 0{,}89$. Warto zauważyć, że w większości przypadków nie wykazano znaczących zmian profilu uwalniania PTX z nanocząstek po napromieniowaniu. W przypadku nanocząstek PLACL i PCLGA poddanych działaniu promieniowania γ zaobserwowano jednak znaczny wzrost szybkości uwalniania PTX, co może wynikać ze zwiększonego udziału mechanizmu erozyjnego na skutek degradacji polimerowych nośników leku poddanych działaniu promieniowania γ (publikacja P3).

W kolejnym etapie pracy (publikacja P4) kontynuowano badania nad wpływem promieniowania jonizującego na nowo opracowane systemy terapeutyczne o kontrolowanym uwalnianiu PTX w odniesieniu do ich potencjalnej sterylizacji. W pracy przedstawiono rezultaty badań dotyczących syntezy, analizy fizykochemicznej i mikrostrukturalnej kopolimeru L-LA i GA (PLGA) oraz wpływ promieniowania jonizującego (25 kGy, promieniowanie γ i EB) na mikrostrukturę i właściwości fizykochemiczne zsyntetyzowanej matrycy oraz otrzymanych nanocząstek zawierających PTX. Dodatkowo, przeprowadzono analizę kinetyki uwalniania substancji leczniczej w warunkach in vitro oraz wpływu promieniowania jonizującego na profil uwalniania PTX z otrzymanych DDSs.

PLGA został zsyntezowany (tak jak poprzednio) w wyniku reakcji polimeryzacji otwarcia pierścienia L-LA i GA (L-LA : GA = 0,85 : 0,15) w obecności katalizatora $BiOct_3$. Polimeryzację prowadzono w ciągu 5 h w temperaturze 120 °C w atmosferze gazu obojętnego (w celu zachowania odpowiedniej kontroli procesu). Wstępne badania biologiczne nie wykazały cyto- i genotoksyczności próbek polimeru poddanego badaniom, co świadczy o efektywności procesu oczyszczania mieszaniny poreakcyjnej. Otrzymana matryca polimerowa charakteryzowała się $M_n = 13\,800$ g mol^{-1} oraz $Đ = 1{,}833$. Analiza fizykochemiczna PLGA po napromieniowaniu (dawką sterylizacyjną, 25 kGy), wykazała spadek średniej masy molowej polimeru o $\Delta M_n = 14$ % (niezależnie od zastosowanego rodzaju promieniowania, tj. promieniowanie γ oraz EB), któremu towarzyszył nieznaczny wzrost $Đ$. Obniżenie M_n wskazuje na przeważający (nad sieciowaniem) udział procesów rozrywania łańcuchów.

Analiza widm ^{1}H i ^{13}C NMR wykazała obecność charakterystycznych dla PLGA sygnałów, w tym, sygnałów pochodzących od sekwencji -LGL- oraz -GLG-, wskazujących na obecność procesu transestryfikacji II rodzaju, towarzyszącego reakcjom polimeryzacji. Uzyskane widma NMR nie wykazały znaczących różnic w udziale jednostek komonomerycznych przed i po napromieniowaniu. Zmianie uległy jednak średnie długości bloków laktydylowych (l_{LL}). Średnie długości l_{LL} były jednak mniejsze po napromieniowaniu fotonami γ ($l_{LL}^{non\text{-}irr} = 4{,}33$; $l_{LL}^{\gamma} = 3{,}35$), co korespondowało z ubytkiem średniej masy molowej polimeru. W przypadku PLGA poddanego działaniu EB, l_{LL} nieznacznie wzrosły ($l_{LL}^{EB} = 4{,}61$), co sugeruje na zwiększony udział mechanizmu sieciowania, konkurującego z degradacją radiacyjną polimeru.

Analiza termiczna (DSC) PLGA przed i po napromieniowaniu nie wykazała znaczących zmian T_g, T_c i T_m po napromieniowaniu. Wykryto jednak zmniejszenie udziału fazy krystalicznej (X_c) PLGA poddanego działaniu promieni γ (z $X_c^{non\text{-}irr} = 16{,}40$ % do $X_c^{\gamma} = 7{,}29$ %), co mogło wynikać

ze skrócenia średnich długości bloków laktydylowych, po napromieniowaniu (γ), a tym samym wpłynęło na pogorszenie struktury fazy krystalicznej i prawdopodobnie obniżyło jej zawartość w polimerze.

Nanocząstki zawierające PTX zostały, tak jak poprzednio, otrzymane z wykorzystaniem matrycy PLGA metodą pojedynczej emulsji (o/w) z odparowaniem rozpuszczalnika. W ten sposób otrzymano sferyczne cząstki o średniej wielkości 253,5 nm. Analiza DLS nie wykazała znaczących zmian wielkości cząstek po napromieniowaniu. Badania uwalniania substancji leczniczej z otrzymanych nanocząstek zostały przeprowadzone za pomocą techniki HPLC. Wykazano, że nanocząstki uwolniły w ciągu 36 dni ponad 90 % substancji leczniczej, niezależnie od tego, czy były, czy nie były poddane procesowi sterylizacji radiacyjnej. Wykazano, że PTX uwalniał się w sposób kontrolowany, zgodnie z profilem kinetyki I rzędu. Analiza matematyczna wykazała wysokie dopasowanie współczynników korelacji uzyskanych danych do modeli matematycznych opisujących uwalnianie substancji leczniczej z nośnika polimerowego, tj. modelu Higuchi`ego oraz Korsmeyer`s–Peppas`a. Wartość współczynnika wykładniczego n (n = 0,7928) wskazuje na udział mechanizmu dyfuzyjnego oraz erozji matrycy w procesie uwalniania PTX z otrzymanych nanocząstek. Na uwagę zwraca nieznaczny wzrost współczynnika n obliczonego dla profilu uwalniania PTX z nanocząstek poddanych działaniu promieniowania jonizującego (n^{γ} = 0,8570; n^{EB} = 0,8574), co może wynikać ze zwiększenia udziału mechanizmu erozyjnego w procesie uwalniania PTX, prawdopodobnie spowodowanego degradacją radiacyjną matrycy polimerowej. Wyniki te korelują z analizą fizykochemiczną matryc polimerowych, która wykazała spadek po napromieniowaniu M_n matrycy polimerowej.

10. Wnioski końcowe

1) Polimeryzacja z otwarciem pierścienia (ROP) L-LA, CL i GA w obecności katalizatora $BiOct_3$ oraz koinicjatora PEG200 jest efektywną metodą otrzymywania nietoksycznych matryc polimerowych do zastosowań biomedycznych (publikacja P2, P4).
2) Prowadzenie procesu ROP L-laktydu (L-LA), ε-kaprolaktonu (CL) i glikolidu (GA) w obecności katalizatora $BiOct_3$ w temperaturze 110 °C – 130 °C, w warunkach gazu obojętnego pozwala na otrzymanie z wysoką wydajnością (≥ 70 %) polimerów o założonej średniej masie molowej oraz charakteryzujących się niskim współczynnikiem dyspersyjności (≤ 2) (publikacja P2, P4).
3) $BiOct_3$ jest efektywnym katalizatorem w procesie ROP laktonów (L-LA, CL, GA), umożliwiającym uzyskanie wysokiej konwersji monomerów (niemal całkowita konwersja monomerów w przypadku PCL, PLA, PLACL i PCLGA oraz powyżej 94 % konwersji L-LA w przypadku PLGA) (publikacja P2, P4).
4) Analiza mikrostruktury otrzymanych kopolimerów L-LA, CL i GA wykazała, że w obecności katalizatora $BiOct_3$, reaktywność komonomerów wzrastała w kierunku CL < L-LA < GA (publikacja P2, P4).

5) Transestryfikacja II rodzaju, towarzysząca procesowi polimeryzacji, w znacznym stopniu przyczyniła się do otrzymania polimerów, których łańcuchy mają strukturę statystyczną, zbudowanych są z krótkich sekwencji bloków (publikacja P2, P4).
6) Analiza NMR matryc PCLGA i PLACL nie wykazała zmian w mikrostrukturze polimerów po poddaniu ich działaniu promieniowania jonizującego dawką sterylizacyjną 25 kGy (publikacja P3). W przypadku matrycy PLGA, analiza mikrostrukturalna wykazała skrócenie średnich długości bloków laktydylowych po napromieniowaniu próbki fotonami γ oraz nieznaczny wzrost l_{LL} kopolimeru poddanego działaniu EB (publikacja P4).
7) W przypadku wszystkich badanych polimerów poddanych działaniu promieni γ (25 kGy) wykazano zmniejszenie M_n, wskazujące na przeważający udział mechanizmu rozrywania łańcuchów polimerów w warunkach prowadzonego procesu sterylizacji. Zmniejszenie M_n kopolimerów poddanych działaniu promieni γ było większe ($\Delta M_n^{PLACL} = -12{,}7$ %, $\Delta M_n^{PCLGA} = -28{,}2$ %, $\Delta M_n^{PLGA} = -13{,}8$ %) niż w przypadku homopolimerów ($\Delta M_n^{PCL} = -9{,}2$ %, $\Delta M_n^{PLA} = -7{,}9$ %) (publikacja P3, P4).
8) Otrzymano systemy terapeutyczne o kontrolowanym uwalnianiu paklitakselu (PTX) w postaci nanocząstek poliestrowych (PCL, PLA, PLACL, PCLGA i PLGA). Otrzymane cząstki miały kształt sferyczny o średniej wielkości w zakresie 172,4 nm – 257,9 nm (publikacja P3, P4).
9) Analiza morfologiczna (SEM) oraz analiza średniej wielkości cząstek (DLS) nie wykazały istotnych zmian po napromieniowaniu otrzymanych nanocząstek zawierających PTX (publikacja P3, P4).
10) W zależności od rodzaju matrycy polimerowej (PCL, PLA, PLACL, PCLGA i PLGA), otrzymane systemy terapeutyczne charakteryzowały się różną kinetyką uwalniania PTX w warunkach in vitro. PTX uwalniał się najszybciej z nośników PLACL i PLGA (niemal całkowite uwolnienie PTX po 5 tygodniach inkubacji w roztworze PBS), natomiast najwolniej z nośników PCL (53 % uwolnienia PTX po 56 dniach inkubacji w roztworze PBS) (publikacja P3, P4).
11) Otrzymane nośniki (matryce PCL, PLA, PLACL, PCLGA i PLGA) są w stanie zapewnić długotrwałe, kontrolowane uwalnianie PTX w warunkach in vitro (publikacja P3 i P4).
12) Uzyskane wyniki badań in vitro wskazują, że PTX uwalniał się w sposób kontrolowany, zgodnie z profilem zbliżonym do kinetyki I rzędu. Dopasowanie otrzymanych profili do modelu Korsmeyer'a-Peppas'a ($0{,}45 < n < 0{,}89$) wykazało, że proces uwalniania PTX z nanocząstek odbywał się zgodnie z mechanizmem anomalnym, łączącym proces dyfuzji oraz erozji matrycy na skutek degradacji polimeru, niezależnie od rodzaju nośnika (publikacja P3, P4).
13) Analiza wpływu promieniowania jonizującego na otrzymane DDSs nie wykazała znaczących zmian w profilach uwalniania substancji leczniczej z nanocząstek poddanych działaniu wiązki elektronów (EB, dawka 25 kGy) (publikacja P3, P4). Istotny wzrost szybkości uwalniania PTX zaobserwowano jednak w przypadku nanocząstek PLACL i PCLGA poddanych działaniu promieni γ (dawka 25 kGy). Analiza współczynnika *n* modelu Korsmeyer`a-Peppas`a wykazała wzrost wartości współczynnika *n*, co sugeruje zwiększony udział mechanizmu erozyjnego podczas uwalniania PTX z nośników PLACL

i PCLGA napromieniowanych kwantami γ. Wyniki te korelują z obserwowanym spadkiem M_n matryc PLACL i PCLGA po napromieniowaniu (publikacja P3).

14) Analiza HPLC nie wykazała obecności substancji rozkładu PTX w nanocząstkach poddanych działaniu promieniowania jonizującego, co wskazuje na odporność PTX na działanie promieniowania γ i EB (25 kGy) (publikacja P3, P4).
15) Analiza fizykochemiczna i strukturalna wykazała, że badane poliestrowe nośniki substancji leczniczej były bardziej odporne na promieniowanie jonizujące za pomocą wiązki elektronów. Różnice między właściwościami fizykochemicznymi matryc polimerowych sterylizowanymi kwantami γ i EB były niewielkie (publikacja P3, P4).
16) Opracowane układy mogą stanowić potencjalne systemy terapeutyczne o kontrolowanym uwalnianiu substancji leczniczej.
17) Zastosowanie promieniowania jonizującego stanowi potencjalną metodę sterylizacji poliestrowych nośników substancji leczniczych, wrażliwych na działanie podwyższonej temperatury, przy czym optymalne jest wykorzystanie w tym celu wiązki wysokoenergetycznych elektronów.

11. Spis literatury

[1] WHO. Cancer Fact Sheet. 2022. Dostęp online: https://www.who.int/news-room/fact-sheets/detail/cancer (26 May 2022).

[2] Sobczak, M., Korzeniowska, A., Goś, P., Kolodziejski, W.L., Preparation and characterization of polyester- and poly(ester-carbonate)-paclitaxel conjugates. *Eur. J. Med. Chem.* **2011**, 46, 3047–3051. DOI: 10.1016/j.ejmech.2011.04.046.

[3] Szczepański, M., Grzanka, A., Izdebska, M., Mikrotubule – cel terapii przeciwnowotworowej. *J. Oncol.* **2007**, 57, 579–585, 2007.

[4] Sharifi-Rad J., i in., Paclitaxel: Application in Modern Oncology and Nanomedicine-Based Cancer Therapy. *Oxid. Med. Cell. Longev.* **2021**, 2021, 1–24. DOI: 10.1155/2021/3687700.

[5] Haddad, R., Alrabadi, N., Altaani, B., Li, T., Paclitaxel Drug Delivery Systems: Focus on Nanocrystals' Surface Modifications. *Polymers* **2022**, 14, 658. DOI: 10.3390/polym14040658.

[6] Paclitaxel. Dostęp online https://pubchem.ncbi.nlm.nih.gov/compound/Paclitaxel (12.07.2023).

[7] Surapaneni, M.S., Das, S.K., Das, N.G., Designing Paclitaxel Drug Delivery Systems Aimed at Improved Patient Outcomes: Current Status and Challenges. *ISRN Pharmacol.*2012, **2012**, 1–15. DOI: 10.5402/2012/623139.

[8] Stefanowicz, Z., Sobczak, M., Piętniewicz, A., Kołodziejski, W.L., Macromolecular conjugates of paclitaxel: Synthesis, characterization, and *In Vitro* paclitaxel release studies based on HPLC validated method. *Acta Chromatogr.* **2016**, 28, 99–117. DOI: 10.1556/AChrom.28.2016.1.8.

[9] Abraxane. Dostęp online: https://www.ema.europa.eu/en/documents/product-information/abraxane-epar-product-information_pl.pdf (16.03.2023).

[10] Charakterystyka produktu leczniczego Aneks I Abrexane. Dostęp online: https://www.ema.europa.eu/en/documents/product-information/abraxane-epar-product-information_pl.pdf (12.07.2023)

[11] Andrzejewska, A., Topoliński, T., Polimery Biodegradowalne Do Zastosowań Biomedycznych. *Postępy w Inż. Mech. Dev. Mech. Eng.* **2015**, 6, 5–12.

[12] Jerome, C., Lecomte, P., Recent advances in the synthesis of aliphatic polyesters by ring-opening polymerization. *Adv. Drug Deliv. Rev.* **2008**, 60, 1056–1076. DOI: 10.1016/j.addr.2008.02.008.

[13] Budnicka, M., Gadomska-Gajadhur, A., Ruskowski, P., Synoradzki, L., Biodegradable polymers for the treatment of tuberculosis Part II. Requirements and characteristics of materials. *Polimery* **2018**, 63, 1–9. DOI: 10.14314/polimery.2018.1.1.

[14] Labet, M., Thielemans, W., Synthesis of polycaprolactone: a review. *Chem. Soc. Rev.* **2009**, 38, 3484. DOI: 10/ffcnqp.

[15] Lecomte, P., Jérôme, C., Recent Developments in Ring-Opening Polymerization of Lactones. *Synthetic Biodegradable Polymers*, B. Rieger, A. Künkel, G. W. Coates, R. Reichardt, E. Dinjus, i T. A. Zevaco, Red., w *Advances in Polymer Science* **2011**, 245, 173–217. DOI: 10.1007/12_2011_144.

[16] Ulery, B.D., Nair, L.S., Laurencin, C.T., Biomedical applications of biodegradable polymers. *J. Polym. Sci. Part B Polym. Phys.* **2011**, 49, 832–864. DOI: 10.1002/polb.22259.

[17] Loureiro, J.A., Pereira, M.C., PLGA Based Drug Carrier and Pharmaceutical Applications: The Most Recent Advances. *Pharmaceutics* **2020**, 12, 903. DOI: 10.3390/pharmaceutics12090903.

[18] Council of Europe. Suppl. 9.2. European Directorate for the Quality of Medicines & HealthCare; Council of Europe: London, UK, 2017, 4333–4350.
[19] Çalış, S., Bozdağ, S., Kaş, H.S., Tunçay, M., Hıncal, A.A., Influence of irradiation sterilization on poly(lactide-co-glycolide) microspheres containing anti-inflammatory drugs. *Il Farm.* **2002**, 57, 55–62. DOI: 10/cv8wtq.
[20] Claybourn, M., Gray, H., Murphy, D.M., Purnell, I.J., Rowlands, C.C., Electron magnetic resonance study of gamma-irradiated poly(lactide-co-glycolide) microspheres. *J. Controlled Release* **2003**, 91, 431–438. DOI: 10/bwwv8w.
[21] Cheetham, A.G., Zhang, P., Lin, Y., Lock, L.L., Cui, H., Supramolecular Nanostructures Formed by Anticancer Drug Assembly. *J. Am. Chem. Soc.* **2013**, 135, 2907–2910. DOI: 10/f4njv2.
[22] Plikk, P., Odelius, K., Hakkarainen, M., Albertsson, A.C., Finalizing the properties of porous scaffolds of aliphatic polyesters through radiation sterilization. *Biomaterials* **2006**, 27, 5335–5347. DOI: 10/dwqz5s.
[23] Athanasiou, K., Sterilization, toxicity, biocompatibility and clinical applications of polylactic acid/ polyglycolic acid copolymers. *Biomaterials* **1996**, 17, 93–102. DOI: 10/d95272.
[24] Dai, Z., Ronholm, J., Tian, Y., Sethi, B., Cao, X., Sterilization techniques for biodegradable scaffolds in tissue engineering applications. *J. Tissue Eng.* **2016**, 7, 204173141664881. DOI: 10/gfw84q.
[25] Kryczka, T., *i in.*, Effect of gamma-irradiation on cladribine and cladribine-containing biodegradable copolymers. *J. Controlled Release* **2003**, 89, 447–456. DOI: 10/d3jj9r.
[26] Domańska, I.M., Oledzka, E., Sobczak, M., Sterilization process of polyester based anticancer-drug delivery systems. *Int. J. Pharm.* **2020**, 587, 119663. DOI: 10.1016/j.ijpharm.2020.119663.
[27] Pogocki, D., Oddziaływanie promieniowania jonizującego z materią. IV Szkoła Sterylizacji Radiacyjnej Sprzętu Medycznego, Przeszczepów, Farmaceutyków i Kosmetyków. Instytut Chemii i Techniki Jądrowej, Warszawa, 1997.
[28] Szymański, W., *Chemia jądrowa: zarys problematyki przemian jądrowych*. Warszawa: Wydawnictwo Naukowe PWN, 1996.
[29] Nuclear Decay Data in the MIRD Format. Dostęp online: https://www.nndc.bnl.gov/nudat3/mird/ (05.06.2023).
[30] Panganiban, R.-A., Snow, A., Day, R., Mechanisms of Radiation Toxicity in Transformed and Non-Transformed Cells. *Int. J. Mol. Sci.* **2013**, 14, 15931–15958. DOI: 10/f5czq6.
[31] Internationale Atomenergie-Organisation, Red., *Trends in radiation sterilization of health care products*. Vienna: Internat. Atomic Energy Agency, 2008.
[32] Yokoya, A., Shikazono, N., Fujii, K., Urushibara, A., Akamatsu, K., Watanabe, R., DNA damage induced by the direct effect of radiation. *Radiat. Phys. Chem.* **2008**, 77, 1280–1285. DOI: 10/dtwmw6.
[33] Gluszewski, W., Zagorski, Z.P., Radiation processing as an unique method of modification of properties of polymers (INCT--1-2/A/2002), Poland, 2002.
[34] Gupta, M.C., Deshmukh, V.G., Radiation effects on poly(lactic acid). *Polymer* **1983**, 24, 827–830. DOI: 10/cndvqd.
[35] Hooper, K.A., Cox, J.D., Kohn, J., Comparison of the effect of ethylene oxide and γ-irradiation on selected tyrosine-derived polycarbonates and poly(L-lactic acid). *J. Appl. Polym. Sci.* **1997**, 63, 1499–1510. DOI: 10/cgwm8x.
[36] Mansouri, M., Berrayah, A., Beyens, C., Rosenauer, C., Jama, C., Maschke, U., Effects of electron beam irradiation on thermal and mechanical properties of poly(lactic acid) films. *Polym. Degrad. Stab.* **2016**, 133, 293–302. DOI: 10/f88zhv.

[37] Głuszewski W., Zagórski, Z.P., Radiation effects in polypropylene/polystyrene blends as the model of aromatic protection effects. *NUKLEONIKA* **2008**, 53, S21–S24.
[38] Volland, C., Wolff, M., Kissel, T., The influence of terminal gamma-sterilization on captopril containing poly(d,l-lactide-co-glycolide) microspheres. *J. Controlled Release* **1994**, 31, 293–305. DOI: 10/dmxtsv.
[39] Tapia-Guerrero, Y.S., *i in.*, Effect of UV and Gamma Irradiation Sterilization Processes in the Properties of Different Polymeric Nanoparticles for Biomedical Applications. *Materials* **2020**, 13, 1090. DOI: 10.3390/ma13051090.
[40] Maksimenko, O., *i in.*, Doxorubicin-loaded PLGA nanoparticles for the chemotherapy of glioblastoma: Towards the pharmaceutical development. *Int. J. Pharm.* **2019**, 572, 118733. DOI: 10.1016/j.ijpharm.2019.118733.
[41] Song, T.-T. *i in.*, Preparation of injectable paclitaxel sustained release microspheres by spray drying for inhibition of glioma *in vitro*. *J. Appl. Polym. Sci.* **2010**, 115, 1534–1539. DOI: 10.1002/app.31105.
[42] Wang, J. *i in.*, Release of paclitaxel from polylactide-co-glycolide (PLGA) microparticles and discs under irradiation. *J. Microencapsul.* **2003**, 20, 317–327. DOI: 10.3109/02652040309178072.
[43] Kricheldorf, H.R., Serra, A., Polylactones: 6. Influence of various metal salts on the optical purity of poly(L-lactide). *Polym. Bull.* **1985**, 14, 1985. DOI: 10.1007/BF00271606.
[44] Yang, P.B., Davidson, M.G., Edler, K.J., Brown, S., Synthesis, Properties, and Applications of Bio-Based Cyclic Aliphatic Polyesters. *Biomacromolecules* **2021**, 22, 3649–3667. DOI: 10.1021/acs.biomac.1c00638.
[45] Kricheldorf, H.R., Weidner, S.M., Scheliga, F., Synthesis of cyclic poly(L -lactide) catalyzed by Bismuth Salicylates—A combination of two drugs. *J. Polym. Sci. Part Polym. Chem.* **2019**, 57, 2056–2063. DOI: 10.1002/pola.29473.
[46] Jiang, Z., Deng, X., Hao, J., Thermogelling hydrogels of poly(ε-caprolactone-co-D,L-lactide)–poly(ethylene glycol)–poly(ε-caprolactone-co-D,L-lactide) and poly(ε-caprolactone-co-L-lactide)–poly(ethylene glycol)–poly(ε-caprolactone-co-L-lactide) aqueous solutions. *J. Polym. Sci. Part Polym. Chem.* **2007**, 45, 4091–4099. DOI: 10.1002/pola.22222.
[47] Kasperczyk, J., Copolymerization of glycolide andε-caprolactone, 1. Analysis of the copolymer microstructure by means of1H and13C NMR spectroscopy. *Macromol. Chem. Phys.* **1999**, 200, 903–910. DOI: 10/fg584r.
[48] Kasperczyk, J., Bero, M., Coordination polymerization of lactides, 4. The role of transesterification in the copolymerization of L,L-lactide and ε-caprolactone. *Makromol. Chem.* **1993**, 194, 913–925. DOI: 10.1002/macp.1993.021940315.
[49] Liu, C.B. *i in.*, Thermoreversible gel–sol behavior of biodegradable PCL-PEG-PCL triblock copolymer in aqueous solutions. *J. Biomed. Mater. Res. B Appl. Biomater.* **2008**, 84B, 165–175. DOI: 10.1002/jbm.b.30858.
[50] Olędzka, E., Sobczak, M., Kołodziejski, W.L., Polimery w medycynie — przegląd dotychczasowych osiągnięć. *Polimery* **2007**, 52, 795–803.
[51] EMA. Guideline on the Sterilisation of the Medicinal Product, Active Substance, Excipient and Primary Container. EMA/CHMP/CVMP/QWP/850374/2015, European Medicines Agency, 2019. Dostęp online: https://www.ema.europa.eu/en/documents/scientific-guideline/guideline-sterilisation-medicinal-product-active-substance-excipient-primary-container_en.pdf (18.05.2023).

12. Kopia publikacji stanowiących podstawę postępowania w sprawie o nadanie stopnia naukowego doktora

International Journal of Pharmaceutics 587 (2020) 119663

Contents lists available at ScienceDirect

International Journal of Pharmaceutics

journal homepage: www.elsevier.com/locate/ijpharm

Review

Sterilization process of polyester based anticancer-drug delivery systems

Izabela M. Domańska, Ewa Oledzka, Marcin Sobczak*

Department of Biomaterials Chemistry, Chair of Analytical Chemistry and Biomaterials, Faculty of Pharmacy, Medical University of Warsaw, 1 Banacha St., Warsaw 02-097, Poland

ARTICLE INFO

Keywords:
Anticancer drug delivery systems
Biodegradable polymers
Polyester
Sterilization
Radiation sterilization
Gamma-irradiation
E-beam irradiation

ABSTRACT

Recently, growing interest in biodegradable polyesters as drug carriers in the development of innovative anticancer drug delivery systems (DDSs) has been observed. These compounds are thermally unstable, and are therefore, particularly demanding due to the limited number of available sterilization techniques. Furthermore, the DDSs sterilization process is often limited to aseptic filtration. Ensuring aseptic production is very demanding and costly, and it is therefore necessary to work on the application of new sterilization methods. In view of this, this review presents the current state of knowledge regarding the radiation sterilization process of some anticancer drugs as well biodegradable polyester carriers (such as polylactide, polyglycolide, poly(ε-caprolactone), poly(trimethylene carbonate) and co- or terpolymers of lactide, glycolide, ε-caprolactone and trimethylene carbonate). The structural changes in anticancer DDSs under the influence of ionizing radiation and the potential degradation mechanisms of both, polyester carriers and cytostatics during the sterilization process of ionizing radiation as well as their effects on the microstructure and properties of DDSs have been discussed in this paper.

1. Introduction

Nowadays, nanocarriers with specifically programmed anticancer drug release kinetics have become a big part of scientists' interest in an innovative pharmacy. The most desirable are Drug Delivery Systems (DDSs) composed of biodegradable and biocompatible polyesters with controlled drug release, most of which, copolymers of lactide (LL) and glycolide (GG) are used (Fredenberg et al., 2011). The advantage of nanocarriers is their size, below 100 nm, that could contribute to the accumulation of an active substance in the tumor tissue (so-called passive targeting) (Duan et al., 2010).

Drugs used for medical treatment usually need to comply with pharmacopoeia requirements that could be achieved in two ways: either by processing under aseptic conditions or by terminal sterilization of the product. The processing under aseptic conditions is often the only way to ensure product sterility, however, it is not preferred because of the relatively high risk of microbial contamination. Furthermore, working under aseptic conditions requires to comply with high standards, which entails higher costs as well complicated and intensive labour (Çalış et al., 2002; Claybourn et al., 2003). Therefore, terminal sterilization is the easiest form from the technological and economical point of view (Igartua et al., 2008). Nonetheless, for parenterally administered drugs, the choice and the validation of the sterilization method is a major challenge. Adopting of the suitable sterilization method is one of the crucial elements of placing developed drug on the market. The encapsulation of a hydrophobic drug in hydrophilic vehicles successfully increases pharmacokinetic properties and drug biodistribution profiles, however, the critical issue is possible toxic by-products coming out from polymer as well as drug degradation arising from the chosen sterilization method (Cheetham et al., 2013). Therefore, it should be kept in mind, that the sterilization process must be capable to eliminate undesirable microbes while having no detrimental effect on targeted DDSs. The sterilization process may affect the structure of the polymer carrier, which determines biodegradation and drug release kinetics. It is also important to remember, that the process may have an adverse effect on the active substance itself. That implies the need of detailed reseach on the impact of sterilization process for each molecule individually.

Abbreviations: 5-FU, 5-fluorouracil; CL, ε-caprolactone; CPA, cyclophosphamide; CPT, camptothecin; DAU, daunorubicin; DDSs, drug delivery systems; DOX, doxorubicin; DTX, docetaxel; e-beam, electron beam; EPI, epirubicin; EtO, ethylene oxide; *E*, energy; FDA, Food and Drug Administration; GG, glycolide; ISO, International Organization of Standarization; LET, Linear Energy Transfer; LL, lactide; M_n, number average molecular weight; MTX, methotrexate; M_w, weight average molecular weight; PACL, paclitaxel; PCL, poly(ε-caprolactone); PDLA, poly(D-lactide); PGA, polyglycolide; Ph. Eur., Pharmacopoeia European; PLA, polylactide/poly(lactic acid); PLCL, copolymer of lactide and ε-caprolactone; PLGA, copolymer of lactide and glycolide; PLLA, poly(L-lactide); PTMC, poly(trimethylene carbonate); SAL, Sterity Assurance Level; $T_{1/2}$, half life; T_g, glass transition temperature; T_m, melting point; TMC, trimethylene carbonate

* Corresponding author.
E-mail addresses: idomanska@wum.edu.pl (I.M. Domańska), eoledzka@wum.edu.pl (E. Oledzka), marcin.sobczak@wum.edu.pl (M. Sobczak).

https://doi.org/10.1016/j.ijpharm.2020.119663
Received 7 April 2020; Received in revised form 2 July 2020; Accepted 14 July 2020
Available online 20 July 2020
0378-5173/

To the best of our knowledge, there is no detailed study summarizing the effect of ionizing radiation on anticancer-DDSs. The currently available reviews on the sensitivity of pharmaceuticals to the ionizing radiation concentrate on a wide variety of medications, of which, anticancer drugs are studied in a limited degree. Subsequently, these works were focused primarily on the radiation effect on the polymer matrix and the change in drug release kinetics, although very little attention is given to the active agent itself. Therefore, our article explains the current method of gamma-rays and electron-beam (e-beam) sterilization of the anticancer DDSs. Due to the biocompatibility and biodegradability, our attention is addressed into polylactide (PLA), polyglycolide (PGA), poly(ε-caprolactone) (PCL), poly(trimethylene carbonate) (PTMC) and co- or terpolymers of LL, GG, ε-caprolactone (CL) and trimethylene carbonate (TMC) - polyesters having a prominent role in the technology of DDSs. Furthermore, because of the wide spectrum of anticancer activity, doxorubicin (DOX), camptothecin (CPT) analogs, paclitaxel (PACL), cyclophosphamide (CPA) and 5-fluorouracil (5-FU) are discussed in details.

2. Sterilization techniques

The purpose of the sterilization process is to obtain material free from microorganisms (Ph. Eur. – suppl. 9.2, 2017). Among commonly used sterilization methods are dry heat, filtration under aseptic conditions, ionizing radiation, steam, and the use of chemicals (Igartua et al., 2008). Filtration and radiation are the most widely used methods for thermosensitive materials. Among other methods, heat and steam sterilization require high temperatures, which can cause drug and polymer material degradation. The use of chemicals such as ethylene oxide (EtO) is not beneficial due to its toxic residues (Igartua et al., 2008). Nevertheless, according to Pharmacopoeia European (Ph. Eur.), the most reliable sterilization methods are saturated steam under pressure and hot air (Ph. Eur. – suppl. 9.2, 2017). They should be used whenever possible. In order to ensure no deterioration of product stability and its properties, it is also emphasized to properly validate the procedure used for each type of sterilized product, irrespective of the sterilization technique (Ph. Eur. – suppl. 9.2, 2017). Table 1 summarizing the wiedly used sterilization techniques.

Sterility Assurance Level (SAL) parameter has been proposed for the quantitative assessment of sterility (Ph. Eur. – suppl. 9.2, 2017). SAL is derived mathematically and it defines the probability of a viable microorganism being present on an individual product unit after the sterilization process. SAL is assigned at the level of 10^{-6} microorganisms/ml or g of the product (Maksimenko et al., 2008a; IAEA, 2008; Ph. Eur. (Pharmacopoeia European) – suppl. 9.2, 2017).

2.1. Techniques of ionizing radiation sterilization

Currently, the sterilization of drugs and medical devices with ionizing radiation is an alternative to the heat sterilization method. This so-called “cold process” is a method suitable especially for drugs or drug carriers heat-sensitive. However, since the radiation may alter the chemical and physical properties of nanocarriers and the drugs used, detailed studies of potential degradation by-products need to be performed (Masson et al., 1997).

There are five types of industrially available ionizing radiation sources: γ-rays, X-rays, e-beam, α-particles and neutrons. The last two cannot be industrially used for sterilization purposes because of their specific properties: α-particles are poorly penetrative and neutron sources activate irradiated material (Sakar et al., 2017). The most commonly used are two ionizing radiation sterilization methods: highly-penetrating with low dose rate γ-irradiation from isotopic sources and less penetrating, but with high dose rate e-beam from accelerators (Sakar et al., 2017).

For the sterilization of medical devices and pharmaceutical products, 25 kGy is a recommended dose with no further need of providing any biological validation. In case of lower irradiation doses, Ph. Eur. advises to provide validation of dose bactericidal effect (Ph. Eur. – suppl. 9.2, 2017). Validation of the sterilization process is proposed to be conducted with a bioindicator: *Bacillus pumilus* (e.g. ATCC 27142, NCTC 10327, NCIMB 10692 or CIP 77.25) with the dose exceeding 10^7 spores per indicator (Ph. Eur. – suppl. 9.2, 2017). The latest recommendations of the International Organization for Standardization (ISO) are to set the sterilization dose for each type of the product depending on its bioburden (Igartua et al., 2008; IAEA, 2008).

2.2. Dry-heat sterilization

Dry-heat sterilization is a suitable method for heat-stable and non-aqueous materials. According to Ph. Eur., for effective sterilization, materials should be put in the oven for at least 2 h at minimum temperature 160 °C. It is also recommended to use *Bacillus atropheaus* (e.g. ATCC 9372, NCIMB 8058, NRRL B-4418 or CIP 77.18), minimum 10^6 spores as a bioindicator of a validation process in the sterilization method used (Athanasiou et al., 1996; Ph. Eur. – suppl. 9.2, 2017). As it is well known, aliphatic polyesters are heat- and moist sensitive, what makes sterilization methods conducted at high temperatures useless. There is a possibility of plastic deformation and destruction of chemical or porous structure (Plikk et al., 2006).

2.3. Steam sterilization

Steam sterilization is conducted in saturated steam for 15 min at

Table 1
Techniques of sterilization (Athanasiou et al., 1996; Dai et al., 2016; Harrell et al., 2018; Ph. Eur. – suppl. 9.2, 2017; Plikk et al., 2006; Wang et al., 2017).

Technique	Advantages	Disadvantages
gamma-radiation	no toxic residues, high bactericidal effect, high penetration through sample, temperature and pressure independent, minimal effect on polymer 3D structure of porous polymer scaffold, rapid process, easy to control	low energy content, possible chain scission, polymer degradation and instability, damage of polycrystalline structure, formation of smaller particles or aggregates
e-beam	high energy content, possible use for thermolabile substances, short sterilization time, minimal effect on polymer 3D structure of porous polymer scaffold, no toxic residues	low penetration through the sample, possible chain scission, polymer degradation, damage of polycrystalline structure, formation of smaller particles or aggregates
gas sterilization	low temperature, small extent of the polymer degradation	possible toxic residues, long process, flammable and explosive nature of gas used, process difficult to control
steam sterilization	no toxic residues	hydrolytic degradation, thermal degradation
dry heat sterilization	no toxic residues, fast, simple, good penetration	not applicable for thermal sensitive materials, possible change in physical and mechanical properties, possible material degradation, decomposition, drug aggregation
asceptic filtration	not affecting nanoparticles properties, possible use for thermolabile substances	size limitations
plasma	low temperature, fast, improved cell interaction	possible change in physical and mechanical properties of polymers, the presence of residual reactive species after the sterilization

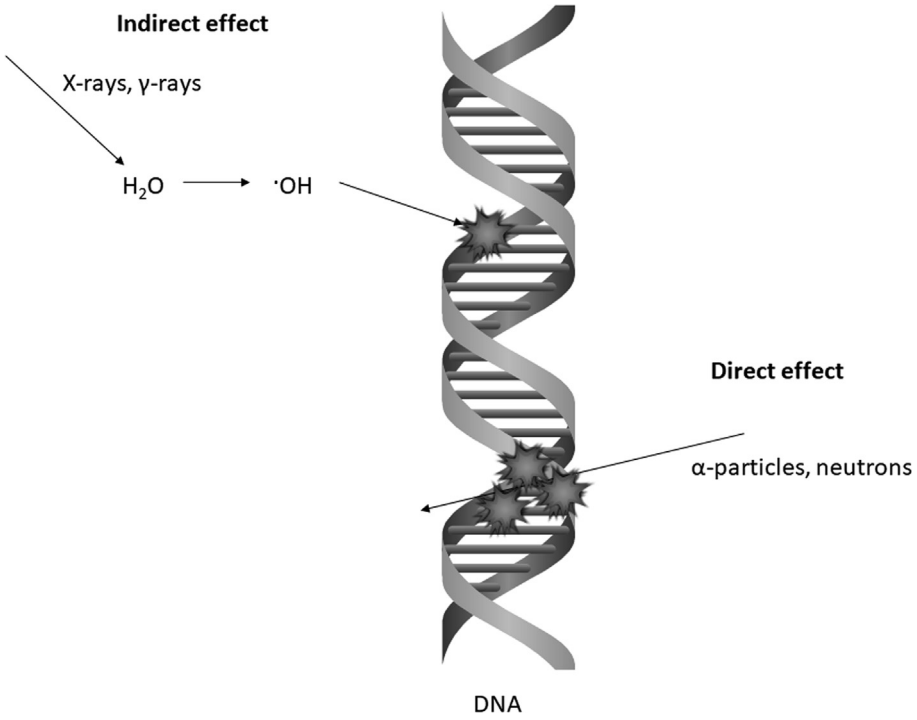

Fig. 1. Mechanisms of microbial cell damage.

121 °C (Ph. Eur. – suppl. 9.2, 2017). Ph. Eur. recommends to use *Geobacillus stearothermophilus* (e.g. ATCC 7953, NCTC 10007, CIP 52.81, NCIMB 8157, ATCC 12980), minimum $5x10^5$ spores as a bioindicator (Ph. Eur. – suppl. 9.2, 2017). High temperatures used in the sterilization process may exceed thermal transition of proceeded given material and, in consequence, alter its physicochemical and mechanical properties, thereby altering degradation kinetics of the polymer (Athanasiou et al., 1996).

2.4. UV sterilization

UV sterilization is used to sterilize the surface of the material and the transparent scaffolds. Its limited application results from the different sensitivity of the microorganism to UV radiation. As is reported, 260 nm is the most lethal wavelength for sterilization purposes. Another critical parameter is UV exposure time, which should be well chosen to ensure effective sterilization without any significant change in material properties (Dai et al., 2016).

According to Rychter et al., who studied sterilization efficiency of porous materials, the disadvantage of using UV sterilization preceded by immersion of the sample in 70% (v/v) ethanol, is its inefficiency. The inability to destroy all types of microorganisms (i.e. hydrophilic viruses and bacterial spores), classifies it as decontamination rather than sterilization (Rychter et al., 2016).

2.5. Gas sterilization

The most commonly used gas for the sterilization process is EtO, however, other highly volatile substances, such as formaldehyde can also be used. This is an alternative method for heat- and moist-sensitive materials. However, due to possible harmful residues remaining on the surface or within the polymer matrix, the sterilization process should be carefully performed (Athanasiou et al., 1996; Plikk et al., 2006). EtO exhibits broad antimicrobial activity by the permanent suppression of cell metabolism and division (Dai et al., 2016). Moreover, EtO is a strong alkylating agent and may alter polymer physicochemical and biological properties by reacting with its functional groups (Kryczka et al., 2003).

When this method is applied, it needs to be remembered about proper degassing and aeration of the sample in order to get rid of all EtO residues (Athanasiou et al., 1996). Because of process difficulty, and many parameters affecting proper sterilization quality, Ph. Eur. recommends to verify method efficiency with the use of bioindicators such as *Bacillus atrophaeus* (e.g. ATCC 9372, CIP 77.18, NCIMB 8058 or NRRL B-4418) or *Bacillus stearothermophilus* with about 10^6 spores per indicator (Ph. Eur. – suppl. 9.2, 2017).

2.6. Filtration technique sterilization

Asceptic filtration is mainly used for thermosensitive solutions, however, attention should be paid on possible adsorption of the solution on the filter and, as a result, to the loss and clogging of the filter. This results from similar filter pore size to nanosuspensions (Sommerfeld et al., 1998). For the sterilization purpose are used sterile bacteria-retaining filters such as membranes, plastics, porous ceramics or suitable sintered glass filters. Membranes of max. 0.22 μm nominal pore size are recommended for use, what will prevent from passing microorganisms through the filter (Ph. Eur. – suppl. 9.2, 2017). *Brevundimonas diminuta* (e.g. ATCC 19146, NCIMB 11091, CIP 103020), min. 10^7 spores/cm^2 is recommended as a bioindicator (Ph. Eur. – suppl. 9.2, 2017).

2.7. Plasma sterilization

Plasma sterilization process is based on the generation of reactive species by subjecting gas to pulsed discharges and therefore electron excitation, dissociation and ionization. In order to inactivate highly resistant microorganisms, reactive gas mixtures with high oxygen content are preferred over inert gases. However, using reactive gas plasmas may cause cross-linking and degradation of the material, thus changing its physical properties (Dai et al., 2016).

3. Ionizing radiation

DDSs must be free from harmful microorganisms. Biological effects caused by ionizing radiation are mainly resulting from DNA damage, which is particularly sensitive to radiation (Hall, 2000).

It is generally recognized that, in the case of living cells, DNA is the main target of radiation due to its essential role in cell replication and proliferation. The mechanism of microbial destruction through ionizing radiation (Fig. 1) identifies two types of cell damage by the radiation effect of biological molecules (Panganiban et al., 2013). For living cells, the most significant is an indirect effect with the interaction of DNA with ·OH radicals formed by radiolysis in the hydration layer around DNA molecule. The indirect effect is assigned to about 60% of DNA lesions caused by X- or γ-rays with low Linear Energy Transfer (LET). This rate decreases with increasing LET value up to 30% for α-particles characterized by high LET. The second type is direct energy deposition in DNA, leading to its immediate damage and is dominant for neutrons or α-particles with high LET (IAEA, 2008; Yokoya et al., 2008).

As was pointed out by Panganiban et al., recent investigations have shown proteins to be another crucial target of ionizing radiation. The indirect effect of radicals formed (e.g. ·OH, O_2^-) may cause changes or breaks in amino acid chains, leading to the loss of protein functions (Panganiban et al., 2013).

3.1. Gamma-irradiation

Gamma irradiation is the second most commonly used sterilization method on the market after EtO (Buchanan, 2008). The main advantage of using photon irradiation is its high penetration power and the isothermal process of sterilization, preferred for heat-sensitive materials (Sakar et al., 2017). Depending on the energy given, density and the composition of the matter, the intensity of radiation passing through the matter decrease with depth (the dose rate decrease), what is referred as a depth-dose distribution (IAEA, 2008). 25 kGy is a traditionally applied dose in the sterilization process, at which, certain undesirable changes, such as chain scission caused by ionization and hence fragmentation of covalent bond may occur, leading to a rapid decrease in molecular weight of polymers (Sakar et al., 2017). It has been noted, that the decrease in molecular weight increases with a dose of γ-radiation. This phenomenon was more noticeable for the number average molecular weight (M_n) compared to weight average molecular weight (M_w). This suggests higher impact of photon radiation on short polymer chains. As a result, compared to non-irradiated copolymer of lactide and glycolide (PLGA), faster degradation of copolymers under *in vivo* conditions was observed (Athanasiou et al., 1996).

In contrary to e-beam, γ-radiation may be used for irradiation of nonuniform and high-density products, due to its strong penetration of matter (Sakar et al., 2017). On the other hand, γ-radiation may reduce the nominal drug content by drug radiolytic degradation and potential formation of toxic by-products. Polymer degradation may also affect drug release kinetic and resorption under *in vivo* conditions, therefore causing a reduction of shelf-life and material instability (Masson et al., 1997).

The most commonly used sources of γ-radiation are ^{60}Co and ^{137}Cs. ^{60}Co with its half-life ($T_{1/2}$) of 5.27 years has relatively high energy (E) of radiation quantum (avg. 1.25 MeV), what makes it the most suitable source for γ-irradiation. The second one, ^{137}Cs ($T_{1/2}$ = 30.1 years, E = 0.661 MeV), is typically used for blood and insect sterilization (IAEA, 2008; Szymański, 1996).

3.2. Electron-beam radiation

E-beam accelerators suitable for sterilization require high energy up to 10 MeV, which provides the highest penetration thickness of 38 mm for unit density (that is almost 8 times lower than for γ-irradiated materials) (IAEA, 2008). Furthermore, sterilization efficiency varies on the material used and thus, the implemented process must be thoroughly investigated before applying to use (Dai et al., 2016).

E-beam irradiation is still a minority of the worldwide sterilization, however, it is gaining an increasing interest in its use. Despite its low penetration rate, e-beam sterilization is instantaneous, with high dose delivery (Sakar et al., 2017).

4. Sterilization of drug delivery systems

4.1. Degradation of polymers as sterilization effect

The influence of irradiation on the degradation of polymers is one of the most important concerns of the scientific interest. Unpredictable degradation may influence the drug release kinetics and thus affect the efficacy and safety of treatment. It is therefore crucial to analyze in depth the possible effects of DDSs sterilization.

It was observed by several authors, that the type of degradation mechanism strictly depends on the irradiation dose, polymer chain length, its microstructure and monomer composition (Gupta and Deshmukh, 1983; Hooper et al., 1997; Mansouri et al., 2016; Plikk et al., 2006). As it was observed, low irradiation doses result in predominating chain scission over cross-linking. This causes the degradation of polymers and accelerates of the drug release kinetics (Hooper et al., 1997). According to Mansouri et al., the irradiation dose 45 kGy (well above typical sterilization dose), is a transition zone from predominating chain scission into cross-linking (Mansouri et al., 2016).

The influence of polymer microstructure and the monomer composition on the polyester degradation mechanisms was examined by Plikk et al. (Plikk et al., 2006). As it was noted, the sensitivity towards radiation depends on polymer‘s side groups, end groups, and the backbone chemistry. And so, ester linkage and the tertiary carbon atom (for branched polyesters) are the most important sites for bond cleavage during radiolysis caused by γ-radiation (Gupta and Deshmukh, 1983; Plikk et al., 2006). That may confirm higher poly(lactide-*co*-ε-caprolactone (PLCL) radiation stability comparing to PLA, which has more tertiary carbon atoms in the structure (Plikk et al., 2006).

Chain length dependency was observed by Volland et al. in relation to primary radicals formed in PLGA (Volland et al., 1994). It was noticed that polymers with shorter chain lengths favor recombination over undergoing further reactions. It was explained by the cage effect, where longer chains characterize lower flexibility and chain mobility, and thus, increase radical lifetime leading to competitive reactions over recombination. It resulted in the formation of more breakdown products (Volland et al., 1994). Detailed research on the impact of ionizing radiation (i.e. γ-radiation and e-beam) on biodegradable polyesters used in anticancer DDSs has been presented in next chapters.

The sterilization process can affect physical properties, e.g. by changing the hydrophobicity/hydrophilicity of a drug carrier (Sommerfeld et al., 1998). Polar oxygen containing groups, such as hydroperoxyl, hydroxyl, carbonyl, and carboxyl groups, resulting from oxidative degradation, ought to increase the hydrophilicity of the sample (Walo et al., 2011). The formation of hydrophilic groups upon radiolytic chain scission (e-beam, doses 10 – 100 kGy) was assigned as a reason of increased hydrophilicity of PLA nanofibers. The comparative study of poly(L-lactide) (PLLA) and PLLA blend with poly(D-lactide) (PDLA) showed a higher increase in hydrophilicity of PLLA nanofibers. It was associated with higher radiation stability of the stereocomplex PLLA/PDLA blend of crystalline structure than the homocrystalline PLLA structure (Zhang et al., 2010). Augustine et al. showed a significant effect of γ-irradiation on the formation of polar surface functional groups, which increased the hydrophilicity of PCL membrane (Augustine et al., 2015). With an increase in the dose of irradiation, the PCL water contact angle decreased. Along with increasing polymer wettability, PCL crystallinity increased, however, at the maximum applied dose (65 kGy), a slight decrease in crystallinity was observed (Augustine et al., 2015). The five-month comparative study of Walo

et al. on γ-irradiated (25 kGy) semicrystalline polyesters, e.i. PLLA and PCL have shown the opposite trend. The contact angle increased over time, which determined the increase in the hydrophobicity of the irradiated samples. The phenomenon has been explained by the migration of hydrophobic segments towards the surface (Walo et al., 2011). Valente et al. related the increase in PLLA random fiber hydrophobicity to surface chemical and roughness changes that occurred during the sterilization process (25 kGy, γ-ray) (Valente et al., 2016). The relationship between contact angle and surface roughness has been studied by Jo et al. As shown, the increase in the dose of irradiation decreased the contact angle of PLGA (85:15) due to increased formation of crystallites, thereby increasing surface roughness. The impact of the chemical changes in the PLGA structure on its hydrophilicity was excluded as there was no indication of the formation of hydrophilic groups upon irradiation (Jo et al., 2012). Another study conducted by Keles et al., showed faster hydration of γ-irradiated PLGA (50:50) microparticles. It was associated with more hydrophilic polymer products after irradiation compared to non-irradiated PLGA (Keles et al., 2015).

4.1.1. Degradation of polylactide/poly(lactic acid)

PLA is a biocompatible and biodegradable polymer (Mansouri et al., 2016) with glass transition temperature (T_g) of 55–63 °C (Burg, 2014). The monomer configuration strictly affects its physicochemical properties, thereby resulting in different radiation sensitivity of each enantiomer. PLA degrades by bulk hydrolysis (Bat et al., 2011). The high thermosensitivity is the key problem in the choice of an effective sterilization method. Although methods with the use of high temperatures are excluded and chemical sterilization by gases may leave some toxic residues, ionizing radiation seems to be the most promising one in order to overcome drawbacks resulting from PLA thermodependency (Plikk et al., 2006).

The effect of e-beam and the radiation-induced degradation mechanisms of PLA was studied by Mansouri et al. As it was reported, PLA degradation under e-beam was caused by random chain scission, resulting in the reduction of M_n and M_w (Mansouri et al., 2016). Radiation-induced chain scission mechanism for PLA and PLGA was previously proposed by Loo et al., where PLA and PLGA hydrolyze into lactic and lactic and glycolic acids, respectively. They are subsequently metabolized in the body and eliminated as CO_2 and water. The chain-scission mechanism was confirmed by lowering M_n, T_g, and by increasing degree of crystallinity with increasing radiation dose (Loo et al., 2004). As it was noted, PLLA was characterized by higher stability against e-beam radiation compared to PLGA. This finding was explained by higher PLA crystallinity (Table 2) (Loo et al., 2004). It should be noted, however, that they used doses ranging from 50 kGy to 500 kGy (Loo et al., 2004), significantly higher than 25 kGy - a standard dose that ensures complete sterilization. These findings are consistent with Song et al. outcomes of γ-irradiation of PACL-loaded PLA microspheres. As it was stated, the sterilization process decreased slightly PACL encapsulation efficiency in microspheres, however, it had only a "little influence on the release profile" (Song et al., 2010).

4.1.2. Degradation of poly(ε-caprolactone)

PCL is a hydrophobic and semi-crystalline polymer. Its low melting point (T_m) (63 °C) and low T_g (−60 °C) (Saad and Suter, 2001) make it demanding with reference to choosing a suitable sterilization method (Table 2).

Masson et al. reported that γ-irradiation of PCL is a selective process that induces reactions in amorphous regions in which two opposite processes take part: chain scission (M_n reduction) and cross-linking (M_w increase) (Masson et al., 1997). Gamma-Irradiation was not proposed as a sterilization method of PCL nanospheres due to possible altered polymer properties, and thus disturbed drug release kinetic (Masson et al., 1997). The negative influence of γ-irradiation was also confirmed by Cottam et al., who noted a significant decrease in PCL degradation rate and the effect of the sterilization on mechanical properties by lowering T_g (Cottam et al., 2009). On the other hand, Filipczak et al. observed no deterioration in mechanical properties of irradiated PCL (Filipczak et al., 2006). According to Filipczak et al., very important is also a post-irradiation effect of the sterilization process. Radicals formed can live for some time after the irradiation causing significant changes in M_w, even in 14 days after the sterilization (Filipczak et al., 2006).

4.1.3. Degradation of poly(trimethylene carbonate)

PTMC is an amorphous, flexible material, that found its potential application in medicine in soft tissue engineering. Comparing to PLA, it degrades *in vivo* by surface erosion. High molecular weight PTMC subjected irradiation with sufficiently high doses of γ-rays causes its cross-linking with the formation of a gel fraction (Bat et al., 2011). As was pointed by Jozwiakowska et al., the formation of insoluble, crosslinked structure allows to radially sterilize PTMC with no considerable deterioration of properties under e-beam irradiation with a dose 25 kGy (Jozwiakowska et al., 2011).

According to Pêgo et al., even below the sterilization dose of 25 kGy, with increasing γ-irradiation dose, a step decrease in M_n and a linear decrease in polydispersity index (PDI) of copolymer of TMC and D,L-lactide was observed (Pêgo et al., 2003). In addition, the irradiation changed polymer's solubility and caused the creation of a gel fraction with increased irradiation dose. Those findings suggested increasing input of cross-linking depending on the air presence (Pêgo et al., 2003).

4.1.4. Degradation of copolymers of lactide and glycolide

Nowadays, PLGA plays very important role as a drug carrier in novel DDSs. Despite several favorable properties, low T_g of about 40 °C, excludes it from thermal and steam sterilization techniques (Bushell et al., 2005). EtO sterilization is also not recommended because of toxic residues remained after the process. Therefore, radiation sterilization is proposed to be the most suitable terminal sterilization method (Athanasiou et al., 1996; Çalış et al., 2002).

According to Claybourn et al., the irradiation of PLGA causes the formation of free radicals, identified as carbon-based secondary alkyl radicals (R·) and alkyl peroxy radicals (RO_2·), which increase the concentration with the radiation dose and GG content of the polymer. It may subsequently affect the polymer properties and drug release kinetics (Claybourn et al., 2003). The impact of the GG content on the PLGA instability caused by the irradiation process was also confirmed by Williams et al. It was emphasized that PLGA microspheres were more stable than the raw polymer during the irradiation process (Williams et al., 2006). As it was shown in both works (Claybourn et al.,

Table 2
Physicochemical properties of biodegradable polyesters.

Polymer	Crystallinity	T_g (°C)	T_m (°C)
PD,L-LA	amorphous (Burg, 2014)	55 (Burg, 2014)	–
PL,L-LA	37% semicrystalline (Burg, 2014)	63 (Burg, 2014)	170–180 (Burg, 2014)
PCL	50% semicrystalline (Mclauchlin and Thomas, 2012; Saad and Suter, 2001)	−60 (Saad and Suter, 2001)	63 (Saad and Suter, 2001)
PGA	45–55% semicrystalline (Burg, 2014)	35 (Burg, 2014)	225 (Burg, 2014)
PLGA	amorphous (Bushell et al., 2005)	40 (Bushell et al., 2005)	–
PTMC	amorphous (Edlund and Albertsson, 2002)	−17 (Edlund and Albertsson, 2002)	–

2003; Williams et al., 2006), the crystallinity is the leading parameter affecting polymer susceptibility to irradiation (next to irradiation dose).

Previous PLGA EPR studies showed that radicals are formed from both, LL and GG components, and it was also reported that comparing to microspheres, radicals formed in raw polymers are less stable and are formed an order of magnitude slower (Claybourn et al., 2003). It was also noticed that comparing to the free COOH group, polymers with esterified COOH group are less sensitive to γ-irradiation (Claybourn et al., 2003), what suggests a different manner of affecting raw polymers and their processed microspheres (Bushell et al., 2005). Additionally, the irradiation of hydrophilic (with free COOH group) polymers and microspheres resulted in higher amount of more stable radicals in comparison to polymers and microspheres with esterified COOH group (Montanari et al., 1998). The EPR study conducted by Bushell et al. identified 3 main radicals formed in PLGA exposed to ionizing radiation: –C·(H)O–, –C·(CH_3)O– and –C·(CH_3)OR, which relative distribution in the polymer varies depending on the LL to GG ratio (Bushell et al., 2005). It has also been revealed that the overall radical content increases with the lactidyl units in the polymer. What was noted, comparing to e-beam irradiated PLGA microspheres, γ-irradiation generates approximately twice more radicals in PLGA microspheres (Bushell et al., 2005). The radiolysis mechanism was studied in detail by Montanari et al. (Montanari et al., 1998), who described the main contribution of primary radicals –CH·(CH_3), resulting from the PLGA chain scission. During heating (above 77 K), hydrogen abstraction at tertiary, and also secondary carbon atoms occurs, generating -C·(CH_3)- and -C·(H)– radicals, respectively. The admission of oxygen generates corresponding peroxyl radicals, which subsequently initiate a chain hydroperoxidative process (Montanari et al., 1998, 2001). The mechanism of γ-radiolysis of PLGA is shown in Fig. 2.

As it was pointed by Volland et al., different *in vitro* drug release results from PLGA have been reported (Volland et al., 1994). In some cases, drug release has been unaffected and in others, it has been positively or negatively altered by γ-irradiation. M_w has been perceived as the main parameter affecting drug release profile (Volland et al., 1994). It appears that the change in the release profile of encapsulated drugs should be similar to the impact of the radiation dose on PLGA instability, but, as Igartua et al. noted, depending on the active substance encapsulated, different outcomes have been reported in terms of the drug release profile, such as a decrease in the drug release profile (Igartua et al., 2008). In comparison, Çaliş et al. reported an accelerated release of drugs with the administered dose (Çalış et al., 2002). Furthermore, as it was shown by Volland et al., higher initial M_w strongly increases PLGA sensitivity towards γ-irradiation (Volland et al., 1994). It was also confirmed by Fernández-Carballido et al., who studied the effect of γ-irradiation on drug loaded PLGA microspheres. As it was reported, it was advantageous to use low molecular weight PLGA, as practically no degradation of DDSs was observed (Fernández-Carballido et al., 2004). This occurrence is consistent with the results of Lee et al., who analyzed the influence of γ-irradiation on PLGA (50:50) of different M_w's. As it was reported, the 25 kGy dose did not significantly affect near first order BCNU release profile from 8 kDa PLGA. It could be related to a minor reduction of M_w (0.9%) compared to 45% M_w drop of high-M_w PLGA (110 kDa) (it should be noted, there was no study on drug release from 110 kDa PLGA) (Lee et al., 2003). The independent test conducted in de Oliveira's study showed low values of the similarity factor (around 50). Nonetheless, no acceleration of the release of methotrexate (MTX) from PLGA (50:50) due to γ-irradiation has been confirmed (de Oliveira et al., 2017). The application of PLGA (50:50) with higher M_w − 42 kDa revealed a loss of about 3% M_w at 10 kGy γ-irradiation. The release profile was continuous until the 18th day of incubation when the drug release rate increased. In comparison, the increase of drug release for non-irradiated sample started around 29th day of incubation (based on the graph given) (Wang et al., 2003). Recent work on DOX-charged PLGA (50:50, M_w 14–15 kDa) nanoparticles has shown no effect of ionizing radiation up to a dose of 15 kGy on the drug release profile, irrespective of the form of irradiation (e-beam and γ-ray). As it was noted, only γ-irradiation at the dose of 25 kGy showed substantial changes in the drug release profile, along with a 5–8% decrease in PLGA M_w (Maksimenko et al., 2019).

4.1.5. Co- and terpolymers of lactide, glycolide, ε-caprolactone and trimethylene carbonate

Very promising conclusion was made by Kryczka et al., who recommended γ-irradiation (doses 15–25 kGy) as a sterilization method of DDSs based on PLGA and PLCL for medical purposes. The cytostatic drugs as well as drug loaded copolymers, showed stability upon the irradiation process and some slight changes in properties did not considerably affect the drug release kinetic (Kryczka et al., 2003).

Musiał-Kulik et al. conducted a comparative study between γ-irradiation and e-beam sterilization of PACL loaded copolymer of TMC and LL. As it was observed, the presence of PACL reduced polymer degradation (less M_w loss) upon the sterilization process. Despite both sterilization techniques altered physical properties of the analyzed materials, e-beam sterilization has been proposed as a better sterilization method (Musiał-Kulik et al., 2013).

According to Rychter et al., who studied the influence of gamma sterilization on the morphology of LL, GG, CL and TMC terpolymers porous scaffolds, strong degradation rates, of up to 40% of relative molecular mass lost were observed, especially with terpolymers containing TMC units, i.e. LL-GG-TMC terpolymers (Rychter et al., 2016). Gamma-irradiation changed thermal properties of the sterilized polymers by affecting amorphous regions of polymers. It resulted in lowering T_g, while T_m remained intact. This did not suggest any impact on the ordered, crystalline regions of irradiated polymers. Comparative studies with the use of e-beam sterilization showed lower degradation rates. However, the irradiation affected the surface morphology of the porous scaffold, resulting in the melting of the polymer matrix (Rychter et al., 2016). All of these factors have a negative impact on mechanical properties of the material, thereby questioning the legitimacy of

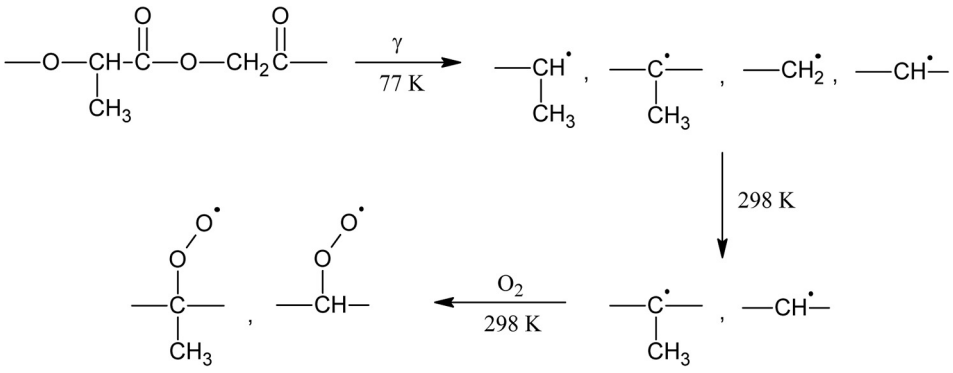

Fig. 2. Mechanism of PLGA radiolysis (Montanari et al., 1998, 2001).

Table 3
The influence of ionizing radiation on anticancer drugs.

Drug	Decomposition/ melting point (°C)	Irradiation conditions	Drug form	Stability of active substance	Irradiation effects	Reference
5-Fluorouracil (5-FU)	283 (Lide, 2009)	4–33 kGy γ-ray (^{60}Co)	5-FU-loaded PLGA microparticles	without studies on 5-FU stability	- drug release study: increased rate of drug release with increasing of the irradiation dose	(Faisant et al., 2002)
Camptothecin (CPT)	275–277 (Volkmann et al., 1971)	25 kGy γ-ray (^{60}Co)	bulk CPT	considered as stable for 2 months after irradiation (storage at 4 °C)	- HPLC analysis: no drug degradation	(Berrada et al., 2005)
Carmustine (BCNU)	31 (Lide, 2009)	25, 50, 75 kGy γ-ray (^{60}Co), dry-ice	BCNU-loaded PLGA wafers	no studies on BCNU stability	- drug release study: almost unchanged BCNU release profile at 25 kGy - GPC: 0.9% M_w reduction of PLGA (8000 g/mole) at 25 kGy; further reduction with irradiation dose - DSC: T_g reduction with increasing irradiation dose - EPR: appearance of –C·(CH_3)– radical	(Lee et al., 2003)
Cisplatin (CIS)	270 (O'Neil, 2006)	28.4 kGy, 37.7 kGy γ-ray (^{60}Co), 10% humidity	CIS-loaded PLA and PLGA microspheres	no studies on CIS stability	- GPC: 30–40% M_w loss of the polymeric carrier, - drug release study: reduction of controlled release time from 60 (non-irradiated) to 8 days at 37.7 kGy	(Spenlehauer et al., 1989)
Cladribine (CLA)	215 (PubChem, 2020a)	15, 20, 25, 100, 200 kGy, γ-ray (^{60}Co)	bulk CLA	considered as stable at doses 15–25 kGy	- TLC: no evidence of CLA decomposition - HPLC analysis: 3.5% CLA contamination with 2-chloroadenine at 200 kGy - DSC: 19–25 °C reduction in CLA melting point - UV; IR; SEM, rentgenography: no appreciable changes	(Kryczka et al., 2003)
Cyclophosphamide (CPA)	60/50 (Varshney and Dodke, 2004)	5, 10, 15, 30, 50 kGy e-beam, room temp./ liquid nitrogen), air; γ-ray (^{60}Co), room temp., air	bulk CPA	considered as stable at 5 kGy	- DSC/TGA: no significant change in the melting point and drug purity up to 30 kGy (γ-ray) and 15 kGy (e-beam) - EPR: linear increase of the radical content with increasing irradiation dose up to 15 kGy - DRS, UV/VIS: drug discoloration - HPLC analysis: the amount of degradants increases with the dose of irradiation (5 kGy: 0.7% degradation; 30 kGy: < 2% degradation)	(Varshney and Dodke, 2004)
Daunorubicin (DAU)	190/208 (Lide, 2009; PubChem, 2020b)	25, 50, 100, 200, 400 kGy e-beam	bulk DAU	considered as stable at 25 kGy	- EPR: weak EPR signals, radical decay $T_{1/2}$ 4 days - SEM, IR, UV/VIS: no significant change - HPLC analysis: no significant change in impurities and drug content at 25 kGy	(Kaczmarek et al., 2013)
Docetaxel (DTX)	232 (PubChem, 2020c)	10, 15, 20 kGy γ-ray (^{60}Co), room temp.	DTX-loaded folate-modified PLGA nanoparticles	considered as stable at 10 kGy for 12 months	- TEM: mostly unchanged spherical shape and particle size - HPLC analysis: decrease in DTX content with more severe irradiation	(Poltavets et al., 2019)
Doxorubicin (DOX)	200/230 (Lide, 2009; Varshney and Dodke, 2004)	5, 10, 15, 30, 50 kGy e-beam, room temp./ liquid nitrogen), air; γ-ray (^{60}Co), room temp., air	DOX hydrochloride	considered as stable at 25 kGy	- HPLC analysis: no significant difference; one new degradant at 30 kGy (< 0.01% degradation) - EPR: radicals present - DRS, UV/VIS - no significant changes	(Varshney and Dodke, 2004)
Epirubicin (EPI)	185 (O'Neil, 2006)	25, 50, 100, 200, 400 kGy e-beam	bulk EPI	considered as stable at 25 kGy	- EPR: weak EPR signals, radical decay $T_{1/2}$ 7 days - SEM, IR, UV/VIS: no significant change - HPLC analysis: no significant change in the impurities and drug content at 25 kGy	(Kaczmarek et al., 2013)
Methotrexate (MTX)	185–202 (PubChem, 2020d)	15, 25, 30 kGy γ-ray (^{60}Co)	MTX-loaded PLGA microparticles	no studies on MTX stability	- SEM: decrease in the sphericity of microparticles, independently of the dose of radiation - EPR: increase of free radical formation with enhancement of drug loading in microparticles - HPLC analysis: no degradation, no changes in the drug content - IR: no changes in the absorption pattern - UV–VIS: no significant acceleration of drug release (attention should be paid to low similarity factors (around 50))	(de Oliveira et al., 2017)

(*continued on next page*)

Table 3 (*continued*)

Drug	Decomposition/ melting point (°C)	Irradiation conditions	Drug form	Stability of active substance	Irradiation effects	Reference
Paclitaxel (PACL)	214 (Lide, 2009)	25 kGy γ-ray (^{60}Co)	bulk PACL	considered as stable for 2 months after irradiation (storage at 4 °C)	- HPLC analysis: no significant changes, no degradation	(Ruel-Gariépy et al., 2004)

radiation sterilization.

4.2. Stability of active substances during the sterilization process

Due to thermal susceptibility, ionizing radiation appears to be the most appropriate sterilization method for many thermosensible active substances. As Varshney et al. have indicated, solid pharmaceuticals undergo from 1 to 5% degradation when radially sterilized at dose of 25 kGy (Varshney and Dodke, 2004). However, as has also been noted, high doses of e-beam irradiation for heat-sensitive active substances are not preferred due to local heating (Varshney and Dodke, 2004). This implies the need for research on the degradation profiles and the effects of radiation sterilization of each cytostatic drug.

The effects of ionizing radiation on the commonly using cytostatic drugs has been discussed in next chapters. The summary of the influence of ionizing radiation on anticancer drugs was presented in Table 3.

4.2.1. Doxorubicin

As it was shown by Maksimienko et al., the benefit of using nanoparticles is altering medicinal agents' distribution in the body. It is known that DOX does not penetrate the blood–brain barrier, however, the utilization of its nanosomal form allows to obtain its therapeutic concentration in the brain. Furthermore, the use of nanosomal form of DOX does not increase its acute toxicity and, what is more, decreases its cardiotoxicity (Maksimenko et al., 2008b). The drug decomposes at about 200 °C (Varshney and Dodke, 2004), what is significantly higher than the temperature used in heat sterilization, which opens up the possibility to use other than asceptic filtration, sterilization methods, such as autoclaving.

As it has already been shown by Varshney et al., DOX hydrochloride can be sterilized at 25 kGy. No major improvement in its physicochemical properties has been observed. Ater the irradiation at 30 kGy, < 0.01% of radiation degradation products have been observed (Varshney and Dodke, 2004). According to Maksimienko et al., the chemical structure of DOX was stable after an irradiation dose of 25 kGy and an optimum sterilization dose of 15 kGy was identified, with a bioburden not exceeding 100 microorganisms/g (Maksimenko et al., 2008a,b). The *Bacillus pumilus* was used as the official test microorganism to test the efficiency of γ-sterilization (Maksimenko et al., 2008a). The irradiation did not impact the stability of DOX and the properties of nanoparticles such as mean particle size, polydispersity and aggregation stability. The sterilization process was successfully achieved at doses beginning at 15 kGy with γ-irradiation as well as with e-beam (Maksimenko et al., 2008a,b). In addition, DOX has been shown to be a radioprotector by decreasing the amount of stable radicals produced by the irradiation of nanoparticles (IAEA, 2008).

DOX, along with daunorubicin (DAU) and epirubicin (EPI) are commonly used anthracycline antibiotic agents (Chiorcea-Paquim et al., 2017; Kaczmarek et al., 2013; Paszel-Jaworska et al., 2016). The comperative study of DAU, DOX and EPI stability to radiation sterilization has been carried out by Kaczmarek et al. The study confirmed radiation resistance of the anthracycline agents to sterilization dose of 25 kGy (Kaczmarek et al., 2013). A continuation of the study was the research conducted by Paszel-Jaworska et al. on the influence of ionizing radiation on DOX, DAU and EPI in relation to their cytotoxic activity (Paszel-Jaworska et al., 2016). As it was noted, ionizing radiation (25 kGy, e-beam) improves the biological activity of drugs in multidrug-resistant CCRF-VCR1000 cells. This finding was related to the formation of free radicals upon the irradiation process (Paszel-Jaworska et al., 2016).

4.2.2. Camptothecin and its analogs

CPT is a hydrophobic, alkaloid drug, derived from a Chinese tree – *Camptotheca acuminate* (Cao et al., 2005). CPT and its derivatives show anticancer activity against solid malignancies such as colon, breast, liver, lung, prostate, and pancreatic cancer cells (Amna et al., 2012).

Their antitumor properties rely on inhibition of DNA topoisomerase I, resulting in single-stranded DNA breaks (Amna et al., 2012; Cortesi et al., 1997). Although CPT shows anticancer activity, human trials were discontinued in the 1970s, due to its toxicity. To the best of our knowledge, there is no work on the radiation stability of CPT and its analogs approved by Food and Drug Administration (FDA), i.e., topotecan and irinotecan (Amna et al., 2012). Nevertheless, γ-irradiation was used as a sterilization method of CPT in Berrada et al. survey (Berrada et al., 2005). For the sterilization process, traditionally applied 25 kGy dose from ^{60}Co source was used. The drug stability was verified by HPLC, which confirmed no degradation caused by γ-irradiation compared to non-irradiated samples (Berrada et al., 2005).

4.2.3. Paclitaxel

PACL is a potent anticancer agent, approved for use by the FDA in 1992. Its parenteral use requires delivery systems to withstand harsh conditions of the sterilization process. As a result, the understanding of mechanisms of drug degradation taking place under the sterilization process is of significant concern of the current studies (Il'ichev and Alquier, 2011).

According to Il'ichev et al., PACL is expected to be susceptible to hydrolytic degradation into Baccatin III, *N*-benzoyl-3-phenyl-*iso*-serine and 10-deacetylpaclitaxel (Il'ichev and Alquier, 2011). Nonetheless, PACL is reported to being stable to typically used sterilization dose 25 kGy (^{60}Co source) (Ruel-Gariépy et al., 2004). Ruel-Gariépy et al., based on HPLC analysis, did not observed drug degradation. Moreover, drug was stable when stored at 4 °C for at least 2 months after the sterilization process (Ruel-Gariépy et al., 2004). The effect of the sterilization dose of 30 kGy (^{60}Co γ-irradiation source) on thermal properties of PACL-loaded PCL was analyzed by Winternitz et al. As they observed, γ-irradiation did not significantly affect its thermal properties and drug release properties (Winternitz et al., 1996). Higher PACL stability to ionizing radiation reaching 46 kGy (e-beam) and 36 kGy (γ-irradiation), was confirmed by Dilcher et al., who observed no significant difference in the amount of PACL's degradation products, i.e. nontaxane, 10-deacetyltaxol and 7-epitaxol (Dilcher et al., 2004).

Il'ichev et al., investigated the effect high dosed of e-beam irradiation on stents and PACL/PLGA films (Il'ichev and Alquier, 2011). As it was reported, hydrolytic and oxidative processes together with the isomerization, have a significant impact on PACL degradation under e-beam sterilization. PACL exposure to irradiation dose of 75 kGy revealed no significant change in the drug release profile. It should be noted, however, that the irradiation dose was three times the sterilization value and, as stated, PACL degradation products were produced at a relatively low level. The possible degradation mechanism of PACL under e-beam suggested by Il'ichev et al. is shown in Fig. 3 (Il'ichev and Alquier, 2011).

4.2.4. Cyclophosphamide

The radiation effects on CPA have been studied by Varshney et al. (Varshney and Dodke, 2004). Several degradation products have been observed upon CPA irradiated at 30 kGy (γ-irradiation and e-beam). As it was observed, N,N-bis (2-chloroethyl) group in CPA is particularly sensitive to irradiation. Three of the degradation products have been reported (Fig. 4. b). A higher degradation profile of CPA was observed during e-beam application relative to γ-irradiation. This result was explained by a local temperature increase in the sample caused by an e-beam (Varshney and Dodke, 2004).

4.2.5. 5-Fluorouracil

5-FU is a well known radiosensitizing agent, used in cancer treatment (Byfield, 1989). Although there is no extensive research on the susceptibility of 5-FU to ionizing radiation, some references to 5-FU being radially sterilized can be found. As an example, γ-irradiation (4–33 kGy) of 5-FU-loaded PLGA microparticles has ben studied by Faisant et. al. (Faisant et al., 2002). As it was stated, only the initial phase of drug release was fastened with an increased dose of irradiation. The immediate, constant drug release phase was not impaired by γ -irradiation (Faisant et al., 2002). In another work, 5-FU-loaded PLGA implants were radially sterilized (25 kGy, γ-irradiation) by Huhtala et al. (Huhtala et al., 2009). However, none of the research aimed to test the stability of 5-FU against ionizing radiation.

5. Conclusions and perspectives

This review addresses the current state of the sterilization methods used in biomedical materials. The most widely used sterilization methods and issues related to the use of biodegradable polyester irradiation and standard anticancer drugs have been described.

Radiation sterilization is a commonly used method for the sterilizing of medical products. Although it has great potential, it should be used wisely due to the different sensitivity of polyesters to ionizing radiation. Up to now, there have been many publications on the study of the impact of the radiation sterilization on the polyester DDSs and drug release kinetics in the case of ionizing radiation; however, little attention is given to the safety of the active substances themselves and their potential use in radiation sterilization of the anticancer-DDSs. Nonetheless, a significant increase in interest in the use of ionizing radiation in the drugs sterilization (especially thermosensitive anticancer-DDSs) has recently been observed due to the possibility of conducting the process at room temperature. So far, two mechanisms (i.e. chain scission and cross-linking) that participate simultaneously in the process of polyester irradiation have been confirmed. Their mutual intensity depends on the individual properties of the polymer (molar mass, microstructure, comonomers ratio, etc.). The radiation sterilization process for each DDSs must therefore be validated with an individual selection of process conditions (temperature, environment, type of radiation etc.).

Importantly, electron beam sterilization over gamma radiation has been demonstrated as shown by the lower number of radicals formed

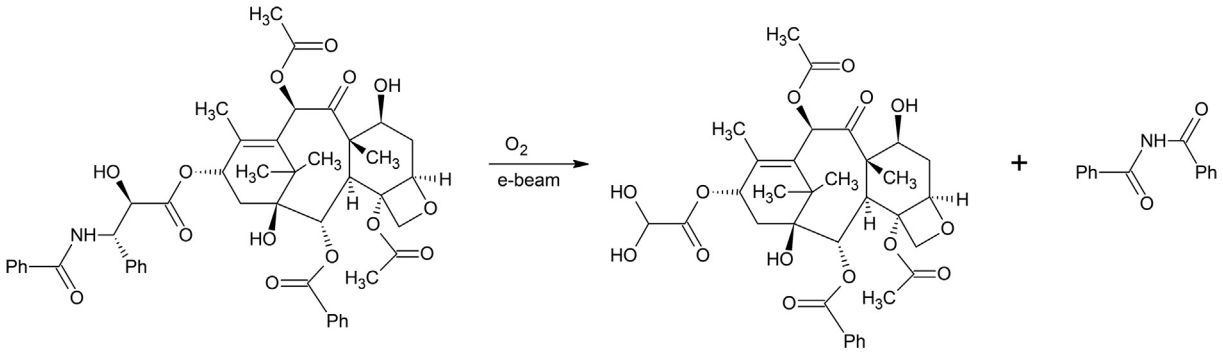

Fig. 3. Mechanism of oxidadative PACL degradation (Il'ichev and Alquier, 2011).

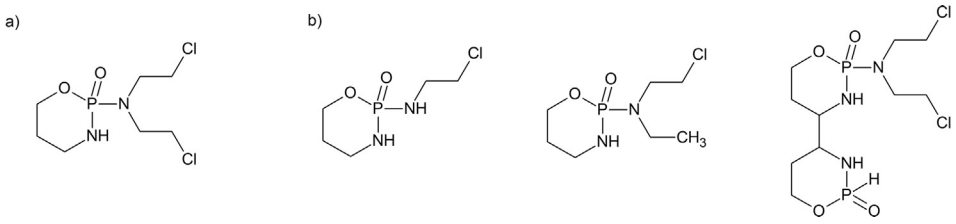

Fig. 4. The structures of: a) basic CPH, b) degradation products of CPH (Varshney and Dodke, 2004).

due to the shorter process. The reduction in temperature and the use of inert gas was also positive. In addition, an increase in the resistance of polymers to ionizing radiation was observed with an increase in their crystallinity and a decrease in M_w. It is also worth to mention that the mechanism of polymer degradation using a pharmacopoeial dose (25 kGy) has repeatedly been verified as a chain-scission, leading to the degradation of polyesters and changes in their physicochemical properties (including adjustments in the drug release kinetics). As the applied dose increases, the degradation of the polymer matrix and drug release kinetics have been increased. Hence, it is necessary to study the optimization of the sterilization process (i.e. the maximum reduction of the ionizing radiation dose) for each DDSs. Importantly, there is evidence of further degradation of polyester over time, thus detailed research on the effect of radiation on the physicochemical properties of DDSs and drug release profile long after the sterilization process need to be carry out.

Most of the tested anticancer substances have been shown to be sterilized at a dose of 25 kGy with a lack or very little improvement in their degradation profile after irradiation. However, the radio-effect of the drug incorporated into the polymeric matrix has been observed in relation to the degradation of DDSs. Nonetheless, further work is required to explain the stabilizing effect of the polymer matrix by certain drugs.

Declaration of Competing Interest

The authors declare that they have no known competing financial interests or personal relationships that could have appeared to influence the work reported in this paper.

Acknowledgments

The contribution of Izabela Domańska was realized within Project No POWR.03.02.00-00-I009/17-00 (Operational Project Knowledge Education Development 2014-2020 co-financed by European Social Fund).

References

Amna, T., Hassan, Nam, Bing, Khil, Kim, 2012. Preparation, characterization, and cytotoxicity of CPT/Fe2O3-embedded PLGA ultrafine composite fibers: a synergistic approach to develop promising anticancer material. Int. J. Nanomed. 2012, 1659–1670. https://doi.org/10.2147/IJN.S24467.

Athanasiou, K.A., Niederauer, G.G., Agrawal, C.M., 1996. Sterilization, toxicity, biocompatibility and clinical applications of polylactic acid/ polyglycolic acid copolymers. Biomaterials 17, 93–102. https://doi.org/10.1016/0142-9612(96)85754-1.

Augustine, R., Saha, A., Jayachandran, V.P., Thomas, S., Kalarikkal, N., 2015. Dose-dependent effects of gamma irradiation on the materials properties and cell proliferation of electrospun polycaprolactone tissue engineering scaffolds. Int. J. Polymeric Mater. Polymeric Biomater. 64, 526–533. https://doi.org/10.1080/00914037.2014.977900.

Bat, E., van Kooten, T.G., Feijen, J., Grijpma, D.W., 2011. Crosslinking of trimethylene carbonate and D, L-lactide (co-) polymers by gamma irradiation in the presence of pentaerythritol triacrylate. Macromol. Biosci. 11, 952–961. https://doi.org/10.1002/mabi.201100031.

Berrada, M., Serreqi, A., Dabbarh, F., Owusu, A., Gupta, A., Lehnert, S., 2005. A novel non-toxic camptothecin formulation for cancer chemotherapy. Biomaterials 26, 2115–2120. https://doi.org/10.1016/j.biomaterials.2004.06.013.

Buchanan, F. (Ed.), 2008. Degradation rate of bioresorbable materials: prediction and evaluation, Woodhead publishing in materials. CRC Press [u.a.], Boca Raton, Fla.

Burg, K., 2014. Poly(α-ester)s. In: Kumbar, S.G., Laurencin, C.T., Deng, M. (Eds.), Natural and Synthetic Biomedical Polymers. Elsevier, pp. 115–121.

Bushell, J.A., Claybourn, M., Williams, H.E., Murphy, D.M., 2005. An EPR and ENDOR study of γ- and β-radiation sterilization in poly (lactide-co-glycolide) polymers and microspheres. J. Control. Release 110, 49–57. https://doi.org/10.1016/j.jconrel.2005.09.009.

Byfield, J.E., 1989. 5-Fluorouracil radiation sensitization – a brief review. Invest New Drugs 7, 111–116. https://doi.org/10.1007/BF00178197.

Çalış, S., Bozdağ, S., Kaş, H.S., Tunçay, M., Hıncal, A.A., 2002. Influence of irradiation sterilization on poly(lactide-co-glycolide) microspheres containing anti-inflammatory drugs. Il Farmaco 57, 55–62. https://doi.org/10.1016/S0014-827X(01)01171-5.

Cao, Z., Mendoza, J., Dejesus, A., Giovanella, B., 2005. Synthesis and anti-tumor activity of alkenyl camptothecin esters. Acta Pharmacol. Sin. 26, 235–241. https://doi.org/10.1111/j.1745-7254.2005.00031.x.

Cheetham, A.G., Zhang, P., Lin, Y., Lock, L.L., Cui, H., 2013. Supramolecular nanostructures formed by anticancer drug assembly. J. Am. Chem. Soc. 135, 2907–2910. https://doi.org/10.1021/ja3115983.

Chiorcea-Paquim, A.-M., Oliveira, S.C.B., Diculescu, V.C., Oliveira-Brett, A.M., 2017. Applications of DNA-electrochemical biosensors in cancer research. In: Palchetti, I., Hansen, P.-.D., Barceló, D. (Eds.), Comprehensive Analytical Chemistry. Elsevier, pp. 287–336. https://doi.org/10.1016/bs.coac.2017.06.003.

Claybourn, M., Gray, H., Murphy, D.M., Purnell, I.J., Rowlands, C.C., 2003. Electron magnetic resonance study of gamma-irradiated poly(lactide-co-glycolide) microspheres. J. Control. Release 91, 431–438. https://doi.org/10.1016/S0168-3659(03)00269-4.

Cortesi, R., Esposito, E., Maietti, A., Menegatti, E., Nastruzzi, C., 1997. Formulation study for the antitumor drug camptothecin: liposomes, micellar solutions and a microemulsion. Int. J. Pharm. 159, 95–103. https://doi.org/10.1016/S0378-5173(97)00275-5.

Cottam, E., Hukins, D.W.L., Lee, K., Hewitt, C., Jenkins, M.J., 2009. Effect of sterilisation by gamma irradiation on the ability of polycaprolactone (PCL) to act as a scaffold material. Med. Eng. Phys. 31, 221–226. https://doi.org/10.1016/j.medengphy.2008.07.005.

Dai, Z., Ronholm, J., Tian, Y., Sethi, B., Cao, X., 2016. Sterilization techniques for biodegradable scaffolds in tissue engineering applications. J. Tissue Eng. 7, 1–13. https://doi.org/10.1177/2041731416648810.

de Oliveira, A.R., Mesquita, P.C., Machado, P.R.L., Farias, K.J.S., de Almeida, Y.M.B., Fernandes-Pedrosa, M.F., Cornélio, A.M., do Egito, E.S.T., da Silva-Júnior, A.A., 2017. Monitoring structural features, biocompatibility and biological efficacy of gamma-irradiated methotrexate-loaded spray-dried microparticles. Mater. Sci. Eng.: C 80, 438-448. doi: 10.1016/j.msec.2017.06.013.

Dilcher, C., Chan, R., Hellinga, D., Seabron, R., Pakala, R., Kuchulakanti, P.K., Richard, R., Chan, K., Zhong, S., Barry, J.J., Waksman, R., 2004. Effect of ionizing radiation on the stability and performance of the TAXUS Express^2 paclitaxel-eluting stent. Cardiovascular Radiation Med. 5, 136–141. https://doi.org/10.1016/j.carrad.2004.06.002.

Duan, K., Zhang, X., Tang, X., Yu, J., Liu, S., Wang, D., Li, Y., Huang, J., 2010. Fabrication of cationic nanomicelle from chitosan-graft-polycaprolactone as the carrier of 7-ethyl-10-hydroxy-camptothecin. Colloids Surf., B 76, 475–482. https://doi.org/10.1016/j.colsurfb.2009.12.007.

Edlund, U., Albertsson, A.-C., 2002. Degradable Polymer Microspheres for Controlled Drug Delivery, in: Albertsson, A.-C. (Ed.), Degradable Aliphatic Polyesters. Advances in Polymer Science. Springer, pp. 67-12.

Faisant, N., Siepmann, J., Oury, P., Laffineur, V., Bruna, E., Haffner, J., Benoit, J.P., 2002. The effect of gamma-irradiation on drug release from bioerodible microparticles: a quantitative treatment. Int. J. Pharm. 242, 281–284. https://doi.org/10.1016/S0378-5173(02)00188-6.

Fernández-Carballido, A., Herrero-Vanrell, R., Molina-Martínez, I.T., Pastoriza, P., 2004. Sterilized ibuprofen-loaded poly(D, L-lactide-co-glycolide) microspheres for intra-articular administration: effect of γ -irradiation and storage. J. Microencapsul. 21, 653–665. https://doi.org/10.1080/09687860400008437.

Filipczak, K., Wozniak, M., Ulanski, P., Olah, L., Przybytniak, G., Olkowski, R.M., Lewandowska-Szumiel, M., Rosiak, J.M., 2006. Poly(ε-caprolactone) Biomaterial Sterilized by E-Beam Irradiation. Macromol. Biosci. 6, 261–273. https://doi.org/10.1002/mabi.200500215.

Fredenberg, S., Wahlgren, M., Reslow, M., Axelsson, A., 2011. The mechanisms of drug release in poly(lactic-co-glycolic acid)-based drug delivery systems—a review. Int. J. Pharm. 415, 34–52. https://doi.org/10.1016/j.ijpharm.2011.05.049.

Gupta, M.C., Deshmukh, V.G., 1983. Radiation effects on poly(lactic acid). Polymer 24, 827–830. https://doi.org/10.1016/0032-3861(83)90198-2.

Hall, E.J., 2000. Radiobiology for the Radiologist, 5th ed. Lippincott Williams & Wilkins, Philadelphia.

Harrell, C.R., Djonov, V., Fellabaum, C., Volarevic, V., 2018. Risks of using sterilization by gamma radiation: the other side of the coin. Int. J. Med. Sci. 15, 274–279. https://

doi.org/10.7150/ijms.22644.
Hooper, K.A., Cox, J.D., Kohn, J., 1997. Comparison of the effect of ethylene oxide and γ-irradiation on selected tyrosine-derived polycarbonates and poly(L-lactic acid). J. Appl. Polym. Sci. 63, 1499–1510. https://doi.org/10.1002/(SICI)1097-4628(19970314)63:11<1499::AID-APP12>3.0.CO;2-Y.
Huhtala, A., Rönkkö, S., Teräsvirta, M., Puustjärvi, T., Sihvola, R., Vehanen, K., Laukkanen, A., Anttila, J., Urtti, A., Pohjonen, T., Uusitalo, H., 2009. The Effects of 5-fluorouracil on ocular tissues in vitro and in vivo after controlled release from a multifunctional implant. Invest. Ophthalmol. Vis. Sci. 50, 2216–2223. https://doi.org/10.1167/iovs.08-3016.
IAEA (International Atomic Energy Agency), 2008. Trends in radiation sterilization of health care products. IAEA, Vienna.
Igartua, M., Hernández, R.M., Rosas, J.E., Patarroyo, M.E., Pedraz, J.L., 2008. γ-Irradiation effects on biopharmaceutical properties of PLGA microspheres loaded with SPf66 synthetic vaccine. Eur. J. Pharm. Biopharm. 69, 519–526. https://doi.org/10.1016/j.ejpb.2007.12.014.
Il'ichev, Y.V., Alquier, L., 2011. Effects of E-BEAM sterilization on drug-eluting stents: paclitaxel degradation elucidated by LC-MS-MS with information-dependent acquisition. J. Chromatogr. Sci. 49, 807–817.
Jo, S.-Y., Park, J.-S., Gwon, H.-J., Shin, Y.-M., Khil, M.-S., Nho, Y.-C., Lim, Y.-M., 2012. Degradation behavior of poly(L-lactide-co-glycolide) films through gamma-ray irradiation. Radiat. Phys. Chem. 81, 846–850. https://doi.org/10.1016/j.radphyschem.2012.03.013.
Jozwiakowska, J., Wach, R.A., Rokita, B., Ulanski, P., Nalawade, S.P., Grijpma, D.W., Feijen, J., Rosiak, J.M., 2011. Influence of electron beam irradiation on physico-chemical properties of poly(trimethylene carbonate). Polym. Degrad. Stab. 96, 1430–1437. https://doi.org/10.1016/j.polymdegradstab.2011.05.010.
Kaczmarek, A., Cielecka-Piontek, J., Garbacki, P., Lewandowska, K., Bednarski, W., Barszcz, B., Zalewski, P., Kycler, W., Oszczapowicz, I., Jelińska, A., 2013. Radiation sterilization of anthracycline antibiotics in solid state. Scientific World J. 2013, 1–7. https://doi.org/10.1155/2013/258758.
Keles, H., Naylor, A., Clegg, F., Sammon, C., 2015. Investigation of factors influencing the hydrolytic degradation of single PLGA microparticles. Polym. Degrad. Stab. 119, 228–241. https://doi.org/10.1016/j.polymdegradstab.2015.04.025.
Kryczka, T., Marciniec, B., Popielarz-Brzezinska, M., Bero, M., Kasperczyk, J., Dobrzyński, P., Kazimierczuk, Z., Grieb, P., 2003. Effect of gamma-irradiation on cladribine and cladribine-containing biodegradable copolymers. J. Control. Release 89, 447–456. https://doi.org/10.1016/S0168-3659(03)00156-1.
Lee, J.S., Chae, G.S., Khang, G., Kim, M.S., Cho, S.H., Lee, H.B., 2003. The effect of gamma irradiation on PLGA and release behavior of BCNU from PLGA wafer. Macromol. Res. 11, 352–356. https://doi.org/10.1007/BF03218376.
Lide, D.R., 2009. CRC Handbook of Chemistry and Physics, 90th ed. CRC Press/Taylor and Francis, Boca Raton, FL.
Loo, S.C.J., Ooi, C.P., Boey, Y.C.F., 2004. Radiation effects on poly(lactide-co-glycolide) (PLGA) and poly(l-lactide) (PLLA). Polym. Degrad. Stab. 83, 259–265. https://doi.org/10.1016/S0141-3910(03)00271-4.
Maksimenko, O., Malinovskaya, J., Shipulo, E., Osipova, N., Razzhivina, V., Arantseva, D., Yarovaya, O., Mostovaya, U., Khalansky, A., Fedoseeva, V., Alekseeva, A., Vanchugova, L., Gorshkova, M., Kovalenko, E., Balabanyan, V., Melnikov, P., Baklaushev, V., Chekhonin, V., Kreuter, J., Gelperina, S., 2019. Doxorubicin-loaded PLGA nanoparticles for the chemotherapy of glioblastoma: towards the pharmaceutical development. Int. J. Pharm. 572, 118733. https://doi.org/10.1016/j.ijpharm.2019.118733.
Maksimenko, O., Pavlov, E., Toushov, E., Molin, A., Stukalov, Y., Prudskova, T., Feldman, V., Kreuter, J., Gelperina, S., 2008a. Radiation sterilisation of doxorubicin bound to poly(butyl cyanoacrylate) nanoparticles. Int. J. Pharm. 356, 325–332. https://doi.org/10.1016/j.ijpharm.2008.01.010.
Maksimenko, O.O., Pavlov, E.P., Tushov, É.G., Molin, A.A., Stukalov, Yu.V., Prudskova, T.N., Sveshnikov, P.G., Kreuter, J., Gel'perina, S.É., 2008b. Radiation sterilization of medicinal formulations of doxorubicin bound to poly(butylcyanoacrylate) nanoparticles. Pharm. Chem. J. 42, 363–367. https://doi.org/10.1007/s11094-008-0128-4.
Mansouri, M., Berrayah, A., Beyens, C., Rosenauer, C., Jama, C., Maschke, U., 2016. Effects of electron beam irradiation on thermal and mechanical properties of poly (lactic acid) films. Polym. Degrad. Stab. 133, 293–302. https://doi.org/10.1016/j.polymdegradstab.2016.09.005.
Masson, V., Maurin, F., Fessi, H., Devissaguet, J.P., 1997. Influence of sterilization processes on poly(ε-caprolactone) nanospheres. Biomaterials 18, 327–335. https://doi.org/10.1016/S0142-9612(96)00144-5.
Mclauchlin, A.R., Thomas, N.L., 2012. Biodegradable polymer nanocomposites. In: Gao, F. (Ed.), Advances in Polymer Nanocomposites. Woodhead Publishing, Padstow, pp. 398–430.
Montanari, L., Costantini, M., Signoretti, E.C., Valvo, L., Santucci, M., Bartolomei, M., Fattibene, P., Onori, S., Faucitano, A., Conti, B., Genta, I., 1998. Gamma irradiation effects on poly(dl-lactictide-co-glycolide) microspheres. J. Control. Release 56, 219–229. https://doi.org/10.1016/S0168-3659(98)00082-0.
Montanari, L., Cilurzo, F., Valvo, L., Faucitano, A., Buttafava, A., Groppo, A., Genta, I., Conti, B., 2001. Gamma irradiation effects on stability of poly(lactide-co-glycolide) microspheres containing clonazepam. J. Control. Release 75, 317–330. https://doi.org/10.1016/S0168-3659(01)00401-1.
Musiał-Kulik, M., Gębarowska, K., Janeczek, H., Pastusiak, M., Kasperczyk, J., Dobrzyński, P., 2013. Radiation sterilization of bioresorbable copolymers with the cytostatic drug. Eng. Biomater. 16, 18–22.
O'Neil, M.J. (Ed.), 2006. The Merck Index: An Encyclopedia of Chemicals, Drugs, and Biologicals, 14th ed. Merck, Whitehouse Station, N.J.
Panganiban, R.-A.M., Snow, A., Day, R., 2013. Mechanisms of radiation toxicity in transformed and non-transformed cells. IJMS 14, 15931–15958. https://doi.org/10.3390/ijms140815931.
Paszel-Jaworska, A., Totoń, E., Dettlaff, K., Kaczmarek, A., Bednarski, W., Oszczapowicz, I., Jelińska, A., Rybczyńska, M., 2016. Increased proapoptotic activity of electron beam irradiated doxorubicin and epirubicin in multidrug-resistant human leukemic cells. Chem. Biol. Interact. 258, 69–78. https://doi.org/10.1016/j.cbi.2016.08.011.
Pêgo, A.P., Siebum, B., Van Luyn, M.J.A., Gallego y Van Seijen, X.J., Poot, A.A., Grijpma, D.W., Feijen, J., 2003. Preparation of Degradable Porous Structures Based on 1,3-Trimethylene Carbonate and D,L-Lactide (Co)polymers for Heart Tissue Engineering. Tissue Engineering 9, 981–994. doi: 10.1089/107632703322495628.
Ph. Eur. (Pharmacopoeia European) – suppl. 9.2, 2017. European Directorate for the Quality of Medicines & HealthCare, Council of Europe, pp. 4333-4350.
Plikk, P., Odelius, K., Hakkarainen, M., Albertsson, A.C., 2006. Finalizing the properties of porous scaffolds of aliphatic polyesters through radiation sterilization. Biomaterials 27, 5335–5347. https://doi.org/10.1016/j.biomaterials.2006.06.024.
Poltavets, Y.I., Zavarzina, V.V., Kuznetsov, S.L., Krasheninnikova, A.A., Dronov, D.O., Gukasova, N.V., Shuvatova, V.G., Balabanyan, V.Y., 2019. Development of docetaxel-loaded folate-modified poly(lactic-co-glycolic acid) particles. J. Reports Pharmaceutical Sci. 8, 253–261.
PubChem Database. National Center for Biotechnology Information. 2020a Cladribine, CID=20279, https://pubchem.ncbi.nlm.nih.gov/compound/Cladribine (accessed 23 March 2020).
PubChem Database. National Center for Biotechnology Information. 2020b Daunorubicin hydrochloride, CID=62770, https://pubchem.ncbi.nlm.nih.gov/compound/Daunorubicin-hydrochloride (accessed 25 February 2020).
PubChem Database. National Center for Biotechnology Information. 2020c Docetaxel, CID=148124, https://pubchem.ncbi.nlm.nih.gov/compound/Docetaxel (accessed 08 June 2020).
PubChem Database. National Center for Biotechnology Information. 2020d Methotrexate, CID=126941, https://pubchem.ncbi.nlm.nih.gov/compound/Methotrexate (accessed on June 15, 2020).
Ruel-Gariépy, E., Shive, M., Bichara, A., Berrada, M., Le Garrec, D., Chenite, A., Leroux, J.-C., 2004. A thermosensitive chitosan-based hydrogel for the local delivery of paclitaxel. Eur. J. Pharm. Biopharm. 57, 53–63. https://doi.org/10.1016/S0939-6411(03)00095-X.
Rychter, P., Śmigiel-Gac, N., Pamuła, E., Smola-Dmochowska, A., Janeczek, H., Prochwicz, W., Dobrzyński, P., 2016. Influence of radiation sterilization on properties of biodegradable lactide/glycolide/trimethylene carbonate and lactide/glycolide/ε-caprolactone porous scaffolds with shape memory behavior. Materials 9, 64. https://doi.org/10.3390/ma9010064.
Saad, B., Suter, U.W., 2001. Biodegradable polymeric materials. In: Buschow, K.H.J., Flemings, M.C., Kramer, E.J., Veyssière, P., Cahn, R.W., Ilschner, B., Mahajan, S. (Eds.), Encyclopedia of Materials: Science and Technology, 2nd ed. Elsevier, pp. 551–555.
Sakar, F., Özer, A.Y., Erdogan, S., Ekizoglu, M., Kart, D., Özalp, M., Colak, S., Zencir, Y., 2017. Nano drug delivery systems and gamma radiation sterilization. Pharm. Dev. Technol. 22, 775–784. https://doi.org/10.3109/10837450.2016.1163393.
Sommerfeld, P., Schroeder, U., Sabel, B.A., 1998. Sterilization of unloaded poly-butylcyanoacrylate nanoparticles. Int. J. Pharm. 164, 113–118. https://doi.org/10.1016/S0378-5173(97)00394-3.
Song, T.-T., Yuan, X.-B., Sun, A.-P., Wang, H., Kang, C.-S., Ren, Y., He, B., Sheng, J., Pu, P.-Y., 2010. Preparation of injectable paclitaxel sustained release microspheres by spray drying for inhibition of glioma in vitro. J. Appl. Polym. Sci. 115, 1534–1539. https://doi.org/10.1002/app.31105.
Spenlehauer, G., Vert, M., Benoit, J., Boddaert, A., 1989. In vitro and In vivo degradation of poly(D, L lactide/glycolide) type microspheres made by solvent evaporation method. Biomaterials 10, 557–563. https://doi.org/10.1016/0142-9612(89)90063-X.
Szymański, W., 1996. Chemia jądrowa: zarys problematyki przemian jądrowych, 2nd ed. Wydawnictwo Naukowe PWN, Warszawa.
Valente, T.A.M., Silva, D.M., Gomes, P.S., Fernandes, M.H., Santos, J.D., Sencadas, V., 2016. Effect of sterilization methods on electrospun poly(lactic acid) (PLA) fiber alignment for biomedical applications. ACS Appl. Mater. Interfaces 8, 3241–3249. https://doi.org/10.1021/acsami.5b10869.
Varshney, L., Dodke, P.B., 2004. Radiation effect studies on anticancer drugs, cyclophosphamide and doxorubicin for radiation sterilization. Radiat. Phys. Chem. 71, 1103–1111. https://doi.org/10.1016/j.radphyschem.2003.12.052.
Volkmann, R., Danishefsky, S., Eggler, J., Solomon, D.M., 1971. Total synthesis of (+-)-camptothecine. J. Am. Chem. Soc. 93, 5576–5577. https://doi.org/10.1021/ja00750a045.
Volland, C., Wolff, M., Kissel, T., 1994. The influence of terminal gamma-sterilization on captopril containing poly(d, l-lactide-co-glycolide) microspheres. J. Control. Release 31, 293–305. https://doi.org/10.1016/0168-3659(94)90012-4.
Walo, M., Przybytniak, G., Nowicki, A., Świeszkowski, W., 2011. Radiation-induced effects in gamma-irradiated PLLA and PCL at ambient and dry ice temperatures. J. Appl. Polym. Sci. 122, 375–383. https://doi.org/10.1002/app.34079.
Wang, J., NG, C.W., Win, K.Y., Shoemakers, P., Lee, T.K.Y., Feng, S.S., Wang, C.H., 2003. Release of paclitaxel from polylactide-co-glycolide (PLGA) microparticles and discs under irradiation, J. Microencapsulation, 20, 317-327. doi: 10.3109/02652040309178072.
Wang, L., Du, J., Zhou, Y., Wang, Y., 2017. Safety of nanosuspensions in drug delivery. Nanomedicine: Nanotechnology, Biology and Medicine 13, 455–469. https://doi.org/10.1016/j.nano.2016.08.007.
Williams, H.E., Huxley, J., Claybourn, M., Booth, J., Hobbs, M., Meehan, E., Clark, B., 2006. The effect of γ-irradiation and polymer composition on the stability of PLG polymer and microspheres. Polym. Degrad. Stab. 91, 2171–2181. https://doi.org/10.

1016/j.polymdegradstab.2006.01.006.
Winternitz, C.I., Jackson, J.K., Oktaba, A.M., Burt, H.M., 1996. Development of a polymeric surgical paste formulation for taxol. Pharm. Res. 13, 368–375.
Yokoya, A., Shikazono, N., Fujii, K., Urushibara, A., Akamatsu, K., Watanabe, R., 2008. DNA damage induced by the direct effect of radiation. Radiat. Phys. Chem. 77, 1280–1285. https://doi.org/10.1016/j.radphyschem.2008.05.021.
Zhang, X., Kotaki, M., Okubayashi, S., Sukigara, S., 2010. Effect of electron beam irradiation on the structure and properties of electrospun PLLA and PLLA/PDLA blend nanofibers. Acta Biomater. 6, 123–129. https://doi.org/10.1016/j.actbio.2009.06.007.

molecules

MDPI

Article

A Comprehensive Investigation of the Structural, Thermal, and Biological Properties of Fully Randomized Biomedical Polyesters Synthesized with a Nontoxic Bismuth(III) Catalyst

Izabela M. Domańska [1], Anna Zgadzaj [2], Sebastian Kowalczyk [3], Aldona Zalewska [3], Ewa Oledzka [1], Krystyna Cieśla [4], Andrzej Plichta [3] and Marcin Sobczak [1,5,*]

1 Department of Biomaterials Chemistry, Chair of Analytical Chemistry and Biomaterials, Faculty of Pharmacy, Medical University of Warsaw, 1 Banacha Str., 02-097 Warsaw, Poland; izabela.domanska@wum.edu.pl (I.M.D.); ewa.oledzka@wum.edu.pl (E.O.)
2 Department of Environmental Health Sciences, Faculty of Pharmacy, Medical University of Warsaw, 1 Banacha Str., 02-097 Warsaw, Poland; anna.zgadzaj@wum.edu.pl
3 Faculty of Chemistry, Warsaw University of Technology, 3 Noakowskiego Str., 00-664 Warsaw, Poland; skowalczyk@ch.pw.edu.pl (S.K.); aldona.zalewska@pw.edu.pl (A.Z.); andrzej.plichta@pw.edu.pl (A.P.)
4 Institute of Nuclear Chemistry and Technology, 16 Dorodna Str., 03-195 Warsaw, Poland; k.ciesla@ichtj.waw.pl
5 Military Institute of Hygiene and Epidemiology, 4 Kozielska Str., 01-163 Warsaw, Poland
* Correspondence: marcin.sobczak@wum.edu.pl; Tel.: +48-22-572-0783

Abstract: Aliphatic polyesters are the most common type of biodegradable synthetic polymer used in many pharmaceutical applications nowadays. This report describes the ring-opening polymerization (ROP) of L-lactide (L-LA), ε-caprolactone (CL) and glycolide (Gly) in the presence of a simple, inexpensive and convenient PEG200-$BiOct_3$ catalytic system. The chemical structures of the obtained copolymers were characterized by ^{1}H- or ^{13}C-NMR. GPC was used to estimate the average molecular weight of the resulting polyesters, whereas TGA and DSC were employed to determine the thermal properties of polymeric products. The effects of temperature, reaction time, and catalyst content on the polymerization process were investigated. Importantly, the obtained polyesters were not cyto- or genotoxic, which is significant in terms of the potential for medical applications (e.g., for drug delivery systems). As a result of transesterification, the copolymers obtained had a random distribution of comonomer units along the polymer chain. The thermal analysis indicated an amorphous nature of poly(L-lactide-*co*-ε-caprolactone) (PLACL) and a low degree of crystallinity of poly(ε-caprolactone-*co*-glycolide) (PCLGA, X_c = 15.1%), in accordance with the microstructures with random distributions and short sequences of comonomer units (l = 1.02–2.82). Significant differences in reactivity were observed among comonomers, confirming preferential ring opening of L-LA during the copolymerization process.

Keywords: biodegradable polymers; aliphatic polyesters; poly(ε-caprolactone); poly(L-lactide); poly(ε-caprolactone-*co*-glycolide); poly(L-lactide-co-ε-caprolactone); bismuth(III) 2-ethylhexanoate; ring opening polymerization

Citation: Domańska, I.M.; Zgadzaj, A.; Kowalczyk, S.; Zalewska, A.; Oledzka, E.; Cieśla, K.; Plichta, A.; Sobczak, M. A Comprehensive Investigation of the Structural, Thermal, and Biological Properties of Fully Randomized Biomedical Polyesters Synthesized with a Nontoxic Bismuth(III) Catalyst. *Molecules* **2022**, *27*, 1139. https://doi.org/10.3390/molecules27031139

Academic Editors: Giuseppe Cirillo, Manuela Curcio and Orazio Vittorio

Received: 21 January 2022
Accepted: 4 February 2022
Published: 8 February 2022

1. Introduction

Bio-based polymeric materials are widely used in medicine and pharmacy (e.g., tissue engineering, drug delivery systems (DDSs), etc.). The most desirable are drug carriers derived from biocompatible polyesters, of which homo- and copolymers containing ε-oxycaproyl (Cap), glycolidyl (GG) and lactidyl (LL) units are the most commonly used biomaterials [1,2]. Concomitantly, the advantage of polyester drug carriers is their biodegradability. These polymers, once introduced into the organism, are well tolerated, metabolically decomposed, and eliminated via normal metabolic pathways [1]. The most attractive catalytic systems for the synthesis of polyesters are those consisting of metals

(Zn, Sn, Zr, Fe). Nevertheless, the resulted polymers may contain traces of metal pollutants, leading to their high toxicity, which is undesirable for biomedical application [3]. As a result, they have been studied extensively over the last few decades, and significant progress has been made in terms of their synthesis using well-defined metalloorganic catalysts [4]. Among these, the use of alternative green catalysts has received particular consideration. Ring-opening polymerization (ROP) of lactones, such as L-lactide (L-LA), *rac*-lactide (*rac*-LA), ε-caprolactone (CL), and glycolide (Gly), using tin compounds as catalysts (e.g., tin(II) 2-ethylhexanoate ($SnOct_2$)), is one of the methods of producing polyesters applied in medicine and pharmacy. Although the Food and Drug Administration (FDA) has approved $SnOct_2$ as a food additive, tin(II) and tin(IV) ions or compounds tend to bind to the SH groups of proteins. In view of this, the catalyst is cytotoxic to some extent [5], and, thus, the resulting polymers should not be considered fully biocompatible [1]. Among other catalysts considered as non-toxic are Zn- and Zr- based compounds [3]. Our previous studies have shown that the polymers synthesized in the presence of diethylzinc [3] and zirconium(IV) acetylacetonate [6] may be considered as non-toxic in terms of cyto- and genotoxicity and thereby be suitable for pharmaceutical and medical applications.

Given the foregoing, in this work we will concentrate on bismuth(III) 2-ethylhexanoate (bismuth octoate, $BiOct_3$), a potential nontoxic organometallic catalyst. Bi(III) is one of the ultratrace elements and its salts have long been used in medicine as both externally and internally administered drugs [4,7,8]. For example, bismuth(III) subsalicylate (BiSS) is a commercial drug for travelers' diarrhea, nonulcer dyspepsia, and gastrointestinal complaints [7]. Furthermore, toxicity studies reveal that Bi(III) is not toxic even at the highest dose tested and it proved less toxic than Zn on cultured human kidney tubular cells [9]. According to Kowalik et al., bismuth-based complexes exhibit not only antimicrobial and anticancer activity, but recent results also reveal the ability to reduce some side effects of cisplatin in cancer therapy [10]. Bi(III) salts (such as $BiCl_3$, $BiAc_3$, BiO_3, Bi(n-hexanoate)$_3$ and BiSS) have previously been reported to act as catalysts in the copolymerization of CL, Gly, and L-LA in particular [8,11]. These compounds are stable in storage and, most importantly, nontoxic in the quantities needed [8]. Comparing to other nontoxic metal catalysts, bismuth (III) compounds are, therefore, well suited to ROP of lactides [4] and may lead to unusual, random Cap and LL sequences in the polymeric chain [11].

However, there are few reports of bismuth organometallic compounds being used as catalysts of the ROP of lactones. Kricheldorf and Serra [12] published the first reference using $BiOct_3$. They highlighted its high effectivity and low tendency of racemization of lactides, even in high temperatures (180 °C) [12]. Though the synthesis of polyesters in the presence of $BiOct_3$ has already been published, the purpose of this study was to extend the prior research of Kricheldorf and Serra [12] towards the synthesis of the copolymers of cyclic carboxylic esters, with a potential use as drug carriers in oncology, as well as to evaluate the resulting polymers in relation to their thermal properties and microstructure. The microstructure of polymers influences the kinetics of biodegradation process [13] and is therefore important regarding drug release and, thus, pharmaceutical application.

In this paper, we describe the synthesis of CL, Gly, and L-LA homo- and copolymers in the presence of a biosafe bismuth(III) catalyst system. The structural, physicochemical, and biological properties of these biodegradable polymers were investigated. Low molar mass and dispersity characterize the developed products. Furthermore, they have a random distribution of comonomer units along the polymer chain, resulting in the polyesters being amorphous or having a low degree of crystallinity. Most importantly, the polymers formed are non-toxic. We hope that the polyesters produced can be used in DDSs technology.

2. Materials and Methods

2.1. Materials

L-Lactide (L-LA, (3S)-*cis*-3,6-Dimethyl-1,4-dioxane-2,5-dione, 98%), ε-caprolactone (CL, 2-Oxepanone, 98 %) and poly(ethylene glycol) (PEG200, M_n = 200 Da) were purchased from Sigma-Aldrich Co. (Poznań, Poland). Glycolide (Gly, 1,4-Dioxane-2,5-dione, 98%) was

purchased from TCI Europe N.V. Co. (Zwijndrecht, Belgium) and bismuth 2-ethylhexanoate from Alfa Aesar Co., part of Thermo Fisher Scientific (Kandel, Germany). Methanol (CH_3OH, analytical pure), chloroform ($CHCl_3$, analytical pure), dichloromethane (DCM, CH_2Cl_2, analytical pure) and hydrochloric acid (HCl, 35–38%) were obtained from POCH Co. (Gliwice, Poland).

2.2. Synthesis of Homo- and Copolymers via ROP

The polymeric materials were formed in bulk by the ROP of CL, Gly, and L-LA in the presence of a PEG200-$BiOct_3$ catalytic system. In brief, appropriate amounts of monomers and PEG200 (1 to 5 g in total) were placed in dry glass ampules (the initiator to monomer ratio was constant as 1:100). Under dry argon, the reaction tubes were degassed and the catalytic amounts of $BiOct_3$ were charged. The reaction vessels were sealed and placed in a thermostated oil bath under various conditions, i.e., time and temperature. When the reaction was completed, the polymerization products were dissolved in DCM or chloroform and precipitated in a cold methanol solution containing 5% of HCl (twice) and a cold methanol (last precipitation). The procedure was carried out a total of three times. The isolated polymer was dried in a vacuum oven to a constant weight and stored at 4 °C.

2.3. Methods

2.3.1. Structural Analysis of Polymers

Analyses of hydrogen nuclear magnetic resonance (^{1}H NMR) and carbon-13 nuclear magnetic resonance (^{13}C NMR) were carried out on an Agilent 400 MHz spectrometer at room temperature using $CDCl_3$ as a solvent. The spectra were collected using 32 scans (^{1}H NMR) or 5000 scans (^{13}C NMR) with a 1 s acquisition time.

The copolymer microstructure was characterized by means of the parameters calculated from ^{1}H NMR and ^{13}C NMR spectra according to the equations presented in the literature: the average length of the lactidyl (l^e_{LL}), glycolidyl (l^e_{GG}) and caproyl (l^e_{Cap}) blocks, randomization ratio (R), and transesterification of the second mode (T_{II}) [14–17].

The monomer conversion ($conv_i$) was calculated using ^{1}H NMR by comparing integrated signals of equivalent protons from the monomer and the polymer, as follows:

$$conv_i = \frac{I_i}{I_i + I_I} \tag{1}$$

where I_i and I_I are the integral intensities of signals from equivalent protons in the monomer and polymer, respectively.

The microstructures of the obtained copolymers were examined using ^{1}H NMR for PCLGA and ^{13}C NMR for PLACL in the most convenient spectrum ranges, namely the methylene proton region of GG units and the ε-methylene proton region of Cap units (PCLGA), as well as the carbonyl carbon range of Cap and LL units (PLACL). By analogy with the literature [14–17], spectral lines were assigned to corresponding comonomeric sequences.

^{1}H NMR and ^{13}C NMR spectra allow for the calculation of l^e_{GG} and l^e_{LL} using the Equation (2) and l^e_{Cap} using the Equation (3) for ^{1}H NMR spectrum and the Equation (4) for ^{13}C NMR spectrum, as well as the determination of the contribution of sequences formed as a result of a transesterification process [18].

$$l^e_{XX} = \frac{1}{2} \times \frac{XXX + XXCap + CapXX + CapXCap}{CapXCap + \frac{1}{2}(XXCap + CapXX)} \tag{2}$$

$$l^e_{Cap} = \frac{CapCap + XCap}{XCap} \tag{3}$$

$$l^e_{Cap} = \frac{XCapX + CapCapX + XCapCap + CapCapCap}{XCapX + \frac{1}{2}(CapCapX + XCapCap)} \tag{4}$$

where X represents glycolyl unit $-OCH_2CO-$ (G) or lactyl unit $-OCH(CH_3)CO-$ (L), Cap is caproil unit $-O(CH_2)_5CO-$, and XCap, XXX, XXCap, and so forth are two- and three-element sequences in the polymer chain.

T_{II} may cause scission of glycolidyl or lactidyl units in the copolymer chain leading to the formation of characteristic CapGCap or CapLCap sequences. The yield of T_{II} is a quantitative determination of the second mode of transesterification process in the copolymer chain, and was calculated according to the Equation (5):

$$T_{II} = \frac{[\text{CapXCap}]}{[\text{CapXCap}]_R} \quad (5)$$

where [CapXCap] is the experimental concentration of CapXCap sequence and the $[\text{CapXCap}]_R$ is the concentration of CapXCap sequence in a completely random chain.

The $[\text{CapXCap}]_R$ can be described by the following relation (Equation (6)) when the ratio of [X]/[Cap] is denoted as *k*':

$$[\text{CapXCap}]_R = \frac{k'^3}{(k'+1)^3} \quad (6)$$

A degree of the randomness of the copolymer chain was calculated from the Equation (7):

$$R = \frac{l_{XX}^R}{l_{XX}^e} \quad (7)$$

where l_{XX}^R and l_{Cap}^R represent the average lengths of glycolidyl or lactidyl (Equation (8)) and caproyl blocks (Equation (9)), respectively, in a completely random copolymer chain.

$$l_{XX}^R = \frac{k'+1}{2k'} \quad (8)$$

$$l_{Cap}^R = k'+1 \quad (9)$$

2.3.2. Gel Permeation Chromatography

The molar mass (M_n) and molecular mass distribution ($Đ$) were determined by gel permeation chromatography (GPC) on a Viscotek system comprising GPCmax and TDA 305 (triple detection array (TDA): RI, IV, LS) equipped with DVB Jordi gel column(s) (linear, mixed bed) in DCM as an eluent at 30 °C at a flow rate of 1.0 mL min^{-1}.

2.3.3. Cyto- and Genotoxicity

To assess the toxicity of polymeric materials, cytotoxicity and genotoxicity tests were carried out. In brief, the cytotoxicity of polymeric matrices was assessed using the neutral red uptake (NRU) test using BALB/c T3T clone A31 mice fibroblast cell line (American Type Culture Collection) in accordance with the International Organization for Standardization (ISO) 10993-5:2009 Annex A guideline [19]. The polymeric extracts for the assay were formed by incubating the sample in 1 mg mL^{-1} DMEM medium with 5% bovine serum for 24 h at 37 °C. Polyethylene film and latex were used as reference materials.

Genotoxicity of the polymeric materials was evaluated according to ISO 13829:2000 guideline [20] by the *Umu*-test with and without metabolic activation using *Salmonella typhimurium* TA3515/psk1002 (Deutsche Sammlung von Mikroorganismen und Zellkulturen GmbH, Braunschweig, Germany). The polymeric samples were incubated in PBS buffer (GIBCO) for 24 h at 37 °C. The 2-aminoanthracene and 4-nitroquinoline N-oxide were used as positive controls.

2.3.4. Thermal Properties

Thermogravimetric analysis (TGA) was performed with a TGA Q500 V20.7 (TA Instruments) under nitrogen flow (60 mL min^{-1}). The measurements were carried out at temperatures ranging from 35 to 600 °C, with a heating rate of 10 °C min^{-1} for the samples placed in an open platinum pan. In order to describe the process of thermal decomposition, the temperatures at which the sample lost 5%, 50%, and 95% of mass ($T_{5\%}$, $T_{50\%}$, and $T_{95\%}$ respectively), as well as the final temperature of thermal decomposition (T_f), were presented. Additionally, the temperature of the maximum rate of thermal decomposition (T_{max}) was determined as the maximum of differential TGA (DTGA) curve. Furthermore, the mass loss of the sample, i.e., the mass loss as a result of evacuation of residual solvents and moisture at the temperature of 150 °C (Δm_{150}), and total mass loss of the sample at a temperature of 600 °C (Δm_t), were calculated. Δm_t values were calculated in relation to the masses at 150 °C.

Differential scanning calorimetry (DSC) measurements were performed using a DSC Q200 instrument (TA Instruments) under nitrogen flow in the temperature range from −140 to 250 °C for the sample placed in aluminum pans, applying a heating rate of 10 °C min^{-1}.

For the characterization of the melting and the cold crystallization processes, peak temperatures (T_m and T_c respectively), onset temperatures (T_{on}), and melting and crystallization enthalpies (ΔH_m and ΔH_c, respectively) were determined. Based on the enthalpy values, the crystalline phase content (crystallinity, X_c) was calculated according to the following Equation (10):

$$X_c = \frac{\Delta H_m - \Delta H_c}{\sum_i (W_i \times \Delta H_{mi,100\%})} \quad (10)$$

where ΔH_m is enthalpy of melting, ΔH_c is enthalpy of cold crystallization and $\Delta H_{mi,100\%}$ is enthalpy of melting for a fully (100%) crystalline homopolymer (literature data). The values of 106 J g^{-1} [21], 136 J g^{-1} [22] and 191 J g^{-1} [23] for $\Delta H_{m,100\%}$ of PLA, PCL and polyglycolide were used respectively. W_i is the weight fraction of the Cap, LL and GG co-units in copolymers; for homopolymers, $W_i = 1$.

The glass transition temperature (T_g) was evaluated as its midpoint based on the first derivative of DSC curve (dDSC). The temperature value of the minimum of the effect generated on the dDSC curve was taken for this purpose [24]. Additionally, in order to estimate T_g of the copolymers, a simple Fox Equation (11) was used [25].

$$\frac{1}{T_g} = \frac{w_1}{T_{g1}} + \frac{w_2}{T_{g2}} \quad (11)$$

where T_g is the glass transition of copolymers constructed from components 1 and 2 with weight fractions w_1 and w_2, respectively. T_{g1} and T_{g2} are the glass transitions of the individual homopolymers 1 and 2, respectively.

3. Results and Discussion

3.1. Synthesis and Characterization of Polyesters

Four different polymer matrices were synthesized via ROP of CL, Gly and L-LA in the presence of the simple, inexpensive and nontoxic PEG200-$BiOct_3$ catalytic system. Bifunctional PEG200 was applied as a co-initiator, resulting in hydroxyl end-capped linear polyesters. The polymerization process was carried out at 110 °C and 130 °C. The molar ratio of the monomers to the catalyst was 100:1. The number average molecular weight (M_n) of synthesized polymers was controlled by the molar ratio of monomer to co-initiator, which was constant and equal to 100:1.

The ^1H NMR and ^{13}C NMR spectra of the synthesized polymers confirmed their structures. The polymers were obtained with a good monomer conversion (almost equilibrium conversion), acceptable yield and moderately narrow dispersities ($Đ$ = 1.23–2.59) (Table 1). The theoretical M_n of the polyesters was determined based on the original monomer and PEG200 content. However, the M_n values obtained by GPC were found to be different

(lower in most cases) from the theoretical ones. The most probable reason is contamination of the sample with moisture, which results in hydrolysis of monomer to hydroxyl byproducts capable of initiating polymerization. As a result, polyesters with lower M_n fractions (Figure 1) were produced, leading to an increase in $Đ$ [26].

Another explanation for the discrepancy in the data might be a transesterification process that occurred during the polymer chain growth. As a consequence, bond cleavage occurs, creating a modification in the distribution of comonomeric units in the polymer chain [17].

Figure 2 depicts the kinetics of the polymerization process. After 24 h, all monomers show complete conversion, verifying the mentioned earlier hypothesis that bismuth derivative catalysts are effective for ROP of cyclic esters. During the polymerization of PLACL, preferential ring opening towards lactide units was observed. L-LA conversion was almost quantitative after 5 h, but CL conversion was substantially slower, reaching 76%, 86%, and 100% after 5 h, 7 h, and 24 h, respectively. A similar trend was observed for homopolymers (PLA vs PCL). PLA reached almost quantitative conversion of L-LA after 7 h, compared to 93% conversion of CL for PCL.

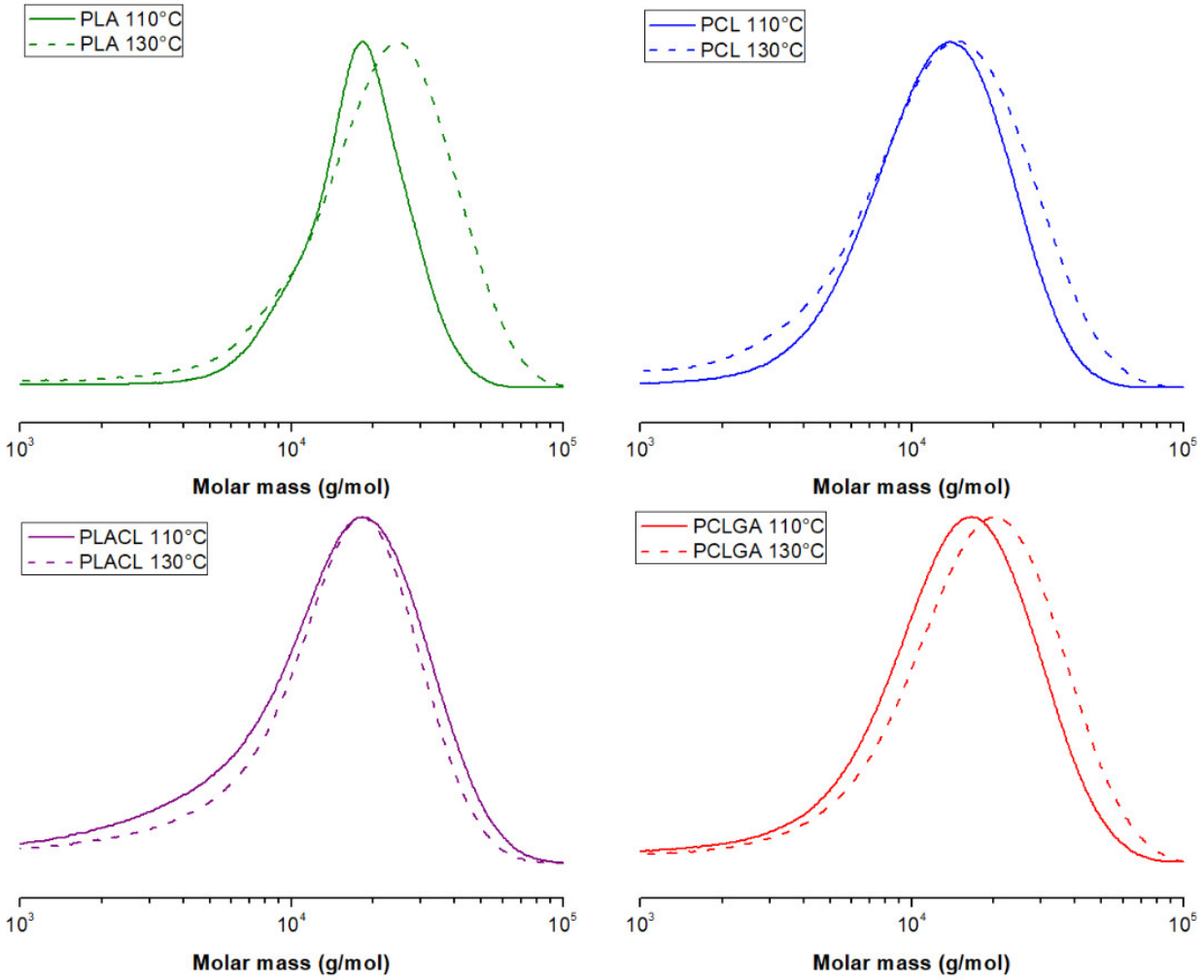

Figure 1. GPC traces for the polymers synthesized in 110 °C (solid line) vs. 130 °C (dashed line).

Table 1. Homo- and copolymerization of CL, Gly and L-LA. Temperature-dependent optimization (24 h, PEG200:$BiOct_3$ = 1:1).

Sample	Molar Ratio	Temp. (°C)	Yield (%)	$Conv_i$ [a] (%)	M_n [b] (kDa)	M_n [c] (kDa)	$Đ$ [c]
PLA poly(L-lactide)	L-LA = 1.0	110	73	100	11.7	15.5	1.23
	L-LA = 1.0	130	85	100	13.9	15.3	1.64
PCL poly(ε-caprolactone)	CL = 1.0	110	50	94	11.4	8.8	1.67
	CL = 1.0	130	68	100	12.2	6.9	2.33
PLACL poly(L-lactide-*co*-ε-caprolactone)	L-LA = 0.45 CL = 0.55	110	64	99 (L-LA) 90 (CL)	13.6	7.3	2.50
	L-LA = 0.50 CL = 0.50	130	56	100 (L-LA) 100 (CL)	10.2	9.7	1.87
CLGA poly(ε-caprolactone-*co*-glycolide)	CL = 0.84 GG = 0.16	110	60	100 (Gly) 99 (CL)	11.5	6.8	2.59
	CL = 0.86 GG = 0.14	130	73	100 (Gly) 100 (CL)	10.3	11.8	1.66

[a]—calculated from ^{1}H NMR; [b]—calculated from the feed ratio [c]—determined from GPC.

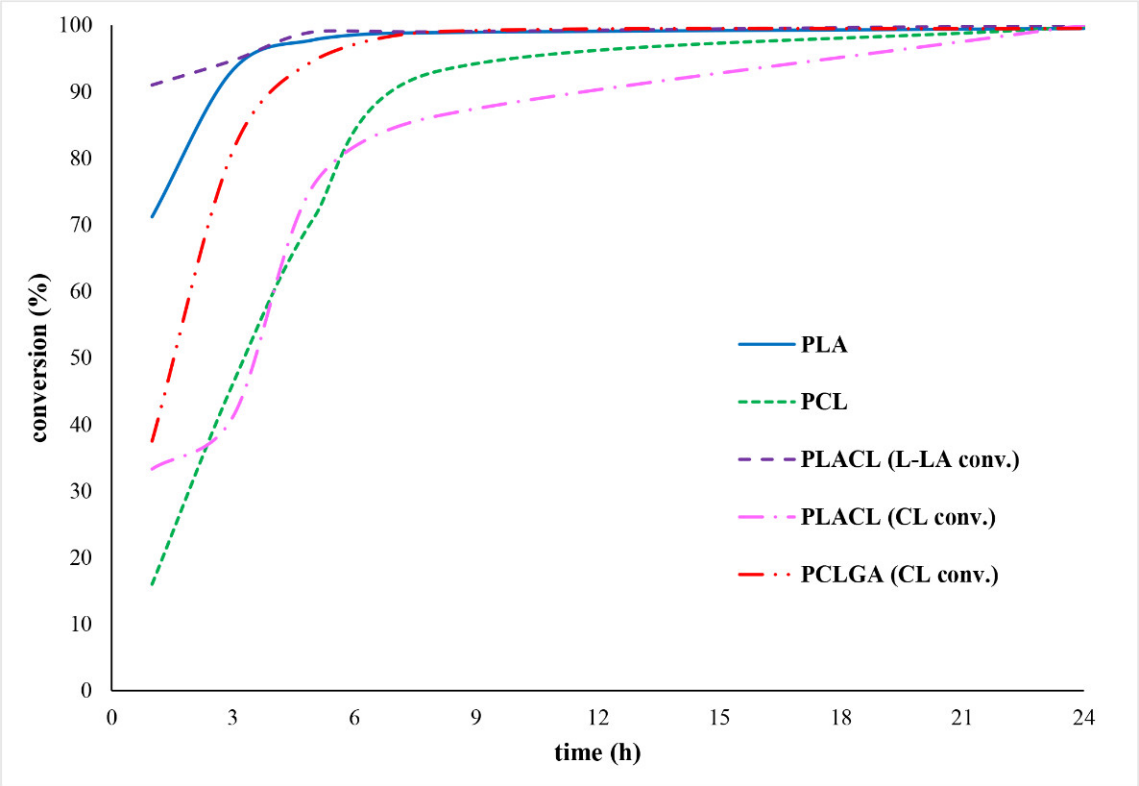

Figure 2. The polymerization kinetics of polymeric carriers (130 °C, PEG200:$BiOct_3$ = 1:1).

The polymerization conditions were optimized in terms of time, temperature, and catalyst content, and were selected based on monomer conversion, yield, and M_n agreement with the theoretical value. The optimal polymerization conditions were set at 24 h and 130 °C, with the exception of PLA, which had an optimum temperature of 110 °C.

The polymerization process was then optimized for the lowest catalyst content while not influencing the properties of the formed polymer matrices (conversion degree, M_n, polydispersity index). Polymers were produced with a high yield and a monomer conversion close to 1. The dispersity values ranged between 1.29 and 1.75, of which the lowest value

was observed for PLA. The M_n of the synthesized polymers was sufficiently consistent with the theoretically expected values (Table 2).

Table 2. Homo- and copolymerization of CL, Gly and L-LA. Catalyst content-dependent optimization (24 h, 130 °C (110 °C for PLA), monomer:PEG200 = 100:1).

Sample	Monomer/ Catalyst Molar Ratio	Molar Ratio	Yield (%)	$Conv_i$ [a] (%)	M_n [b] (kDa)	M_n [c] (kDa)	$Đ$ [c]
PLA	500	L-LA = 1.0	90	98	12.1	12.3	1.29
PCL	400	CL = 1.0	70	100	11.7	10.8	1.59
PLACL	300	L-LA = 0.52 CL = 0.48	79	99 (L-LA) 99 (CL)	12.6	14.9	1.55
PCLGA	1000	CL = 0.85 GG = 0.15	78	100 (Gly) 98 (CL)	11.8	10.4	1.75

[a]—calculated from ^{1}H NMR; [b]—calculated from the feed ratio; [c]—determined from GPC.

TGA and DTGA curves are presented in Figure 3a,b. The characteristic values of temperature, where the samples reach particular decomposition steps of 5%, 50% and 95% ($T_{5\%}$, $T_{50\%}$ and $T_{95\%}$), as well as T_f and T_{max}, are summarized in Table 3. Only small amounts of residues were observed at 600 °C, suggesting complete thermal decomposition of polymers into volatile products.

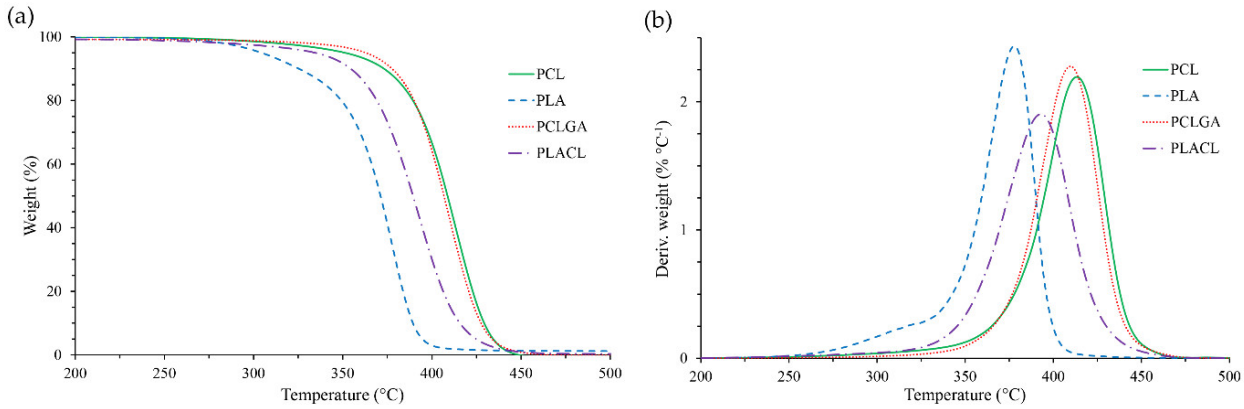

Figure 3. TGA (**a**) and DTGA (**b**) plots of the obtained polymeric carriers.

Table 3. Thermal decomposition of polymeric matrices.

Sample	Δm_{150} (%)	Δm_t (%)	$T_{5\%}$ (°C)	$T_{50\%}$ (°C)	$T_{95\%}$ (°C)	T_{max} (°C)	T_f (°C)
PLA	0.02	98.77	304.5	371.2	394.6	377.9	414.9
PCL	0.01	100.00	351.4	408.8	434.4	413.3	464.5
PLACL	0.62	99.03	339.3	389.6	424.9	393.3	464.0
PCLGA	0.58	99.50	365.4	406.9	433.8	409.8	475.6

The data show the following sequence of thermal stability PCL ≥ PCLGA > PLACL > PLA. It was found that PLA was the least thermally stable polymer. However, the presence of Cap units in the copolymer chain significantly increased the thermal stability of PLACL, as shown by the shift of temperature of particular decomposition steps of thermal decomposition (compare PLACL and PLA, Table 3). For example, the shift of T_{max} value was equal to 15 °C in relation to PLA. To the contrary, only a small effect of GG units on thermal stability of PCLGA in relation to PCL was observed. In such cases, T_{max} shifted 3.5 °C down.

The curves display a one-step degradation in the case of PCL, PCLGA and PLACL (Figure 3a,b). This confirms high homogeneity of both co-polymers, like the PCL homopolymer. However, in the case of PLA, a slight shoulder on DTGA curve (with max at ca. 320 °C, Figure 3b) was observed. This suggests the occurrence of an additional step of polymer decomposition. Despite very low dispersity of PLA ($Đ$ = 1.26), it can be supposed that in the first step (at low temperature), the fraction of the polymer characterized by the lower M_n (Figure 1) started to decompose.

Temperatures of glass transition (T_g), cold crystallization (T_c) and melting (T_m), as well as onset temperatures (T_{on}) of melting and crystallization, enthalpy of melting (ΔH_m), enthalpy of cold crystallization (ΔH_c) and degree of crystallinity (X_c), are listed in Table 4.

Table 4. Thermal parameters of polymeric matrices determined from DSC.

Sample	T_g (°C)	T_c (°C)	T_{on} [a] (°C)	T_m (°C)	T_{on} [b] (°C)	ΔH_c (J g^{-1})	ΔH_m (J g^{-1})	X_c (%)
PLA	54.4	104.6	102.1	158.9	156.9	15.5	51.4	33.9
PCL	−62.9	nd	nd	60.8	55.7	nd	128.5	98.1
PLACL	−12.3	nd	nd	nd	nd	nd	nd	0.0 [c]
PCLGA	−56.2	−23.1	−29.1	20.0 28.3	13.8	54.7	76.5	15.1

[a]—cold crystallization process; [b]—melting process; [c]—amorphous; nd—not detected.

The distribution of the crystallites organization is an important factor influencing the processes. As seen in the DSC thermogram, upon heating of the PLA sample (Figure 4a) at temperature above glass transition, two processes are observed, i.e., crystallization (so called cold crystallization; exothermal effect), followed by melting (endothermal effect). The exothermal process may result from the release of energy due to rearranging of molecules into a lower energy configuration. This results in formation of the better organized (crystalline) phase [27,28]. The molten polymer is characterized by a higher energy compared to the crystalline phase. Due to the changes in the polymer energy states taking place at heating, energy is released or absorbed, which can be observed as exothermal or endothermal effects. Similarly, in the case of PCLGA, both crystallization and melting are observed at heating (Figure 4c). In comparison, only the melting endotherm was observed during heating of PCL (Figure 4b), which can be related to the high crystalline phase content determined for this polymer (X_c = 98%). On the contrary, no effects of crystallization or melting are observed in the case of PLACL. This suggests an amorphous nature of the copolymer.

The single glass transition (Table 4) was observed in all cases, confirming good homogeneity of the obtained polymers. This process is clearly visible in the case of PLA (from 51.0 °C to 56.4 °C), PLACL (from −15.7 °C to −8.8 °C) and PCLGA (from −59.2 to −54.4 °C), and very difficult for detection in the case of PCL (from −63.1 °C to −62.5 °C). Additionally, the values of T_g, calculated from the Equation (11), for both copolymers PLACL (−17.0 °C) and PCLGA (−52.4 °C) are in good agreement with the measurements (−12.3 °C and −56.2 °C, respectively).

Thermal properties of all synthesized polymers are in close agreement with the literature data: PLA (X_c = 35% [29], T_g = 55–65 °C, T_m = 145–183 °C [30,31]); PCL (T_g = −60 °C, T_m = 60 °C [32]; PLACL/50:50 (T_g = 4 °C, T_m = 158 °C [33]); PCLGA of low Gly content (T_g = −60 °C, T_m = 54 °C [34,35]). It is known that molecular weight, monomer composition, and crystalline and rigid amorphous fractions development strictly affect thermal properties of polymers [30,33,36]. Therefore, some discrepancies in the results are probably due to chemical and structural differences in materials.

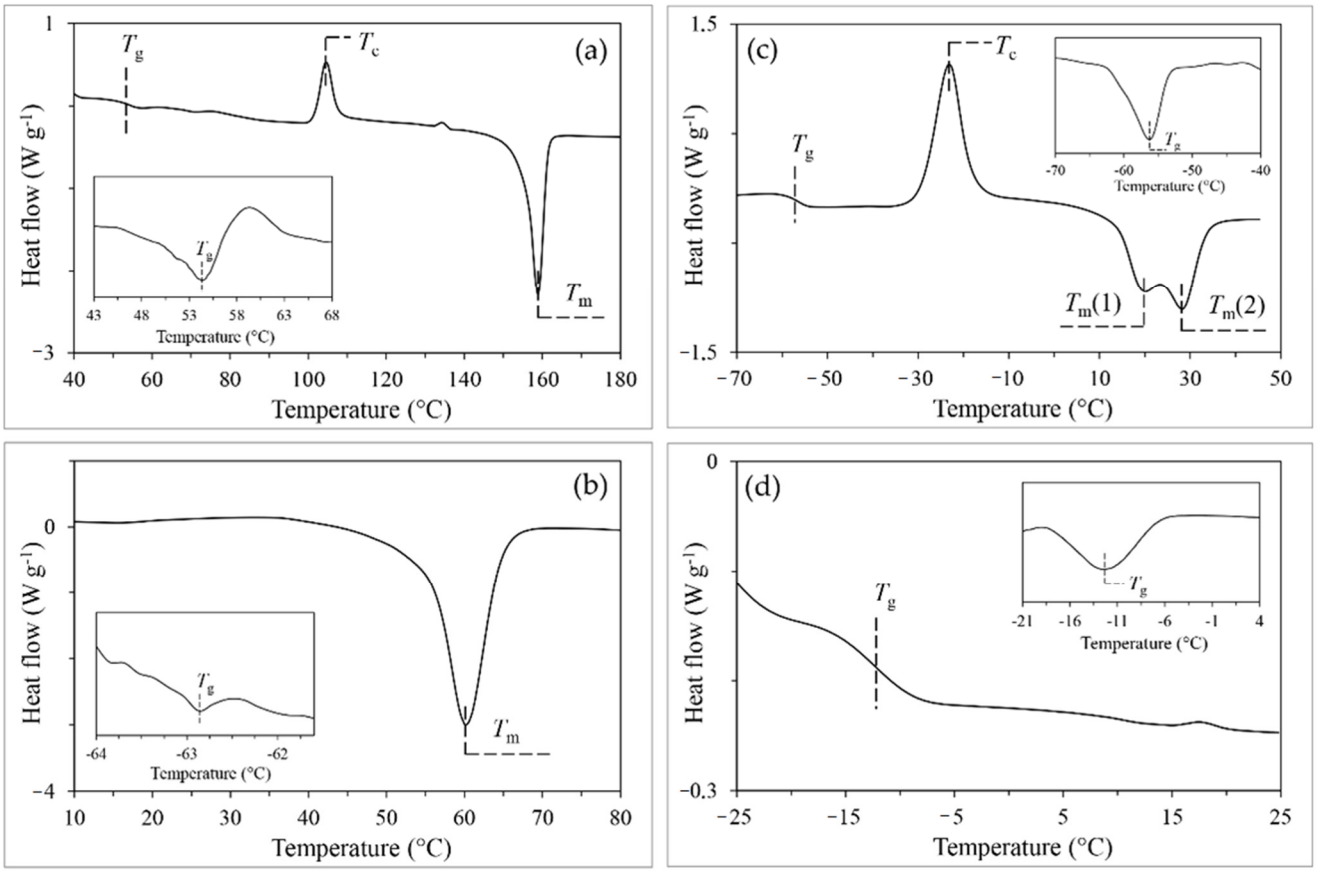

Figure 4. DSC thermograms of (**a**) PLA, (**b**) PCL, (**c**) PCLGA and (**d**) PLACL. DDSC curves in miniatures (determination of T_g).

The differences between thermal properties of homo- and copolymers might be discussed in terms of the differences in composition and the reactions leading to their syntheses. Therefore, while PLA and PCL polymers are both crystalline (Figure 3a,b), PLACL is amorphous (Figure 4d). The amorphous state of PLACL may be due to transesterification reactions occurring during the synthesis. Bond scissions in comonomeric units of the copolymer chain lead to shortening of LL and Cap block segments. As a result, the transesterification process increases the randomness of comonomer units along the chain and disrupts the crystallization process, hence reducing the size of crystallites. This conclusion corresponds to the results of D'Auria et al. [33], who analyzed random copolymers of LA and CL. The authors concluded that distribution of comonomers along the chain affects thermal behavior of the copolymer. The copolymers with low comonomer content (LA = 0.1 and CL = 0.1) and long sequences of the prevailing comonomer unit (l_{Cap} = 12.2 and l_{LL} = 11.1 respectively) were crystalline, while the copolymer with LA content (LA = 0.3) was amorphous, and only small amounts of crystalline phase were observed for the copolymers with the compositions LA = 0.7 and LA = 0.5, for which average lengths of comonomer sequences (l_{LL} and l_{Cap}) were in the range of 1.3–3.2.

In the case of the PCLGA, the melting endotherm with two minima in the temperature range of 10–40 °C was observed (Figure 4c). This might be connected to the presence of two types of crystallites differing in size and/or morphology. Accordingly, small, poorly organized crystallites start melting at lower temperature, while the larger crystallites characterized by the better ordered structure melt at higher temperature. Among the others, this might result due to the possible presence of two different blocks in the copolymer chain: Cap units reach domain and GG units reach domain. However, this explanation seems insufficient considering the appearance of the single glass transition and the course of the thermal decomposition process showing rather good homogeneity of the material. Cold

crystallization occurring during heating at low temperature might also lead to the formation of less perfect crystallites due to possible reorganization of the amorphous fraction, as well as the improvement of the structure of the crystallites resulting directly after synthesis. This may result in a diversification of the material, in which blocks of different organization will become present. However, the most likely hypothesis (remaining in substantial consent with the above), seems to be that in this temperature range, two processes (endothermal and exothermal) occur simultaneously, and the thermal effects of these processes overlap. Initially, the melting of the less crystallized fraction (endothermal) begins, followed by melt crystallization (exothermal). The new crystallites formed gradually in this way, with a higher degree of organization, melt at a higher temperature, which is still accompanied by an endothermal effect.

3.2. Structural Characterization of the Synthesized Polyester Carriers

As previously stated, the type of catalyst used and the transesterification process during synthesis have a strong influence on the microstructure of the polymers formed [1]. It was demonstrated that the structure of polymers may be controlled by modifying the kind of catalyst and the polymerization process parameters. Higher ROP process temperatures, for example, result in more random copolymers as a result of T_{II}, which induces redistribution of comonomer units in the polymer chain [1].

The structure of homopolymers and the chain microstructure of copolymers were investigated using ^{1}H and ^{13}C NMR spectroscopy. The characteristic signals were assigned based on the literature [14,16,37,38] and verified the structure of the obtained PCL, PLA, PLACL and PCLGA.

The ^{1}H NMR spectrum of the synthesized PCL: 4.22 ppm (-O-$(CH_2)_5$- C(O)-O-C**H$_2$**-CH_2-O-CH_2-CH_2-O-), 4.06 ppm (-O-C**H$_2$**-CH_2-CH_2-CH_2-CH_2-C(O)-), 3.69 ppm (-O-$(CH_2)_5$-C(O)-O-CH_2-C**H$_2$**-O-CH_2-CH_2-O-), 3.65 ppm (HO-C**H$_2$**-CH_2-CH_2-CH_2-CH_2-C(O)-) + (-O-$(CH_2)_2$-O-C**H$_2$**-C**H$_2$**-O-$(CH_2)_2$-O-), 2.31 ppm (-O-CH_2-CH_2-CH_2-CH_2-C**H$_2$**-C(O)-), 1.65 ppm (-O-CH_2-C**H$_2$**-CH_2-C**H$_2$**-CH_2- C(O)-), 1.38 ppm (-OC-CH_2-CH_2-C**H$_2$**-CH_2-CH_2- C(O)-).

The ^{1}H NMR spectrum of the synthesized PLA: 5.17 ppm (-O(O)C-(**H**)C(CH_3)-), 4.36 ppm (-O(O)C-(**H**)C(CH_3)-OH), 4.28 ppm (-O-CH_2-C**H$_2$**-O(O)C-$(CH_2)_5$-O-), 3.68 ppm (-O-C**H$_2$**-CH_2-O(O)C-$(CH_2)_5$-O-), 3.62 ppm (-O-$(CH_2)_2$-O-C**H$_2$**-C**H$_2$**-O-$(CH_2)_2$-O-), 1.59 ppm (-O(O)C-(H)C(C**H$_3$**)-).

The examination of the copolymers spectra, namely the ^{1}H NMR spectra of PCLGA (CL:Gly = 85:15) (Figure 5) and the ^{13}C NMR spectra of PLACL (CL:L-LA = 50:50) (Figure 6), allowed us to assign spectral lines to corresponding comonomeric sequences of PCLGA (Table 5) and PLACL (Table 6). Using the Equations (2)–(9) [14–16], the distribution of comonomeric units in the polymer chain was determined in accordance with the published data.

The copolymer of low monomer content (Gly = 0.15 and CL = 0.85) characterized longer sequences of prevailing comonomer unit (l_{Cap} = 2.82 and l_G = 1.02) and low crystallinity (X_c = 15.1 %), while PLACL (L-LA = 0.5 and CL = 0.5), having similar average lengths of comonomer sequences (l_L and l_{Cap}) of 2.80 and 1.41 respectively, was amorphous. The quantitative evaluation of their characteristic sequences (CapGCap and CapLCap) clearly demonstrates the effect of T_{II}, which lead to unit redistribution in the examined copolymer chains (Table 7). High T_{II} value and random structure characterize the copolymers (R = 1.07 for PLACL and R = 1.33 for PCLGA).

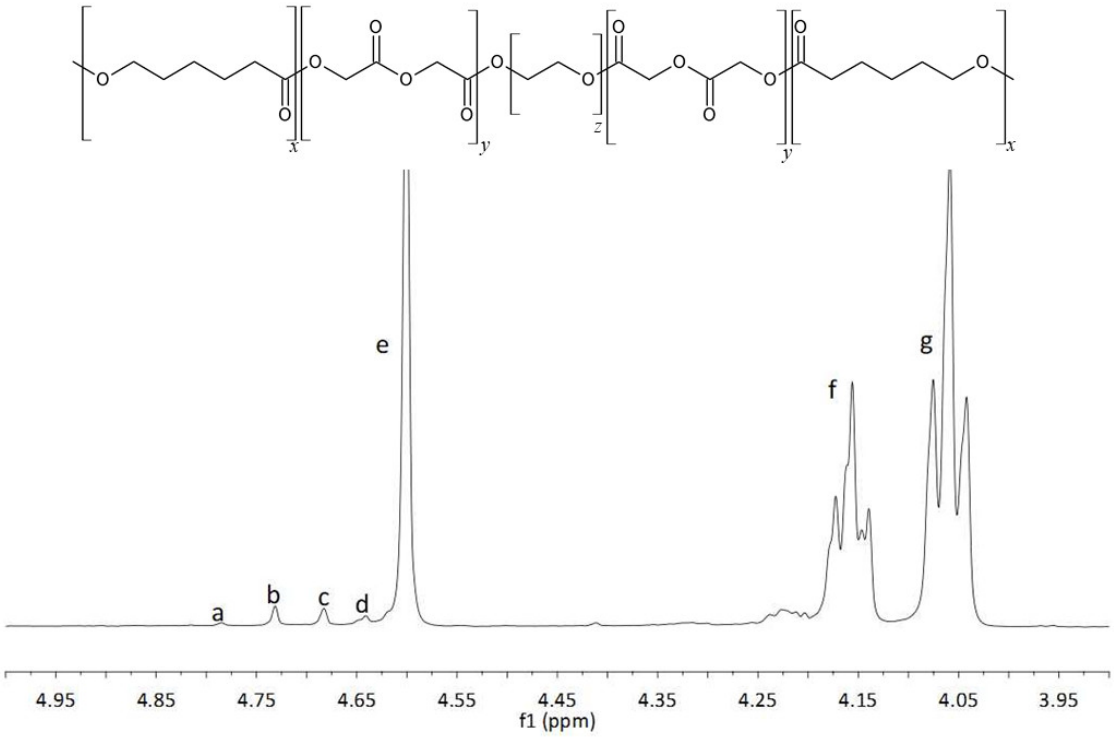

Figure 5. ^{1}H NMR spectrum of PCLGA.

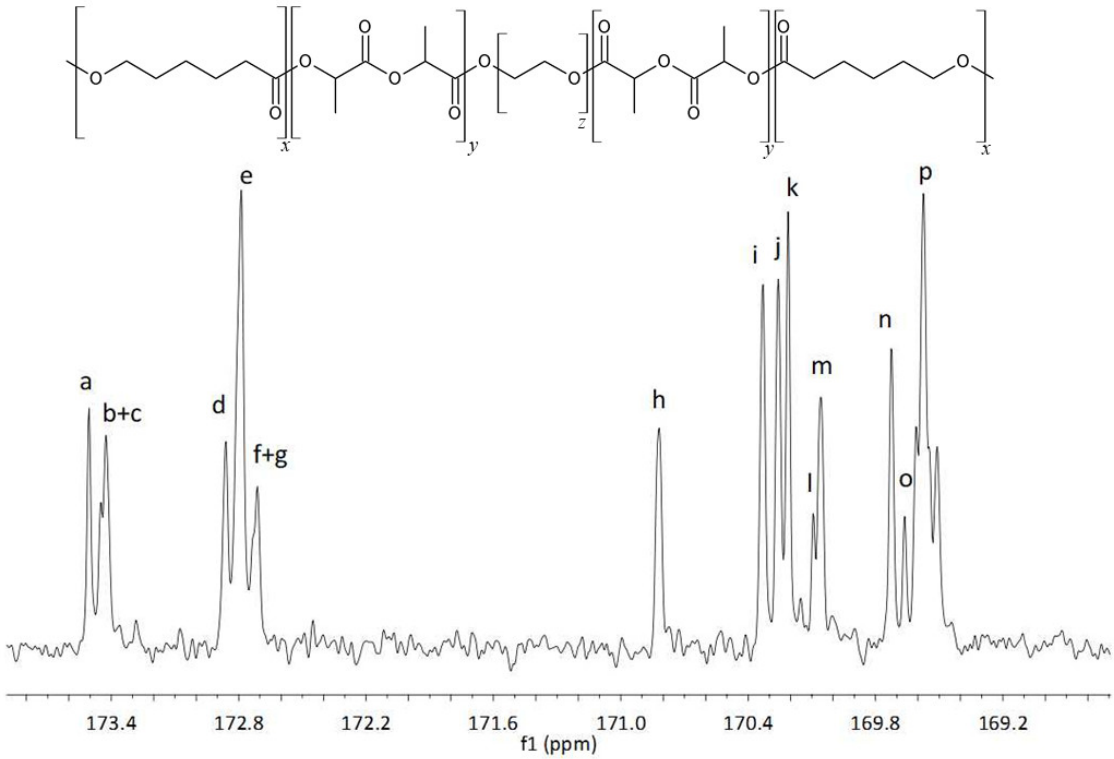

Figure 6. ^{13}C NMR spectrum of PLACL, region of carbonyl carbon atoms of ε-oxycaproyl and lactidyl units.

Table 5. Chemical shifts in ^{1}H NMR spectrum of PCLGA.

Signal	δ [ppm]	Sequence
a	4.79	G G G
b	4.73	Cap **G** G
c	4.68	G **G** Cap
d	4.64	Cap **G G** Cap
e	4.60	Cap **G** Cap
f	4.16	G **Cap**
g	4.06	Cap **Cap**

Table 6. Chemical shifts in ^{13}C NMR spectrum of PLACL, region of carbonyl carbon atoms of ε-oxycaproyl and lactidyl units.

Signal	δ [ppm]	Sequence
a	173.59	Cap **Cap** Cap
b	173.45	Cap L **Cap** Cap
c	173.43	L L **Cap** Cap
d	172.86	Cap **Cap** L L
e	172.79	L L **Cap** L L
f	172.73	Cap L **Cap** L Cap
g	172.71	L L **Cap** L Cap
h	170.82	Cap **L** Cap
i	170.33	Cap L L **L** Cap + L L L **L** Cap
j	170.26	Cap L **L** Cap
k	170.21	Cap **L** L Cap
l	170.09	Cap **L** L L Cap
m	170.06	Cap **L** L L L
n	160.73	L L **L** L Cap
o	169.66	Cap L **L** L Cap
p	169.57	L L **L** L L + Cap L **L** L L

Table 7. Structural characteristics of PLACL and PCLGA (synthesis parameters: 24 h, 130 °C).

Kind of Copolymer/Molar Ratio	The Average Length of the Blocks	T_{II}	R
poly(L-lactide-*co*-ε-caprolactone) PLACL/50:50	l_L^e = 2.80 l_{CL}^e = 1.41	0.70	1.07
poly(ε-caprolactone-*co*-glycolide) PCLGA/85:15	l_G^e = 1.02 l_{CL}^e = 2.82	0.96	1.33

l_L^e—experimental average length of lactyl blocks; l_{CL}^e—experimental average length of caproyl blocks; l_G^e—experimental average length of glycolyl blocks; R—randomization ratio; T_{II}—yield of the second mode of transesterification.

3.3. Cyto- and Genotoxicity

The polyesters produced in this work are intended for biomedical uses, such as drug carriers in anticancer DDSs. Despite the fact that the drug cargo has substantial cytotoxic activity, the polymeric matrices are intended to be cell and gene neutral. As a result, the four

representatives of synthesized polyesters were evaluated for cytotoxicity and genotoxicity (Table 8).

Table 8. Results of the *umu*-test and the NRU test in contrast to the untreated control at the highest concentrations of tested extracts [1 mg mL^{-1}].

Sample	Genotoxicity Assay		Cytotoxicity Assay
	IR [a] **± SD**	***IR*** [b] **± SD**	**Cells Viability ± SD [%]**
PLA	0.96 ± 0.02	0.75 ± 0.11	102 ± 2
PCL	0.94 ± 0.11	0.79 ± 0.08	100 ± 1
PLACL	0.87 ± 0.03	0.82 ± 0.14	108 ± 6
PCLGA	1.04 ± 0.11	0.78 ± 0.14	97 ± 4

[a] version without metabolic activation, [b] version with metabolic activation.

The NRU test was used for the cytotoxicity testing. The quantitative estimation of viable cells in tested cultures was based on their ability to accumulate the dye in their lysosomes. The viability of BALB/c 3T3 cells was not reduced below 70% as compared to the untreated control by any of the tested dilutions. As a result, all examined polymers may be declared nontoxic in the NRU assay.

The *umu*-test was performed to assess the genotoxic potential of the produced polymeric materials. The growth of *Salmonella typhimurium* determining the toxicity of tested samples was evaluated by a measurement of optical density. All tested samples were not toxic for the *Salmonella typhimurium* (bacteria growth > 0.5) with and without metabolic activation. Furthermore, the induction ratio (*IR*), which represents a sample's genotoxic potential, was <1.5 for all examined materials. This indicates that none of the produced polymers were genotoxic.

3.4. The Possibility of Employing the Produced Polymers as Carriers of Therapeutic Drugs

Polyesters are one of the most significant groups of biodegradable polymers. Homo-, co-, and terpolymers of L-LA, *rac*-LA, CL, and Gly are widely employed in medicine, e.g., as drug carriers [3,6,39]. The advantage of DDSs over traditional drug forms is from controlled and sustained drug release in the body, which is influenced, among other things, by the microstructure of the chain [40] and the composition of the polymer carrier [41]. Polyesters are distinguished mostly by their tunable microstructure and chemistry. As a consequence, their properties may be effectively optimized (e.g., drug release profile, degradation time, structure targeting). In our study, the synthesis conditions were optimized in terms of time, temperature, and catalyst content, which is important for biomedical applications because residuals of the catalyst may contaminate the obtained material. ^{1}H and ^{13}C NMR studies confirmed the polymer structures and complete monomer conversion. Low molar mass homopolymers and atactic copolymers synthesized in the presence of $BiOct_3$ exhibit no cyto- or genotoxicity. Based on our previous experience, the obtained polyesters with a statistical microstructure can be used in the technology of short-term DDSs systems. Furthermore, a high randomization ratio of the polyester chains may be favorable owing to a more uniform drug release profile as a result of the polymer's homogeneous hydrolytic degradation.

A recent comparison of data from the synthesis of biodegradable polymers using bismuth catalysts has been published [7]. The results reported herein confirm the existing data and demonstrate the tremendous potential of $BiOct_3$ to create random polymers. The findings are consistent with Kricheldorf's research [5,7,42], who has been investigating the utilization of Bi(III) compounds, such as bismuth subsalicylate and bismuth(III) n-hexanoate, in the polymerization of biodegradable polymers. Similarly, in our study the polymers were obtained with a high yield. The catalyst enabled complete monomer conversion with excellent reactivity. $BiOct_3$ encouraged random distribution of comonomer units along the chain, and the polymerization process produced polymers with low $Đ$.

We are currently conducting additional research on paclitaxel-DDSs derived from these polymers. The preliminary findings of our research enable us to confirm our hypotheses. In our next article, we will present detailed results from structural, physicochemical, and biological investigations (in vitro and in vivo) of these DDSs.

4. Conclusions

Four various biodegradable polymeric matrices were synthesized via ROP of CL, Gly and L-LA in the presence of non-toxic PEG200-$BiOct_3$ catalytic system. The catalyst system characterizes high productivity by means of small amounts of the catalyst needed for the polymerization process. The structures of the resulted polyesters correspond well to theoretical assumptions. The polymers showed low polydispersity index and M_n consistent with theoretical values. The polymers were analyzed by means of their structure and thermal properties. The results are consistent with the literature data. $BiOct_3$ catalysts efficiently promoted homo- and copolymerization of CL, Gly, and L-LA in a variable range of monomer compositions, which were coherent with monomer feed ratios. Nevertheless, the transesterification reactions contributed to some extent to the structures with more randomized distribution of monomers along the copolymer chains.

Thermal analysis showed single glass transition temperatures indicating good homogeneity of the polymers. The amorphous nature of PLACL and low ordering of PCLGA deduced from the DSC curves are in accordance with random microstructures of the copolymers.

The results showed that $BiOct_3$ is a well-suited catalyst, particularly for L-LA, for which preferential ring opening in relation to CL is observed during the polymerization process. The resulted polymers did not show neither cytotoxicity nor genotoxicity. Additionally, taking into account the extraordinarily low toxicity, $BiOct_3$ is a particularly attractive "green" catalyst for ROP of biodegradable polyesters, especially these predicted for contact with the living organisms, including drug delivery systems.

Author Contributions: I.M.D.: conceptualization, chemical, structural, analytical and pharmaceutical research, methodology, investigation, formal analysis, and writing—original draft; A.Z. (Anna Zgadzaj): biological research, methodology, investigation; A.Z. (Aldona Zalewska): DSC measurement and analysis; A.P.: GPC measurement and analysis; S.K.: GPC measurement and analysis; E.O.: investigation, formal analysis, and writing—original draft and editing; K.C.: investigation, formal analysis, and writing—original draft and editing; M.S.: conceptualization, chemical, structural, analytical and pharmaceutical research, investigation, writing—original draft, editing, and supervision. All authors have read and agreed to the published version of the manuscript.

Funding: This work was founded by the FW23/N/21:MAT Statutory Project of Medical University of Warsaw, 1 Banacha St., 02-097 Warsaw, Poland.

Institutional Review Board Statement: Not applicable.

Informed Consent Statement: Not applicable.

Data Availability Statement: The data presented in this study are available on request from the corresponding author.

Acknowledgments: The contribution of Izabela M. Domańska was realized within the Project No POWR.03.02.00-00-I009/17-00 (Operational Project Knowledge Education Development 2014–2020 co-financed by European Social Fund).

Conflicts of Interest: The authors declare that they have no known competing financial interests or personal relationships that could appear to have influenced the work described in this paper.

Sample Availability: Samples of all compounds are available from the authors.

References

1. Orchel, A.; Jelonek, K.; Kasperczyk, J.; Dobrzynski, P.; Marcinkowski, A.; Pamula, E.; Orchel, J.; Bielecki, I.; Kulczycka, A. The Influence of Chain Microstructure of Biodegradable Copolyesters Obtained with Low-Toxic Zirconium Initiator to In Vitro Biocompatibility. *BioMed Res. Int.* **2013**, *2013*, e176946. [CrossRef] [PubMed]
2. Żółtowska, K.; Sobczak, M.; Olędzka, E. Novel Zinc-Catalytic Systems for Ring-Opening Polymerization of ε-Caprolactone. *Molecules* **2015**, *20*, 2816–2827. [CrossRef]
3. Żółtowska, K.; Oledzka, E.; Kuras, M.; Skrzypczak, A.; Nałęcz-Jawecki, G.; Sobczak, M. Cyto- and genotoxicity evaluation of the biomedical polyesters obtained in the presence of new zinc catalytic systems. *Int. J. Polym. Mater. Polym. Biomater.* **2017**, *66*, 768–772. [CrossRef]
4. Yang, P.B.; Davidson, M.G.; Edler, K.J.; Brown, S. Synthesis, Properties, and Applications of Bio-Based Cyclic Aliphatic Polyesters. *Biomacromolecules* **2021**, *22*, 3649–3667. [CrossRef]
5. Kricheldorf, H.R.; Weidner, S.M.; Scheliga, F. Synthesis of cyclic poly(L-lactide) catalyzed by Bismuth Salicylates—A combination of two drugs. *J. Polym. Sci. Part A Polym. Chem.* **2019**, *57*, 2056–2063. [CrossRef]
6. Kasiński, A.; Zielińska-Pisklak, M.; Kowalczyk, S.; Plichta, A.; Zgadzaj, A.; Oledzka, E.; Sobczak, M. Synthesis and Characterization of New Biodegradable Injectable Thermosensitive Smart Hydrogels for 5-Fluorouracil Delivery. *Int. J. Mol. Sci.* **2021**, *22*, 8330. [CrossRef]
7. Kricheldorf, H.R. Syntheses of Biodegradable and Biocompatible Polymers by Means of Bismuth Catalysts. *Chem. Rev.* **2009**, *109*, 5579–5594. [CrossRef]
8. Huang, B.-H.; Dutta, S.; Lin, C.-C. 1.39—Main-Group Catalysts for Lactide Polymerization. In *Comprehensive Inorganic Chemistry*, 2nd ed.; Elsevier: Amsterdam, The Netherlands, 2013; Volume 1, pp. 1217–1249. [CrossRef]
9. Rodilla, V.; Miles, A.T.; Jenner, W.; Hawksworth, G.M. Exposure of cultured human proximal tubular cells to cadmium, mercury, zinc and bismuth: Toxicity and metallothionein induction. *Chem. Biol. Interact.* **1998**, *115*, 71–83. [CrossRef]
10. Kowalik, M.; Masternak, J.; Barszcz, B. Recent Research Trends on Bismuth Compounds in Cancer Chemoand Radiotherapy. *CMC* **2019**, *26*, 729–759. [CrossRef]
11. Kricheldorf, H.R.; Rost, S. A-B-A-Triblock and multiblock copolyesters prepared from ε-caprolactone, glycolide and L-lactide by means of bismuth subsalicylate. *Polymer* **2005**, *46*, 3248–3256. [CrossRef]
12. Kricheldorf, H.R.; Serra, A. Polylactones. 6. Influence of various metal salts on the optical purity of poly(L-lactide). *Polym. Bull.* **1985**, *14*, 497–502. [CrossRef]
13. Żółtowska, K.; Piotrowska, U.; Oledzka, E.; Sobczak, M. Efficient Diethylzinc/Gallic Acid and Diethylzinc/Gallic Acid Ester Catalytic Systems for the Ring-Opening Polymerization of rac-Lactide. *Molecules* **2015**, *20*, 21909–21923. [CrossRef] [PubMed]
14. Kasperczyk, J. Copolymerization of glycolide andε-caprolactone, 1. Analysis of the copolymer microstructure by means of ^{1}H and ^{13}C NMR spectroscopy. *Macromol. Chem. Phys.* **1999**, *200*, 903–910. [CrossRef]
15. Kasperczyk, J.; Bero, M. Coordination polymerization of lactides, 2. Microstructure determination of poly[(L,L-lactide)-co-(ε-caprolactone)] with ^{13}C nuclear magnetic resonance spectroscopy. *Makromol. Chem.* **1991**, *192*, 1777–1787. [CrossRef]
16. Kasperczyk, J.; Bero, M. Coordination polymerization of lactides, 4. The role of transesterification in the copolymerization of L,L-lactide and ε-caprolactone. *Makromol. Chem.* **1993**, *194*, 913–925. [CrossRef]
17. Bero, M.; Czapla, B.; Dobrzyński, P.; Janeczek, H.; Kasperczyk, J. Copolymerization of glycolide and ε-caprolactone, 2[a] Random copolymerization in the presence of tin octoate. *Macromol. Chem. Phys.* **1999**, *200*, 911–916. [CrossRef]
18. Dobrzynski, P. Synthesis of biodegradable copolymers with low-toxicity zirconium compounds. III. Synthesis and chain-microstructure analysis of terpolymer obtained from L-lactide, glycolide, and ε-caprolactone initiated by zirconium(IV) acetylacetonate. *J. Polym. Sci. A Polym. Chem.* **2002**, *40*, 3129–3143. [CrossRef]
19. International Organization for Standardization. *EN ISO 10993-5:2009 Biological Evaluation of Medical Devices—Part 5: Tests for In Vitro Cytotoxicity (ISO 10993-5:2009)*; Annex A Neutral Red Uptake (NRU) Cytotoxicity Test; International Organization for Standardization: Geneva, Switzerland, 2009.
20. International Organization for Standardization. *ISO/FDIS 13829:2000 Water Quality-Determination of the Genotoxocity of Water and Waste Water Using the Umu-Test*; International Organization for Standardization: Geneva, Switzerland, 2000.
21. Sarasua, J.-R.; Prud'homme, R.E.; Wisniewski, M.; Le Borgne, A.; Spassky, N. Crystallization and Melting Behavior of Polylactides. *Macromolecules* **1998**, *31*, 3895–3905. [CrossRef]
22. Tiptipakorn, S.; Keungputpong, N.; Phothiphiphit, S.; Rimdusit, S. Effects of polycaprolactone molecular weights on thermal and mechanical properties of polybenzoxazine. *J. Appl. Polym. Sci.* **2015**, *132*, 41915. [CrossRef]
23. Magazzini, L.; Grilli, S.; Fenni, S.E.; Donetti, A.; Cavallo, D.; Monticelli, O. The Blending of Poly(glycolic acid) with Polycaprolactone and Poly(L-lactide): Promising Combinations. *Polymers* **2021**, *13*, 2780. [CrossRef]
24. Cieśla, K.; Watzeels, N.; Rahier, H. Effect of gamma irradiation on thermophysical properties of plasticized starch and starch surfactant films. *Radiat. Phys. Chem.* **2014**, *99*, 18–22. [CrossRef]
25. Rzepna, M.; Sadło, J.; Przybytniak, G.; Iuliano, A. Impact of electron beam treatment on copolymers of polylactide and poly(trimethylene carbonate) in an air atmosphere. *J. Appl. Polym. Sci.* **2021**, *138*, 50184. [CrossRef]
26. Plichta, A.; Kowalczyk, S.; Olędzka, E.; Sobczak, M.; Strawski, M. Effect of structural factors on release profiles of camptothecin from block copolymer conjugates with high load of drug. *Int. J. Pharm.* **2018**, *538*, 231–242. [CrossRef]

27. Zhao, H.; Zhu, Y.; Sha, L. Study of the relationship between characteristics of aramid fibrids and mechanical property of aramid paper using DSC. *e-Polymers* **2014**, *14*, 139–144. [CrossRef]
28. Derakhshandeh, M.; Noroozi, N.; Schafer, L.L.; Vlassopoulos, D.; Hatzikiriakos, S.G. Dynamics of partially miscible polylactide-poly(ε-caprolactone) blends in the presence of cold crystallization. *Rheol. Acta* **2016**, *55*, 657–671. [CrossRef]
29. Bliley, J.M.; Marra, K.G. Chapter 11—Polymeric Biomaterials as Tissue Scaffolds. In *Stem Cell Biology and Tissue Engineering in Dental Sciences*; Vishwakarma, A., Sharpe, P., Shi, S., Ramalingam, M., Eds.; Academic Press: Boston, MA, USA, 2015; pp. 149–161. [CrossRef]
30. Fernández, J.; Etxeberria, A.; Sarasua, J.-R. Synthesis, structure and properties of poly(L-lactide-co-ε-caprolactone) statistical copolymers. *J. Mech. Behav. Biomed. Mater.* **2012**, *9*, 100–112. [CrossRef] [PubMed]
31. Fukushima, K.; Tabuani, D.; Abbate, C.; Arena, M.; Rizzarelli, P. Preparation, characterization and biodegradation of biopolymer nanocomposites based on fumed silica. *Eur. Polym. J.* **2011**, *47*, 139–152. [CrossRef]
32. Burg, K. Poly(α-ester)s′. In *Natural and Synthetic Biomedical Polymers*; Kumbar, S.G., Laurencin, C.T., Deng, M., Eds.; Elsevier: Oxford, UK, 2014; pp. 115–121. [CrossRef]
33. D'Auria, I.; Lamberti, M.; Rescigno, R.; Venditto, V.; Mazzeo, M. Copolymerization of L-Lactide and ε-Caprolactone promoted by zinc complexes with phosphorus based ligands. *Heliyon* **2021**, *7*, e07630. [CrossRef]
34. Pamula, E.; Dryzek, E. Structural Changes in Surface-Modified Polymers for Medical Applications. *Acta Phys. Pol. A* **2008**, *113*, 1485–1493. [CrossRef]
35. Turek, A.; Stoklosa, K.; Borecka, A.; Paul-Samojedny, M.; Kaczmarczyk, B.; Marcinkowski, A.; Kasperczyk, J. Designing Biodegradable Wafers Based on Poly(L-lactide-co-glycolide) and Poly(glycolide-co-ε-caprolactone) for the Prolonged and Local Release of Idarubicin for the Therapy of Glioblastoma Multiforme. *Pharm. Res.* **2020**, *37*, 90. [CrossRef]
36. Ahmed, J.; Varshney, S.K. Polylactides—Chemistry, Properties and Green Packaging Technology: A Review. *Int. J. Food Prop.* **2011**, *14*, 37–58. [CrossRef]
37. Liu, C.B.; Gong, C.Y.; Huang, M.J.; Wang, J.W.; Pan, Y.F.; Zhang, Y.D.; Li, G.Z.; Gou, M.L.; Wang, K.; Tu, M.J.; et al. Thermoreversible gel–sol behavior of biodegradable PCL-PEG-PCL triblock copolymer in aqueous solutions. *J. Biomed. Mater. Res.* **2008**, *84B*, 165–175. [CrossRef] [PubMed]
38. Jiang, Z.; Deng, X.; Hao, J. Thermogelling hydrogels of poly(ε-caprolactone-co-D,L-lactide)–poly(ethylene glycol)–poly(ε-caprolactone-co-D,L-lactide) and poly(ε-caprolactone-co-L-lactide)–poly(ethylene glycol)–poly(ε-caprolactone-co-L-lactide) aqueous solutions. *J. Polym. Sci. A Polym. Chem.* **2007**, *45*, 4091–4099. [CrossRef]
39. Efthimiadou, E.K.; Theodosiou, M.; Toniolo, G.; Abu-Thabit, N.Y. Stimuli-responsive biopolymer nanocarriers for drug delivery applications. In *Stimuli Responsive Polymeric Nanocarriers for Drug Delivery Applications*; Makhlouf, A.S.H., Abu-Thabit, N.Y., Eds.; Woodhead Publishing: Sawston, UK, 2018; pp. 405–432. [CrossRef]
40. Żółtowska, K.; Piotrowska, U.; Oledzka, E.; Luchowska, U.; Sobczak, M.; Bocho-Janiszewska, A. Development of biodegradable polyesters with various microstructures for highly controlled release of epirubicin and cyclophosphamide. *Eur. J. Pharm. Sci.* **2017**, *96*, 440–448. [CrossRef]
41. Xu, Y.; Kim, C.-S.; Saylor, D.M.; Koo, D. Polymer degradation and drug delivery in PLGA-based drug-polymer applications: A review of experiments and theories. *J. Biomed. Mater. Res. B Appl. Biomater.* **2017**, *105*, 1692–1716. [CrossRef]
42. Kricheldorf, H.R.; Bornhorst, K.; Hachmann-Thiessen, H. Bismuth(III) *n*-Hexanoate and Tin(II) 2-Ethylhexanoate Initiated Copolymerizations of ε-Caprolactone and L -Lactide. *Macromolecules* **2005**, *38*, 5017–5024. [CrossRef]

Journal of Drug Delivery Science and Technology 90 (2023) 105115

Contents lists available at ScienceDirect

Journal of Drug Delivery Science and Technology

journal homepage: www.elsevier.com/locate/jddst

The influence of electron beam and gamma irradiation on paclitaxel-loaded nanoparticles of fully randomized copolymers in relation to potential sterilization

Izabela M. Domańska [a], Aldona Zalewska [b], Krystyna Cieśla [c], Andrzej Plichta [b], Wojciech Głuszewski [c], Monika Łyczko [c], Sebastian Kowalczyk [b], Ewa Oledzka [a], Marcin Sobczak [a,*]

[a] Department of Pharmaceutical Chemistry and Biomaterials, Faculty of Pharmacy, Medical University of Warsaw, 1 Banacha Str., 02-097, Warsaw, Poland
[b] Faculty of Chemistry, Warsaw University of Technology, 3 Noakowskiego Str., 00-664, Warsaw, Poland
[c] Institute of Nuclear Chemistry and Technology, 16 Dorodna Str., 03-195, Warsaw, Poland

ARTICLE INFO

Keywords:
Drug delivery systems
Radiation sterilization
Electron beam
Gamma irradiation
Paclitaxel
Biodegradable polymers
Aliphatic polyesters
Nanoparticles

ABSTRACT

The presented report describes the evaluation of the influence of e-beam and γ-radiation on properties of the newly developed anticancer drug delivery systems (DDSs) based on biodegradable polymeric matrices: poly (ε-caprolactone) (PCL), poly(L-lactide) (PLA), poly(L-lactide-*co*-ε-caprolactone) (PLACL) and poly(ε-caprolactone-*co*-glycolide) (PCLGA), in relation to potential sterilization process. The physicochemical properties of the pharmaceutical formulations of paclitaxel (PTX)-loaded nanoparticles, as well as the basic polymeric matrices, were studied after irradiation with γ-rays and e-beam at sterilization dose 25 kGy. The structure of the polymers was found to be practically intact after the irradiation. Importantly, no PTX-related degradation products were detected after the irradiation. The results demonstrate, that the polyester based DDSs can realize sustained and controlled release of PTX. The kinetics of drug release were defined as first order with non-Fickian diffusion for all systems. The obtained results demonstrated a great potential of e-beam for the sterilization purposes of polymeric nanoparticles. In comparison, some effect on PTX release from the γ-irradiated copolymeric nanoparticles was observed due to faster polymer degradation.

1. Introduction

Cancer is one of the main causes of death worldwide. According to World Health Organization, in 2020, cancer was responsible for nearly one in six deaths [1]. It is therefore of great importance to provide new solutions and new drug forms in combination with the drugs already used in the cancer treatment. Paclitaxel (PTX) is one of the most effective antineoplastic agent, widely used in the treatment of breast, ovarian, and non-small cell lung cancers, along with Kaposi's sarcoma, leukemias and urologic malignancies [2,3]. However, despite natural origin, its low aqueous solubility is challenging in relation to the method of administration [3]. Therefore, efforts are being made in order to develop new PTX delivery systems.

Encapsulation is a well-known technique for the incorporation of an active substance in another inert material. It allows to isolate the external environment from the drug, and thus reduce the side effects of the active ingredient, enhance tumor deposition and improve therapeutic efficacy. Nevertheless, drug carriers must meet a number of criteria, such as biocompatibility and the stability during processing and sterilization. One of the most important polymers used in the drug delivery systems (DDSs) technology are biodegradable and bioresorbable aliphatic polyesters. However, these polyesters are sensitive to heat and moisture. The high temperatures utilised in the sterilization process may affect the physicochemical and mechanical characteristics of the polymer matrix, influencing the drug release profile. The use of chemicals (e.g. ethylene oxide) may leave some toxic residues and filtration under aseptic conditions is limited by the pores of membrane (Ø = 0.22 μm). As an alternative final sterilization technique, European Pharmacopoeia (Ph. Eur.) allows the exposure to ionizing radiation in the form of γ-rays

* Corresponding author.
E-mail addresses: izabela.domanska@wum.edu.pl (I.M. Domańska), aldona.zalewska@pw.edu.pl (A. Zalewska), k.ciesla@ichtj.waw.pl (K. Cieśla), andrzej.plichta@pw.edu.pl (A. Plichta), w.gluszewski@ichtj.waw.pl (W. Głuszewski), m.lyczko@ichtj.waw.pl (M. Łyczko), sebastian.kowalczyk@pw.edu.pl (S. Kowalczyk), eoledzka@wum.edu.pl (E. Oledzka), marcin.sobczak@wum.edu.pl (M. Sobczak).

https://doi.org/10.1016/j.jddst.2023.105115
Received 5 April 2023; Received in revised form 19 October 2023; Accepted 27 October 2023
Available online 7 November 2023

Abbreviations

ACN	acetonitrile
$BiOct_3$	bismuth(III) 2-ethylhexanoate
^{13}C NMR	carbon-13 nuclear magnetic resonance
CL	ε-caprolactone
Cap	ε-oxycaproyl unit
Đ	dispersity index (GPC)
DCM	dichloromethane
DDSs	drug delivery systems
DLS	dynamic light scattering
DSC	differential scanning calorimetry
EE	encapsulation efficiency
G	glycolyl unit
GG	glycolidyl unit
Gly	glycolide
GPC	gel permeation chromatography
ΔH_C	enthalpy of cold crystallization
ΔH_m	enthalpy of melting
^1H NMR	hydrogen nuclear magnetic resonance
HPLC	high-performance liquid chromatography
l	average length of blocks
L	lactyl unit
L-LA	L-lactide
LL	lactidyl unit
MC	macrocyclic content
M_n	number average molecular mass
n	number of replicates
PBS	phosphate-buffered saline
PCL	poly(ε-caprolactone)
PCLGA	copolymer of glycolide and ε-caprolactone
PDI	dispersity index (DLS)
PEG200	polyethylene glycol (M_n = 200 Da)
PGA	polyglycolide
Ph. Eur.	European Pharmacopoeia
PLA	poly(L-lactide)
PLACL	copolymer of L-lactide and ε-caprolactone
PTX	paclitaxel
PVA	poly(vinyl alcohol)
R	randomization ratio
ROP	ring opening polymerization
SEM	scanning electron microscopy
T_C	temperature of cold crystallization
TFA	trifluoroacetic acid
T_g	glass transition temperature
TGA	thermogravimetric analysis
T_{II}	transesterification of the second mode
T_m	temperature of melting
$T_{5\%}$	temperature of 5 % weight loss
$T_{50\ \%}$	temperature of 50 % weight loss
$T_{95\ \%}$	temperature of 95 % weight loss
T_f	final temperature of thermal decomposition
T_{max}	temperature of the maximum rate of thermal decomposition
X_C	degree of crystallinity
ZP	zeta potential

or fast electrons. A dose of 25 kGy is recommended for this purpose [4,5]. This method is particularly suitable for the polymers heat-sensitive. However, during irradiation, crosslinking and degradation processes might be induced in the polymers [6]. There is a number of already published research dealing with the effect of radial sterilization on polymeric matrices [7–11]. However, a detailed research on the influence of ionizing radiation on each particular medicinal formulation need to be carry out independently for each formulation [5].

In the present study, we investigate the influence of ionizing radiation (sterilization dose, 25 kGy) on PTX-loaded nanoparticles based on synthesized polymer matrices enabling sustained delivery of the drug substance. In addition, we examined the impact of ionizing radiation on PCL, PLA, PLACL, and PCLGA using two types of ionizing radiation (γ-rays, EB). We present a potential "green" catalyst system based on bismuth 2-ethylhexanoate.

2. Materials and methods

2.1. Materials

L-Lactide (L-LA, (3S)-*cis*-3,6-Dimethyl-1,4-dioxane-2,5-dione, 98 %), ε-caprolactone (CL, 2-Oxepanone, 98 %), poly(vinyl alcohol) (PVA, M_w = 13–23 kDa, 87–89 % hydrolyzed), Cremophor® EL and poly(ethylene glycol) (PEG200, M_n = 200 Da) were purchased from Sigma-Aldrich Co. (Poznań, Poland). Glycolide (Gly, 1,4-Dioxane-2,5-dione, 98 %) was purchased from TCI Europe N.V. Co. (Zwijndrecht, Belgium) and bismuth 2-ethylhexanoate ($BiOct_3$) from Alfa Aesar Co., part of Thermo Fisher Scientific (Kandel, Germany). Methanol (CH_3OH, analytical pure), chloroform ($CHCl_3$, analytical pure), dichloromethane (DCM, CH_2Cl_2, analytical pure) and hydrochloric acid (HCl, 35–38 %) were obtained from POCH Co. (Gliwice, Poland). Acetonitrile (ACN, gradient grade for liquid chromatography) and trifluoroacetic acid (TFA, ≥99.0 %) were purchased from Merck KGaA (Darmstadt, Germany), and phosphate-buffered saline (PBS, pH = 7.4) from Carl Roth GmbH + Co. KG (Karlsruhe, Germany). Paclitaxel (PTX, T45) was a generous gift from Medical University of Gdańsk (Gdańsk, Poland).

2.2. Methods

2.2.1. Synthesis of homo- and copolymers via ring opening polymerization

The polymeric matrices were synthesized in bulk by the ring opening polymerization (ROP) of CL, Gly and L-LA in various monomer compositions. As a result, 4 polymeric matrices were obtained, i.e.: poly(L-lactide) (PLA), poly(ε-caprolactone) (PCL), copolymer of L-LA and CL (PLACL, L-LA:CL = 1:1), and copolymer of Gly and CL (PCLGA, Gly:CL = 0.15:0.85).

The polymerization process was conducted in bulk, under dry argon atmosphere at 130 °C (or 110 °C for PLA), in the presence of PEG200 as a co-initiator and $BiOct_3$ as a catalyst. The catalyst to monomer ratios (C:M) were as follows: 1:500 (PLA), 1:400 (PCL), 1:300 (PLACL) and 1:1000 (PCLGA). The co-initiator to monomer ratio (I:M) was constant and was 1:100. After 24 h, more than 98 % of the monomer conversion was obtained for all polymers. The resulted polymers were precipitated with cold methanol and then dried under vacuum. The polymeric matrices were stored at 4 °C until further usage. A detailed course of the polymerization was described previously [12].

2.2.2. Preparation of paclitaxel-loaded nanoparticles

The nanoparticles were prepared by a single emulsion (o/w) solvent evaporation technique. Briefly, PTX was dissolved in DCM to a final concentration of 2 mg ml^{-1}. The solution was poured to a pre-weighed polymer and sonicated for 5 min in an ultrasonic cleaner (EMAG, Germany) to assure polymer proper dissolution. The drug to polymer ratio was 1:10 (w/w). The solution was added dropwise to a 1 % aqueous solution of PVA and emulsified using a high shear homogenizer, with 10,000 rpm (T25 digital ULTRA-TURRAX®, IKA) and then sonicated for 5 min with the amplitude of 70 % (Vibra Cell 505, SONICS & MATERIALS, INC, USA). The phase volume ratio of the emulsion was o/w =

1:10. The emulsion was left overnight on a magnetic stirrer (400 rpm) to remove the organic solvent and to solidify the nanoparticles. The suspension was then centrifuged with 20,000 rpm, 30 min (Optima XPN-80 Ultracentrifuge, BECKMAN COULTER) and washed twice to remove the residual emulsifier. The resulting nanoparticles were freeze-dried and stored at 4 °C for further usage.

2.2.3. Irradiation of nanoparticles and polymeric matrices

Gamma irradiation of both, polymeric matrices and PTX-loaded nanoparticles was performed using ^{60}Co source in Gamma Chamber 5000 (BRIT, India). The samples were irradiated with a dose of 25 kGy at a dose rate of 1.8 kGy h^{-1} in air and at ambient temperature.

Electron irradiation was done in the linear electron accelerator Elektronika 10/10 with e-beam energy of 10 MeV using a dose of 25 kGy in air and at ambient temperature.

The irradiation process was performed at the Institute of Nuclear Chemistry and Technology in Warsaw, Poland.

2.2.4. Structural analysis of polymers

To determine the microstructure of the copolymers' chains NMR analysis was used. The ^{1}H spectra of the polymers were recorded at 400 MHz resonance frequency on an Agilent spectrometer, with 32 scans and 2.56 s acquisition time. The ^{13}C NMR spectra were obtained on a 300 MHz Varian spectrometer, with 10,000 scans and 1.73 s acquisition time. Deuterated chloroform was used as a solvent. The measurements were carried out at room temperature.

The microstructure of the copolymers was characterized by the characteristic parameters, such as the average lengths of lactidyl (l^{e}_{LL}), glycolidyl (l^{e}_{GG}) and caproyl (l^{e}_{Cap}) blocks, randomization ratio (R), and yield of the transesterification of the second mode (T_{II}). The parameters were calculated according to the equations presented in the literature [13,14].

As it is described in the literature [12,13,15], transesterification of the first mode is an intermolecular exchange of the lactidyl (–LL–) and glycolidyl (–GG–) units. Compared, transesterification of the second mode leads to the formation of lactyl (–L–) and glycolyl (–G–) units in the copolymer chain, due to intramolecular bond cleavage in the lactidyl or glycolidyl units. As a result, characteristic sequences, such as: CapLCap or CapGCap are formed. Quantitative analysis of the resulted comonomeric sequences clearly illustrates changes in polymer microstructure, caused by transesterification process, leading to redistribution of units in the copolymer chain. The yield of transesterification of lactyl ($T_{II}^{CapLCap}$) or glycolyl units ($T_{II}^{CapGCap}$) by a caproyl segment is described by the following equations:

$$T_{II}^{CapLCap} = \frac{[CapLCap]}{[CapLCap]_R} \tag{1}$$

$$T_{II}^{CapGCap} = \frac{[CapGCap]}{[CapGCap]_R} \tag{2}$$

where [CapLCap] and [CapGCap] are the experimental concentrations of CapLCap and CapGCap sequences respectively and $[CapLCap]_R$ and $[CapGCap]_R$ are the corresponding sequence in a completely randomized distribution of units in the copolymer chain.

Additionally, polymers' microstructure may be described by a coefficient R (eqs. (3) and (4)), that illustrates degree of randomness of a copolymer chain and attains the value of 0 for block structure, and 1 for a completely randomized copolymer chain [13]. The value of the coefficient R is the ratio of the average lengths of caproyl (l_{Cap}), lactidyl (l_{LL}) or glycolidyl (l_{GG}) microblocks calculated according to Bernoullian statistics (l^{R}) and the average lengths of respective microblocks determined experimentally (l^{e}):

$$R^{PLACL} = \frac{l^{R}_{Cap}}{l^{e}_{Cap}} = \frac{l^{R}_{LL}}{l^{e}_{LL}} \tag{3}$$

$$R^{PCLGA} = \frac{l^{R}_{Cap}}{l^{e}_{Cap}} = \frac{l^{R}_{GG}}{l^{e}_{GG}} \tag{4}$$

2.2.5. Gel permeation chromatography

The number average molecular mass (M_n) and dispersity index ($Đ$) were determined by gel permeation chromatography (GPC) on a Viscotek system comprising GPCmax and TDA 305 (triple detection array (TDA): RI, IV, LS) and equipped with DVB Jordi gel column(s) (linear, mixed bed). The analysis was performed in DCM as an eluent, at 30 °C and flow rate of 1.0 mL min^{-1}. The results were calculated using conventional calibration with set of 12 sharp polystyrene standards and refractometer as concentration detector.

2.2.6. MALDI-TOF-MS

MALDI-TOF Mass Spectrometry (MALDI-TOF-MS) was applied to estimate the content of macrocycles in the homopolymers (PCL and PLA). The experiments were performed in a linear mode using an ultrafleXtreme™ (Bruker Daltonics, Coventry, UK) mass spectrometer, equipped with a nitrogen laser and using a DCTB matrix. The PCL and PLA samples were dissolved in THF (5 mg mL^{-1}) and mixed with a solution of DCTB. The macrocyclic content (*MC*) was estimated based on the ratio of peak intensities for cyclic and linear polymers.

2.2.7. Thermal properties

Differential scanning calorimetry (DSC) measurements were conducted with a Q200 apparatus (TA Instruments) under nitrogen flow, in temperature range from −140 to 250 °C. The heating rate was 10 °C min^{-1}. Temperatures of melting (T_m), and of cold crystallization (T_c) were determined as the temperatures of the maxima of DSC thermal effect. Beside, enthalpies of melting (ΔH_m) and of cold crystallization (ΔH_c) were calculated basing these effects. Glass transition temperature (T_g) was determined as temperature of peak minimum on DDSC curve (derivative of DSC).

Additionally, crystalline phase content (crystallinity index, X_c) was calculated based on the enthalpy values (eq. (5)):

$$X_c = \frac{\Delta H_m - \Delta H_c}{\sum_i \left(W_i \times \Delta H_{mi,100\%}\right)} \tag{5}$$

where ΔH_m and ΔH_c are the enthalpies of melting and cold crystallization respectively, W_i is the weight fraction of the comonomeric units in the polymer and $\Delta H_{mi,100\ \%}$ is the enthalpy of melting for 100 % crystalline polymer: 106 J g^{-1} (PLA) [16], 136 J g^{-1} (PCL) [17] and 191 J g^{-1} (polyglycolide (PGA)) [18].

Thermogravimetric analysis (TGA) was performed with a TGA Q500 V20.7 (TA Instruments). The measurements were carried out under nitrogen flow (60 mL min^{-1}), in temperature range from 35 to 600 °C. The heating rate was 10 °C min^{-1}. Thermal decomposition of the polymers was analyzed by the temperatures at which the mass loss reached 5 %, 50 %, and 95 % ($T_{5\%}$, $T_{50\ \%}$, and $T_{95\ \%}$ respectively). The final temperature of decomposition (T_f) and the temperature at the maximum decomposition rate (T_{max} – peak temperature at the DTGA curve) were also determined.

2.2.8. Hydrolytic degradation of polymers

Hydrolytic degradation of the polymers was performed in PBS solution (pH = 7.4). Briefly, approx. 10–20 mg of a polymeric matrix was weighted and filled with 2 ml of medium. The samples were prepared individually for each measuring point. The polymers were incubated in 37 °C with shaking at 100 rpm. After certain time intervals, the medium was collected and dried in vacuum. The amount of polymer degradation products was calculated as a mass loss over the hydrolytic degradation time.

2.2.9. Dynamic light scattering

The average size, Z-average and dispersity index (PDI) of the prepared nanoparticles were measured by dynamic light scattering (DLS) using a Zetasizer Nano ZS analyzer (Malvern Panalytical Ltd, United Kingdom). For this purpose, an appropriate amount of the freeze-dried samples was resuspended in purified deionized water. The zeta-potential (ZP) was determined by electrophoresis in a capillary cell.

2.2.10. Scanning electron microscopy

The morphology of the PTX-loaded nanoparticles was examined by scanning electron microscopy (SEM), using the Ultra Plus microscope (ZEISS, Germany). The samples were placed on a metal stub and sputter-coated with a nanometric gold layer before the measurements.

2.2.11. HPLC analysis

The amount of PTX was determined by HPLC using a Beckman Coulter system (Miami, Florida, USA), equipped with a Triathlon 900 autosampler (Spark Holland B.V.; Emmen, the Netherlands). The system consisted of a secondary pump (System Gold® 125NM Solvent Module; Fullerton, CA, USA) and a UV/VIS detector (System Gold® 166 Detector; Fullerton, CA, USA). All controlled with LP-chrom software (version 2.61). Chromatographic separations were carried out using a thermostated column (Luna C18(2), 25 cm, 5 μm, 100A, Phenomenex).

The concentrations of PTX in the samples were determined by HPLC at $\lambda = 229$ nm, according to Stefanowicz et al. [3]. For this purpose, isocratic elution with a flow rate of 1 ml min^{-1} was applied. The mobile phase was the mixture of ACN, water and methanol = 60:2:38, with the addition of TFA (0.1 %). The temperature in the column was maintained at 30 °C.

To determine the drug content, a certain amount of freeze-dried nanoparticles was dissolved in ACN and sonicated for 5 min in ultrasonic cleaner. The concentration of PTX in the samples was measured by high-performance liquid chromatography (HPLC) at $\lambda = 229$ nm, using a calibration curve in the concentration range from 0.10 to 80.0 μg ml^{-1} ($R^2 = 0.9999$).

Encapsulation efficiency (*EE*) is the amount of the drug incorporated into nanoparticles in relation to the total drug added, and it was calculated according to the following equation (eq. (6)).

$$EE(\%) = \frac{m_e}{m_t} \times 100\% \tag{6}$$

where m_e is the amount of the drug entrapped in the nanoparticles and m_t is the total amount of drug added.

2.2.12. In vitro drug release study

In vitro drug release studies were carried out in PBS (pH = 7.4), using dialysis method. Importantly, in order to prevent the precipitation of the released PTX, Cremophor® EL (0.5 % (w/v)) was added to the buffer solution [3].

The freeze-dried nanoparticles, containing approx. 400 μg of PTX, were resuspended in the medium and introduced into a dialysis bag (MWCO = 3500 Da, Spectra/Por®). The end sealed dialysis membrane was submerged fully in 20 ml of the medium. The volume ratio of the inner to the outer phase was 1:10. The in vitro PTX release studies were carried out in triplicate at 37 °C in orbital shaker-incubator (ES-20, Biosan) over the time of 34 days for PLA and PLACL drug carriers. In case of PCL and PCLGA drug carriers, the study was extended to 56 days. At appropriate time intervals, 2 ml aliquots were withdrawn and replaced with equal volume of fresh medium. In order to prevent PTX degradation, the samples were stored at −20 °C for further analysis. The amount of PTX released from the nanoparticles was calculated in relation to the actual amount of the encapsulated drug.

2.2.13. Mathematical models

The results of PTX release were analyzed according to zero-order, first-order, Higuchi and Korsmeyer-Peppas mathematical models, according to equations 7–10 [19,20].

Zero order:

$$F = kt \tag{7}$$

First order:

$$logF = log\ F_0 - \frac{kt}{2.303} \tag{8}$$

Higuchi model:

$$F = k\sqrt{t} \tag{9}$$

Korsmeyer-Peppas model:

$$F = kt^n, for\ F < 0.6 \tag{10}$$

where: F – fraction of drug released in time (t); F_0 – initial concentration of the drug; k – model constant; n – release exponent.

To find out the mechanism of drug release, the release exponent n from Korsmeyer-Peppas model was used, as described in Table 1.

3. Results and discussion

3.1. Synthesis and characterization of polymers

We previously reported [12] $BiOct_3$ as an active initiator in the ROP of CL, Gly and L-LA, providing polymers with expected M_n and with low $Đ$. In the presence of PEG200 as a co-initiator, $BiOct_3$ showed a moderate activity in the ROP of CL and high reactivity in the case of L-LA and Gly. Importantly, the obtained polymers were not cyto- and genotoxic [12], what is critical in terms of biomedical applications.

Radiation sterilization of pharmaceutical products based on polyester nanoparticles is difficult because these polymers may undergo chain scission and/or cross-linking when exposed to radiation. As a result, the physicochemical properties of the DDSs may change, resulting in changes in drug release kinetic profiles. Therefore, a thorough investigation into the effects of ionizing radiation on the synthesized polymeric matrices was conducted in this study.

The microstructure of a polyester chain may be considered as a unique fingerprint of the polymer. It is an important factor influencing its other properties, such as crystallinity, that in turn affects degradation kinetic of the polymer. Therefore, a detailed analysis of characteristic parameters, such as average lengths of blocks (l) and randomization ratio of the copolymers was also performed.

The structures of the polymers before and after irradiation were investigated by means of ^1H and ^{13}C nuclear magnetic resonance (NMR) spectroscopy. The characteristic spectral lines were assigned to corresponding comonomeric sequences (Figs. 1 and 2) by analogy according to the literature [13,14,22,23]. Based on the presented results and our previous study [12], the obtained copolymers were of random structure and short average lengths of blocks, as the effect of transesterification reactions of the second mode, accompanying the polymerization process. No difference were found between the NMR spectra of the

Table 1
Interpretation of drug release mechanism using Korsmeyer-Peppas model [21].

n	Mechanism of drug transport
0.45	Fickian diffusion
$0.45 < n < 0.89$	non-Fickian
0.89	case II transport
>0.89	super case II transport

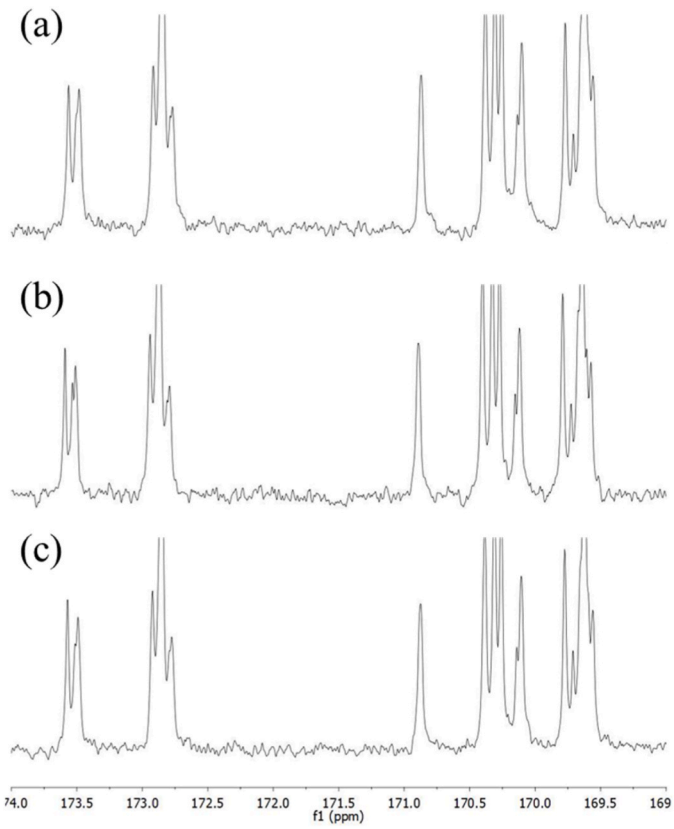

signal	δ [ppm]	sequence
a	173.59	Cap **Cap** Cap
b	173.45	Cap L **Cap** Cap
c	173.43	L L **Cap** Cap
d	172.86	Cap **Cap** L L
e	172.79	L L **Cap** L L
f	172.73	Cap L **Cap** L Cap
g	172.71	L L **Cap** L Cap
h	170.82	Cap **L** Cap
i	170.33	Cap L L **L** Cap + L L L **L** Cap
j	170.26	Cap L **L** Cap
k	170.21	Cap **L** L Cap
l	170.09	Cap **L** L L Cap
m	170.06	Cap **L** L L L
n	160.73	L L **L** L Cap
o	169.66	Cap L **L** L Cap
p	169.57	L L **L** L L + Cap L **L** L L

Fig. 1. The influence of ionizing radiation on ^{13}C NMR spectra of PLACL: non-irr (a), irr-γ (b) and irr-e$^-$ (c). Chemical shifts in ^{13}C NMR spectrum of PLACL, region of carbonyl carbon atoms of ε-oxycaproyl and lactidyl units.

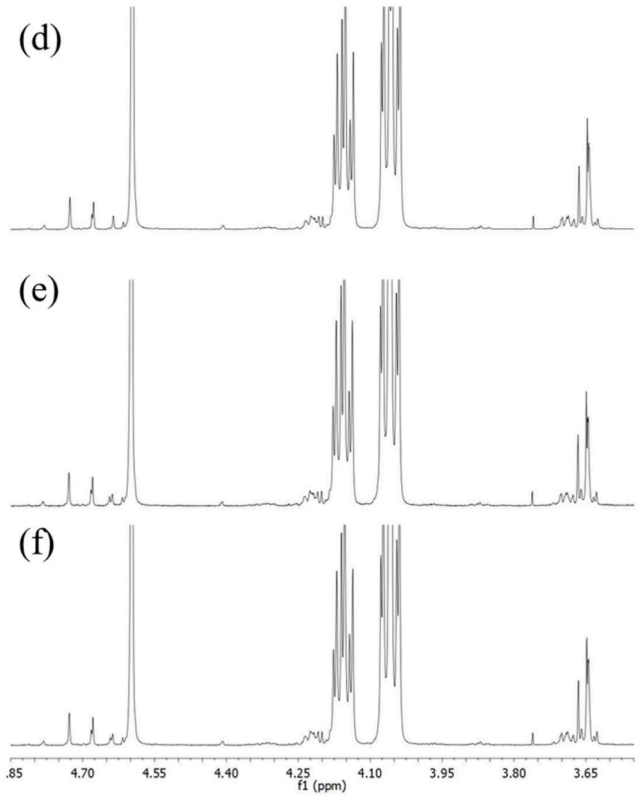

signal	δ [ppm]	sequence
a	4.79	G **G** G
b	4.73	Cap **G** G
c	4.68	G **G** Cap
d	4.64	Cap **G G** Cap
e	4.60	Cap **G** Cap
f	4.16	G **Cap**
g	4.06	Cap **Cap**

Fig. 2. The influence of ionizing radiation on ^{1}H NMR spectra of PCLGA non-irr (d), irr-γ (e) and irr-e$^-$ (f). Chemical shifts in ^{1}H NMR spectrum of PCLGA.

non-irradiated and the irradiated samples, independently whether irradiation was performed with γ-rays or with e-beam (Figs. 1 and 2). As shown in Table 2, irradiation had no effect on the distribution of comonomeric units in PLACL or PCLGA chains. A negligible change in randomization ratio after the irradiation of PLACL ($R_{non\text{-}irr} = 1.05$, $R_{irr\text{-}\gamma} = 1.09$, $R_{irr\text{-}e} = 1.06$) and PCLGA ($R_{non\text{-}irr} = 1.23$, $R_{irr\text{-}\gamma} = 1.20$, $R_{irr\text{-}e} = 1.22$) was observed. Concomitantly, the average lengths of copolymer blocks remained unaffected, that clearly demonstrates no substantial influence of the ionizing radiation at the sterilization dose on the microstructure of the analyzed polymers.

3.2. The influence of ionizing radiation on the molecular structure and physicochemical properties of polyesters

The presence of PEG200 with two hydroxyl end groups leads to the formation of linear polyesters. However, due to intramolecular transesterification, macrocyclic products may be formed in some extent [24]. In order to find whether cyclic oligo- and polyesters were formed during the polymerization process, the homopolymers were subjected to MALDI-TOF mass spectrometry. The results (Table 3) showed *MC* of 27.8 % in the case of PCL. In comparison, the *MC* of PLA was lower and was 13.4 %. The difference in the content of macrocycles between the homopolymers might be caused by the lower temperature applied during the polymerization process of PLA (110 °C) as compared to PCL (130 °C).

The synthesized polymers were irradiated using γ-rays and e-beam (25 kGy). As it is shown in Fig. 3, neither type of irradiation had a substantial effect on M_n of the homopolymers (≤10 % loss of initial M_n was noticed in case of PCL and PLA). Interestingly, only a very small difference between the influence of γ-rays and e-beam on the average molecular mass of the homopolymers was observed. These data are consistent with the *MC* values estimated by MALDI-TOF MS, showing a negligible difference between the non-irradiated and irradiated PCL and PLA. Altogether, the results suggested good resistance of PCL and PLA to irradiation.

In comparison, relatively higher decrease of M_n was observed for γ-irradiated copolymers. This effect was particularly noticeable for PCLGA, for which 28 % loss of initial M_n was observed (Table 3). Simultaneously, the results showed some increase in $Đ$ with decreasing M_n. This data may indicate, that chain scission is a dominant process taking place during the irradiation of the polymers in the gamma chamber at applied irradiation dose (25 kGy). The results showed, that the copolymers were more susceptible to γ-rays compared to the homopolymers. This may result from higher impact of γ-rays on short copolymer chains (compared to homopolymers studied), as already described by Athanasiou et al. [25].

Table 2
The influence of irradiation on the microstructure of PLACL and PCLGA.

Irradiation	PLACL			PCLGA		
	non-irr	γ-irr	e^--irr	non-irr	γ-irr	e^--irr
Mole Fraction of Units in the Copolymer	F_{LL} = 0.48	F_{LL} = 0.48	F_{LL} = 0.48	F_{GG} = 0.16	F_{GG} = 0.16	F_{GG} = 0.16
The Average Length of the Blocks	l^e_L = 2.70 l^e_{Cap} = 1.46	l^e_L = 2.69 l^e_{Cap} = 1.39	l^e_L = 2.82 l^e_{Cap} = 1.41	L^e_G = 1.14 l^e_{Cap} = 2.81	L^e_G = 1.18 l^e_{Cap} = 2.81	L^e_G = 1.15 l^e_{Cap} = 2.82
R	1.05	1.09	1.06	1.23	1.20	1.22
T_{II}	0.85	0.81	0.78	0.93	0.92	0.93

F_{LL} – mole fraction of lactidyl units in the copolymer; F_{GG} – mole fraction of glycolidyl units in the copolymer; l^e_L – experimental average length of lactyl blocks; l^e_{Cap} – experimental average length of caproyl blocks; l^e_G – experimental average length of glycolyl blocks; R – randomization ratio, T_{II} – yield of the second mode of transesterification.

Table 3
The influence of irradiation on structure and physicochemical properties of the polymeric matrices.

Polymer	Molar ratio	Irradiation	M_n (kDa)[a]	ΔM_n (%) [ab]	$Đ$[a]	MC[c] (%)
PCL	CL = 1.0	non-irr	20.7	n.a.	1.62	27.8 ± 7.9
		irr-γ	18.8	−9.2	1.68	27.9 ± 5.6
		irr-e^-	19.5	−5.8	1.58	31.1 ± 1.7
PLA	L-LA = 1.0	non-irr	20.2	n.a.	1.17	13.4 ± 2.0
		irr-γ	18.6	−7.9	1.21	14.9 ± 1.3
		irr-e^-	18.8	−6.9	1.21	12.4 ± 3.0
PLACL	L-LA = 0.5	non-irr	11.0	n.a.	2.40	n.a.
		irr-γ	9.6	−12.7	2.59	n.a.
	CL = 0.5	irr-e^-	11.6	+5.5	2.30	n.a.
PCLGA	Gly = 0.15	non-irr	12.4	n.a.	1.55	n.a.
		irr-γ	8.9	−28.2	2.15	n.a.
	CL = 0.85	irr-e^-	12.8	+3.2	1.51	n.a.

n.a. – not applicable; [a] – determined by GPC; [b] – M_n change compared to non-irradiated sample; [c] – determined by MALDI-TOF-MS.

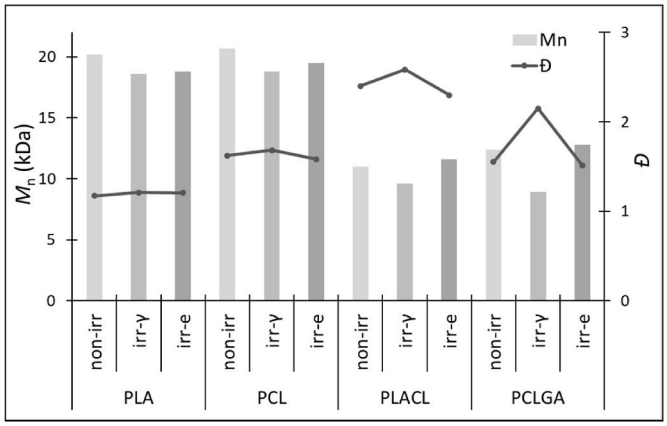

Fig. 3. The influence of ionizing radiation (dose 25 kGy) on the average molecular mass and dispersity index of the polymers.

In opposite, a slight overall increase of M_n was observed for the copolymers subjected to e-beam irradiation (5.5 % for PLACL and 3.2 % for PCLGA) along with decreasing their dispersity. Additionally, a detailed analysis of molar mass distribution (Fig. 4) clearly shows some increase in polymer fraction characterized by both, low and high values of molecular mass. It may suggest the contribution of cross-linking process along with chain scission during the irradiation of the copolymers with e-beam.

M_n change for all samples irradiated with e-beam was lower as compared to the samples irradiated with γ-rays. It may result from longer time of irradiation with γ-rays compared to e-beam in order to attain the equivalent dose. The ^{60}Co source characterized relatively low activity (dose rate of 1.8 kGy h^{-1}), that required long exposure time of the samples to γ-rays (ca. 14 h, while the use of e-beam required less than 1 min). Prolonged exposure of the polymers to irradiation could lead to continuous formation of new radicals over the time. Additionally, radicals density during irradiation in gamma chamber with such source was low and the possibility for recombination of two radicals at adjacent macromolecules was low. Therefore, degradation processes might occur with a high efficiency. To the contrary, in the case of electron irradiation, a high effective dose rate was applied leading to formation of a huge amount of radicals in short time. Therefore, due to

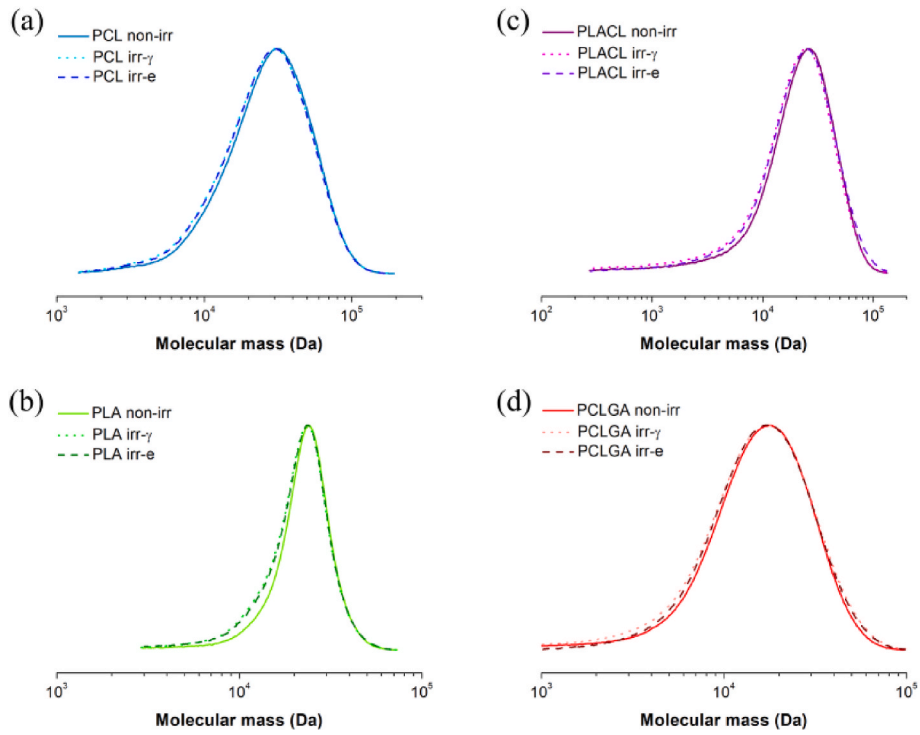

Fig. 4. The influence of ionizing radiation on the molecular mass distribution of polymers: PCL (a), PLA (b), PLACL (c), and PCLGA (d).

high density of free radicals in the material, the probability of meeting radicals formed on adjacent chains increased, and thus the subsequent reactions between these radicals with the formation of cross-links occurred with the higher efficiency. Accordingly, such conditions made more possible creation of crosslinks between the neighboring macromolecules. This might result in some increase in molecular mass of polymers.

Simultaneously, the differences between the relationship of degradation and cross-linking processes taking place in gamma chamber and in e-beam might be explained in terms of different exposure of polymers to air [26]. Irradiation in aerobic atmosphere allows alkyl radicals to react with oxygen, that result in the formation of peroxyl radicals, and thus oxidation products. Therefore, prolonged γ-irradiation in air leads to chain cleavage, accompanied by polymer oxidative degradation. To the contrary, the rapid irradiation with high dose of electrons acts similarly as irradiation in an inert gas atmosphere. This is because that diffusion of oxygen inwards the material is strongly limited in such a short time, therefore, the outer layers favor oxidative degradation, while crosslinking may occur inside the material [26]. This may explain the simultaneous occurrence of two processes: chain scissions and cross linking that can be concluded in the copolymers irradiated in e-beam, and finally the shift of the global resulting processes towards crosslinking.

The differences between the effect of irradiation in e-beam and in gamma chamber might be thus explained in terms of the concurrence of degradation and crosslinking processes.

3.3. *The influence of ionizing radiation on thermal properties of polyesters*

Even small changes in the microstructure or physicochemical properties (e.g. average molecular mass), can significantly affect thermal properties of the polymers. It may be related to the homogeneity and supramolecular structure of the polymers alike relationship between participation and distribution of the crystalline and amorphous regions. Therefore, a detailed thermal characterization is very important for comprehensive characterization of the polymers. In the present study, changes of thermal properties of the polymers as a result of their irradiation were analyzed commensurate with their microstructure and physicochemical properties. DSC measurements were repeated after subsequent 2 and 8 months in purpose to determine the possible changes in crystallinity of the semicrystlline polymers due to their storage.

The analyzed herein polymers characterized single T_g indicating their homogeneity, alike in our previous work [12]. DSC data (Table 4) proved high crystallinity of PCL (X_c almost 100 %), shown by large heat of melting. Simultaneously, PLA has appeared semicrystalline (X_c ca. 38 %). As concerns the copolymers, crystalline phase was observed only for PCLGA (Table 4), characterized by the predominance of caproyl blocks in PCLGA chain. It is shown by the appeareance of melting endotherm in

Table 4
The influence of ionizing radiation on thermal parameters of polymeric matrices determined from DSC.

Polymer	Irradiation	T_g (°C)	T_c (°C)	T_m (°C)	ΔH_c (J g^{-1})	ΔH_m (J g^{-1})	X_c (%)
PCL	non-irr	−62.9	nd	60.8	nd	128.5	98.1
	irr-γ	−59.4	nd	60.8	nd	130.4	99.5
	irr-e[-]	−59.7	nd	60.1	nd	131.1	100.0
PLA	non-irr	54.4	104.6	158.9	15.5	51.4	33.9
	non-irr[a]	60.0	108.1	163.0	23.4	63.6	37.9
	irr-γ[a]	58.8	105.7	160.2	22.8	68.6	43.2
	irr-e-[a]	58.1	106.1	160.6	23.8	68.2	41.9
PLACL	non-irr	−12.3	nd	nd	nd	nd	0.0[c]
	irr-γ	−9.8	nd	nd	nd	nd	0.0[c]
	irr-e[-]	−9.9	nd	nd	nd	nd	0.0[c]
PCLGA	non-irr	−56.2	−23.1	20.0 28.3	54.7	76.5	15.1
	non-irr[b]	−49.5	nd	20.4 44.9	nd	85.6	59.4
	irr-γ[b]	−52.9	nd	23.7 42.2	nd	73.9	51.3
	irr-e-[b]	−49.9	nd	26.9 43.5	nd	79.0	54.8

[a] – 2nd series of measurements (8 months storage).
[b] – 2nd series of measurements (2 months storage).
[c] – amorphous; nd – not detected.

DSC curve. In comparison, PLACL (LA:CL = 0.5:0.5) was amorphous, despite both homopolymers (PLA and PCL) were crystalline or at least contained crystalline blocks (Table 4, Fig. 6 a). It could result from high randomization of the units in the copolymer chain ($R = 1.05$) and short lactidyl and caproyl blocks ($l_{LL} = 1.59$ and $l_{Cap} = 1.46$), that were not able to form crystallites large enough to be detected as a crystalline phase.

Interestingly, the storage of partially crystalline PLA and PCLGA samples revealed some changes in the course of the process taking place at heating (Fig. 5a and b). In the case of these polymers, cold crystallization (followed by melting) was observed during the first serie of measurements. At re-measurements (undertaken after storage), the course of DSC analysis of PLA was generally similar to that observed during the first serie, with that difference that the temperature of all processes (glass transition, cold crystallization and melting) as well as the enthalpies of cold crystallization and melting were higher (Fig. 5a, Table 4). This showed that storage induced reorganization of the polymer structure probably with formation of larger faction of the better ordered crystalline phase that might be additionally improved during heating (as shown by occurrence of cold crystallization).

In the case of PCLGA, cold crystallization was not observed during re-measurements (Fig. 5b). Moreover, during the first analysis two minima were observed on the melting endotherm (that were recorded in the temperature range 10 °C–35 °C). At re-measurement, melting was shifted to higher temperature. The major endothermal effect was recorded in the temperature range 30–55 °C), while only small endotherm was noticed in the temperature region corresponding to the double endothermal effect occurring during the first analysis. Both, disappeareance of cold crystallization and the change in the temperature and the profile of melting endotherm, is probably connected to secondary crystallization taking place during the storage of the PCLGA sample.

Accordingly to the occurrence of cold crystallization at heating, the crystallinities indexes were evaluated for the raw material before it was subjected to heating in the DSC calorimeter. For this purpose, the enthalpy of cold crystallization was substracted from the enthalpy of melting and the resulting value was taken for final calculation of X_C. Considering that the total enthalpy of melting is related to two components: the crystallinity occurring in the sample before DSC measurement and the crystallinity additionally formed during cold crystallization process, the raw crystallinity was calculated basing the enthalpy value obtained after subtracting the cold crystallization enthalpy from the final melting enthalpy (eq. (5)).

The re-measurements of the samples revealed some increase of the crystallinity of partially crystalline PLA and PCLGA samples after storage. X_c of PCLGA increased from 15.1 % [12] to 59.4 % after 2 months, while in case of PLA, X_c increased in longer time of 8 months from 33.9 % to 37.9 %.

The increase in the crystalline ordering may be attributed to the possible reorganization of polymer chains from amorphous fraction and those forming less perfect crystallites during storage. This results in increase of the crystallites content, enlargement of their size and improvement of their structure. Our observations remined somewhat the observation of Phillipson et al. [27], who explained this phenomenon as caused by a diffusion controlled process of secondary crystallization due to the thickening of lamellae [27]. The amorphous regions of polymers' chains may re-align to a more ordered state, explaining the increase of apparent crystallinity with time. This hypothesis fits also to explanation given by Hay [28], who has attributed the increase in the crystalline ordering during storage of the semicrystalline polymers to physical ageing and enthalpic relaxation, changing their thermal properties. The crystallites already formed are supposed to act as points of reinforcement, constraining amorphous regions surrounding the crystallites [28].

The above results show the instability of the amorphous phase and might be related to the study of Arias et al. [29], who observed the increase of crystallinity during the hydrolysis of semicrystalline polyesters. This resulted from the faster of hydrolytic degradation of the polymers in their amorphous regions as compared to the crystalline phase.

Simultaneously, it can be noticed, that the temperature of glass

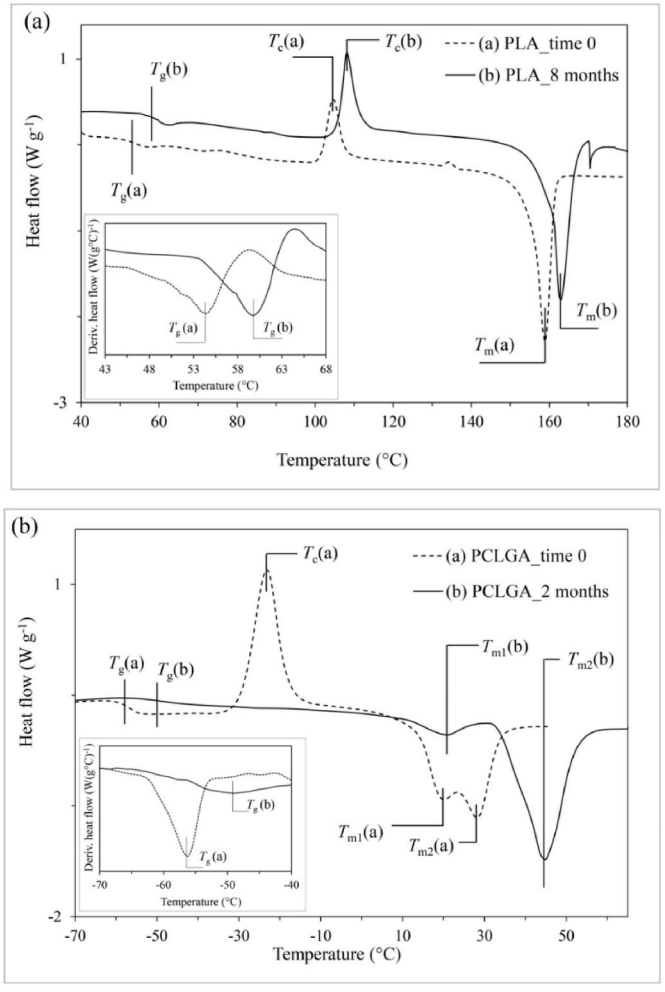

Fig. 5. DSC curves of PLA (a) and PCLGA (b) change in time (serie 1 – time 0, serie 2 – re-measurement after storage). DDSC curves in miniatures.

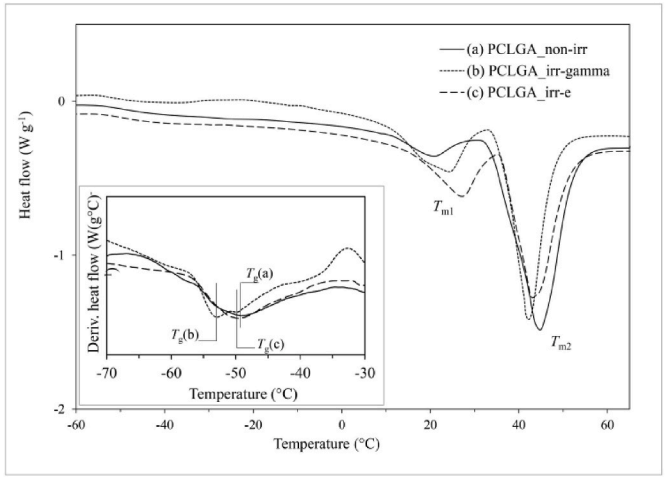

Fig. 6. DSC curves of PCLGA: non-irr (a), irr-γ (b) and irr-e (c).

transition was higher in both cases (PLA, PCLGA) at re-measurements as compared to the first analyses (Fig. 6a and b, Table 4, [12]). This result might be explained in terms of the increase of the ordering of the amorphous phase due to storage of the samples.

The influence of ionizing radiation on thermal properties of the polymers was assessed by thermogravimetry and DSC studies. As shown in Table 4, both types of irradiation (γ-rays and electrons) were found to alter somewhat the temperatures of glass transition, cold crystallization and melting of the polymers. However, in most cases, temperature change was more pronounced for the γ-irradiated samples. This results can be related to the change of molecular mass of the polymers under both types of irradiation (Table 3), for which, γ-irradiation induced decrease of M_n of the polymers in a greater extent comparing to e-beam. The prevalence of the mechanism of chain scission taking place during irradiation of the polymers may be confirmed by the shifts of characteristic temperatures showed in DSC curve of PCLGA (Fig. 6). Two minima observed on PCLGA endotherm can be attributed to the presence of two types of crystallites differing in size and possibly in morphology [12]. Different crystallites may be formed depending on the polymer chain length. Accordingly, PCLGA of lower M_n starts to melt (T_{m1}), while PCLGA of longer chains melts at higher temperature (T_{m2}). The apparent shift of endotherm minima may result from polymer degradation upon irradiation. It can be noticed that the irradiated PCLGA start to melt at lower temperature as compared to the non-irradiated sample. Moreover, the profiles of endothermal effects indicate, that a greater fraction of the polymer melts in the frame of the first endothermal effect. Accordingly, the minimum of this effect shifts to higher temperature. Simultaneously, the second minimum related to the crystallites formed by the polymer of longer chains (higher M_n) shifted towards lower temperatures probably as a result of chain scission and the formation of shorter chains. This seems to be in accordance with TGA data, showing decrease in the temperature of decomposition of the major fraction (Fig. 7). Additionally, a greater temperature decrease was observed for γ-irradiated PCLGA. This result is in accordance with a substantial decrease of M_n of γ-irradiated PCLGA, while in the case of PCLGA irradiated with e-beam, M_n slightly increased suggesting competitive mechanisms of chain-scission and cross-linking upon irradiation (Table 3).

The change in T_g after irradiation may be related to the change in ordering of molecules in amorphous region. Therefore, some increase in T_g observed in the case of PCL and PLACL is probably caused by an increase in the ordering of the amorphous phase, while decrease of T_g noticed in the case of PLA might be connected to a decrease in the ordered distribution of macromolecules in the amorphous region. It seems worth to mention that the amorphous regions possibly are built by the macromolecules characterized by a low molecular mass.

The characteristic values of polymers' degradation temperatures are depicted in Table 5. Except PLA, neither type of irradiation influenced significantly polymers' degradation. DTGA plots (Fig. 7) show, that the

Table 5
The influence of ionizing radiation on thermal decomposition of the polymeric matrices.

Polymer	Irradiation	$T_{5\%}$ (°C)	$T_{50\ \%}$ (°C)	$T_{95\ \%}$ (°C)	T_{max} (°C)	T_f (°C)
PCL	non-irr	351.4	408.8	434,4	413.3	464.5
	irr-γ	360.9	410.3	440.5	414.0	467.3
	irr-e$^-$	359.8	409.6	437.0	413.4	466.3
PLA	non-irr	304.5	371.2	394.6	377.9	414.9
	irr-γ	324.3	372.4	394.3	377.2	416.1
	irr-e$^-$	322.5	372.1	393.8	376.9	415.5
PLACL	non-irr	339.3	389.6	424.9	393.3	464.0
	irr-γ	338.4	389.6	423.9	393.6	466.5
	irr-e$^-$	332.3	388.2	425.9	391.8	465.3
PCLGA	non-irr	365.4	406.9	433.8	409.8	475.6
	irr-γ	351.5	405.5	434.8	409.1	475.9
	irr-e$^-$	351.7	405.0	431.6	408.7	476.0

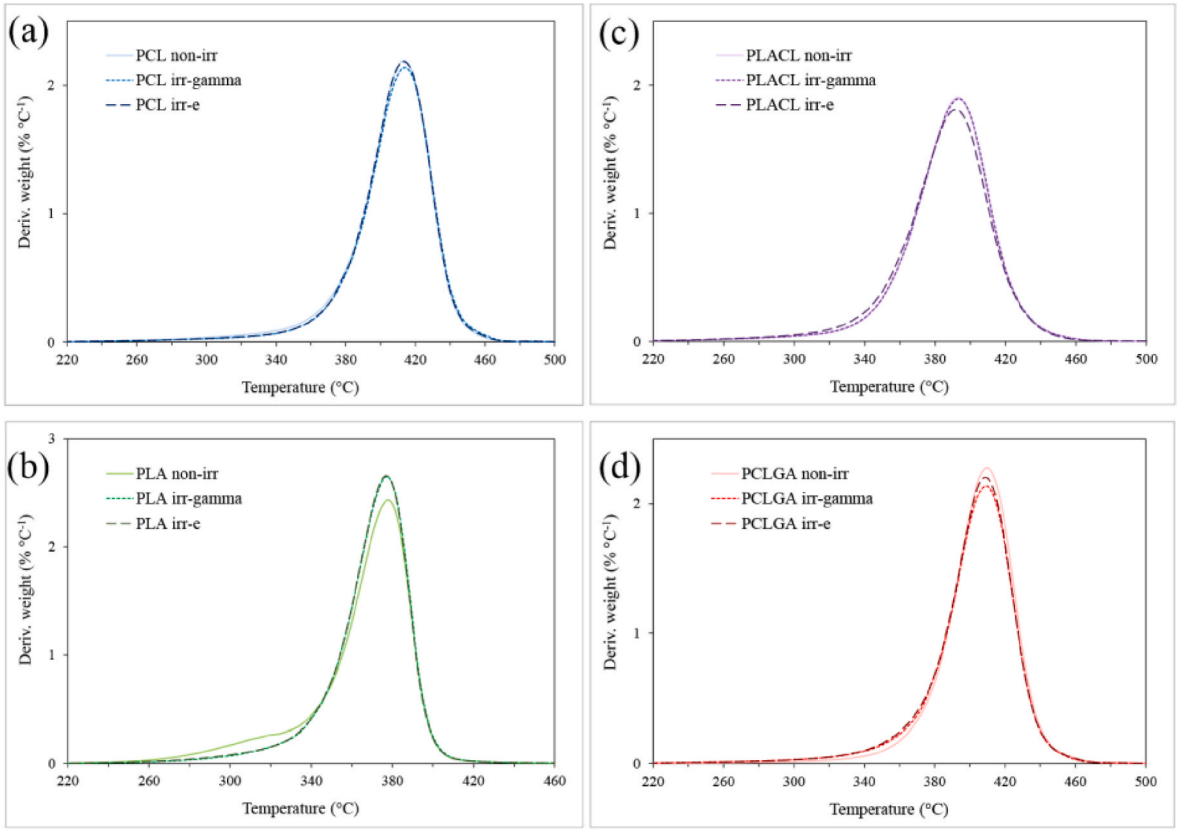

Fig. 7. The influence of ionizing radiation on thermal decomposition of the polymers: PCL (a), PLA (b), PLACL (c) and PCLGA (d).

non-irradiated PLA characterized two-step degradation. In the frame of low temperature step (taking place till ca. 330 C, shown by a shoulder on DTGA curve) the low molecular mass fraction decomposed. In the case of the irradiated samples, the first step of thermal decomposition was not separated. Simultaneously, data collected in Table 5 have shown the increase of $T_{5\%}$ parameter. This shows, that the beginning of decomposition of PLA was shifted towards higher temperature after irradiation. When the first step of degradation consist on decomposition of the polymer fraction characterized by a low molecular mass, it can be thus concluded that some crosslinking of this fraction was induced by irradiation.

This result might be explained in terms of two concurring processes taking place under gamma irradiation: chain scission and cross-linking. Overall, despite slight decrease of the average molecular mass of PLA, suggesting the predominance of chain scission mechanism during the irradiation, the shift of the first step of thermal decomposition towards higher temperatures may suggests the concomitant occurrence of cross-linking of short chains.

Although no separated thermal effect was observed, a detailed analysis of the DTGA curves has shown that thermal decomposition, that can be attributed to the fractions with a lower molecular mass, occurred at higher temperature also in the case of PCL irradiated with both, γ-rays and electrons (Table 5). However, the temperature shift was only negligible (Fig. 7a). To the contrary, in the cases of both copolymers (PLACL and PCLGA), thermal decomposition of the low molar fractions started at lower temperature, suggesting the predominance of chain scission mechanism at irradiation of these polymers.

3.4. The influence of ionizing radiation on hydrolytic degradation of polymers

The mass loss of the polymers occurred slowly. After 98 days of hydrolytic degradation, more than 70 % of mass remained in case of all non-irradiated polymers. Importantly, no rapid mass loss was observed in early degradation of the polymers, proving their relatively homogeneous composition. However, degradation profiles of the homo- and copolymers differed significantly. The homopolymers showed a one-step degradation profile with a slow, continuous decrease in mass over the time of hydrolytic degradation (Fig. 8). Compared, PLACL and PCLGA presented a two-stage degradation profile with a fast mass loss during the first step of degradation, followed by a slow and continuous mass loss. As expected, the slowest degradation was observed in the case of PCL (less than 10 % mass loss in 98 days) and the fastest was detected in the case of PLACL (28 % mass loss in 98 days).

The changes in degradation profiles observed for the irradiated polymers correlated with the changes in their average molecular mass. As seen in Fig. 8, irradiation did not influence degradation profiles of the homopolymers considerably. However, some acceleration in mass loss for the γ-irradiated polymers over the time of hydrolytic degradation was observed (from 8 % to 10 % for PCL, from 11 % to 12 % mass loss for PLA, from 28 % to 39 % mass loss for PLACL and from 25 % to 40 % mass loss for PCLGA samples after 98 days of hydrolytic degradation). These results are in accordance with the changes in average molecular mass of irradiated polymers. Similarly to mass loss recorded for hydrolytic degradation, greater decrease of M_n was observed for the copolymers irradiated with γ-rays than to e-beam (12.7 % for γ-irradiated PLACL and 28.2 % molecular mass loss for γ-irradiated PCLGA), that in turn might contributed to faster degradation of these polymers.

3.5. Preparation of PTX-loaded nanoparticles

PTX-loaded nanoparticles were obtained by a single solvent evaporation technique. For this purpose, low molecular mass polyvinyl alcohol was used as a functional excipient, that acts as a steric stabilizer for the resulting nanosuspensions [9]. According to Maksimenko et al. [9], degree of PVA hydrolysis (<90 %) is an important factor increasing stabilizing effects during the formation of nanoparticles. Therefore, in the present study, PVA with molecular mass of 13–23 kDa and 87–89 % hydrolyzed was used. As shown in Table 6, this approach allowed for the formation of nanoparticles with 64.5–72.3 % yield. The encapsulation efficiency (*EE*) varied depending on the polymer used, nonetheless, in all cases was satisfying. It reached 69.3 %, 82.6 %, 69.0 % and 79.4 % for PCL, PLA, PLACL and PCLGA matrices respectively (Table 6). The nanosuspensions obtained characterized good homogeneity and particle

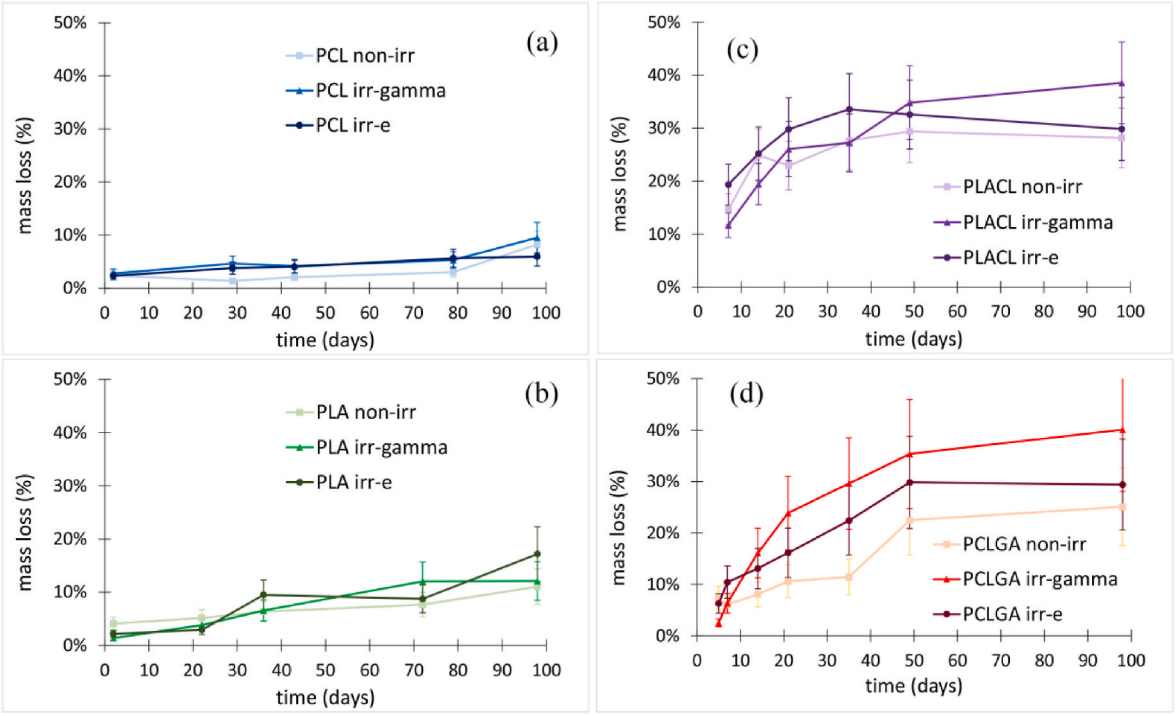

Fig. 8. Hydrolytic degradation of non-irradiated and irradiated polymers: PCL (a), PLA (b), PLACL (c), and PCLGA (d); $n = 3$.

Table 6
The influence of ionizing radiation on PTX-loaded nanoparticles determined by DLS, $n = 3$.

Sample	Yield (%)	EE (%)	Irradiation	Size[a] (nm)	Z-average (nm)	PDI	ZP[b] (mV)
PCL-PTX	68.7 ± 3.3	69.3 ± 9.4	non-irr	172.4 ± 6.6	204.6 ± 5.7	0.33 ± 0.02	−8.20 ± 0.29
			irr-γ	181.3 ± 2.4	150.7 ± 2.2	0.18 ± 0.01	−19.70 ± 3.78
			irr-e$^-$	186.9 ± 2.9	155.3 ± 1.2	0.16 ± 0.01	−23.68 ± 0.23
PLA-PTX	72.3 ± 9.5	67.5 ± 5.4	non-irr	257.9 ± 19.3	248.5 ± 8.3	0.20 ± 0.03	−22.96 ± 0.80
			irr-γ	272.6 ± 8.6	259.4 ± 9.3	0.23 ± 0.03	−30.42 ± 1.06
			irr-e$^-$	256.4 ± 29.6	196.0 ± 30.4	0.31 ± 0.14	−26.20 ± 0.58
PLACL-PTX	64.5 ± 8.6	51.5 ± 2.7	non-irr	196.7 ± 3.4	176.9 ± 0.5	0.09 ± 0.02	−30.54 ± 5.52
			irr-γ	209.8 ± 12.5	186.2 ± 1.8	0.15 ± 0.03	−8.51 ± 1.16
			irr-e$^-$	197.1 ± 5.6	176.7 ± 3.7	0.10 ± 0.01	−17.04 ± 1.23
PCLGA-PTX	69.0 ± 6.1	79.4 ± 4.4	non-irr	254.1 ± 21.9	285.9 ± 18.1	0.33 ± 0.02	−11.58 ± 0.71
			irr-γ	213.3 ± 4.9	205.4 ± 2.3	0.32 ± 0.03	−6.25 ± 0.32
			irr-e$^-$	262.9 ± 35.1	313.4 ± 18.1	0.35 ± 0.06	−5.78 ± 0.28

[a] – at maximum of particle size distribution.
[b] – zeta-potential (mV).

size of approx. 172.4 nm (PCL), 257.9 nm (PLA), 196.7 nm (PLACL), and 254.1 nm (PCLGA) (Table 6). However, after lyophilization and re-suspension of PCL-based nanoparticles, homogeneity was lost, necessitating extended sonication in an ultrasonic cleaner. It could be due to the polymer's more hydrophobic nature as a result of its six-carbon backbone (as compared to PLA) [30], and thus, leading to agglomeration of the nanoparticles. Additionally, PCL characterized the highest degree of crystallinity, preventing the association of the surface of nanoparticles with hydrophilic PVA molecules.

3.6. Evaluation of the stability of PTX-loaded nanoparticles to irradiation

Since the DDSs obtained herein are intended for parenteral administration, they need to be sterilized. Although the use of the pharmacopoeia-recommended dose (25 kGy) is considered adequate for sterilizing purpose [7,31,32], it is recommended to investigate any changes in physicochemical properties for each type of sterilized product. The impact of ionizing radiation on the physicochemical properties of medicinal formulations was determined by measuring the size and size distribution of nanoparticles, testing PTX stability in the presence of impurities, and analyzing any changes in PTX release kinetic profiles.

The influence of irradiation on the stability of PTX-loaded polymeric nanoparticles was evaluated by HPLC. The chromatograms of PTX extracted from the nanoparticles showed no additional peaks upon irradiation. It suggests that the irradiation did not lead to the formation of any PTX-related degradation products. The obtained results confirmed the stability of PTX encapsulated into polymeric carriers to both, γ-irradiation and e-beam at dose 25 kGy.

In this study, the average size of nanoparticles was in the range of 172.4–257.9 nm, depending on the polymer matrix used (Table 6). Such size preclude their sterile filtration. For that reason we investigated the influence of ionizing radiation in relation to the sterilization process of the produced DDSs. The zeta-potential of the nanoparticles was negative and took the values of −8.20 (±0.29) mV for PCL nanoparticles, −22.96 (±0.80) mV for PLA nanoparticles, −30.54 (±5.52) mV for PLACL nanoparticles, and −11.58 (±0.71) mV for PCLGA nanoparticles. The negative values of ZP were caused by terminal carboxylic groups in the polymers in water [33,34].

The data presented in Table 6 show that the applied radiation dose (25 kGy) did not significantly change the mean particle size of PTX-

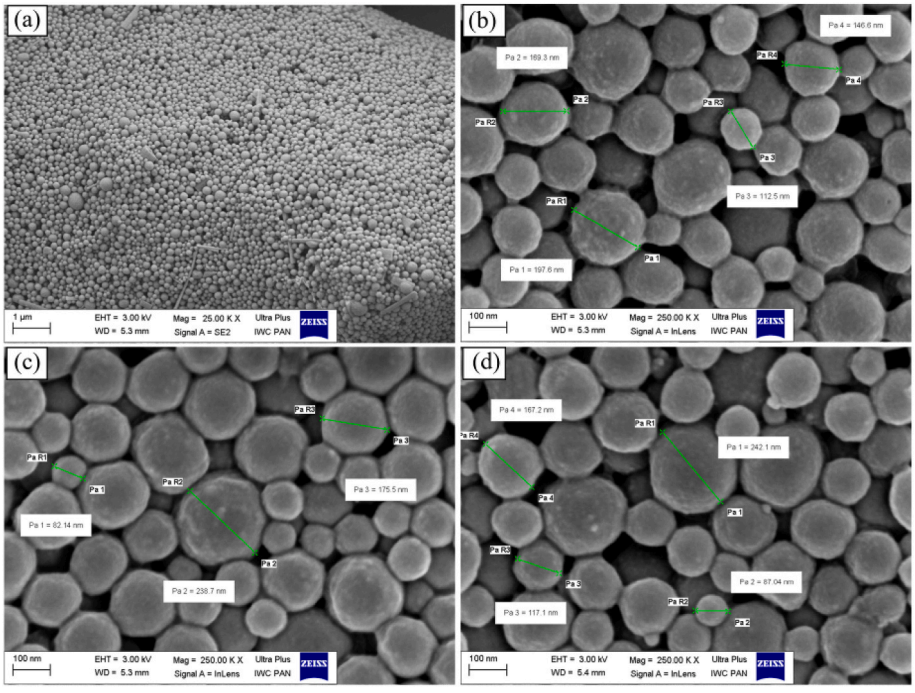

Fig. 9. Example SEM micrographs of lyophilized PTX-loaded nanoparticles: (a) distribution of PLA nanoparticles and the morphology of PLA nanoparticles: (b) non-irr, (c) irr-γ, and (d) irr-e.

loaded nanoparticles, regardless the type of polymeric matrix and the type of irradiation.

Fig. 9 presents SEM images of the irradiated and non-irradiated PTX-loaded nanoparticles. The particles exhibited spherical shape, were arranged in clusters and had a bimodal particle size distribution. The smaller fraction was in size of 70–120 nm and the bigger was of approx. 130–250 nm. Importantly, no change in the morphology of the nanoparticles was observed after irradiation and the irradiated nanoparticles kept the same shape as the non-irradiated ones.

3.7. In vitro PTX release from nanoparticles

Fig. 10 depicts a comparative study of in vitro PTX release from non-irradiated DDSs that differed in polymeric drug carrier (PCL, PLA, PLACL, and PCLGA) and the solution containing free PTX as a control. As presented, the course of PTX release profile strictly depends on the type of polymer matrix used. The slowest release of PTX was observed for PCL (53 % after 56 days of incubation) and the fastest for PLACL; 100 % of PTX was released after 34 days. This fact could be explained using polymer morphology. Because PLACL was amorphous, the polymeric chains were disordered and loosely arranged, allowing drug particles to diffuse through the polymeric matrix. Furthermore, rapid hydrolytic degradation of PLACL (25 % mass loss in 14 days) increased the role of the erosion mechanism in drug release. PCL, on the other hand, is crystalline, which, combined with its hydrophobic properties, slowed its hydrolytic degradation (less than 10 % mass loss over 98 days) and decreased the permeability to hydrophobic drug molecules (PTX) towards the release medium. This confirms that the kinetic profile of drug release is strictly dependent on degree of polymer degradation [35] (apart from drug diffusion coefficient). In opposite to slow biodegradation of a hydrophobic and crystalline PCL, PGA possess more hydrophilic character leading to a faster degradation [35]. Taking this into account, PCLGA degradation should result in relatively faster degradation (when compared to PCL), and thus faster drug release. However, within the first 21 days of incubation, the kinetic profiles of PTX release from PCL and PCLGA nanoparticles were comparable (Fig. 10). This is consistent with the polymer degradation studies (section 3.4). As shown in Fig. 8a and d, PCL and PCLGA exhibit slow mass loss during the first stage of hydrolytic degradation. However, after 35 days, a significant mass loss of the PCLGA matrix was observed. Simultaneously, PTX release from PCLGA nanoparticles increased, reaching 50 % after 41 days (compared to 38 % for PCL nanoparticles). The results obtained are consistent with the literature. Some similar observations have already been noted by Turek et al. [35] and Li et al. [36] and were related to the resistance of CapGCap and CapGGGCap sequences (resulted from the second mode of transesterification) to hydrolysis. It was confirmed by some insignificant changes in chain microstructure during degradation

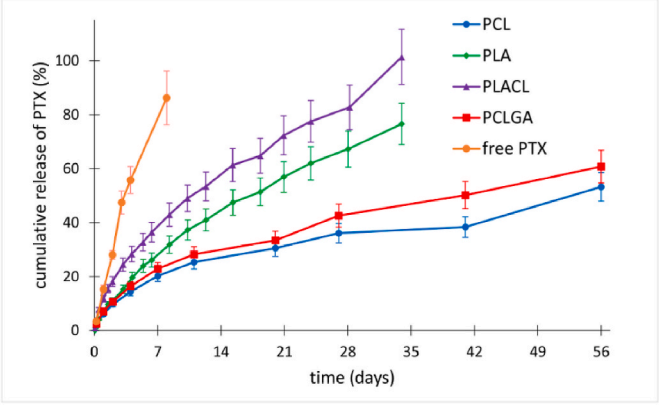

Fig. 10. The comparison of the kinetic profiles of free PTX release and PTX release from various non-irradiated polymeric drug carriers, $n = 3$.

[35]. This may explain the similar profiles of PTX release from PCLGA and PCL nanoparticles in the first 21 days of the study. In our work, PCLGA demonstrated a high randomization ratio as well as high content of the resistant to hydrolytic process CapGCap sequences (reaching approx. 80 % in the polymer chain in relation to the total amount of glycolyl units) [35]. As a result, PCLGA degradation occurs at a similar rate as PCL degradation in the first stage, and thus similar drug release profiles are observed in both cases during the first 21 days.

Fig. 11 depicts plots demonstrating the effect of irradiation on the kinetic profiles of PTX release from polymeric drug carriers. To assess the kinetic profiles of drug release, the data were fitted to zero-order, first-order, Higuchi and Korsmeyer-Peppas mathematical models (Table 7). The values of R^2 for zero-order and first-order kinetics suggest that the drug release profiles from all polymeric matrices followed the first-order kinetic, regardless of irradiation. Additionally, the data well fitted to the Higuchi and Korsmeyer-Peppas mathematical models. The analysis of the release exponent from the Korsmeyer-Peppas model clearly shows the drug release with non-Fickian diffusion ($0.45 < n < 0.89$). It indicates two mechanisms taking part in drug release, i.e. diffusion of the drug through the polymeric matrix and erosion of the polymer. Furthermore, a detailed examination of the release exponent (n) reveals some differences in drug release mechanisms between DDSs that differ in polymeric matrix. As shown in Fig. 10, PCL and PCLGA nanoparticles are characterized by prolonged drug release. The release exponent of drug release from these nanoparticles takes the values characteristic for non-Fickian diffusion, nonetheless, the values are relatively low ($n_{PCL} = 0.62$; $n_{PCLGA} = 0.52$) and close to the values expected for Fickian diffusion mechanism ($n = 0.45$). It may indicate anomalous drug release with the predominance of the contribution of diffusion mechanism over polymer erosion.

Simultaneously the higher n-values, determined for PLA and PLACL ($n_{PLA} = 0.74$; $n_{PLACL} = 0.72$) can be related to the more prominent share of the erosion mechanism (along with the diffusion mechanism) as compared to PCL and PCLGA nanoparticles. The progressive erosion of the polymeric matrix contributes to faster diffusion of the drug through this matrix and to its faster release.

Only negligible differences (in the frame of the scatter of experimental data) in the kinetic profiles of PTX release from PCL and PLA drug carriers were observed after the irradiation. However, in the case of PLACL and PCLGA matrices, γ-irradiation increased to some extent the amount of PTX released from the nanoparticles (Fig. 11). These data are in accordance with the results arising from the studies of the influence of irradiation on the molecular structure of the polymeric matrices. As described, chain scission was the main mechanism taking place during irradiation of PLACL and PCLGA with γ-rays. It is shown by decrease of M_n of the copolymers (Fig. 3) and resulted in increased mass loss during hydrolysis (section 3.4). That in turn, increased the contribution of erosion mechanism facilitating the release of drug molecules from the polymer matrices. This is well shown by some increase of the exponent of drug release from γ-irradiated nanoparticles (from $n_{non\text{-}irr} = 0.72$ to $n_{irr\text{-}\gamma} = 0.79$ for PLACL nanoparticles and from $n_{non\text{-}irr} = 0.52$ to $n_{irr\text{-}\gamma} = 0.61$ for PCLGA nanoparticles). This hypothesis is also consistent with the change of the release exponent n for PLA nanoparticles irradiated with both, γ-rays and electrons. Along with decrease of M_n of the polymer ($\Delta M_{nPLA\ \gamma\text{-}irr} = 7.9$ % and $\Delta M_{nPLA\ e\text{-}irr} = 6.9$ %), the release exponent increased from n = 0.74 to n = 0.83 after the irradiation, regardless of γ-rays and e-beam. This suggests polymer degradation and, as a result, an increase in the role of the erosion mechanism in drug release. In comparison, despite some decrease of M_n, only negligible differences of the release exponent n were observed for the irradiated PCL nanoparticles (from $n = 0.62$ to $n = 0.63$). This may result from the resistance of PCL to irradiation due to its hydrophobicity and high crystalline index, that in turn, allow to maintain the arrangement of the polymer chains.

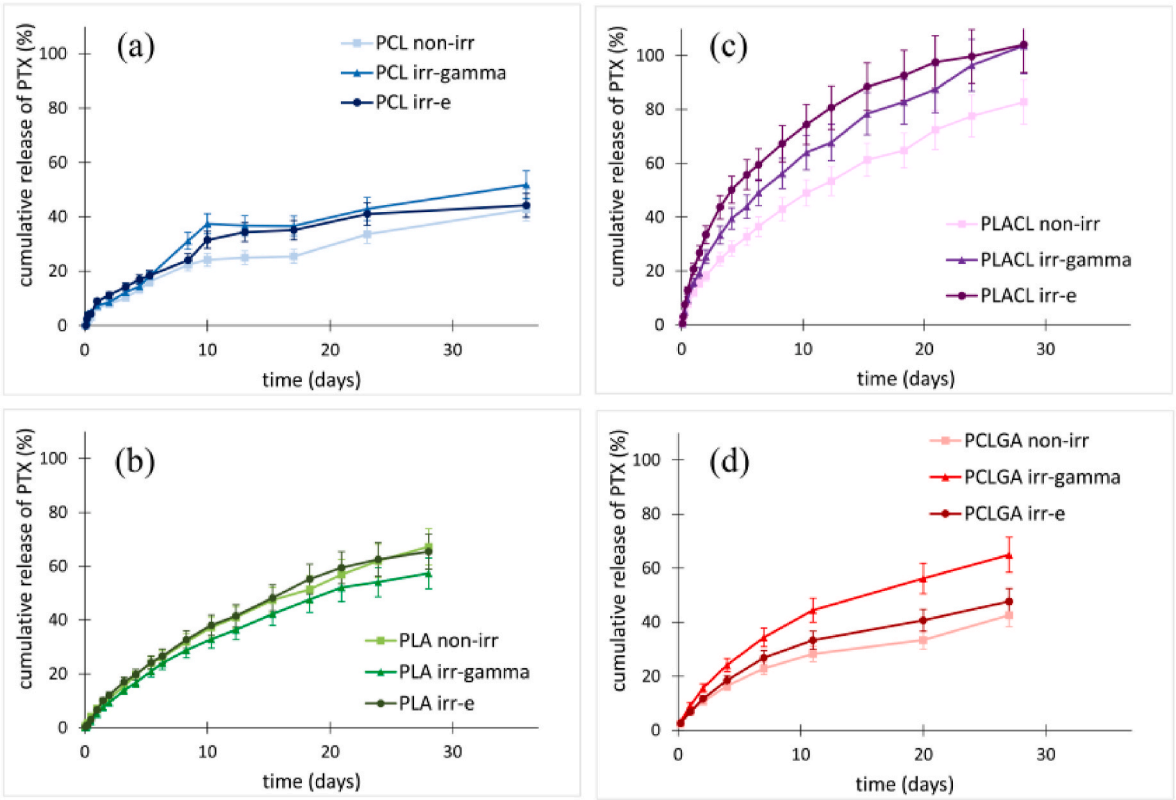

Fig. 11. The influence of irradiation on kinetic profiles of PTX release from the nanoparticles obtained with: PCL (a), PLA (b), PLACL (c), and PCLGA (d), $n = 3$.

Table 7
Data analysis of PTX release from polymeric nanoparticles.

Sample	Irradiation	Zero Order	First Order	Higuchi		Korsmeyer–Peppas	
		R^2	R^2	R^2	K_H[a]	R^2	n[b]
PCL	non-irr	0.8982	0.9385	0.9869	7.356	0.9873	0.615
	irr-γ	0.8386	0.8890	0.9546	9.583	0.9713	0.631
	irr-e	0.8267	0.8721	0.9702	8.401	0.9770	0.601
PLA	non-irr	0.9659	0.9960	0.9948	13.790	0.9932	0.741
	irr-γ	0.9454	0.9871	0.9951	12.158	0.9818	0.829
	irr-e	0.9487	0.9937	0.9958	13.851	0.9768	0.827
PLACL	non-irr	0.9442	0.9956	0.9990	16.497	0.9858	0.717
	irr-γ	0.9226	0.9956	0.9983	20.633	0.9645	0.790
	irr-e	0.8558	0.9940	0.9808	21.430	0.9796	0.718
PCLGA	non-irr	0.9295	0.9764	0.9950	8.097	0.9930	0.521
	irr-γ	0.8484	0.9550	0.9743	11.222	0.9909	0.612
	irr-e	0.8272	0.8926	0.9642	8.018	0.9690	0.519

[a] – release rate constant.
[b] – release exponent.

4. Conclusions

During the design and development of anticancer DDSs, it is critical to select the optimal sterilization method that allows for the avoidance or at least limitation of undesirable side effects. It may be especially difficult in the case of biodegradable polyesters due to their low thermal stability. With this regard we propose the use of ionizing radiation for the sterilization purposes of the PTX-loaded polymeric nanoparticles. It can be stated, that the obtained copolymers were of random structure, as a result of the transesterification of the second mode, accompanying the polymerization process. Importantly, neither γ-rays nor e-beam was found to impact the microstructure of the polymers. The results showed, that the main mechanism taking part during the irradiation of the examined polymers was chain scission. This caused decrease in M_n and thus altered thermal properties of the polymers (T_g, T_c, T_m). As a result, hydrolytic degradation of the polymers was accelerated. The most noticeable decrease of M_n was for the γ-irradiated copolymers characterized random microstructure and short average lengths of blocks (12.7 % and 28.2 % of average molecular mass loss for PLACL and PCLGA respectively).

The PTX-loaded nanoparticles were obtained with a high encapsulation efficiency and a size range of 172.4–257.9 nm (DLS). The obtained results indicated good control of release of PTX. The kinetic profiles of drug release were defined as first order with non-Fickian diffusion (anomalous mechanism), irrespective to polymeric drug carrier and applied irradiation. It can be concluded, that no substantial effect of e-beam (25 kGy) on PTX release from the examined polymeric matrices was observed. However, a noticeable increase of the amount of PTX release over the time was observed for γ-irradiated copolymer drug carriers. The enhanced drug release may result from higher degradation

of the copolymers irradiated with γ-rays (compared to the non-irradiated copolymers), that increased the contribution of the erosion mechanism, facilitating the release of hydrophobic drug outwards the nanoparticles. This results may be interesting in relation to possible modification of the controlled release of active substances [37]. Therefore, it may be beneficial to use γ-irradiation in purpose to accelerate drug release.

Simultaneously, our results have proved, a great potential of e-beam for the sterilization purposes of polyesters micro– and nanoparticles, especially, when it is desirable to protect the polymer matrix from undesirable changes that might be induced by thermal or chemical sterilization.

It should be taken into account, that the increased chain scission of the polymers irradiated with γ-rays (compared to e-beam) may be due to the longer time of irradiation, that was necessary to receive the sterilization dose of 25 kGy, causing both the constant formation of new radicals affecting the polymers and prolonged contact with air, leading to more advanced oxidative degradation.

CRediT author statement

I declare, that: a) all authors have read and agreed to the published version of the manuscript. b) the authors' contribution is as follows:

Izabela M. Domańska: conceptualization, chemical, structural, analytical and pharmaceutical research, methodology, investigation, formal analysis, and writing – original draft; **Aldona Zalewska**: DSC measurement and analysis; **Krystyna Cieśla**: interpretation of thermal analysis data, investigation, formal analysis, and writing – original draft, editing and supervision; **Andrzej Plichta**: GPC measurement and analysis; **Wojciech Głuszewski**: irradiation of samples; **Monika Łyczko**: DLS measurement; **Sebastian Kowalczyk**: GPC measurement; **Ewa Oledzka**: discussion, editing; **Marcin Sobczak**: conceptualization, chemical, structural, analytical and pharmaceutical research, investigation, writing – original draft, editing, and supervision.

Funding

The work was performed as part of the Project number FW231/1/F/MBS/N/21, which was carried out from 2021 to 2023 and was funded by a scientific financial support obtained from the Medical University of Warsaw (Poland).

Institutional review board statement

Not applicable.

Informed consent statement

Not applicable.

Sample availability

Samples of all compounds are available from the authors.

Declaration of competing interest

The authors declare that they have no known competing financial interests or personal relationships that could have appeared to influence the work reported in this paper.

Data availability

Data will be made available on request.

Acknowledgments

The contribution of Izabela M. Domańska was realized within the Project No POWR.03.02.00–00-I009/17-00 (Operational Project Knowledge Education Development 2014–2020 co-financed by European Social Fund).

References

[1] WHO - cancer fact sheet. https://www.who.int/news-room/fact-sheets/detail/cancer.
[2] M.S. Surapaneni, S.K. Das, N.G. Das, Designing paclitaxel drug delivery systems aimed at improved patient outcomes: current status and challenges, ISRN Pharmacology 2012 (Aug. 2012) 1–15, https://doi.org/10.5402/2012/623139.
[3] Z. Stefanowicz, M. Sobczak, A. Piętniewicz, W.L. Kołodziejski, Macromolecular conjugates of paclitaxel: synthesis, characterization, and *in Vitro* paclitaxel release studies based on HPLC validated method, Acta Chromatogr. 28 (1) (Mar. 2016) 99–117, https://doi.org/10.1556/AChrom.28.2016.1.8.
[4] 'European Pharmacopoeia - Supplement 9.2, Jan. 2017, pp. 4333–4350'.
[5] I.M. Domańska, E. Oledzka, M. Sobczak, Sterilization process of polyester based anticancer-drug delivery systems, Int. J. Pharm. 587 (Sep. 2020), 119663, https://doi.org/10.1016/j.ijpharm.2020.119663.
[6] A. Iuliano, M. Nowacka, K. Rybak, M. Rzepna, The effects of electron beam radiation on material properties and degradation of commercial PBAT/PLA blend, J. Appl. Polym. Sci. 137 (11) (Mar. 2020), 48462, https://doi.org/10.1002/app.48462.
[7] R. Dorati, et al., The effect of γ-irradiation on PLGA/PEG microspheres containing ovalbumin, J. Contr. Release 107 (1) (Sep. 2005) 78–90, https://doi.org/10.1016/j.jconrel.2005.05.029.
[8] R. Dorati, et al., Long-term effect of gamma irradiation on the functional properties and cytocompatibility of multiblock Co-polymer films, J. Biomater. Sci. Polym. Ed. 23 (17) (Dec. 2012) 2223–2240, https://doi.org/10.1163/156856211X613915.
[9] O. Maksimenko, et al., Doxorubicin-loaded PLGA nanoparticles for the chemotherapy of glioblastoma: towards the pharmaceutical development, Int. J. Pharm. 572 (Dec. 2019), 118733, https://doi.org/10.1016/j.ijpharm.2019.118733.
[10] M. Walo, G. Przybytniak, A. Nowicki, W. Świeszkowski, Radiation-induced effects in gamma-irradiated PLLA and PCL at ambient and dry ice temperatures, J. Appl. Polym. Sci. 122 (1) (Oct. 2011) 375–383, https://doi.org/10.1002/app.34079.
[11] D. Milicevic, E. Suljovrujic, The resistance of poly-(l-lactide) to gamma radiation: effect of initial preparation and crystallinity, Polym. Bull. 77 (5) (May 2020) 2659–2677, https://doi.org/10.1007/s00289-019-02880-2.
[12] I.M. Domańska, et al., A comprehensive investigation of the structural, thermal, and biological properties of fully randomized biomedical polyesters synthesized with a nontoxic bismuth(III) catalyst, Molecules 27 (3) (Feb. 2022) 1139, https://doi.org/10.3390/molecules27031139.
[13] J. Kasperczyk, M. Bero, Coordination polymerization of lactides, 4. The role of transesterification in the copolymerization of L,L-lactide and ε-caprolactone, Makromol. Chem. 194 (3) (Mar. 1993) 913–925, https://doi.org/10.1002/macp.1993.021940315.
[14] J. Kasperczyk, Copolymerization of glycolide andε-caprolactone, 1. Analysis of the copolymer microstructure by means of1H and13C NMR spectroscopy, Macromol. Chem. Phys. 200 (4) (Apr. 1999) 903–910, 10/fg584r.
[15] P. Dobrzynski, J. Kasperczyk, H. Janeczek, M. Bero, Synthesis of biodegradable copolymers with the use of low toxic zirconium compounds. 1. Copolymerization of glycolide with l -lactide initiated by Zr(acac) $_4$, Macromolecules 34 (15) (Jul. 2001) 5090–5098, https://doi.org/10.1021/ma0018143.
[16] J.-R. Sarasua, R.E. Prud'homme, M. Wisniewski, A. Le Borgne, N. Spassky, Crystallization and melting behavior of polylactides, Macromolecules 31 (12) (Jun. 1998) 3895–3905, https://doi.org/10.1021/ma971545p.
[17] S. Tiptipakorn, N. Keungputpong, S. Phothiphiphit, S. Rimdusit, Effects of polycaprolactone molecular weights on thermal and mechanical properties of polybenzoxazine, J. Appl. Polym. Sci. 132 (18) (May 2015), https://doi.org/10.1002/app.41915 n/a-n/a.
[18] L. Magazzini, S. Grilli, S.E. Fenni, A. Donetti, D. Cavallo, O. Monticelli, The blending of poly(glycolic acid) with polycaprolactone and poly(l-lactide): promising combinations, Polymers 13 (16) (Aug. 2021) 2780, https://doi.org/10.3390/polym13162780.
[19] A. Kasiński, et al., Synthesis and characterization of new biodegradable injectable thermosensitive smart hydrogels for 5-fluorouracil delivery, IJMS 22 (15) (Aug. 2021) 8330, https://doi.org/10.3390/ijms22158330.
[20] S. Dash, P. N. Murthy, L. Nath, and P. Chowdhury, 'KINETIC MODELING ON DRUG RELEASE FROM CONTROLLED DRUG DELIVERY SYSTEMS', p. 7.
[21] G. Singhvi, M. Singh, REVIEW: IN-VITRO DRUG RELEASE CHARACTERIZATION MODELS, 2011, p. 8.
[22] C.B. Liu, et al., Thermoreversible gel–sol behavior of biodegradable PCL-PEG-PCL triblock copolymer in aqueous solutions, J. Biomed. Mater. Res. 84B (1) (Jan. 2008) 165–175, https://doi.org/10.1002/jbm.b.30858.
[23] Z. Jiang, X. Deng, J. Hao, Thermogelling hydrogels of poly(ε-caprolactone-co-D,L-lactide)–poly(ethylene glycol)–poly(ε-caprolactone-co-D,L-lactide) and poly(ε-caprolactone-co-L-lactide)–poly(ethylene glycol)–poly(ε-caprolactone-co-L-lactide) aqueous solutions, J. Polym. Sci. Polym. Chem. 45 (17) (Sep. 2007) 4091–4099, https://doi.org/10.1002/pola.22222.

[24] G. Rokicki, A. Piotrowska, P. Pawlowski, Macrocyclic vs. Linear polymer formation in the coordination- insertion polymerization of cyclic carbonates, Polym. J. 35 (2) (Feb. 2003) 133–140, https://doi.org/10.1295/polymj.35.133.
[25] K. Athanasiou, Sterilization, toxicity, biocompatibility and clinical applications of polylactic acid/polyglycolic acid copolymers, Biomaterials 17 (2) (Jan. 1996) 93–102, 10/d95272.
[26] M. Walo, M. Rzepna, RECENT DEVELOPMENTS IN RADIATION PROCESSING OF POLYMERS, Institute of Nuclear Chemistry and Technology, 2020.
[27] K. Phillipson, M. J Jenkins, J. N Hay, The ageing of poly(ϵ-caprolactone): ageing of poly(ϵ-caprolactone), Polym. Int. 64 (12) (Dec. 2015) 1695–1705, https://doi.org/10.1002/pi.4969.
[28] J.N. Hay, The physical ageing of amorphous and crystalline polymers, Pure Appl. Chem. 67 (11) (Jan. 1995) 1855–1858, https://doi.org/10.1351/pac199567111855.
[29] V. Arias, A. Höglund, K. Odelius, A.-C. Albertsson, Tuning the degradation profiles of poly(l -lactide)-Based materials through miscibility, Biomacromolecules 15 (1) (Jan. 2014) 391–402, https://doi.org/10.1021/bm401667b.
[30] F. Ahmed, D.E. Discher, Self-porating polymersomes of PEG–PLA and PEG–PCL: hydrolysis-triggered controlled release vesicles, J. Contr. Release 96 (1) (Apr. 2004) 37–53, https://doi.org/10.1016/j.jconrel.2003.12.021.
[31] A. Fernandezcarballido, P. Puebla, R. Herrerovanrell, P. Pastoriza, Radiosterilisation of indomethacin PLGA/PEG-derivative microspheres: protective effects of low temperature during gamma-irradiation, Int. J. Pharm. 313 (1–2) (Apr. 2006) 129–135, https://doi.org/10.1016/j.ijpharm.2006.01.034.
[32] Mar. 06, 'da'. EMA/CHMP/CVMP/QWP/850374/2015, 2019 [Online]. Available: https://www.ema.europa.eu/en/documents/scientific-guideline/guideline-sterilisation-medicinal-product-active-substance-excipient-primary-container_en.pdf.
[33] S. Nandhakumar, M.D. Dhanaraju, V.D. Sundar, B. Heera, Influence of surface charge on the in vitro protein adsorption and cell cytotoxicity of paclitaxel loaded poly(ε-caprolactone) nanoparticles, Bullet. Faculty Pharm. 55 (2) (Dec. 2017) 249–258, https://doi.org/10.1016/j.bfopcu.2017.06.003. Cairo University.
[34] T. Musumeci, et al., PLA/PLGA nanoparticles for sustained release of docetaxel, Int. J. Pharm. 325 (1–2) (Nov. 2006) 172–179, https://doi.org/10.1016/j.ijpharm.2006.06.023.
[35] A. Turek, et al., Designing biodegradable wafers based on poly(L-lactide-co-glycolide) and poly(glycolide-co-ε-caprolactone) for the prolonged and local release of idarubicin for the therapy of glioblastoma multiforme, Pharm. Res. (N. Y.) 37 (5) (May 2020) 90, https://doi.org/10.1007/s11095-020-02810-2.
[36] S. Li, P. Dobrzynski, J. Kasperczyk, M. Bero, C. Braud, M. Vert, Structure−Property relationships of copolymers obtained by ring-opening polymerization of glycolide and ε-caprolactone. Part 2. Influence of composition and chain microstructure on the hydrolytic degradation, Biomacromolecules 6 (1) (Jan. 2005) 489–497, https://doi.org/10.1021/bm049458+.
[37] S.J. Holland, B.J. Tighe, P.L. Gould, Polymers for biodegradable medical devices. 1. The potential of polyesters as controlled macromolecular release systems, J. Contr. Release 4 (3) (Oct. 1986) 155–180, https://doi.org/10.1016/0168-3659(86)90001-5.

applied sciences

MDPI

Article

The Influence of Ionizing Radiation on Paclitaxel-Loaded Nanoparticles Based on PLGA

Izabela M. Domańska [1], Ramona Figat [2], Aldona Zalewska [3], Krystyna Cieśla [4], Sebastian Kowalczyk [3], Karolina Kędra [5] and Marcin Sobczak [1,*]

[1] Department of Pharmaceutical Chemistry and Biomaterials, Faculty of Pharmacy, Medical University of Warsaw, 1 Banacha Str., 02-097 Warsaw, Poland; izabela.domanska@wum.edu.pl
[2] Department of Toxicology and Bromatology, Faculty of Pharmacy, Medical University of Warsaw, 1 Banacha Str., 02-097 Warsaw, Poland; ramona.figat@wum.edu.pl
[3] Faculty of Chemistry, Warsaw University of Technology, 3 Noakowskiego Str., 00-664 Warsaw, Poland; aldona.zalewska@pw.edu.pl (A.Z.); sebastian.kowalczyk@pw.edu.pl (S.K.)
[4] Institute of Nuclear Chemistry and Technology, 16 Dorodna Str., 03-195 Warsaw, Poland; k.ciesla@ichtj.waw.pl
[5] Institute of Physical Chemistry, Polish Academy of Sciences, 44/52 Kasprzaka St., 01-224 Warsaw, Poland; kkedra@ichf.edu.pl
* Correspondence: marcin.sobczak@wum.edu.pl; Tel.: +48-22-572-0783

Abstract: The effect of ionizing radiation (γ-rays and electron beam) on anticancer drug delivery systems (DDSs) properties was evaluated concerning potential sterilization. For this purpose, paclitaxel (PTX)-loaded nanoparticles were obtained using a biodegradable, self-developed copolymer of L-lactide and glycolide (PLGA), synthesized in the presence of bismuth 2-ethylhexanoate catalyst. The nanoparticles were obtained with a high encapsulation efficiency of PTX (*EE* = 94.2%). The average size of the nanoparticles was 253.5 nm. The influence of irradiation (sterilization dose, 25 kGy) on the microstructure and the physicochemical and thermal properties of the polymer matrix was investigated, as well as the effect of irradiation on the morphology and physicochemical properties of the pharmaceutical formulations of the nanoparticles. Additionally, an in vitro drug release study was conducted regarding any alterations in the kinetic profiles of drug release. It was confirmed that the irradiation with both types of ionizing radiation, i.e., γ-rays and electron-beam (EB), slightly decreased the average molecular weight of the polymer matrix. While only negligible changes in the microstructure and thermal properties of PLGA were observed after irradiation with EB, the average length of lactidyl blocks (l_{LL}) in the copolymer chains irradiated with γ-rays decreased from 4.33 to 3.35. Moreover, the contribution of crystalline phase (X_c) in γ-irradiated samples decreased significantly from 35.1% to 22.7%, suggesting a dominant mechanism of chain scission over cross-linking in PLGA samples irradiated with γ-rays. In vitro drug release results demonstrate a sustained and controlled release of PTX from the nanoparticles based on PLGA. The kinetics of drug release was defined as first order with non-Fickian diffusion. Only negligible differences in the kinetic profiles of PTX release from PLGA drug carriers were observed after irradiation. The overall results suggest good resistance of PLGA nanoparticles to irradiation within the conditions used and the great potential of EB in the sterilization process of the polymeric DDSs.

Keywords: drug delivery systems; radiation sterilization; electron beam; gamma irradiation; paclitaxel; biodegradable polymers; L-lactide and glycolide copolymers; nanoparticles

Citation: Domańska, I.M.; Figat, R.; Zalewska, A.; Cieśla, K.; Kowalczyk, S.; Kędra, K.; Sobczak, M. The Influence of Ionizing Radiation on Paclitaxel-Loaded Nanoparticles Based on PLGA. *Appl. Sci.* **2023**, *13*, 11052. https://doi.org/10.3390/app131911052

Academic Editor: Domenico Lombardo

Received: 5 September 2023
Revised: 30 September 2023
Accepted: 5 October 2023
Published: 7 October 2023

1. Introduction

Cancer is a leading cause of death worldwide. According to the World Health Organization (WHO), the most common cancer types in 2020 were breast and lung cancer. Although breast cancer is characterized by a high cure rate when detected early, lung cancer was the most common cause of cancer deaths in 2020 (1.8 million deaths) [1]. It is,

therefore, of great importance to provide new solutions and new drug forms for anticancer therapy in combination with drug substances already placed on the market. Paclitaxel is a potent anticancer agent of natural origin that was originally isolated from yew bark (*Taxus brevifolia*). PTX is widely used in anticancer therapy, namely, in the treating of breast, ovarian, and non-small cell lung cancers, along with malignant melanoma and leukemias [2,3]. However, its low aqueous solubility is challenging considering the method of administration. For this reason, the entrapment of PTX into nanoparticulate systems has been extensively studied. Polymeric nanospheres reduce the side effects of cytostatics, enhance their tumor deposition and improve therapeutic efficacy. The advantage of DDSs over traditional drug forms results from controlled and sustained drug release in the body [4]. The most desirable drug carriers are obtained from biodegradable and biocompatible polyesters. These polymers, when introduced to the organism, are metabolically decomposed into completely removable and non-toxic products. Nevertheless, polymer drug carriers administered parenterally, are required to withstand the harsh conditions of the sterilization process. Considering biodegradable polyester drug carriers, the assurance of sterility is particularly challenging. Polyesters are thermally unstable; therefore, the number of potentially available sterilization methods is limited, mainly to aseptic filtration. The assurance of sterility under this method is very costly and demanding, and most importantly, for sterile filtration, membranes of a max. 0.22 μm pore size are recommended for use [5]. This, in turn, limits the use of this method in relation to particles size. Moreover, sterile filtration may be questioned from the safety point of view due to feasible microbiological contamination. Therefore, it is of great interest to find an effective, alternative method to enable the maintenance of sterility criteria without altering the physicochemical properties of the sterilized material. Among other commonly used sterilization methods are dry-heat, ionizing radiation, steam, the use of chemicals, and UV. Due to high temperatures applied, dry-heat and steam are excluded for heat- and moisture-sensitive polyester-based materials. High temperatures used in the sterilization process may alter the physicochemical and mechanical properties of polymer matrix and consequently alter the kinetic profile of drug release. Recently, Tapia-Guerrero et al. [6] presented preliminary studies on the use of UV and gamma photons for the sterilization of PLGA nanoparticles. They indicated that the use of UV can be an effective sterilization procedure and, at the same time, not cause significant changes in the physicochemical parameters of nanoparticles. However, the penetration depth of UV rays is very low [7] and therefore is limited mainly to surfaces and transparent scaffolds. The use of chemicals, such as gaseous ethylene oxide, or other highly volatile substances such as formaldehyde, may be applicable for heat- and moisture-sensitive materials. However, some harmful residues may remain within the polymer matrix [8]. Furthermore, using chemicals may alter the polymer's physicochemical properties by reacting with its functional groups [9]. On the other hand, ionizing radiation is the method of choice, gaining an increasing interest of scientists for terminal sterilization of DDSs. The use of the pharmacopeial recommended dose, 25 kGy, is considered adequate for sterilizing purposes [5,10–13]. Irradiation may be conducted under various conditions, including the presence of an inert gas atmosphere, room temperature, or cryogenic conditions. Two types of ionizing radiation are commonly used in the sterilization process, i.e., γ-irradiation and EB. The main advantage of irradiation with γ photons is its high penetration power. Gamma irradiation may be applied for non-uniform and high-density products. Like γ-ray, sterilization with EB is also instantaneous with high-dose delivery. However, it should be considered that sterilization efficiency varies depending on the material used.

Overall, radiation sterilization may be suitable for heat-sensitive drugs or drug carriers. It is a fast and effective process, providing high penetration power through the material. Nevertheless, specific undesirable changes caused by ionizing radiation may occur. Radiation-induced chain scission may lead to polymer fragmentation and consequently a decrease in average molecular mass (M_n) [14]. Moreover, the diminution in M_n is expected to increase with increased irradiation dose. In turn, this may alter the physicochemical

properties of drug carriers [15]. It is, therefore, essential to properly validate the sterilization procedure concerning any potential effects of irradiation, irrespectively, for each type of sterilized product.

In this study, we investigate the influence of γ-rays and EB (25 kGy) on the sterilization process of PTX-loaded polymeric nanoparticles based on self-synthesized polymer matrices. For this purpose, biodegradable copolymers of L-lactide (L-LA) and glycolide (GA) were synthesized in the presence of a bismuth catalyst system, and the effect of irradiation on this polyester DDSs was examined as well.

There is a number of already-published studies on the influence of ionizing radiation on polymeric matrices. However, only a few studies have dealt with the use of γ and EB irradiation for the sterilization purposes of polyester micro-/nanoparticles containing PTX (e.g., Wang et al. [16], who analyzed PTX-loaded PLGA microparticles (LA:GA = 50:50), and Song et al. [17], who analyzed PTX-loaded polylactide microspheres). Our study tries to fill this gap. What is more, these articles are based on the polymers of different monomer composition, therefore cannot be directly compared.

2. Materials and Methods

2.1. Materials

L-Lactide (L-LA, (3S)-*cis*-3,6-Dimethyl-1,4-dioxane-2,5-dione, 98%), poly(vinyl alcohol) (PVA, M_w = 13–23 kDa, 87–89% hydrolyzed), Cremophor® EL and poly(ethylene glycol) (PEG, M_n = 200 Da) were purchased from Sigma-Aldrich Co. (Poznań, Poland). Glycolide (GA, 1,4-Dioxane-2,5-dione, 98%) was purchased from TCI Europe N.V. Co. (Zwijndrecht, Belgium), and bismuth 2-ethylhexanoate ($BiOct_3$) was obtained from Alfa Aesar Co., which is part of Thermo Fisher Scientific (Kandel, Germany). Methanol (CH_3OH, analytical pure), chloroform ($CHCl_3$, analytical pure), dichloromethane (DCM, CH_2Cl_2, analytical pure) and hydrochloric acid (HCl, 35–38%) were obtained from POCH Co. (Gliwice, Poland). Acetonitrile (ACN, gradient grade for liquid chromatography) and trifluoroacetic acid (TFA, ≥99.0%) were purchased from Merck KGaA (Darmstadt, Germany), and phosphate-buffered saline (PBS, pH = 7.4) from Carl Roth GmbH + Co. KG (Karlsruhe, Germany). Paclitaxel (PTX, T45) was received from the Medical University of Gdańsk (Gdańsk, Poland).

2.2. Synthesis of Homo- and Copolymers via *Ring-Opening Polymerization*

The polymeric matrices were synthesized in bulk by the ring-opening polymerization (ROP) of L-LA and glycolide. The monomer composition was 0.85:0.15 (L-LA:GA). The polymerization process was performed under a dry argon atmosphere at 120 °C in the presence of a bio-safe bismuth catalyst system consisting of $BiOct_3$ (catalyst) and PEG200 (co-initiator). The monomer to PEG200 ratio was 100:1. The resulting polymers were purified using the precipitation method (with cold methanol) and dried under a vacuum. The polymers were stored at 4 °C until further usage.

2.3. Preparation of Paclitaxel-Loaded Nanoparticles

The nanoparticles were prepared by a single emulsion (*o*/*w*) solvent evaporation technique. For this purpose, PTX was dissolved in DCM and then poured into a pre-weighed polymer. The drug-to-polymer ratio was 1:10 (*w*/*w*), with a drug concentration of 2 mg mL^{-1}. After complete dissolution, the solution was added dropwise to a 1% PVA aqueous solution to form an o/w emulsion and emulsified (10,000 rpm, T25 digital ULTRA-TURRAX®, IKA, Staufen, Germany). The emulsion obtained was sonicated with 70% amplitude (Vibra Cell 505, SONICS & MATERIALS, INC., Newtown, CT, USA). After the evaporation of the organic solvent, the suspension was centrifuged at 20,000 rpm (Optima XPN-80 Ultracentrifuge, BECKMAN COULTER, Indianapolis, IN, USA) and washed twice to remove the residual emulsifier. The resulting nanoparticles were freeze-dried and stored at 4 °C for further usage.

2.4. Irradiation of Nanoparticles and Polymeric Matrices

The gamma irradiation of the samples was performed using ^{60}Co source in Gamma Chamber 5000 (BRIT, Navi Mumbai, India). The samples were irradiated with a dose of 25 kGy at a dose rate of 1.8 kGy h^{-1} in air and at ambient temperature.

Electron irradiation was performed in a linear electron accelerator Elektronika 10/10 with e-beam energy of 10 MeV using a dose of 25 kGy in air and at ambient temperature.

2.5. Structural Analysis of Polymers

The ^{1}H spectra of the polymers were acquired using an Agilent spectrometer (400 MHz) with 32 scans and a 2.56 s acquisition time. Deuterated chloroform was used as a solvent. The measurements were carried out at room temperature with 32 scans and 2.56 s acquisition time.

The ^{13}C NMR spectra of the samples were recorded at 300 MHz using a Varian spectrometer. Deuterated chloroform was used as a solvent. The measurements were carried out at room temperature with 10,000 scans and 1.73 s acquisition time.

The conversion of the reaction was determined by ^{1}H NMR spectroscopy. Polymer composition, chain microstructure and the yield of transesterification processes were defined by means of ^{13}C NMR spectroscopy measurements [18,19].

2.6. Gel Permeation Chromatography

The M_n value and dispersity index ($Đ$) of each sample were determined by gel permeation chromatography (GPC) using a Viscotek system comprising GPCmax and TDA 305 (triple detection array (TDA): RI, IV, LS) and equipped with DVB Jordi gel column(s) (linear, mixed bed). GPC was performed at 30 °C with DCM as an eluent with a flow rate of 1.0 mL min^{-1}. The calibration was performed using a set of 12 sharp polystyrene standards and a refractometer as a concentration detector.

2.7. Biological Assay

The cytotoxicity of the polymer was evaluated according to the ISO 10993-5:2009 guideline [20], i.e., by the neutral red uptake (NRU) test using BALB/c 3T3 clone A31 mice fibroblasts cell line (American Type Culture Collection). The BALB/3T3 clone A31 line used in the assay is recommended by ISO experts for the NRU cytotoxicity assessment test [20]. The polymeric extracts were prepared by incubating the samples in 1 mg mL^{-1} DMEM medium with 10% bovine serum (24 h, 37 °C) with stirring. The extracts were sterilized using a syringe filter. Highly cytotoxic latex and non-cytotoxic polyethylene were used as reference materials. The samples were considered cytotoxic if they reduced cell survival below 70% when compared to the untreated cells.

The genotoxicity of the polymeric materials was evaluated according to ISO 13829:2000 guideline [21], i.e., by the umu-test using *Salmonella typhimurium* TA3515/psk1002 (Deutsche Sammlung von Mikroorganismen und Zellkulturen GmbH, Germany). The principle of genotoxicity assessment by the umu-test is based on the use of the genetically engineered *Salmonella typhimurium* strain TA3515/psk1002, carrying the umuC-lacZ fusion plasmid. When the SOS response is induced by genotoxins, the umuC-lacZ fusion gene is expressed, and the umuC-lacZ fusion product protein is induced. Since this protein has β-galactosidase activity, it is possible to check the inductivity of umuC gene expression by measuring its activity colorimetrically. The experiment was conducted with and without metabolic activation (S9 rat liver fraction). The polymeric samples were incubated in PBS buffer (GIBCO) for 24 h at 37 °C. The extracts were sterilized by filtration before the assay. The 2-aminoanthracene and 4-nitroquinoline N-oxide were used as positive controls. The genotoxic potential of the samples was determined by Induction Ratio (*IR*). Samples were considered genotoxic when the *IR* value was min. 1.5.

2.8. Thermal Properties

DSC studies were carried out for the polymer matrix that was (a) non-irradiated, (b) γ-irradiated, and (c) irradiated with EB by using a Q200 apparatus (TA Instruments, New Castle, DE, USA). The measurements were performed in a heating/cooling/heating cycle from −50 °C to 180 °C and at a heating/cooling rate of 10 °C min^{-1}. The samples were placed in closed aluminum pans under a constant nitrogen flow. The characteristic temperatures of the occurring crystallization and melting processes were determined as the maximum or minimum of the exothermal (crystallization) and endothermal (melting) processes (T_c, T_m, T_{min}).

The crystalline phase content (X_c) was calculated based on the enthalpy values (Equation (1)) determined from the first heating run:

$$X_c = \frac{\Delta H_m - \Delta H_c}{\sum_i (W_i \times \Delta H_{mi,100\%})} \quad (1)$$

where ΔH_m and ΔH_c are the enthalpies of melting and cold crystallization, respectively; W_i is the weight fraction of the co-monomeric units in the polymer; and $\Delta H_{mi,100\%}$ is the enthalpy of melting for 100% crystalline polymer, which is set at 106 J g^{-1} (polylactide) [22] and 191 J g^{-1} (polyglycolide) [23].

Glass transition was determined based on DSC curves recorded during the second heating run when the polymer was already stabilized, mainly because the glass transition was difficult to isolate from other processes occurring during the first heating.

2.9. Dynamic Light Scattering

The average size and dispersity index (*PDI*) of the prepared nanoparticles were measured by dynamic light scattering (DLS) using a Zetasizer Nano ZS analyzer (Malvern Panalytical Ltd., Malvern, UK). For this purpose, an appropriate amount of the nanoparticles was resuspended in purified deionized water. The zeta-potential (ZP) was determined by electrophoresis in a capillary cell.

2.10. Surface Morphology

The morphology of the nanoparticles was evaluated by scanning electron microscopy (SEM) using an Ultra Plus microscope (ZEISS, Oberkochen, Germany). For this purpose, a small amount of the samples was stuck on a double-sided tape attached to a metal stub and sputter-coated with a thin layer of gold before the measurements.

2.11. Drug Content

To determine the drug content, a certain amount of PTX-loaded nanospheres was dissolved in ACN. The samples were assayed by high-performance liquid chromatography (HPLC) at λ = 229 nm, according to Stefanowicz et al. [3]. The HPLC system was the Beckman Coulter system (Miami, FL, USA). Chromatographic separations were carried out using a Luna C18(2) column (25 cm, 5 µm, 100 A, Phenomenex, Torrance, CA, USA). Chromatographic conditions were a mobile phase consisting of ACN/water/methanol (60/2/38, *v*/*v*/*v*) with TFA (0.1%), and a flow rate of 1 mL min^{-1}. The analyses were performed at 30 °C.

Encapsulation efficiency (*EE*) was calculated according to the following equation (Equation (2)):

$$EE(\%) = \frac{m_e}{m_t} \times 100\% \quad (2)$$

where m_e is the amount of the drug entrapped in the nanoparticles, and m_t is the total amount of drug added.

Drug loading capacity (*DL*) was calculated according to the following formula (Equation (3)):

$$DL(\%) = \frac{m_e}{m_n} \times 100\% \quad (3)$$

where m_e is the amount of the drug entrapped in the nanoparticles, and m_n is the total weight of nanoparticles.

2.12. In Vitro Drug Release Study

In vitro drug release tests were performed using the dialysis method on free PTX as a control and PTX-loaded nanospheres that were (a) non-irradiated, (b) irradiated with γ-rays, and (c) irradiated with EB. PBS solution (pH = 7.4), containing Cremophor® EL (0.5% (*w*/*v*) as a solubilizer, was used as a release medium. The suspensions were maintained at 37 °C while stirring at 100 rpm (ES-20, Biosan, Riga, Latvia). The amounts of PTX released from the samples were chromatographically determined at λ = 229 nm, according to Section 2.11.

The results of the PTX release were analyzed according to zero-order, first-order, Higuchi and Korsmeyer–Peppas mathematical models, as shown in Equations (4)–(7) [24,25].

Zero order:

$$F = kt \quad (4)$$

First order:

$$logF = logF_0 - \frac{kt}{2.303} \quad (5)$$

Higuchi model:

$$F = k\sqrt{t} \quad (6)$$

Korsmeyer–Peppas model:

$$F = kt^n, for\ F < 0.6 \quad (7)$$

where F is the fraction of drug released in time (t), F_0 is the initial concentration of the drug, k is the model constant, and n is the release exponent.

3. Results and Discussion

The aim of this research was to develop nontoxic PLGA systems for the controlled release of PTX. The DDSs obtained in this work are intended for biomedical application and therefore require sterilization. For this purpose, the use of ionizing radiation (γ-rays and EB, 25 kGy) as a potential sterilization technique was proposed. The influence of irradiation on the structure and physicochemical properties of polymeric nanoparticles, as well as the kinetic profile of PTX release, was analyzed in detail.

3.1. Synthesis and Characterization of Polymers

The copolymer of L-lactide and glycolide with monomer composition L-LA:GA = 0.85:0.15 was synthesized using a bismuth catalyst system, consisting of the catalyst, $Bi(Oct)_3$, and the co-initiator, PEG200, leading to the formation of a linear polyester.

Importantly, the polymeric matrix obtained was neither cyto- nor genotoxic, which is critical in biomedical applications. In order to assess the cytotoxicity of the polymer, the NRU test was performed. It was observed that for the highest concentrations of the extracts tested (1 mg mL^{-1}), the cell survival rate was 106 ± 6% when compared to untreated cells (Table 1). These results confirmed the lack of cytotoxic effect of the PLGA sample tested. The umu-test with and without metabolic activation was used to assess the

genotoxicity of the polymer. At the highest concentration tested (1 mg mL^{-1}), the PLGA samples did not inhibit the growth of Salmonella typhimurium cells (G > 0.5). This, together with the induction ratio (IR) being lower than 1.5, indicates the lack of genotoxicity of the polymer (Table 1).

Table 1. Results of umu- and NRU tests (concentration 1 mg mL^{-1}).

Sample	Genotoxicity Assay				Cytotoxicity Assay
	−S9 [a]		+S9 [b]		
	G	IR [a]	G	IR [b]	Cells Viability (%)
PLGA	0.97 ± 0.07	0.80 ± 0.07	0.97 ± 0.07	1.31 ± 0.40	106 ± 6
Positive Control	1.04 ± 0.01	3.30 ± 0.28	0.87 ± 0.04	2.53 ± 0.41	1 ± 1
Negative Control	1.00 ± 0.01	1.00 ± 0.05	1.00 ± 0.04	1.00 ± 0.08	111 ± 1

[a] version without metabolic activation; [b] version with metabolic activation.

The results of the copolymerization of L-lactide with glycolide are presented in Table 2. The polymerization reached 94.5% conversion of L-LA and the near-complete conversion of GA. The synthesized polymer was irradiated using γ-rays and EB with a dose of 25 kGy. Molecular masses and dispersity coefficients of irradiated and non-irradiated PLGA samples were determined by GPC in triplicate. The resulting polymer was characterized by a low dispersity index ($Đ$ = 1.83), and the average molecular mass M_n = 13.8 kDa (Table 2), which was in line with the calculations based on the monomer feed ratio (M_n ~14.5 kDa). As it is shown in Table 2, a considerable decrease in M_n was observed for the copolymer subjected to both γ-rays and EB (13.8% and 14.1% of M_n decrease for PLGA samples irradiated with γ-rays and EB, respectively) along with an increase in dispersity. Interestingly, no significant difference between the influence of γ-rays and EB on the M_n of PLGA was observed. In comparison, in our previous research [26] describing the influence of irradiation on PTX-loaded nanoparticles of different polymer matrices (poly(L-lactide)—PLA, poly(ε-caprolactone)—PCL, the copolymer of L-LA and ε-caprolactone—PLACL, and the copolymer of GA and ε-caprolactone—PCLGA), a relatively higher decrease in M_n was observed for γ-irradiated copolymers (ΔM_{nPLACL} = −12.7%, ΔM_{nPCLGA} = −28.2%) compared to the copolymers irradiated with EB (ΔM_{nPLACL} = +5.5%, ΔM_{nPCLGA} = +3.2%) [26]. The overall decrease in the molecular mass of PLGA observed after the irradiation process may suggest that the chain scission was a leading mechanism, taking place during the sterilization of the polymer by both γ-rays and EB. This is consistent with the literature, according to which the dominant mechanism for PLGA irradiated with low doses of γ-rays and EB is chain scission [27,28]. During the irradiation, PLGA is excited, and active species, such as free radicals, are formed. The active species initiate further reactions, causing bond cleavage among the polymer chain. As a result, the molecular mass of the polymer is lowered [28].

Table 2. The influence of irradiation on the microstructure and physicochemical properties of PLGA.

Irradiation	M_n (kDa) [a]	ΔM_n (%) [ab]	$Đ$ [a]	F_{GG}	l_{LL} [e]	l_{GG} [e]	$T_{II\ (LGL)}$	$T_{II\ (GLG)}$
non-irr	13.79 ± 0.10	n.a.	1.83 ± 0.01	0.15	4.33	1.23	0.15	1.14
irr-γ	11.89 ± 0.64	−13.82	1.95 ± 0.09	0.16	3.35	1.28	0.13	1.38
irr-e$^-$	11.85 ± 0.15	−14.07	1.96 ± 0.03	0.16	4.61	1.22	0.15	0.79

n.a.—not applicable; [a]—determined by GPC; [b]—M_n change compared to non-irradiated sample; F_{GG}—mole fraction of glycolidyl units in the copolymer chain; l_{LL}[e]—experimental average length of

lactidyl blocks; l_{GG}^{e}—experimental average length of glycolidyl blocks; T_{II}—yield of the second mode of transesterification.

The microstructure of the polymers was investigated using ^{13}C NMR spectroscopy. The characteristic signals were assigned to corresponding co-monomeric sequences by analogy according to the literature [19]. As seen in Figure 1, the signal for consecutive –LLL– sequence (169.65 ppm, Table 3) dominated over other signals due to the high LA-to-GA ratio in the feed (LA:GA = 85:15). However, the presence of odd sequences, such as –LGL– and –GLG–, was also noticed, indicating the participation of the transesterification of the second mode accompanying the polymerization process. As a result, the obtained polymer was of a random structure and short average lengths of blocks (Table 2).

Table 3. Chemical shift in ^{13}C NMR spectrum of PLGA.

Chemical Shift (ppm)	Sequence
169.65	LLLL
169.58	LLGG
169.50	LGLL
169.47	GGLL
169.38	GLG
166.55	GGLG
166.49	GGLL
166.47	GGGG
166.44	LGL
166.38	LLGG

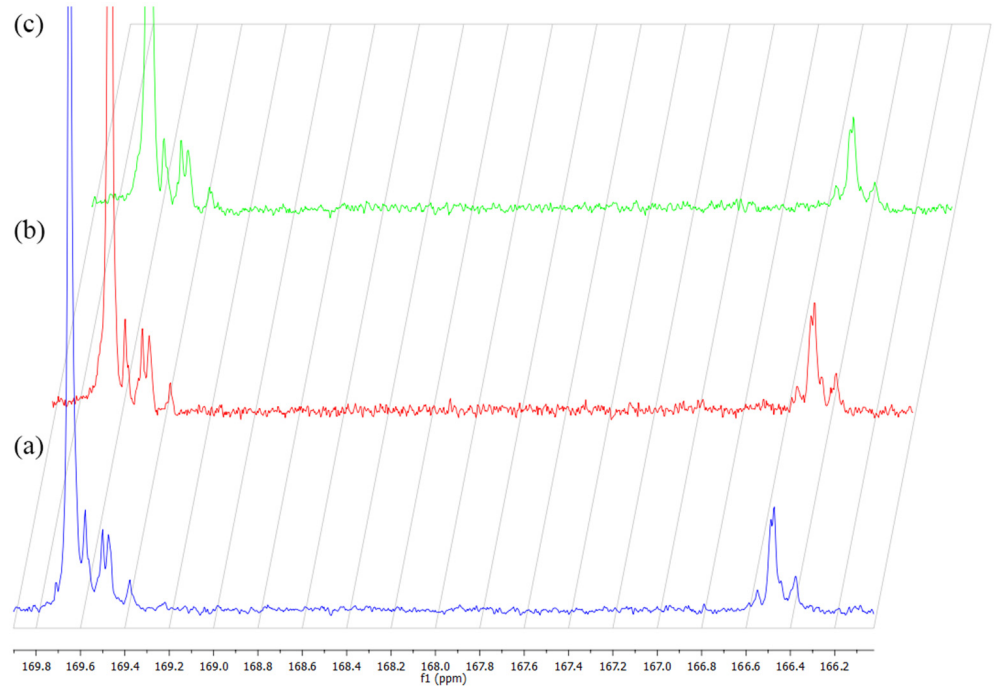

Figure 1. The influence of ionizing radiation on ^{13}C NMR spectra of PLGA non-irr (**a**), irr-γ (**b**) and irr-e^{-} (**c**).

As seen in Figure 1, no additional signals were found in the ^{13}C NMR spectra upon irradiation. Additionally, a detailed analysis of the polymer microstructure revealed only negligible changes in relation to the average length of glycolidyl units (l_{GG}^{e}) and $T_{II[LGL]}$ (Table 2). As seen from the value of T_{II} of lactyl units (L) ($T_{II[GLG]}$ = 1.11), the synthesized polymer was of a random structure. After irradiation with γ-rays, $T_{II[GLG]^{\gamma}}$ increased to

1.38, and the average length of lactidyl units (l_{LL}) decreased from 4.33 to 3.35. These slight differences may suggest that the irradiation might cause some changes in the regions of the lactidyl units of the copolymer chain. It appears that the relative amount of –GLG– sequences in the copolymer increased after irradiation with γ-rays, possibly as a result of chain scission. However, after the irradiation of PLGA with EB, $T_{II[GLG]}$ slightly decreased ($T_{II[GLG]}^{EB}$ = 0.79), and l_{LL} increased from 4.33 to 4.61. It has to be taken into consideration that irradiation with EB was conducted with a high dose rate in considerably lower time compared to irradiation in a gamma chamber. In fact, exposition in a gamma chamber needs a dozen hours to obtain a dose of 25 kGy, and there is enough time that free radicals reactions leading to chain scission may occur with high efficiency, especially in the presence of atmospheric oxygen. On the contrary, during exposition in EB, a considerable amount of radicals are formed in a short time. These (high molecular) radicals might recombine; thus, the processes of cross-linking become more probable. Additionally, due to limited contact with oxygen, degradation processes may also be limited, compared to irradiation with γ rays. As a result, these processes may lead to chain elongation.

The overall results, i.e., decrease in molecular mass and changes in the polymer microstructure after irradiation, may be explained in terms of two concurring processes taking place during irradiation (chain scission and cross-linking). However, the overall decrease in the M_n of PLGA suggests the predominance of chain scission over cross-linking. According to the literature, lactidyl units may be more susceptible to irradiation than glycolyl units (G) due to the presence of tertiary carbon atoms, which, together with ester linkages, are the important sites for bond cleavage [9,27]. Therefore, the changes in the microstructure were more apparent in the values of T_{II} and average block lengths related to lactidyl units.

3.2. The Influence of Ionizing Radiation on Thermal Properties of Polyesters

The influence of ionizing radiation on the thermal properties of PLGA was assessed by DSC. During the first heating of the non-irradiated sample (Figure 2a), a decrease in heat flow was observed at temperatures above 30 °C, possibly connected to the glass transition. It was accompanied by an endothermal effect with the minimum of 77.3 °C. In the higher temperature range, the exothermal effect of cold crystallization (recrystallization of the polymer chains into the structure with lower energy; T_c = 103.7 °C) was observed. It was followed by the endothermal effect with two minima (at 138.0 °C and 147.1 °C). The two minima of the endothermal effect can be related to a superposition of the melting of different supramolecular structures of the polymer and, precisely, to the melting of less- and better-ordered crystals [29]. Loo et al. [30] attributed them to the melting of the more tightly packed linear polymer fraction (at higher temperature) and the more branched chains (at lower temperature).

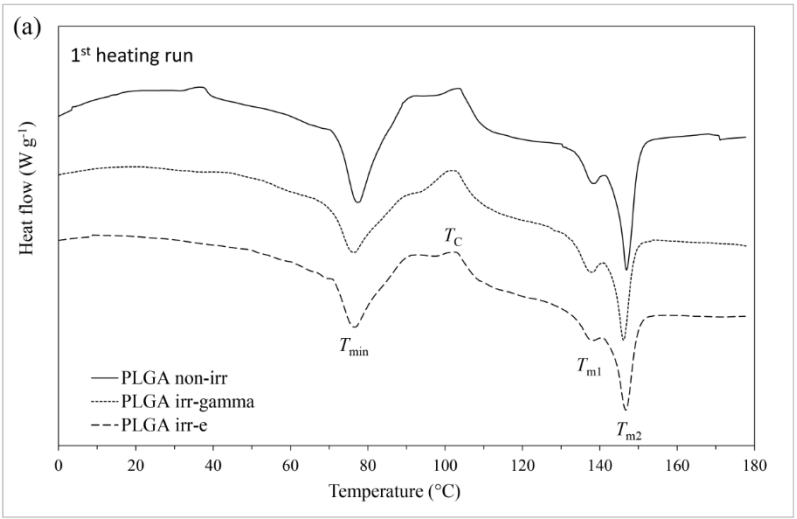

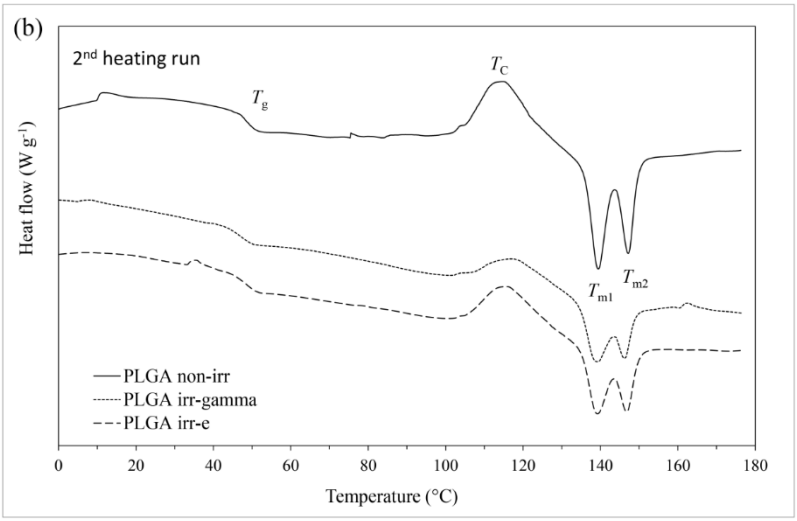

Figure 2. DSC curves of non-irradiated PLGA and PLGA irradiated with γ-rays and EB: (**a**) 1st heating run and (**b**) 2nd heating run.

The genesis of the endotherm accompanying the glass transition (T_{min} = 77.3 °C) is not entirely clear. It can be considered as related to the melting of the low-ordered fractions of PLGA, that are possibly characterized by the polymer of low molecular weight (oligomers). It follows the hypothesis given by Dorati et al. [31], who related the endothermal peak between 20 °C and 40 °C of PEG-PLGA samples to the melting of free PEG-PLGA blocks of the polymer that were formed during storage or as a result of radiation-induced degradation [31].

During the second heating (Figure 2b), the initial sample undergoes recrystallization followed by melting, with the enthalpies of both processes being similar (48–50 J g^{-1}) (indicating that almost all of the melted material was formed during recrystallization occurring at a lower temperature during the same heating cycle). Moreover, these enthalpies were similar to the enthalpy of melting occurring on first heating.

Based on the above data, the copolymer was found to reveal a semicrystalline structure (X_c = 35.1%). Additionally, single T_g indicates good homogeneity of the copolymer. The influence of ionizing radiation on the thermal and crystalline properties of PLGA is shown in Table 4. No change in T_g was observed after irradiation with EB, whereas a relatively small effect was observed after the gamma irradiation (decrease from 48.1 °C to 47.6 °C). However, the changes were noticed in the enthalpies and characteristic temperatures of the crystallization and melting processes (Table 4). This was particularly evident in the enthalpies of the processes. It was also noticed that the effect of gamma irradiation was higher than that of EB.

Table 4. The influence of ionizing radiation on thermal parameters of PLGA determined from DSC.

Irradiation	T_g [b] (°C)	T_{min} [a] (°C)	T_c [a] (°C)	T_m [a] (°C)	ΔH_c [a] (J g^{-1})	ΔH_m [a] (J g^{-1})	X_c [a] (%)
non-irr	48.1	77.3	103.7	138.0 (T_{m1}) / 147.1 (T_{m2})	8.52	50.16	35.1
irr-γ	47.6	76.8	102.6	137.4 (T_{m1}) / 146.2 (T_{m2})	15.00	41.92	22.7
irr-e$^-$	48.2	76.7	103.3	137.3 (T_{m1}) / 146.5 (T_{m2})	4.76	42.06	31.4

[a] determined from the 1st heating run; [b] determined from the 2nd heating run.

It can be concluded that ionizing radiation induces a decrease in the crystalline phase content. However, the effect was much higher after irradiation in the gamma chamber

compared to irradiation with EB (X_c decreased from 35.1% to 22.7% and to 31.4%, respectively).

These results, in combination with GPC data (Table 2), may differentiate both types of irradiation (γ-rays and EB) in regard to the type of mechanism prevailing during the irradiation process (crosslinking and/or chain scission). Importantly, the irradiation of the samples was conducted in air. The presence of atmospheric oxygen enables reactions of alkyl radicals with oxygen. In the case of prolonged exposure to radiation in the gamma chamber, this resulted in high participation in the degradation process. However, rapid irradiation with a high dose (as for EB in our case) acts similarly to the exposure of the material to irradiation in an inert gas atmosphere, which prevents the formation of peroxyl radicals within the interior of the material. This occurs because atmospheric oxygen does not have time to diffuse into the sample and cannot react with its interior. In that case, the outer layer of the material (exposed to oxygen), favors oxidative degradation, while some crosslinking may occur inside the material [32]. This may therefore explain the overall decrease in M_n in the case of both types of irradiation, together with the contradictory results of the microstructure of the polymer, which suggests the slight elongation of lactidyl segments (from 4.33 to 4.61) in the copolymer chain irradiated with EB.

Contrary to the non-irradiated copolymer ($\Delta H_c 2nd^{heating}$ = 48.13 J g^{-1} and $\Delta H_m 2nd^{heating}$ = 49.84 J g^{-1}), in the case of both irradiated samples, recrystallization occurred to a much lesser extent during the second heating (as shown by the lower values of ΔH_c being equal to 22.86 J g^{-1} and 29.17 J g^{-1} in the case of the γ-irradiated and EB-irradiated samples, respectively). However, even though the melting enthalpies were lower (31.90 J g^{-1} and 39.68 J g^{-1} in the case of γ-irradiated and EB-irradiated PLGA samples), this indicated a lower crystalline content. Some of the melting crystalline phase was present in the irradiated samples before the start of this heating cycle (as shown by the lower values of ΔH_c compared to ΔH_m), indicating that it was formed during the preceding cooling cycle (desmeared curves). Simultaneously, the appropriate values of T_c were equal to 115.0 °C, 117.8 °C and 116.2 °C, and the values of T_m were equal to 139.4 and 147.2 °C (PLGA non-irr), 139.0 and 146.1 °C (γ-irr PLGA), and 139.1 and 146.6 °C (EB-irr PLGA).

Therefore, it can be concluded that irradiation also influences the recrystallization and melting processes taking place during cooling and the second heating. Similarly to other cases, the effect was more evident after radiation treatment performed in the gamma chamber compared to EB.

3.3. Evaluation of the Stability of PTX-Loaded Nanoparticles to Irradiation

The PTX-loaded nanoparticles were obtained using single solvent evaporation technique with an encapsulation efficiency of PTX of 94.2 ± 3.0%. The *DL* value of PTX was 8.0 ± 0.2%.

Importantly, the HPLC spectra of the PTX extracted from the irradiated nanoparticles (Figure 3) did not show any additional peaks (compared to non-irradiated samples). Moreover, the areas of the peak of PTX (RT ~6 min) obtained from the chromatograms of the non-irradiated and irradiated samples, and recalculated with a given concentration gave an RSD value of 0.4%. This results confirm that PTX did not degrade after irradiation with both types of ionizing radiation (γ-rays and EB) and suggest the stability of PTX encapsulated in polymeric nanoparticles to irradiation (25 kGy).

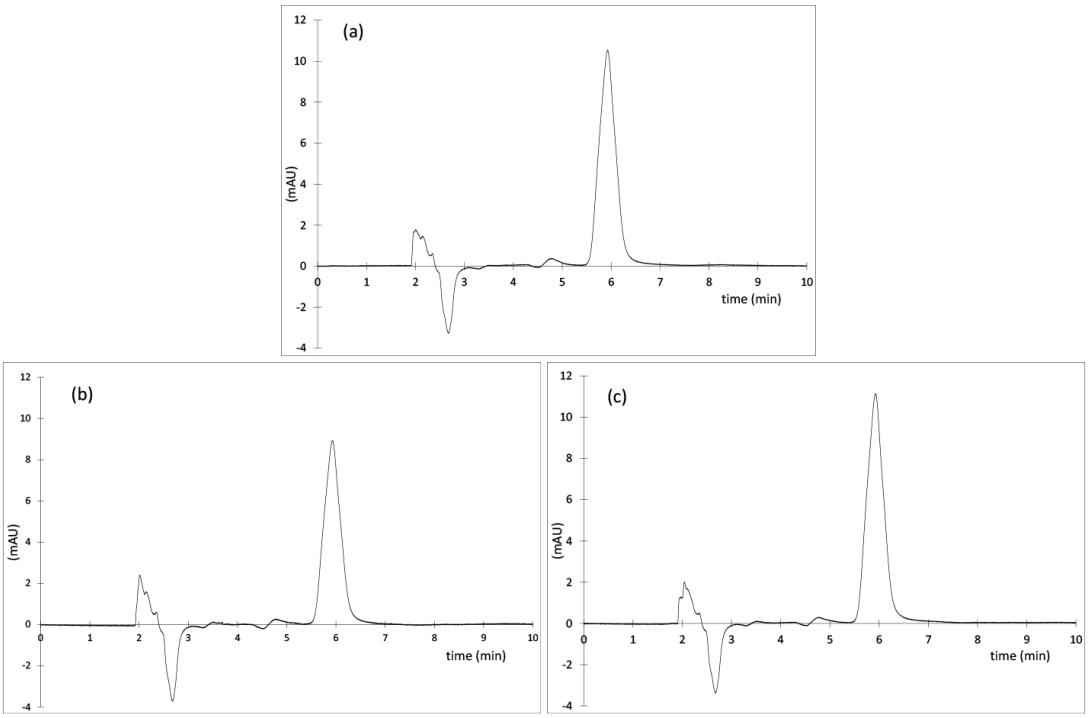

Figure 3. HPLC chromatograms of PTX extracted from the nanoparticles (**a**) non-irradiated (C_{PTX} = 7.6 μg mL^{-1}), (**b**) γ-irradiated (C_{PTX} = 5.6 μg mL^{-1}) and (**c**) irradiated with EB (C_{PTX} = 7.8 μg mL^{-1}).

The resulting particles (independent of drug loading) were spherical in shape (as shown by SEM, Figure 4) and varied in dimensions. No particular differences between the particles morphology were noticed after irradiation. DLS data have shown that the average size of particles was equal to 253.5 ± 3.9 nm with narrow particle size distribution (*PDI* < 0.2) independent of whether the particles were loaded or not (Table 5). No change in average particles size was noticed after the irradiation with γ-rays and EB (compared to non-irradiated samples). The zeta potential of PTX-loaded particles was negative (−20.83 mV) and similar to the formulations prepared without the drug. This might be explained by the lack of ionizable functional groups in PTX molecules [33]. However, after irradiation, *ZP* decreased and reached −36.73 mV and −33.75 mV in the case of γ- and EB-irradiated samples, respectively. This may be attributed to a greater amount of ionized terminal carboxylic groups [34,35] resulting from polymer degradation, which may potentially contribute to the increase in particles stability in suspension.

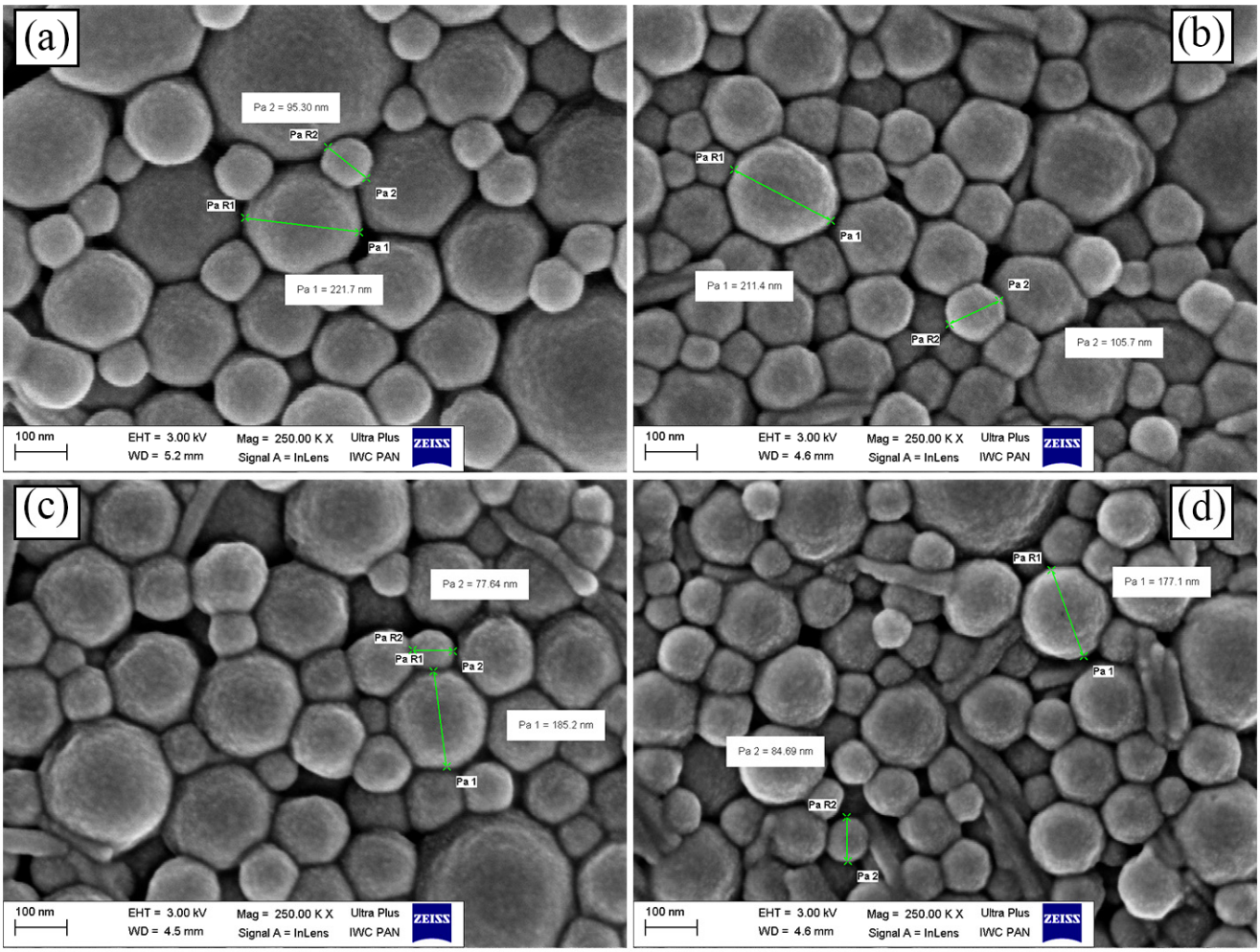

Figure 4. SEM micrographs of lyophilized PLGA nanoparticles: (**a**) placebo, (**b**) non-irr, (**c**) irr-γ and (**d**) irr-e PLGA nanospheres with PTX.

Table 5. The influence of ionizing radiation on PTX-loaded nanoparticles determined by DLS.

Irradiation	Size (nm)	*PDI*	*ZP* (mV)
PLGA	253.6 ± 4.1	0.19 ± 0.03	−22.48 ± 0.41
PLGA-PTX non-irr	253.5 ± 3.9	0.17 ± 0.03	−20.83 ± 1.17
PLGA-PTX irr-γ	256.4 ± 3.1	0.20 ± 0.02	−36.73 ± 1.26
PLGA-PTX irr-e$^-$	253.6 ± 2.1	0.17 ± 0.02	−33.75 ± 0.57

3.4. In Vitro Drug Release

Figure 5 displays cumulative drug release profiles of irradiated and non-irradiated nanoparticle formulations. The release profile of free PTX was added as a control. The release of PTX from PLGA nanoparticles exhibited a monophasic release pattern (no initial burst release was observed). An almost complete drug release was observed after 36 days of the study, independent of applied irradiation. Importantly, the release of free drug was faster compared to the drug release from the nanoparticles. This indicates that the release profiles of the encapsulated drug were not hindered by the dialysis membrane.

The in vitro release mechanism of paclitaxel from the nanoparticles was further evaluated using zero-order, first-order, Higuchi and Korsmeyer–Peppas mathematical release kinetic models (Table 6).

Table 6. Data analysis of PTX release from PLGA nanoparticles.

Irradiation	Zero-Order	First-Order	Higuchi		Korsmeyer–Peppas	
	R^2	R^2	R^2	K_H [a]	R^2	n [b]
non-irr	0.881	0.998	0.981	17.805	0.995	0.793
irr-γ	0.949	0.963	0.991	17.906	0.977	0.857
irr-e	0.946	0.974	0.995	17.820	0.993	0.857

[a]—release rate constant; [b]—release exponent.

The values of R^2 for zero-order and first-order kinetics suggest that the drug release profiles from the PLGA nanoparticles followed the first-order kinetic, regardless of irradiation. Some references, as, e.g., the work of Jusu et.al. [36], demonstrate the zero-order release of paclitaxel from PLGA nanoparticles, and being well characterized by Korsmeyer-Peppas model. However, mathematical models are only a simplification and do not give exact insight into the mechanism of drug release. Moreover, the composition of the comonomers obtained by us is different from those tested by other authors. It should also be noted that the obtained R^2 values for the zero-order and first-order kinetics models are not very different. Probably, in the case of the obtained nanoparticles, we are dealing with a mixed drug release mechanism.

Additionally, the release data fitted well to the Higuchi and Korsmeyer–Peppas mathematical models. A detailed analysis of the release exponent n from the Korsmeyer–Peppas model ($n_{\text{non-irr}} = 0.79$ and $n_{\text{irr-}\gamma,\text{EB}} = 0.86$) indicates drug release with non-Fickian diffusion ($0.45 < n < 0.89$), in which two mechanisms (diffusion and erosion) take part in drug release [37].

Only negligible differences (in the frame of the scatter of experimental data) in the kinetic profiles of PTX release from PLGA drug carriers were observed after irradiation. This suggests the good resistance of PLGA nanoparticles to irradiation. Despite some degradation observed within the polymer matrix itself, drug release profile from the irradiated samples did not vary significantly compared to the non-irradiated samples. This may be explained to some extent by the radio-protective effect of PTX resulting from its molecular structure. Aromatic groups present in PTX structure act as energy sinks via the energy transfer mechanism and stabilize the molecule [38,39].

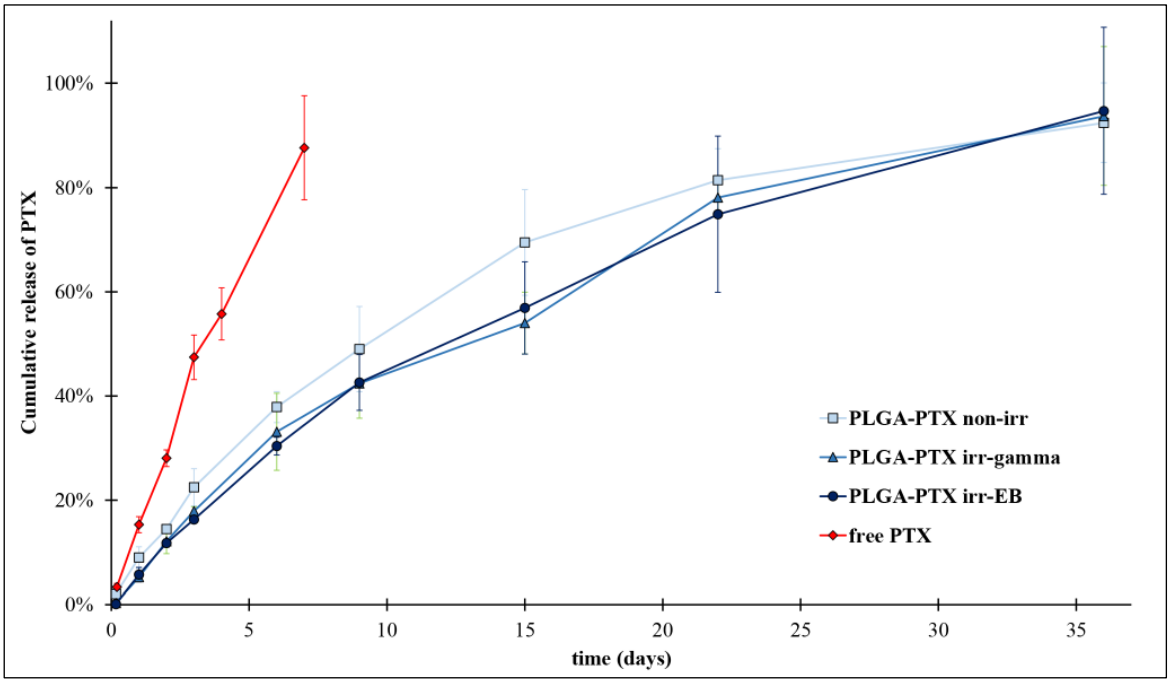

Figure 5. The influence of irradiation on kinetic profiles of PTX release from PLGA nanoparticles.

4. Conclusions

In this study, we demonstrate the feasibility of the radiation sterilization of PLGA nanoparticles containing PTX. Importantly, the polymer matrix synthesized in this study and used as the drug carrier was neither cyto- nor genotoxic, which is required in the case of biomedical applications. The influence of irradiation was analyzed to develop nanoparticles and the polymer matrix itself, and the type of ionizing radiation (γ-rays or EB). Considering the polymer matrix, PLGA exhibited a noticeable degradation degree, given as a decrease in M_n, reaching approx. 14% after irradiation with γ-rays and EB. This result suggests that the main mechanism taking part during the irradiation of PLGA was chain scission. However, the structural changes differed depending on the type of ionizing radiation applied. Gamma-irradiation significantly affected the micro- and macroscopic properties of PLGA by shortening lactidyl segments in the polymer chains. While only negligible changes in characteristic temperatures of the polymer (T_g, T_c, T_m) were observed, the crystallite content decreased from 35.1% to 22.7%. Contrary to irradiation with γ-rays, in the case of the polymer irradiated with EB, a slight elongation of lactidyl blocks was observed. This may be explained by differences in the course of radiation processes. Considering the polymer irradiated with γ-rays, the changes of properties may be assigned with the predominance of chain scission (probably accompanied to some extent by cross-linking), while during irradiation with EB, two processes, that differ in the mechanism of action (chain scission and cross-linking) were likely to occur to a similar extent. While prolonged exposure of the polymer to γ-rays leads to the breakage of polymer chains and the oxidative degradation of the material. In the case of EB, the rapid irradiation of the polymer with a high dose (compared to γ-rays) disables oxygen diffusion into the internal layers of the material. It creates similar conditions as the inert gas atmosphere. As a result, external layers of the polymer undergo oxidative degradation, while cross-linking occurs inside the polymer matrix [32]. This may, therefore, explain the overall decrease in M_n in the case of both types of irradiation and the elongation of lactidyl blocks of PLGA irradiated with EB.

Comparing the effects of the sterilization process with γ-rays and EB on the physicochemical, structural, and thermal properties of PLGA clearly indicates that within this study, EB induced less structural damage to the copolymer.

The nanoparticles were obtained with a high efficiency of PTX encapsulation (*EE* = 94.2 ± 3.0%). The particles characterize a spherical shape and an average size of 253.5 ± 3.9 nm (shown by DLS). The physicochemical analysis of the particles did not reveal any changes in their size and morphology after the sterilization process. A complete release of PTX was achieved within the first 36 days of the study. The nanoparticles released the drug with a first-order kinetic profile and with non-Fickian diffusion (anomalous mechanism). Importantly, the sterilization process (independent of the type of ionization) did not significantly affect the drug's release.

The overall results have shown that PLGA nanoparticles have potential for the sustained delivery of PTX and have proved the great potential of EB for the purposes of sterilization of PLGA-based nanoparticles containing PTX.

Author Contributions: I.M.D.: conceptualization, chemical, structural, analytical and pharmaceutical research, methodology, investigation, formal analysis and writing—original draft; R.F.: biological research, methodology and investigation; A.Z.: DSC measurement and analysis; K.C.: interpretation of thermal analysis data, investigation, formal analysis, writing—original draft, and editing and supervision; S.K.: GPC measurement; M.S.: conceptualization, chemical, structural, analytical and pharmaceutical research, investigation, writing—original draft, editing and supervision. K.K.: interpretation of thermal analysis data, DLS and Zeta potential analysis data, and text correction. All authors have read and agreed to the published version of the manuscript.

Funding: The work was performed as part of Project number FW231/1/F/MBS/N/21, which was carried out from 2021 to 2023 and was funded by the scientific financial support obtained from the Medical University of Warsaw (Poland).

Institutional Review Board Statement: Not applicable.

Informed Consent Statement: Not applicable.

Data Availability Statement: The data presented in this study are available upon request from the corresponding author.

Acknowledgments: The contribution of Izabela M. Domańska was realized within Project No POWR.03.02.00-00-I009/17-00 (Operational Project Knowledge Education Development 2014–2020 co-financed by the European Social Fund).

Conflicts of Interest: The authors declare that they have no known competing financial interest or personal relationships that could appear to have influenced the work described in this paper.

Sample Availability: Samples of all compounds are available from the authors.

Abbreviations

ACN	acetonitrile
$BiOct_3$	bismuth 2-ethylhexanoate
$Đ$	dispersity index (GPC)
DDSs	drug delivery systems
EB	electron-beam
EE	encapsulation efficiency
GA	glycolide
G	glycolyl unit
GG	glycolidyl unit
ΔH_c	enthalpy of cold crystallization
ΔH_m	enthalpy of melting
IR	induction ratio
L	lactyl unit
LL	lactidyl unit
L-LA	L-lactide
l_{GG}	average length of glycolidyl units
l_{LL}	average length of lactidyl blocks
M_n	number average molecular mass

NRU	neutral red uptake
PBS	phosphate-buffered saline
PDI	dispersity index (DLS)
PEG	poly(ethylene glycol)
PLGA	copolymer of L-lactide and glycolide
PTX	paclitaxel
PVA	poly(vinyl alcohol)
ROP	ring-opening polymerization
T_c	temperature of cold crystallization
TFA	trifluoroacetic acid
T_g	glass transition temperature
T_{II}	transesterification of the second mode
T_m	temperature of melting
X_c	crystalline phase content
ZP	zeta potential

References

1. WHO. Cancer Fact Sheet. 2022. Available online: https://www.who.int/news-room/fact-sheets/detail/cancer (accessed on 26 May 2022).
2. Surapaneni, M.S.; Das, S.K.; Das, N.G. Designing Paclitaxel Drug Delivery Systems Aimed at Improved Patient Outcomes: Current Status and Challenges. *ISRN Pharmacol.* **2012**, *2012*, 623139. https://doi.org/10.5402/2012/623139.
3. Stefanowicz, Z.; Sobczak, M.; Piętniewicz, A.; Kołodziejski, W. Macromolecular conjugates of paclitaxel: Synthesis, characterization, and In Vitro paclitaxel release studies based on HPLC validated method. *Acta Chromatogr.* **2016**, *28*, 99–117. https://doi.org/10.1556/AChrom.28.2016.1.8.
4. Martins, K.F.; Messias, A.D.; Leite, F.L.; Duek, E.A.R. Preparation and characterization of paclitaxel-loaded PLDLA microspheres. *Mat. Res.* **2014**, *17*, 650–656. https://doi.org/10.1590/S1516-14392014005000028.
5. Council of Europe. *Suppl. 9.2. European Directorate for the Quality of Medicines & HealthCare*; Council of Europe: London, UK, 2017, pp. 4333–4350.
6. Tapia-Guerrero, Y.S.; Del Prado-Audelo, M.L.; Borbolla-Jiménez, F.V.; Gomez, D.M.G.; García-Aguirre, I.; Colín-Castro, C.A.; Morales-González, J.A.; Leyva-Gómez, G.; Magaña, J.J. Effect of UV and Gamma Irradiation Sterilization Processes in the Properties of Different Polymeric Nanoparticles for Biomedical Applications. *Materials* **2020**, *13*, 1090. https://doi.org/10.3390/ma13051090.
7. Raeiszadeh, M.; Adeli, B. A Critical Review on Ultraviolet Disinfection Systems against COVID-19 Outbreak: Applicability, Validation, and Safety Considerations. *ACS Photonics* **2020**, *7*, 2941–2951. https://doi.org/10.1021/acsphotonics.0c01245.
8. Igartua, M.; Hernández, R.M.; Rosas, J.E.; Patarroyo, M.E.; Pedraz, J.L. γ-Irradiation effects on biopharmaceutical properties of PLGA microspheres loaded with SPf66 synthetic vaccine. *Eur. J. Pharm. Biopharm.* **2008**, *69*, 519–526. https://doi.org/10/cr2vtz.
9. Domańska, I.M.; Oledzka, E.; Sobczak, M. Sterilization process of polyester based anticancer-drug delivery systems. *Int. J. Pharm.* **2020**, *587*, 119663. https://doi.org/10.1016/j.ijpharm.2020.119663.
10. Maksimenko, O.; Pavlov, E.; Toushov, E.; Molin, A.; Stukalov, Y.; Prudskova, T.; Feldman, V.; Kreuter, J.; Gelperina, S. Radiation sterilisation of doxorubicin bound to poly(butyl cyanoacrylate) nanoparticles. *Int. J. Pharm.* **2008**, *356*, 325–332. https://doi.org/10/bkcr7f.
11. Dorati, R.; Genta, I.; Montanari, L.; Cilurzo, F.; Buttafava, A.; Faucitano, A.; Conti, B. The effect of γ-irradiation on PLGA/PEG microspheres containing ovalbumin. *J. Control. Release* **2005**, *107*, 78–90. https://doi.org/10.1016/j.jconrel.2005.05.029.
12. Fernandezcarballido, A.; Puebla, P.; Herrerovanrell, R.; Pastoriza, P. Radiosterilisation of indomethacin PLGA/PEG-derivative microspheres: Protective effects of low temperature during gamma-irradiation. *Int. J. Pharm.* **2006**, *313*, 129–135. https://doi.org/10.1016/j.ijpharm.2006.01.034.
13. EMA. Guideline on the Sterilisation of the Medicinal Product, Active Substance, Excipient and Primary Container. EMA/CHMP/CVMP/QWP/850374/2015, European Medicines Agency, 2019. Available online: https://www.ema.europa.eu/en/documents/scientific-guideline/guideline-sterilisation-medicinal-product-active-substance-excipient-primary-container_en.pdf (accessed on 18 May 2023).
14. Sakar, F.; Özer, A.Y.; Erdogan, S.; Ekizoglu, M.; Kart, D.; Özalp, M.; Colak, S.; Zencir, Y. Nano drug delivery systems and gamma radiation sterilization. *Pharm. Dev. Technol.* **2017**, *22*, 775–784. https://doi.org/10/gfsj3j.
15. Athanasiou, K. Sterilization, toxicity, biocompatibility and clinical applications of polylactic acid/polyglycolic acid copolymers. *Biomaterials* **1996**, *17*, 93–102. https://doi.org/10/d95272.
16. Wang, J.; Ng, C.W.; Win, K.Y.; Shoemakers, P.; Lee, T.K.Y.; Feng, S.S.; Wang, C.H. Release of paclitaxel from polylactide-co-glycolide (PLGA) microparticles and discs under irradiation. *J. Microencapsul.* **2003**, *20*, 317–327. https://doi.org/10.3109/02652040309178072.

17. Song, T.-T.; Yuan, X.-B.; Sun, A.-P.; Wang, H.; Kang, C.-S.; Ren, Y.; He, B.; Sheng, J.; Pu, P.-Y. Preparation of injectable paclitaxel sustained release microspheres by spray drying for inhibition of glioma *in vitro*. *J. Appl. Polym. Sci.* **2010**, *115*, 1534–1539. https://doi.org/10.1002/app.31105.
18. Dobrzynski, P.; Kasperczyk, J.; Janeczek, H.; Bero, M. Synthesis of Biodegradable Copolymers with the Use of Low Toxic Zirconium Compounds. 1. Copolymerization of Glycolide with L -Lactide Initiated by $Zr(Acac)_4$. *Macromolecules* **2001**, *34*, 5090–5098. https://doi.org/10.1021/ma0018143.
19. Jing, Y.; Yang, M.; Dai, S.; Quan, C.; Liu, J.; Jiang, Q.; Zhang, C.; Liu, B. Microwaves promote transesterification in the rapid synthesis of methoxy-poly(ethylene glycol)-block-poly(l-lactide-random-glycolide). *Polymer* **2018**, *136*, 187–193. https://doi.org/10.1016/j.polymer.2017.12.062.
20. *EN ISO 10993-5:2009*; Biological Evaluation of Medical Devices—Part 5: Tests for In Vitro Cytotoxicity (ISO 10993-5:2009). Annex A Neutral Red Uptake (NRU) Cytotoxicity Test. International Organization for Standardization: Geneva, Switzerland, 2009.
21. *ISO/FDIS 13829:2000*. Water Quality-Determination of the Genotoxocity of Water and Waste Water Using the Umu-Test; International Organization for Standarization: Geneva, Switzerland, 2000.
22. Sarasua, J.-R.; Prud'homme, R.E.; Wisniewski, M.; Le Borgne, A.; Spassky, N. Crystallization and Melting Behavior of Polylactides. *Macromolecules* **1998**, *31*, 3895–3905. https://doi.org/10.1021/ma971545p.
23. Magazzini, L.; Grilli, S.; Fenni, S.E.; Donetti, A.; Cavallo, D.; Monticelli, O. The Blending of Poly(glycolic acid) with Polycaprolactone and Poly(l-lactide): Promising Combinations. *Polymers* **2021**, *13*, 2780. https://doi.org/10.3390/polym13162780.
24. Kasiński, A.; Zielińska-Pisklak, M.; Kowalczyk, S.; Plichta, A.; Zgadzaj, A.; Oledzka, E.; Sobczak, M. Synthesis and Characterization of New Biodegradable Injectable Thermosensitive Smart Hydrogels for 5-Fluorouracil Delivery. *Int. J. Mol. Sci.* **2021**, *22*, 8330. https://doi.org/10.3390/ijms22158330.
25. Dash, S.; Murthy, P.N.; Nath, L.; Chowdhury, P. Kinetic Modeling on Drug Release from Controlled Drug Delivery Systems. *Acta Pol. Pharm. Ñ Drug Res.* **2010**, *67*, 217–223.
26. Domańska, I.; Zalewska, A.; Cieśla, K.; Plichta, A.; Głuszewski, W.; Łyczko, M.; Kowalczyk, S.; Oledzka, E.; Sobczak, M. The influence of electron beam and gamma irradiation on paclitaxel-loaded nanoparticles of fully randomized copolymers in relation to potential sterilization. 2023, *manuscript submitted*.
27. Plikk, P.; Odelius, K.; Hakkarainen, M.; Albertsson, A.C. Finalizing the properties of porous scaffolds of aliphatic polyesters through radiation sterilization. *Biomaterials* **2006**, *27*, 5335–5347. https://doi.org/10/dwqz5s.
28. Loo, S.C.J.; Ooi, C.P.; Boey, Y.C.F. Radiation effects on poly(lactide-co-glycolide) (PLGA) and poly(l-lactide) (PLLA). *Polym. Degrad. Stab.* **2004**, *83*, 259–265. https://doi.org/10/c4fc7c.
29. Davison, L.; Themistou, E.; Buchanan, F.; Cunningham, E. Low temperature gamma sterilization of a bioresorbable polymer, PLGA. *Radiat. Phys. Chem.* **2018**, *143*, 27–32. https://doi.org/10.1016/j.radphyschem.2017.09.009.
30. Loo, J.S.C.; Ooi, C.P.; Boey, F.Y.C. Degradation of poly(lactide-co-glycolide) (PLGA) and poly(l-lactide) (PLLA) by electron beam radiation. *Biomaterials* **2005**, *26*, 1359–1367. https://doi.org/10/b2b29p.
31. Dorati, R.; Colonna, C.; Tomasi, C.; Bruni, G.; Genta, I.; Modena, T.; Conti, B. Long-Term Effect of Gamma Irradiation on the Functional Properties and Cytocompatibility of Multiblock Co-Polymer Films. *J. Biomater. Sci. Polym. Ed.* **2012**, *23*, 2223–2240. https://doi.org/10.1163/156856211X613915.
32. Walo, M.; Rzepna, M. *Recent Developments in Radiation Processing of Polymers*; Institute of Nuclear Chemistry and Technology: Warszawa, Poland, 2020.
33. Pandita, D.; Ahuja, A.; Velpandian, T.; Lather, V.; Dutta, T.; Khar, R.K. Characterization and in vitro assessment of paclitaxel loaded lipid nanoparticles formulated using modified solvent injection technique. *Pharmazie* **2009**, *64*, 301–310. https://doi.org/10.1691/ph.2009.8338.
34. Nandhakumar, S.; Dhanaraju, M.D.; Sundar, V.D.; Heera, B. Influence of surface charge on the in vitro protein adsorption and cell cytotoxicity of paclitaxel loaded poly(ε-caprolactone) nanoparticles. *Bull. Fac. Pharm. Cairo Univ.* **2017**, *55*, 249–258. https://doi.org/10.1016/j.bfopcu.2017.06.003.
35. Musumeci, T.; Ventura, C.; Giannone, I.; Ruozi, B.; Montenegro, L.; Pignatello, R.; Puglisi, G. PLA/PLGA nanoparticles for sustained release of docetaxel. *Int. J. Pharm.* **2006**, *325*, 172–179. https://doi.org/10.1016/j.ijpharm.2006.06.023.
36. Jusu, S.M.; Obayemi, J.D.; Salifu, A.A.; Nwazojie, C.C.; Uzonwanne, V.; Odusanya, O.S.; Soboyejo, W.O. Drug encapsulated blend of PLGA PEG microspheres: In vitro and in vivo study of the efects of localized/targeted drug delivery on the treatment of triple negative breast cancer. *Sci. Rep.* **2020**, *10*, 14188. https://doi.org/10.1038/s41598-020-71129-0.
37. Singhvi, G.; Singh, M. Review: In-Vitro Drug Release Characterization Models. *Int. J. Pharm. Stud. Res.* **2011**, *2*, 77–84.
38. Głuszewski, W.; Zagórski, Z.P. Radiation effects in polypropylene/polystyrene blends as the model of aromatic protection effects. *Nukleonika* **2008**, *53*, S21–S24.
39. Ferry, M.; Ngono, Y. Energy transfer in polymers submitted to ionizing radiation: A review. *Radiat. Phys. Chem.* **2021**, *180*, 109320. https://doi.org/10.1016/j.radphyschem.2020.109320.

Warszawa, 09.11.2023 r.

mgr Izabela Domańska
Wydział Farmaceutyczny
Warszawski Uniwersytet Medyczny

OŚWIADCZENIE

Jako pierwszy autor pracy:

Domańska, I.M., Oledzka, E., Sobczak, M.

Sterilization process of polyester based anticancer-drug delivery systems.

***International Journal of Pharmaceutics* 2020, 587, 119663. DOI: 10.1016/j.ijpharm.2020.119663**

oświadczam, iż mój własny wkład merytoryczny w przygotowanie, przeprowadzenie i opracowanie badań oraz przedstawienie pracy w formie publikacji stanowi:

udział w opracowaniu koncepcji, zebranie materiałów dotyczących sterylizacji systemów poliestrowych o kontrolowanym uwalnianiu substancji aktywnych o działaniu przeciwnowotworowym, analiza i interpretacja zebranych danych literaturowych, pisanie oryginalnego tekstu publikacji, jego korekta i dyskusja z recenzentami.

Mój udział procentowy w przygotowaniu publikacji określam jako 80 %

Domańska

.....

(podpis oświadczającego)

Warszawa, 07.11.2023 r.

dr hab. inż. Ewa Olędzka
Wydział Farmaceutyczny
Warszawski Uniwersytet Medyczny

OŚWIADCZENIE

Jako współautor pracy:

Domańska, I.M., Oledzka, E., Sobczak, M.

Sterilization process of polyester based anticancer-drug delivery systems.

***International Journal of Pharmaceutics* 2020, 587, 119663. DOI: 10.1016/j.ijpharm.2020.119663**

oświadczam, iż mój własny wkład merytoryczny w przygotowanie, przeprowadzenie i opracowanie badań oraz przedstawienie pracy w formie publikacji stanowi:

konsultacja naukowa; pisanie oryginalnego tekstu publikacji oraz jego korekta.

Mój udział procentowy w przygotowaniu publikacji określam jako 10 %

Jednocześnie wyrażam zgodę na wykorzystanie w/w pracy jako część rozprawy doktorskiej mgr Izabeli Domańskiej.

.....

(podpis oświadczającego)

Warszawa, 07.11.2023 r.

prof. dr hab. inż. Marcin Sobczak
Wydział Farmaceutyczny
Warszawski Uniwersytet Medyczny

OŚWIADCZENIE

Jako współautor pracy:

Domańska, I.M., Oledzka, E., Sobczak, M.

Sterilization process of polyester based anticancer-drug delivery systems.

***International Journal of Pharmaceutics* 2020, 587, 119663. DOI: 10.1016/j.ijpharm.2020.119663**

oświadczam, iż mój własny wkład merytoryczny w przygotowanie publikacji stanowi:

konsultacja naukowa; pisanie oryginalnego tekstu publikacji, jego korekta oraz dyskusja z recenzentami. Mój udział procentowy w przygotowaniu publikacji określam jako 10 %

Jednocześnie wyrażam zgodę na wykorzystanie w/w pracy jako część rozprawy doktorskiej mgr Izabeli Domańskiej.

.....

(podpis oświadczającego)

Warszawa, 09.11.2023 r.

mgr Izabela Domańska
Wydział Farmaceutyczny
Warszawski Uniwersytet Medyczny

OŚWIADCZENIE

Jako pierwszy autor pracy:

Domańska, I.M., Zgadzaj, A., Kowalczyk, S., Zalewska, A., Oledzka, E., Cieśla, K., Plichta, A., Sobczak, M.

A Comprehensive Investigation of the Structural, Thermal, and Biological Properties of Fully Randomized Biomedical Polyesters Synthesized with a Nontoxic Bismuth(III) Catalyst.

***Molecules* 2022, 27, 1139. DOI: 10.3390/molecules27031139**

oświadczam, iż mój własny wkład merytoryczny w przygotowanie, przeprowadzenie i opracowanie badań oraz przedstawienie pracy w formie publikacji stanowi:

udział w opracowaniu koncepcji projektu badawczego, przeprowadzenie reakcji syntezy oraz badań strukturalnych i fizykochemicznych matryc polimerowych, opracowanie metodyki oraz interpretacja otrzymanych wyników badań, zarządzanie projektem badawczym, pisanie oryginalnego tekstu publikacji, jego korekta oraz dyskusja z recenzentami.

Mój udział procentowy w przygotowaniu publikacji określam jako 60 %

Domańska

.....

(podpis oświadczającego)

Warszawa, 14.06.2023 r.

dr Anna Zgadzaj
Zakład Toksykologii i Bromatologii
Wydział Farmaceutyczny, Warszawski Uniwersytet Medyczny

OŚWIADCZENIE

Jako współautor pracy:

Domańska, I.M., Zgadzaj, A., Kowalczyk, S., Zalewska, A., Oledzka, E., Cieśla, K., Plichta, A., Sobczak, M., A Comprehensive Investigation of the Structural, Thermal, and Biological Properties of Fully Randomized Biomedical Polyesters Synthesized with a Nontoxic Bismuth(III) Catalyst. *Molecules* 2022, 27, 1139. DOI: 10.3390/molecules27031139

oświadczam, iż mój własny wkład merytoryczny w przygotowanie, przeprowadzenie i opracowanie badań oraz przedstawienie pracy w formie publikacji stanowi:

przeprowadzenie badań cyto- i genotoksyczności oraz analiza i interpretacja otrzymanych wyników badań.

Mój udział procentowy w przygotowaniu publikacji określam jako 5 %

Jednocześnie wyrażam zgodę na wykorzystanie w/w pracy jako część rozprawy doktorskiej mgr Izabeli Domańskiej.

Anna Zgadzaj
.....
(podpis oświadczającego)

Warszawa, 07.11.2023 r.

mgr inż. Sebastian Kowalczyk
Wydział Chemiczny
Politechnika Warszawska

OŚWIADCZENIE

Jako współautor pracy:

Domańska, I.M., Zgadzaj, A., Kowalczyk, S., Zalewska, A., Oledzka, E., Cieśla, K., Plichta, A., Sobczak, M.

A Comprehensive Investigation of the Structural, Thermal, and Biological Properties of Fully Randomized Biomedical Polyesters Synthesized with a Nontoxic Bismuth(III) Catalyst.

***Molecules* 2022, 27, 1139. DOI: 10.3390/molecules27031139**

oświadczam, iż mój własny wkład merytoryczny w przygotowanie, przeprowadzenie i opracowanie badań oraz przedstawienie pracy w formie publikacji stanowi:

przeprowadzenie badań techniką GPC (ang. gel permeation chromatography).

Mój udział procentowy w przygotowaniu publikacji określam jako 3 %

Jednocześnie wyrażam zgodę na wykorzystanie w/w pracy jako część rozprawy doktorskiej mgr Izabeli Domańskiej.

(podpis oświadczającego)

Warszawa, 07.11.2023 r.

dr hab. inż., prof. uczelni Aldona Zalewska
Wydział Chemiczny
Politechnika Warszawska

OŚWIADCZENIE

Jako współautor pracy:

Domańska, I.M., Zgadzaj, A., Kowalczyk, S., Zalewska, A., Oledzka, E., Cieśla, K., Plichta, A., Sobczak, M.

A Comprehensive Investigation of the Structural, Thermal, and Biological Properties of Fully Randomized Biomedical Polyesters Synthesized with a Nontoxic Bismuth(III) Catalyst.

***Molecules* 2022, 27, 1139. DOI: 10.3390/molecules27031139**

oświadczam, iż mój własny wkład merytoryczny w przygotowanie, przeprowadzenie i opracowanie badań oraz przedstawienie pracy w formie publikacji stanowi:

przeprowadzenie badań techniką DSC (ang. differential scanning calorimetry) oraz analiza otrzymanych wyników badań.

Mój udział procentowy w przygotowaniu publikacji określam jako 5 %

Jednocześnie wyrażam zgodę na wykorzystanie w/w pracy jako część rozprawy doktorskiej mgr Izabeli Domańskiej.

Aldona Zalewska
.....

(podpis oświadczającego)

Warszawa, 07.11.2023 r.

dr hab. inż. Ewa Olędzka
Wydział Farmaceutyczny
Warszawski Uniwersytet Medyczny

OŚWIADCZENIE

Jako współautor pracy:

Domańska, I.M., Zgadzaj, A., Kowalczyk, S., Zalewska, A., Oledzka, E., Cieśla, K., Plichta, A., Sobczak, M.

A Comprehensive Investigation of the Structural, Thermal, and Biological Properties of Fully Randomized Biomedical Polyesters Synthesized with a Nontoxic Bismuth(III) Catalyst.

***Molecules* 2022, 27, 1139. DOI: 10.3390/molecules27031139**

oświadczam, iż mój własny wkład merytoryczny w przygotowanie, przeprowadzenie i opracowanie badań oraz przedstawienie pracy w formie publikacji stanowi:

konsultacja naukowa; pisanie oryginalnego tekstu publikacji oraz jego korekta.

Mój udział procentowy w przygotowaniu publikacji określam jako 5 %

Jednocześnie wyrażam zgodę na wykorzystanie w/w pracy jako część rozprawy doktorskiej mgr Izabeli Domańskiej.

Ewa Olędzka
.....
(podpis oświadczającego)

Warszawa, 07.11.2023 r.

dr hab. inż. Krystyna Cieśla, Prof. Instytutu
Instytut Chemii i Techniki Jądrowej
ul. Dorodna 16
03-195 Warszawa

OŚWIADCZENIE

Jako współautor pracy:

Domańska, I.M., Zgadzaj, A., Kowalczyk, S., Zalewska, A., Oledzka, E., Cieśla, K., Plichta, A., Sobczak, M.

A Comprehensive Investigation of the Structural, Thermal, and Biological Properties of Fully Randomized Biomedical Polyesters Synthesized with a Nontoxic Bismuth(III) Catalyst.

***Molecules* 2022, 27, 1139. DOI: 10.3390/molecules27031139**

oświadczam, iż mój własny wkład merytoryczny w przygotowanie, przeprowadzenie i opracowanie badań oraz przedstawienie pracy w formie publikacji stanowi:

interpretacja wyników badań analizy termicznej, konsultacja naukowa; udział w pisaniu oryginalnego tekstu publikacji oraz jego korekta.

Mój udział procentowy w przygotowaniu publikacji określam jako 7 %

Jednocześnie wyrażam zgodę na wykorzystanie w/w pracy jako część rozprawy doktorskiej mgr Izabeli Domańskiej.

K. Cieśla

.....

(podpis oświadczającego)

Warszawa, 07.11.2023 r.

dr hab. inż., prof. uczelni Andrzej Plichta
Wydział Chemiczny
Politechnika Warszawska

OŚWIADCZENIE

Jako współautor pracy:

Domańska, I.M., Zgadzaj, A., Kowalczyk, S., Zalewska, A., Oledzka, E., Cieśla, K., Plichta, A., Sobczak, M.

A Comprehensive Investigation of the Structural, Thermal, and Biological Properties of Fully Randomized Biomedical Polyesters Synthesized with a Nontoxic Bismuth(III) Catalyst.

***Molecules* 2022, 27, 1139. DOI: 10.3390/molecules27031139**

oświadczam, iż mój własny wkład merytoryczny w przygotowanie, przeprowadzenie i opracowanie badań oraz przedstawienie pracy w formie publikacji stanowi:

przeprowadzenie badań techniką GPC (ang. gel permeation chromatography) oraz analiza otrzymanych wyników badań.

Mój udział procentowy w przygotowaniu publikacji określam jako 5 %

Jednocześnie wyrażam zgodę na wykorzystanie w/w pracy jako część rozprawy doktorskiej mgr Izabeli Domańskiej.

Andrzej Plichta
.....
(podpis oświadczającego)

Warszawa, 07.11.2023 r.

prof. dr hab. inż. Marcin Sobczak
Wydział Farmaceutyczny
Warszawski Uniwersytet Medyczny

OŚWIADCZENIE

Jako współautor pracy:

Domańska, I.M., Zgadzaj, A., Kowalczyk, S., Zalewska, A., Oledzka, E., Cieśla, K., Plichta, A., Sobczak, M.

A Comprehensive Investigation of the Structural, Thermal, and Biological Properties of Fully Randomized Biomedical Polyesters Synthesized with a Nontoxic Bismuth(III) Catalyst.

***Molecules* 2022, 27, 1139. DOI: 10.3390/molecules27031139**

oświadczam, iż mój własny wkład merytoryczny w przygotowanie, przeprowadzenie i opracowanie badań oraz przedstawienie pracy w formie publikacji stanowi:

udział w opracowaniu koncepcji projektu badawczego, określenie metodyki oraz interpretacja wyników badań strukturalnych, fizykochemicznych, analitycznych i farmaceutycznych, konsultacja naukowa i nadzór nad projektem; pisanie oryginalnego tekstu publikacji, korekta oraz dyskusja z recenzentami.

Mój udział procentowy w przygotowaniu publikacji określam jako 10 %

Jednocześnie wyrażam zgodę na wykorzystanie w/w pracy jako część rozprawy doktorskiej mgr Izabeli Domańskiej.

.....

(podpis oświadczającego)

Warszawa, 09.11.2023 r.

mgr Izabela Domańska
Wydział Farmaceutyczny
Warszawski Uniwersytet Medyczny

OŚWIADCZENIE

Jako pierwszy autor pracy:

Domańska, I.M., Zalewska, A., Cieśla, K., Plichta, A., Głuszewski W., Łyczko, M., Kowalczyk, S., Oledzka, E., Sobczak, M.,

The influence of electron beam and gamma irradiation on paclitaxel-loaded nanoparticles of fully randomized copolymers in relation to potential sterilization.

Journal of Drug Delivery Science and Technology **2023, 90, 105115.**

DOI: 10.1016/j.jddst.2023.105115

oświadczam, iż mój własny wkład merytoryczny w przygotowanie, przeprowadzenie i opracowanie badań oraz przedstawienie pracy w formie publikacji stanowi:

udział w opracowaniu koncepcji projektu badawczego, przeprowadzenie reakcji syntezy oraz badań strukturalnych, fizykochemicznych, analitycznych i farmaceutycznych z matrycą polimerową, opracowanie metodyki oraz interpretacja otrzymanych wyników badań, zarządzanie projektem badawczym, pisanie oryginalnego tekstu publikacji, jego korekta oraz dyskusja z recenzentami.

Mój udział procentowy w przygotowaniu publikacji określam jako 55 %

Domańska

.....

(podpis oświadczającego)

Warszawa, 07.11.2023 r.

dr hab. inż., prof. uczelni Aldona Zalewska
Wydział Chemiczny
Politechnika Warszawska

OŚWIADCZENIE

Jako współautor pracy:

Domańska, I.M., Zalewska, A., Cieśla, K., Plichta, A., Głuszewski W., Łyczko, M., Kowalczyk, S., Oledzka, E., Sobczak, M.,

The influence of electron beam and gamma irradiation on paclitaxel-loaded nanoparticles of fully randomized copolymers in relation to potential sterilization.

***Journal of Drug Delivery Science and Technology* 2023, dostęp online 07.11.2023, 105115.**

DOI: 10.1016/j.jddst.2023.105115

oświadczam, iż mój własny wkład merytoryczny w przygotowanie, przeprowadzenie i opracowanie badań oraz przedstawienie pracy w formie publikacji stanowi:

przeprowadzenie badań techniką DSC (ang. differential scanning calorimetry) oraz analiza otrzymanych wyników badań.

Mój udział procentowy w przygotowaniu publikacji określam jako 5 %

Jednocześnie wyrażam zgodę na wykorzystanie w/w pracy jako część rozprawy doktorskiej mgr Izabeli Domańskiej.

Aldona Zalewska

(podpis oświadczającego)

Warszawa, 07.11.2023 r.

dr hab. inż. Krystyna Cieśla, Prof. Instytutu
Instytut Chemii i Techniki Jądrowej
ul. Dorodna 16
03-195 Warszawa

OŚWIADCZENIE

Jako współautor pracy:

Domańska, I.M., Zalewska, A., Cieśla, K., Plichta, A., Głuszewski W., Łyczko, M., Kowalczyk, S., Oledzka, E., Sobczak, M.,

The influence of electron beam and gamma irradiation on paclitaxel-loaded nanoparticles of fully randomized copolymers in relation to potential sterilization.

***Journal of Drug Delivery Science and Technology* 2023, dostęp online 07.11.2023, 105115.**

DOI: 10.1016/j.jddst.2023.105115

oświadczam, iż mój własny wkład merytoryczny w przygotowanie, przeprowadzenie i opracowanie badań oraz przedstawienie pracy w formie publikacji stanowi:

interpretacja wyników badań analizy termicznej, konsultacja naukowa; udział w pisaniu oryginalnego tekstu publikacji oraz jego korekta.

Mój udział procentowy w przygotowaniu publikacji określam jako 7 %

Jednocześnie wyrażam zgodę na wykorzystanie w/w pracy jako część rozprawy doktorskiej mgr Izabeli Domańskiej.

.....

(podpis oświadczającego)

Warszawa, 07.11.2023 r.

dr hab. inż., prof. uczelni Andrzej Plichta
Wydział Chemiczny
Politechnika Warszawska

OŚWIADCZENIE

Jako współautor pracy:

Domańska, I.M., Zalewska, A., Cieśla, K., Plichta, A., Głuszewski W., Łyczko, M., Kowalczyk, S., Oledzka, E., Sobczak, M.,

The influence of electron beam and gamma irradiation on paclitaxel-loaded nanoparticles of fully randomized copolymers in relation to potential sterilization.

***Journal of Drug Delivery Science and Technology* 2023, dostęp online 07.11.2023, 105115.**

DOI: 10.1016/j.jddst.2023.105115

oświadczam, iż mój własny wkład merytoryczny w przygotowanie, przeprowadzenie i opracowanie badań oraz przedstawienie pracy w formie publikacji stanowi:

przeprowadzenie badań techniką GPC (ang. gel permeation chromatography) oraz analiza otrzymanych wyników badań.

Mój udział procentowy w przygotowaniu publikacji określam jako 5 %

Jednocześnie wyrażam zgodę na wykorzystanie w/w pracy jako część rozprawy doktorskiej mgr Izabeli Domańskiej.

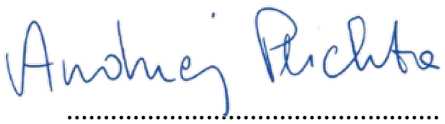

.....

(podpis oświadczającego)

Warszawa, 07.11.2023 r.

dr Wojciech Głuszewski
Instytut Chemii i Techniki Jądrowej

OŚWIADCZENIE

Jako współautor pracy:

Domańska, I.M., Zalewska, A., Cieśla, K., Plichta, A., Głuszewski W., Łyczko, M., Kowalczyk, S., Oledzka, E., Sobczak, M.,

The influence of electron beam and gamma irradiation on paclitaxel-loaded nanoparticles of fully randomized copolymers in relation to potential sterilization.

***Journal of Drug Delivery Science and Technology* 2023, dostęp online 07.11.2023, 105115.**

DOI: 10.1016/j.jddst.2023.105115

oświadczam, iż mój własny wkład merytoryczny w przygotowanie, przeprowadzenie i opracowanie badań oraz przedstawienie pracy w formie publikacji stanowi:

sterylizacja próbek przy użyciu promieniowania γ oraz wiązki elektronów (dawka 25 kGy).

Mój udział procentowy w przygotowaniu publikacji określam jako 5 %

Jednocześnie wyrażam zgodę na wykorzystanie w/w pracy jako część rozprawy doktorskiej mgr Izabeli Domańskiej.

.....

(podpis oświadczającego)

Warszawa, 07.11.2023 r.

dr Monika Łyczko
Instytut Chemii i Techniki Jądrowej

OŚWIADCZENIE

Jako współautor pracy:

Domańska, I.M., Zalewska, A., Cieśla, K., Plichta, A., Głuszewski W., Łyczko, M., Kowalczyk, S., Oledzka, E., Sobczak, M.,

The influence of electron beam and gamma irradiation on paclitaxel-loaded nanoparticles of fully randomized copolymers in relation to potential sterilization.

***Journal of Drug Delivery Science and Technology* 2023, dostęp online 07.11.2023, 105115.**

DOI: 10.1016/j.jddst.2023.105115

oświadczam, iż mój własny wkład merytoryczny w przygotowanie, przeprowadzenie i opracowanie badań oraz przedstawienie pracy w formie publikacji stanowi:

przeprowadzenie badań techniką DLS (ang. dynamic light scattering)

Mój udział procentowy w przygotowaniu publikacji określam jako 5 %

Jednocześnie wyrażam zgodę na wykorzystanie w/w pracy jako część rozprawy doktorskiej mgr Izabeli Domańskiej.

.....

(podpis oświadczającego)

Warszawa, 07.11.2023 r.

mgr inż. Sebastian Kowalczyk
Wydział Chemiczny
Politechnika Warszawska

OŚWIADCZENIE

Jako współautor pracy:

Domańska, I.M., Zalewska, A., Cieśla, K., Plichta, A., Głuszewski W., Łyczko, M., Kowalczyk, S., Oledzka, E., Sobczak, M.,

The influence of electron beam and gamma irradiation on paclitaxel-loaded nanoparticles of fully randomized copolymers in relation to potential sterilization.

***Journal of Drug Delivery Science and Technology* 2023, dostęp online 07.11.2023, 105115.**

DOI: 10.1016/j.jddst.2023.105115

oświadczam, iż mój własny wkład merytoryczny w przygotowanie, przeprowadzenie i opracowanie badań oraz przedstawienie pracy w formie publikacji stanowi:

przeprowadzenie badań techniką GPC (ang. gel permeation chromatography).

Mój udział procentowy w przygotowaniu publikacji określam jako 3 %

Jednocześnie wyrażam zgodę na wykorzystanie w/w pracy jako część rozprawy doktorskiej mgr Izabeli Domańskiej.

Sebastian Kowalczyk

(podpis oświadczającego)

Warszawa, 07.11.2023 r.

dr hab. inż. Ewa Olędzka
Wydział Farmaceutyczny
Warszawski Uniwersytet Medyczny

OŚWIADCZENIE

Jako współautor pracy:

Domańska, I.M., Zalewska, A., Cieśla, K., Plichta, A., Głuszewski W., Łyczko, M., Kowalczyk, S., Oledzka, E., Sobczak, M.,

The influence of electron beam and gamma irradiation on paclitaxel-loaded nanoparticles of fully randomized copolymers in relation to potential sterilization.

***Journal of Drug Delivery Science and Technology* 2023, dostęp online 07.11.2023, 105115.**

DOI: 10.1016/j.jddst.2023.105115

oświadczam, iż mój własny wkład merytoryczny w przygotowanie, przeprowadzenie i opracowanie badań oraz przedstawienie pracy w formie publikacji stanowi:

konsultacja naukowa; korekta tekstu publikacji.

Mój udział procentowy w przygotowaniu publikacji określam jako 5 %

Jednocześnie wyrażam zgodę na wykorzystanie w/w pracy jako część rozprawy doktorskiej mgr Izabeli Domańskiej.

Ewa Olędzka
.....

(podpis oświadczającego)

Warszawa, 07.11.2023 r.

prof. dr hab. inż. Marcin Sobczak
Wydział Farmaceutyczny
Warszawski Uniwersytet Medyczny

OŚWIADCZENIE

Jako współautor pracy:

Domańska, I.M., Zalewska, A., Cieśla, K., Plichta, A., Głuszewski W., Łyczko, M., Kowalczyk, S., Oledzka, E., Sobczak, M.,

The influence of electron beam and gamma irradiation on paclitaxel-loaded nanoparticles of fully randomized copolymers in relation to potential sterilization.

***Journal of Drug Delivery Science and Technology* 2023, dostęp online 07.11.2023, 105115.**

DOI: 10.1016/j.jddst.2023.105115

oświadczam, iż mój własny wkład merytoryczny w przygotowanie, przeprowadzenie i opracowanie badań oraz przedstawienie pracy w formie publikacji stanowi:

udział w opracowaniu koncepcji projektu badawczego, określenie metodyki oraz interpretacja wyników badań strukturalnych, fizykochemicznych, analitycznych i farmaceutycznych, konsultacja naukowa i nadzór nad projektem; pisanie oryginalnego tekstu publikacji, korekta oraz dyskusja z recenzentami.

Mój udział procentowy w przygotowaniu publikacji określam jako 10 %

Jednocześnie wyrażam zgodę na wykorzystanie w/w pracy jako część rozprawy doktorskiej mgr Izabeli Domańskiej.

.....

(podpis oświadczającego)

Warszawa, 09.11.2023 r.

mgr Izabela Domańska
Wydział Farmaceutyczny
Warszawski Uniwersytet Medyczny

OŚWIADCZENIE

Jako pierwszy autor pracy:

Domańska, I.M., Figat, R., Zalewska, A., Cieśla, K., Kowalczyk, S., Kędra, K., Sobczak, M., The Influence of Ionizing Radiation on Paclitaxel-Loaded Nanoparticles Based on PLGA. ***Applied Sciences*** **2023, 13, 11052; DOI: 10.3390/app131911052**

oświadczam, iż mój własny wkład merytoryczny w przygotowanie, przeprowadzenie i opracowanie badań oraz przedstawienie pracy w formie publikacji stanowi:

udział w opracowaniu koncepcji projektu badawczego, przeprowadzenie reakcji syntezy oraz badań strukturalnych, fizykochemicznych, analitycznych i farmaceutycznych z matrycą polimerową, opracowanie metodyki oraz interpretacja otrzymanych wyników badań, zarządzanie projektem badawczym, pisanie oryginalnego tekstu publikacji, jego korekta oraz dyskusja z recenzentami.

Mój udział procentowy w przygotowaniu publikacji określam jako 65 %

Domańska
.....

(podpis oświadczającego)

Warszawa, 10.10.2023 r.

dr n. farm. Ramona Figat
Zakład Toksykologii i Bromatologii
Wydział Farmaceutyczny, Warszawski Uniwersytet Medyczny

OŚWIADCZENIE

Jako współautor pracy:
Domańska, I.M., Figat, R., Zalewska, A., Cieśla, K., Kowalczyk, S., Kędra, K., Sobczak, M., The Influence of Ionizing Radiation on Paclitaxel-Loaded Nanoparticles Based on PLGA. ***Applied Sciences*** **2023, 13, 11052; DOI: 10.3390/app131911052**
oświadczam, iż mój własny wkład merytoryczny w przygotowanie, przeprowadzenie i opracowanie badań oraz przedstawienie pracy w formie publikacji stanowi:

przeprowadzenie badań cyto- i genotoksyczności oraz analiza i interpretacja otrzymanych wyników badań.

Mój udział procentowy w przygotowaniu publikacji określam jako 5 %

Jednocześnie wyrażam zgodę na wykorzystanie w/w pracy jako część rozprawy doktorskiej mgr Izabeli Domańskiej.

Ramona Figat
.....
(podpis oświadczającego)

Warszawa, 07.11.2023 r.

dr hab. inż., prof. uczelni Aldona Zalewska
Katedra Chemii Nieorganicznej
Wydział Chemiczny
Politechnika Warszawska

OŚWIADCZENIE

Jako współautor pracy:

Domańska, I.M., Figat, R., Zalewska, A., Cieśla, K., Kowalczyk, S., Kędra, K., Sobczak, M., The Influence of Ionizing Radiation on Paclitaxel-Loaded Nanoparticles Based on PLGA. ***Applied Sciences*** **2023, 13, 11052; DOI: 10.3390/app131911052**

oświadczam, iż mój własny wkład merytoryczny w przygotowanie, przeprowadzenie i opracowanie badań oraz przedstawienie pracy w formie publikacji stanowi:

przeprowadzenie badań techniką DSC (ang. differential scanning calorimetry) oraz analiza otrzymanych wyników badań.

Mój udział procentowy w przygotowaniu publikacji określam jako 5 %

Jednocześnie wyrażam zgodę na wykorzystanie w/w pracy jako część rozprawy doktorskiej mgr Izabeli Domańskiej.

Aldona Zalewska

.....

(podpis oświadczającego)

Warszawa, 07.11.2023 r.

dr hab. inż. Krystyna Cieśla, Prof. Instytutu
Instytut Chemii i Techniki Jądrowej
ul. Dorodna 16
03-195 Warszawa

OŚWIADCZENIE

Jako współautor pracy:

Domańska, I.M., Figat, R., Zalewska, A., Cieśla, K., Kowalczyk, S., Kędra, K., Sobczak, M., The Influence of Ionizing Radiation on Paclitaxel-Loaded Nanoparticles Based on PLGA. ***Applied Sciences*** **2023, 13, 11052; DOI: 10.3390/app131911052**

oświadczam, iż mój własny wkład merytoryczny w przygotowanie, przeprowadzenie i opracowanie badań oraz przedstawienie pracy w formie publikacji stanowi:

interpretacja wyników badań analizy termicznej, konsultacja naukowa; udział w pisaniu oryginalnego tekstu publikacji oraz jego korekta.

Mój udział procentowy w przygotowaniu publikacji określam jako 7 %

Jednocześnie wyrażam zgodę na wykorzystanie w/w pracy jako część rozprawy doktorskiej mgr Izabeli Domańskiej.

K. Cieśla

.....

(podpis oświadczającego)

Warszawa, 07.11.2023 r.

mgr inż. Sebastian Kowalczyk
Wydział Chemiczny
Politechnika Warszawska

OŚWIADCZENIE

Jako współautor pracy:

Domańska, I.M., Figat, R., Zalewska, A., Cieśla, K., Kowalczyk, S., Kędra, K., Sobczak, M., The Influence of Ionizing Radiation on Paclitaxel-Loaded Nanoparticles Based on PLGA. ***Applied Sciences*** **2023, 13, 11052; DOI: 10.3390/app131911052**

oświadczam, iż mój własny wkład merytoryczny w przygotowanie, przeprowadzenie i opracowanie badań oraz przedstawienie pracy w formie publikacji stanowi:

przeprowadzenie badań techniką GPC (ang. gel permeation chromatography).
Mój udział procentowy w przygotowaniu publikacji określam jako 5 %

Jednocześnie wyrażam zgodę na wykorzystanie w/w pracy jako część rozprawy doktorskiej mgr Izabeli Domańskiej.

Sebastian Kowalczyk
(podpis oświadczającego)

Warszawa, 10.10.2023 r.

dr Karolina Kędra
Instytut Chemii Fizycznej
Polska Akademia Nauk

OŚWIADCZENIE

Jako współautor pracy:

Domańska, I.M., Figat, R., Zalewska, A., Cieśla, K., Kowalczyk, S., Kędra, K., Sobczak, M., The Influence of Ionizing Radiation on Paclitaxel-Loaded Nanoparticles Based on PLGA. ***Applied Sciences*** **2023, 13, 11052; DOI: 10.3390/app131911052**

oświadczam, iż mój własny wkład merytoryczny w przygotowanie, przeprowadzenie i opracowanie badań oraz przedstawienie pracy w formie publikacji stanowi:

interpretacja wyników badań DSC i DLS, korekta tekstu.

Mój udział procentowy w przygotowaniu publikacji określam jako 3 %

Jednocześnie wyrażam zgodę na wykorzystanie w/w pracy jako część rozprawy doktorskiej mgr Izabeli Domańskiej.

Karolina Kędra

……

(podpis oświadczającego)

Warszawa, 10.10.2023 r.

prof. dr hab. inż. Marcin Sobczak
Wydział Farmaceutyczny
Warszawski Uniwersytet Medyczny

OŚWIADCZENIE

Jako współautor pracy:

Domańska, I.M., Figat, R., Zalewska, A., Cieśla, K., Kowalczyk, S., Kędra, K., Sobczak, M., The Influence of Ionizing Radiation on Paclitaxel-Loaded Nanoparticles Based on PLGA. ***Applied Sciences*** **2023, 13, 11052; DOI: 10.3390/app131911052**

oświadczam, iż mój własny wkład merytoryczny w przygotowanie, przeprowadzenie i opracowanie badań oraz przedstawienie pracy w formie publikacji stanowi:

udział w opracowaniu koncepcji projektu badawczego, określenie metodyki oraz interpretacja wyników badań strukturalnych, fizykochemicznych, analitycznych i farmaceutycznych, konsultacja naukowa i nadzór nad projektem; pisanie oryginalnego tekstu publikacji, korekta oraz dyskusja z recenzentami. Mój udział procentowy w przygotowaniu publikacji określam jako 10 %

Jednocześnie wyrażam zgodę na wykorzystanie w/w pracy jako część rozprawy doktorskiej mgr Izabeli Domańskiej.

.....

(podpis oświadczającego)